
Oestrogen and Thyroid Hormone Interactions in the Regulation of Bone Mass

Moira Shang-Mei Cheung

A thesis submitted for the degree of

DOCTOR OF PHILOSOPHY

2014

Molecular Endocrinology Group

Faculty of Medicine, Imperial College London

UK

Abstract

Osteoporosis is characterised by low bone mass, reduced bone mineral density and a deterioration of bone microarchitecture, resulting in increased susceptibility to fragility fractures. Oestrogen deficiency and thyrotoxicosis are established risk factors for osteoporosis. Oestrogen and thyroid hormone have opposing actions on adult bone and I hypothesise that accelerated bone loss at the menopause is due to unopposed actions of thyroid hormone on the skeleton.

To test this hypothesis, I investigated the effect of altered thyroid status on the skeleton in adult sham-operated and ovariectomised wild type and thyroid hormone receptor (TR) α and β knockout mice (TR $\alpha^{0/0}$ and TR $\beta^{-/-}$). Skeletal phenotype analysis included determination of structural, densitometric, histomorphometric and biomechanical parameters.

Skeletal phenotypes of euthyroid wild type mice were compared to hypothyroid and thyrotoxic wild type as well as TR $\alpha^{0/0}$ and TR $\beta^{-/-}$ mice. Bone mass was elevated in TR $\alpha^{0/0}$ and reduced in TR $\beta^{-/-}$ mice despite similar bone formation rates. These data suggest that the differences in bone mass are due to differing osteoclast activity.

The skeletal phenotypes of TR $\alpha^{0/0}$ and TR $\beta^{-/-}$ mice following manipulation of thyroid status were then described in detail. TR $\beta^{-/-}$ and wild type mice rendered hypothyroid, had significantly lower bone formation than hypothyroid TR $\alpha^{0/0}$ mice suggesting that, in the absence of thyroid hormone, TR α may inhibit bone formation.

Finally, the effect of oestrogen withdrawal in each of these groups of mice was also investigated. These studies demonstrate oestrogen deficiency bone loss was greater in hypothyroid compared to hyperthyroid mice, indicating that accelerated bone loss following oestrogen withdrawal cannot result from unopposed actions of thyroid hormones. Nevertheless, the studies contained in this thesis provide new insight regarding the roles of TR α and TR β in bone maintenance and the effects of interactions between oestrogen and thyroid hormones on the regulation of bone mass.

Contents

Abstract.....	2
Contents.....	3
List of Figures.....	7
List of Tables.....	11
Abbreviations.....	12
Declaration of Originality and Copyright Declaration.....	19
Acknowledgements.....	20
The Thesis.....	21
Characterisation of Oestrogen and Thyroid Hormone Interactions in the Regulation of Bone Mass..	21
1 INTRODUCTION.....	23
1.1 BACKGROUND.....	23
1.2 BONE PHYSIOLOGY.....	24
1.2.1 STRUCTURE OF BONE.....	24
1.2.2 COMPOSITION OF BONE.....	26
1.2.2.1 BONE CELLS.....	26
1.2.2.2 BONE MATRIX AND MINERALISATION.....	36
1.2.3 EMBRYONIC DERIVATION OF BONE.....	39
1.2.3.1 INTRAMEMBRANOUS OSSIFICATION.....	39
1.2.3.2 ENDOCHONDRAL OSSIFICATION.....	40
1.2.4 REGULATION OF BONE: MODELLING AND REMODELLING.....	44
1.2.4.1 BONE MODELLING.....	44
1.2.4.2 BONE REMODELLING.....	44
1.2.4.3 OTHER MECHANISMS OF REGULATION OF SKELETAL MASS.....	47
1.3 OSTEOPOROSIS.....	48
1.3.1 RISK FACTORS FOR OSTEOPOROSIS.....	48
1.4 THYROID HORMONE.....	51
1.4.1 HOMEOSTATIC CONTROL OF THYROID HORMONE.....	51
1.4.2 THYROID HORMONE SYNTHESIS.....	53
1.4.3 LOCAL CONTROL OF THYROID HORMONE CONCENTRATIONS.....	55
1.4.4 MOLECULAR MECHANISMS OF THYROID HORMONE ACTION.....	57
1.4.5 THE EFFECTS OF CIRCULATING THYROID HORMONE LEVELS ON THE SKELETON.....	62
1.4.6 THE ROLE OF THYROID HORMONE TRANSPORTERS AND DEIODINASES IN THE SKELETON.....	65
1.4.7 THE ROLE OF TRS IN THYROID HORMONE SIGNALLING IN THE SKELETON.....	67

1.4.8 IMPORTANT SIGNALLING PATHWAYS INVOLVED IN THYROID ACTION IN THE SKELETON .	71
1.4.9 THYROID STIMULATING HORMONE	74
1.5 OESTROGEN	75
1.5.1 OESTROGEN SYNTHESIS	75
1.5.2 HOMEOSTATIC CONTROL OF OESTROGEN	75
1.5.3 LOCAL CONTROL OF OESTROGEN LEVELS.....	78
1.5.4 MOLECULAR MECHANISMS OF OESTROGEN ACTION	78
1.5.5 THE EFFECTS OF REDUCED OESTROGEN SIGNALLING IN THE SKELETON	80
1.5.6 IMPORTANT SIGNALLING PATHWAYS INVOLVED IN OESTROGEN ACTION IN THE SKELETON	85
1.5.7 FOLLICLE STIMULATING HORMONE.....	87
1.6 SIMILARITIES OF OESTROGEN AND THYROID HORMONE ACTION ON BONE.....	88
1.7 EXPERIMENTAL DESIGN	89
1.7.1 Hypothesis.....	89
1.7.2 Aims.....	89
2 MATERIAL AND METHODS.....	91
2.1 GENETICALLY MODIFIED MICE.....	91
2.1.1 TR α ^{0/0} MICE.....	91
2.1.2 TR β ^{-/-} MICE.....	91
2.2 GENOTYPING OF MOUSE STRAINS.....	91
2.2.1 DNA EXTRACTION.....	91
2.2.2 POLYMERASE CHAIN REACTION (PCR).....	91
2.3 OESTROGEN AND THYROID HORMONE MANIPULATION.....	97
2.3.1 WILD TYPE AND TR α ^{0/0} MICE.....	97
2.3.2 TR β ^{-/-} MICE	97
2.4 CALCEIN LABELLING	98
2.5 GROWTH PARAMETERS	98
2.6 SERUM SAMPLES.....	99
2.6.1 THYROID HORMONE AND BONE TURNOVER MARKERS.....	99
2.7 DISSECTION, FIXATION AND STORAGE OF THE SKELETON	100
2.8 BONE IMAGING	100
2.8.1 FAXITRON POINT PROJECTION MICRORADIOGRAPHIC ANALYSIS.....	100
2.8.2 MICRO COMPUTED TOMOGRAPHY (CT) ANALYSIS	104
2.8.3 qBSE-SEM	105

2.8.4 BSE-SEM	107
2.8.5 CONFOCAL MICROSCOPY.....	108
2.8.6 HISTOMORPHOMETRY.....	110
2.9 MECHANICAL LOADING AND BONE STRENGTH.....	111
2.10 STATISTICS.....	113
2.10.1 TYPE I AND TYPE II ERRORS.....	113
3 SKELETAL PHENOTYPING OF WILD TYPE MICE WITH MANIPULATED THYROID STATUS IN COMPARISON TO TR α ^{0/0} AND TR β ^{-/-} MICE.....	115
3.1 BACKGROUND.....	115
3.2 RESULTS.....	117
3.2.1 CIRCULATING THYROID STATUS OF WILD TYPE, TR α ^{0/0} AND TR β ^{-/-} MICE.....	117
3.2.2 ANALYSIS OF BODY WEIGHT AND TAIL LENGTH MEASUREMENTS.....	118
3.2.3 STRUCTURAL PARAMETERS.....	119
3.2.4 BONE MINERAL DENSITY.....	122
3.2.5 BONE FORMATION: P1NP AND BFR.....	129
3.2.6 BONE RESORPTION: CTX, CORTICAL RESORPTION, OSTEOCLAST PARAMETERS.....	133
3.2.7 BIOMECHANICAL TESTING.....	137
3.3 SUMMARY OF RESULTS.....	138
3.4 DISCUSSION.....	139
4 THE EFFECTS OF DIFFERING THYROID STATUS ON THE SKELETAL PHENOTYPE OF TR α ^{0/0} AND TR β ^{-/-} MICE.....	146
4.1 BACKGROUND.....	146
4.2 RESULTS.....	147
4.2.1 CIRCULATING THYROID HORMONE STATUS.....	147
4.2.2 GROWTH.....	149
4.2.3 STRUCTURAL PARAMETERS.....	150
4.2.4 BONE MINERAL DENSITY.....	153
4.2.5 BONE FORMATION: P1NP AND BFR.....	159
4.2.6 BONE RESORPTION: CTX AND ENDOCORTICAL RESORPTION.....	161
4.2.7 BIOMECHANICAL TESTING.....	163
4.3 SUMMARY OF RESULTS.....	164
4.4 DISCUSSION.....	165
4.4.1 Skeletal effects of thyroid status in TR α ^{0/0} mice.....	166
4.4.2 Skeletal effects of thyroid status in TR β ^{-/-} mice.....	167

4.4.3 Changes in BMC in response to alteration in thyroid status in different genotypes.....	169
4.4.4 Summary and salient points.....	171
5 EFFECTS OF OESTROGEN AND THYROID HORMONE INTERACTIONS IN THE REGULATION OF BONE MASS	173
5.1 BACKGROUND	173
5.2 RESULTS.....	173
5.2.1 GROWTH	173
5.2.3 STRUCTURAL PARAMETERS	176
5.2.4 BONE MINERAL DENSITY.....	182
5.2.5 BONE FORMATION: P1NP AND BFR.....	187
5.2.6 BONE RESORPTION: CTX AND CORTICAL RESORPTION	191
5.2.7 BIOMECHANICAL TESTING	193
5.3 SUMMARY OF RESULTS.....	194
5.4 DISCUSSION.....	197
5.4.1 TR α has an osteoprotective effect on oestrogen deficiency bone loss	197
5.4.2 Oestrogen withdrawal associated with increased weight and bone length	198
5.4.3 Oestrogen withdrawal in hypothyroid mice is associated with increased resorption on cancellous surfaces but not endocortical surfaces	199
5.4.4 Hyperthyroid mice do not demonstrate oestrogen deficiency elevation in bone formation	199
5.4.5 Decreased bone formation associated with presence of oestrogen and unliganded TR α	199
5.4.6 Bone remodelling uncoupled in ovariectomised TR $\alpha^{0/0}$ mice	200
6 DISCUSSIONS AND CONCLUSIONS	202
6.1 Effects on the skeleton of oestrogen and thyroid hormone interactions	202
6.2 Bone biology	203
6.3 Future research and ongoing experiments.....	204
APPENDIX.....	206
REFERENCES	223
PUBLICATIONS FROM THESIS.....	239

List of Figures

1.1	Structure of long bones	25
1.2	Mesenchymal progenitor differentiation	26
1.3	Histology image of osteoclast (Oc) resorbing bone and BSE-SEM image of resorbed bone surface	30
1.4	Diagram of resorbing osteoclast	31
1.5	Osteocyte lacunae and dendritic processes in cortical bone	34
1.6	Synthesis and structural organisation of type 1 collagen	37
1.7	Collagen fibrils in woven bone and lamellar bone	39
1.8	Diagram showing the different steps in endochondral ossification	40
1.9	Growth plate	42
1.10	Growth plate signalling	43
1.11	Remodelling cycle	46
1.12	Homeostatic control of thyroid hormone	52
1.13	Thyroid hormone synthesis	54
1.14	Deiodinase activation and inactivation of thyroid hormone	56
1.15	Structure of steroid hormone and TR isoforms	58
1.16	TR control of gene expression	61
1.17	Key signalling pathways in the growth plate	72
1.18	Serum hormone concentrations and follicular growth during the menstrual cycle	77
1.19	ER isoforms	79
1.20	Decline in BMD in men and women	81
2.1	Primer locations for identification of wild type and mutant TR α alleles	93

2.2	Primer locations for identification of wild type and mutant TR β alleles	94
2.3	Example of PCR gel used for identifying wild type and mutant TR α PCR products	95
2.4	Example of PCR gel used for identifying wild type and mutant TR β PCR products	96
2.5	Image processing used for determining BMC	102
2.6	Determining cortical thickness	103
2.7	Micro CT images of a femur	104
2.8	Image of lumbar vertebrae taken by qBSE-SEM	106
2.9	Different densities represented in different colours	106
2.10	BSE-SEM images of the internal cortex of femurs	107
2.11	Montaged confocal image of a lumbar vertebra	108
2.12	Confocal images of double labelling	109
2.13	Osteoclast parameters analysis	111
2.14	Load displacement curves generated from three point bending of femur	112
3.1	Serum free T4 and free T3 levels	117
3.2	Growth parameters	118
3.3	Gross structural parameters	119
3.4	BSE- SEM images showing bone microarchitecture	121
3.5	Bone mineral content of femurs	123
3.6	Bone mineral content of caudal vertebrae	124
3.7	Micro-mineralisation of lumbar vertebrae	126
3.8	Micro-mineralisation of tibial cortical bone	127
3.9	Micro-mineralisation of tibial trabeculae	128
3.10	Dynamic bone formation parameters	130

3.11	Montages of confocal images of lumbar vertebrae of hypothyroid, euthyroid and hyperthyroid wild type mice	131
3.12	Serum P1NP concentrations	132
3.13	Serum bone resorption markers	133
3.14	Endosteal resorption parameters	134
3.15	Sections of proximal humeri showing TRAP stained osteoclasts in red	135
3.16	Analysis of histomorphometric osteoclast parameters	136
3.17	Biomechanical properties	137
4.1	Circulating thyroid hormone status	148
4.2	Growth parameters	149
4.3	Gross structural parameters	150
4.4	SEM images showing bone micro architecture	152
4.5	Bone mineral content of femurs	154
4.6	Bone mineral content of caudal vertebrae	155
4.7	Micro-mineralisation of lumbar vertebrae	157
4.8	Micro-mineralisation of tibial trabeculae and cortical bone	158
4.9	Serum P1NP concentrations	159
4.10	Dynamic bone formation parameters	160
4.11	Serum bone resorption parameters	161
4.12	Bone resorption parameters	162
4.13	Mechanical properties	163
4.14	Proposed model of thyroid hormone induced bone loss in differing genotypes	170
5.1	Growth parameters	174

5.2	Bone length	175
5.3	Cortical parameters	177
5.4	Micro CT assessment of BV/TV	179
5.5	SEM images of bone micro architecture	181
5.6	Bone mineral content of femurs	183
5.7	Bone mineral content of caudal vertebrae	184
5.8	Micro-mineralisation of lumbar vertebrae	186
5.9	Serum P1NP from wild type, TR α ^{0/0} and TR β ^{-/-} mice with differing thyroid status	187
5.10	Graphical representation of BFR	190
5.11	Serum bone resorption markers	192
5.12	Mechanical properties	194

List of Tables

1.1	Bone phenotype of ER deficient mice	85
1.2	Comparison between the actions of TH and E2 in the skeleton	88
2.1	Summary of drugs administered to manipulate thyroid status in each group	98
3.1	Analysis of micro CT data	122
3.2	Summary of skeletal phenotyping	138
4.1	Analysis of micro CT data	153
4.2	Summary of effects of alteration in thyroid status in TR $\alpha^{0/0}$ and TR $\beta^{-/-}$ mice compared to euthyroid status in respective genotype	164
4.3	Table showing the presence of liganded or unliganded TR in the different treatment groups	166
4.4	Summary of changes in BMC in femurs and caudal vertebrae of wild type, TR $\alpha^{0/0}$ and TR $\beta^{-/-}$ mice with differing thyroid status	169
4.5	Table summarising the BFR in each genotype which are hypothyroid and if each TR is liganded or not	171
5.1	Analysis of micro CT data	180
5.2	Analysis of dynamic bone formation parameters	189
5.3	Summary of effects of ovariectomy on the skeletal phenotype of wild type, TR $\alpha^{0/0}$ and TR $\beta^{-/-}$ mice with differing thyroid status shown in genotype grouping	195
5.4	Summary of effects of ovariectomy on the skeletal phenotype of hypo, eu and hyperthyroid mice in different genotypes	196

Abbreviations

AF1/2	Activation function 1/2
ATP	Adenosine triphosphate
ALP	Alkaline phosphatase
ANOVA	Analysis of variance
APC	Adenomatous polyposis coli protein
ApoTR	Unliganded thyroid hormone receptor
BFR	Bone formation rate
BMC	Bone mineral content
BMD	Bone mineral density
BMI	Body mass index
BMP	Bone morphogenic protein
BR	BMP receptor
BRU	Bone remodelling unit
BS	Bone surface
BSE-SEM	Backscattered electron scanning electron microscopy
BSP	Bone sialoprotein
BV/TV	Bone volume per tissue volume
cAMP	Cyclic 3'5' adenosine monophosphate
CART	Cocaine and amphetamine-regulated transcript
CF	Cumulative frequency
c-fms	Colony-stimulating factor-I receptor

Col	Collagen
CSLM	Confocal scanning light microscopy
CT	Computed tomography
CTX	C-terminal cross-linked telopeptide of type I collagen
D1	Iodothyronine deiodinase enzyme type 1
D2	Iodothyronine deiodinase enzyme type 2
D3	Iodothyronine deiodinase enzyme type 3
DBD	DNA binding domain
DHEA	Dehydroepiandrosterone
DHT	5 α -dihdrotestosterone
DIT	Di-iodotyrosine
Dkk	Dikkopf
DMP1	Dentine matrix protein 1
DNA	Deoxyribonucleic acid
DUOX2	Dual oxidase 2
DUOXA2	Dual oxidase maturation factor 2
DXA	Dual energy X-ray absorptiometry
E1	Estrone
E2	17 β -estradiol
ECM	Extra cellular matrix
EMP	Extra cellular matrix proteins
ER	Oestrogen receptor
ERE	Oestrogen response element

ERK	Extra cellular signal regulated kinase
FGF	Fibroblast growth factor
FGFR	Fibroblast growth factor receptor
FOXO	Forkhead box
FSH	Follicle stimulating hormone
GH	Growth hormone
GHR	Growth hormone receptor
GHRH	Growth hormone releasing hormone
GnRH	Gonadotrophin releasing hormone
GPCR	G protein-coupled receptor
GRIP-1	Glucocorticoid receptor interacting protein-1
GSK3β	Glycogen synthase kinase 3 β
GWAS	Genome wide association studies
HAT	Histone acetyltransferase
HPT axis	hypothalamic–pituitary–thyroid axis
Hyt/hyt	Congenital hypothyroid mice with TSHR mutation
HZ	Hypertrophic zone
IGF	Insulin like growth factor
IGFBP	Insulin like growth factor binding protein
Ihh	Indian Hedgehog protein
IL	Interleukin
IP₃	Inositol 1,4,5-triphosphate
i.v.	Intravenous

JAK	janus kinase
JNK	c-jun N-terminal kinase
LAT	L-type amino acid transporter
LBD	Ligand binding domain
LH	Luteinising Hormone
LRP	LDL receptor related protein
LRP5/6	Low density lipoprotein receptor related protein 5/6
M-CSF	Macrophage colony stimulating factor
MAPK	Mitogen activated protein kinase
MAR	Mineral apposition rate
MCT	Monocarboxylate transporter
MIT	Mono-iodotyrosine
MMP	Matrix metalloproteinase
mRNA	Messenger ribonucleic acid
MS	Mineralising surface
MSC	Mesenchymal stem cells
NADPH	Nicotinamide adenine dinucleotide phosphate
NCoR/NCOR	Nuclear receptor co-repressor
NF-κB	Nuclear factor kappa light chain enhancer of activated B cell
NIS	Na ⁺ /I ⁻ symporters
NPP1	Nucleotide pyrophosphates phosphodiesterase1
OATP	Organic anion transporting polypeptide
Oc	Osteoclast

Oc.N	Osteoclast number
Oc.S	Osteoclast surface
OCN	Osteocalcin
OPG	Osteoprotegerin
OPN	Osteopontin
OSN	Osteonectin
OSX	Osterix
OVX	Ovariectomy/ovariectomised
P1NP	Propeptide of type 1 N-terminal procollagen
Pax8	Mice with thyroid agenesis
PCR	Polymerase chain reaction
PHEX	Phosphate-regulating neutral endopeptidase, X-linked
PI3K	Phosphoinositide 3 kinase
PKA	Protein kinase A
PKC	Protein kinase C
PLC	Phospholipase C
PMMA	Poly-methyl-methacrylate
PNS	Parasympathetic nervous system
POP	Pyrophosphate
PPR	PTHrP receptor
PTH	Parathyroid hormone
PTHrP	PTH related protein
PTU	Propylthiouracil

PZ	Proliferative zone
qBSE-SEM	Quantitative backscattered electron scanning electron microscopy
RANK	Receptor activator of nuclear factor-κB
RANKL	Receptor activator of nuclear factor-κB
RF	Relative frequency
ROS	Reactive oxidative stress
rT3	3,3',5'-triiodothyronine
RTH	Resistance to thyroid hormone
Runx2	Runt related transcription factor 2
RXR	Retinoid X receptor
SEM	Standard error of the mean
SHBG	Sex-hormone-binding globulin
SIBLING	Small integrin-binding ligand, N-linked glycoprotein
SMI	Structure module index
SMRT	Silencing mediator for retinoid and thyroid receptors
SNS	Sympathetic nervous system
SRC1	Steroid receptor coactivator-1
STAT	Signal transducer and activator of transcription
T2	3,3'-dideothyronine
T3	3,5,3'-L-tri-iodothyronine
T4	Thyroxine
Tb.N	Trabecular number
Tb.Sp	Trabecular spacing

Tb.Th	Trabecular thickness
Tcf/Lef	T-cell factor/lymphoid enhancer binding factor
Tg	Thyroglobulin
TGB	Thyroxine binding globulin
TGF	Transforming growth factor
TH	Thyroid hormone
THRA/Thra	Human/Mouse thyroid hormone receptor α gene
THRB/Thrb	Human/Mouse thyroid hormone receptor β gene
TMB	3,3',5,5'-Tetramethylbenzidine
TNAP	Tissue nonspecific alkaline phosphatase
TNF(R)	Tumour necrosis factor (receptor)
TPO	Thyroid peroxidase
TR	Thyroid hormone receptor
TRAF	TNF receptor associated factor
TRAF6	TNF receptor-associated factor 6
TRAP	Tartrate resistant acid phosphatase
TRE	Thyroid response element
TRH	Thyrotrophin releasing hormone
TSH	Thyroid stimulating hormone
TSHR	Thyroid stimulating hormone receptor
TTR	Transthyretin
TV	Tissue Volume
WT	Wild type

Declaration of Originality and Copyright Declaration

I declare that the experiments and data presented in this thesis, to the best of my knowledge, were undertaken, collected, analysed and presented by me, unless otherwise acknowledged.

This work contains previously unpublished novel data and provides an original contribution to the knowledge of the scientific fields of thyroid and bone biology.

The copyright of this thesis rests with the author and is made available under a Creative Commons Attribution Non-Commercial No Derivatives licence. Researchers are free to copy, distribute or transmit the thesis on the condition that they attribute it, that they do not use it for commercial purposes and that they do not alter, transform or build upon it. For any reuse or redistribution, researchers must make clear to others the licence terms of this work.

A handwritten signature in black ink that reads "Moira Cheung". The signature is written in a cursive, flowing style.

Moira Shang-Mei Cheung

London, 2014

Acknowledgements

I would like to thank my supervisors, Professor Graham Williams and Professor Duncan Bassett, for their help and scientific mentorship during my time in the laboratory. I have the utmost regard for their scientific abilities and am grateful that they allowed me the freedom to juggle family commitments and work without ever questioning my dedication to my studies.

I would like to acknowledge the Medical Research Council for funding my studies.

I would also like to thank Professor Alan Boyde for assisting me with confocal microscopy and electron microscopy and Maureen Arora for her help with sample preparation for confocal microscopy and BSE-SEM imaging. Alan and Mo, as well as sharing their considerable scientific expertise, always extended their welcome to me and I thoroughly enjoyed my time spent working with them.

I am grateful to Holly Evans who assisted with generating micro CT data and Charlotte Combs who taught me ovariectomy and helped with animal husbandry of TR β ^{-/-} mice. I would also like to thank Dr Mahrokh Nohadani who assisted with the embedding and sectioning of decalcified bones.

I would like to thank the other members of the laboratory who have supported me technically, scientifically and with their friendship. These include Dr Nicolas Bernstein, Dr Charlotte Combs, Dr Thomas Galliford, Dr Apostolos Gogakos, Rebecca Hernandez, Dr John Logan, Jonathan Nicholls and Dr Julian Waung.

I would like to acknowledge and thank my mentors, Dr Jeremy Allgrove, Professor Francis Glorieux, Professor Frank Rauch and Professor Martin Savage who have encouraged and inspired me to pursue a career in bone biology.

I am indebted to my parents and friends for many years of support, prayers and love. I would especially like to thank my mother-in-law, who cared for both my baby boys after my maternity leave, whilst I was studying for this PhD.

Most importantly, I would like to thank my husband, Justin, and children, Naomi, Joseph and Nathaniel for their love, patience and sacrifice.

The Thesis

Characterisation of Oestrogen and Thyroid Hormone Interactions in the Regulation of Bone Mass

Rationale for Investigation

Osteoporosis is a worldwide public health priority that costs €32 billion per annum in Europe alone. Oestrogen deficiency is the major determinant of postmenopausal bone loss and thyrotoxicosis is an established risk factor for osteoporosis. Clinical observations, epidemiological data, experimental evidence from mutant mice and our current understanding of the actions of oestrogen and T3 in bone cells, all support the concept that optimal adult bone mass and strength are maintained by balanced and opposing actions of oestrogen and thyroid hormones.

Hypothesis

I hypothesise that at the menopause, the actions of thyroid hormone on bone are unopposed following oestrogen withdrawal, leading to accelerated bone loss and fracture.

To address this hypothesis, I will determine the skeletal responses to ovariectomy in adult TR α ^{0/0} and TR β ^{-/-} mice which have been maintained euthyroid, hypothyroid and hyperthyroid.

Aims

In order to investigate this hypothesis in a step by step and comprehensive manner, I aim to:

1. Compare the bone phenotypes of TR α ^{0/0} and TR β ^{-/-} mice to hypothyroid and hyperthyroid wild type mice.
2. Establish the effects of altered thyroid status on TR α ^{0/0} and TR β ^{-/-} mice.
3. Characterise the effects of ovariectomy or sham operation on the bone phenotype of thyroid status manipulated wild type, TR α ^{0/0} and TR β ^{-/-} mice.

Chapter 1

Introduction

1 INTRODUCTION

1.1 BACKGROUND

Osteoporotic fractures are a substantial public health burden, costing the NHS approximately £2.1 billion per year and increasing as the ageing population increases (Dennison and Cooper, 2011). Oestrogen deficiency is the leading cause of postmenopausal bone loss and thyrotoxicosis is an established risk factor for osteoporosis (Bassett et al., 2007a). The prevalence of postmenopausal osteoporosis increases with age and the lifetime incidence of fracture for a 50 year old woman in the UK is 40% (Sambrook and Cooper, 2006). Although oestrogen withdrawal is widely recognised as the leading cause of osteoporosis, the contribution of excess thyroid hormone is also substantial. More than 3% of 50 year old women receive thyroid hormone therapy, and over-treatment is common within the population (Parle et al., 1993), suggesting that thyroid abnormalities are underestimated contributors to the osteoporosis burden. Understanding the regulation of bone mass is important for the prevention and treatment of osteoporosis. Oestrogen and thyroid hormones have opposing actions on the skeleton, suggesting that optimal maintenance of bone mass is regulated by the balance of anabolic actions of oestrogen and catabolic actions of thyroid hormone. The experiments in this thesis examine the role and interactions of oestrogen and thyroid hormone in the regulation of bone mass.

1.2 BONE PHYSIOLOGY

To understand thyroid hormone and oestrogen action on the skeleton, it is important to have an understanding of normal bone physiology. The skeleton provides mechanical strength and structure, protects vital organs and acts as a metabolic and endocrine organ. Whilst being strong, it must also be light to enable locomotion. In achieving all these functions, it is a dynamic, adaptive organ, able to respond to external and internal stimuli.

1.2.1 STRUCTURE OF BONE

Structurally, bones can be categorised into two main groups which have distinct developmental derivations: flat bones such as the ileum, skull and scapula and long bones such as the femur, tibia and humerus. Some bones such as the vertebrae and small bones of the hands and feet do not fall into these distinct categories but have features of both.

The gross anatomical structure of long bones can be subdivided into three main sections, as illustrated in Figure 1.1. The diaphysis is the cylindrical section in the centre of the long bone, is composed of compact bone called the cortex and splays at each end to form the metaphysis. The metaphysis commences at the growth plate, under which new bone is being accrued, and tapers down to the diaphysis. At the ends of the long bone, beyond the growth plates, are the epiphyses. The external surface of the bone is enveloped by the periosteum, which during growth is a discrete entity and can be readily identified. After the cessation of growth, the periosteum becomes a thin layer which lines the external bone. The internal surface of the bone, the endosteal surface, includes the inside of the cortex (intramedullary cortical surface) and the trabecular surfaces. The majority of the diaphysis of the long bone is filled with marrow, with little calcified bone, but directly under the growth plate and into the metaphysis, is found a lattice of trabecular or cancellous bone, which supports the growth plate (Baron, 1999).

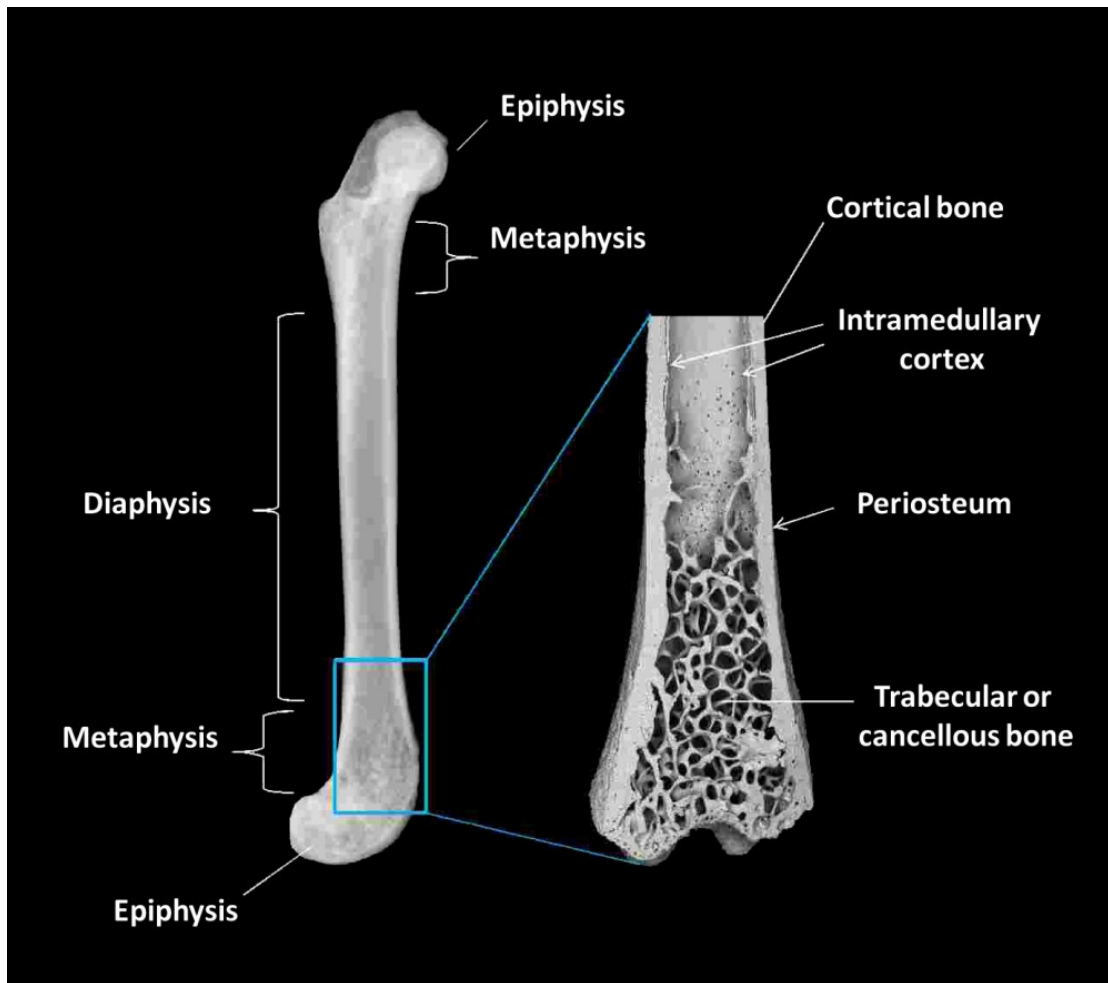


Figure 1.1 Structure of long bones

Backscattered electron-scanning electron microscopy (BSE-SEM) image of femur demonstrating the structure of long bones.

1.2.2 COMPOSITION OF BONE

1.2.2.1 BONE CELLS

1.2.2.1.1 Bone-forming osteoblasts

Osteoblasts are cuboidal, matrix secreting cells found on bone surfaces. They are derived from mesenchymal stem cells (MSCs). MSCs can differentiate into osteoblasts, myocytes, chondrocytes and adipocytes (see Figure 1.2).

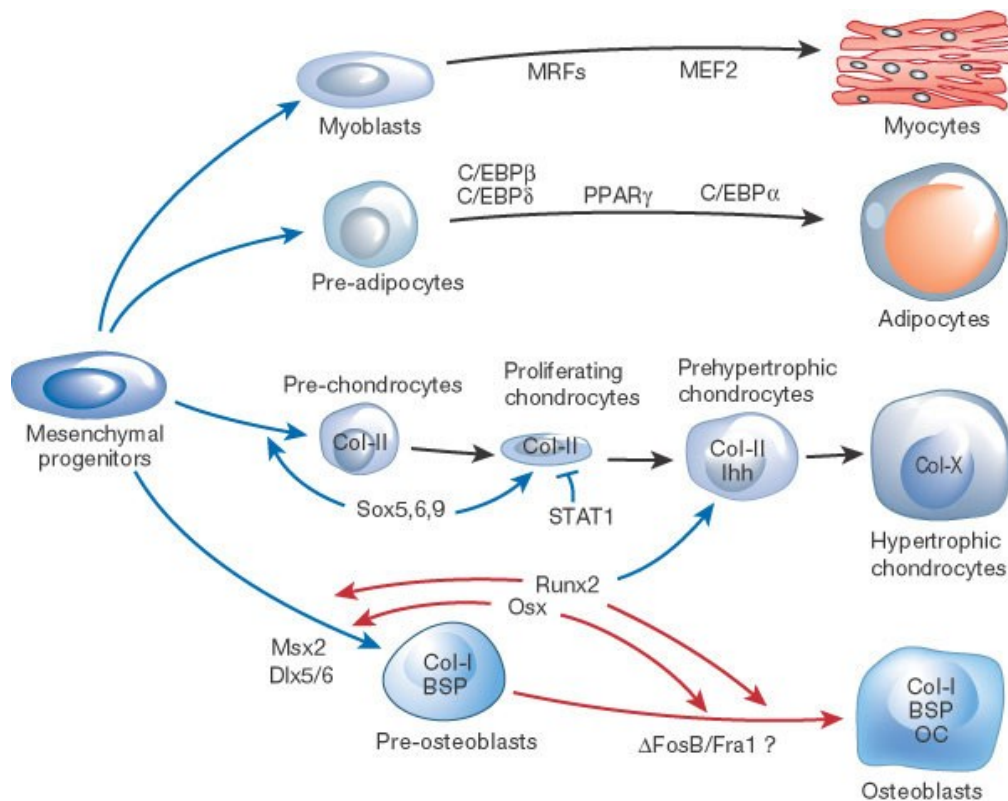


Figure 1.2 Mesenchymal progenitor differentiation

Figure reproduced from Harada et al 2003 with permission (Harada and Rodan, 2003). Mesenchymal progenitor differentiation into osteoblasts, chondrocytes, adipocytes and myocytes is tightly regulated.

Differentiation of osteoblasts requires Runx 2 (runt-related transcription factor 2), which is also involved in chondrocyte maturation. Downstream from Runx 2, osterix (Osx) is also essential for osteoblast maturation, after which osteoblasts express specific markers such as osteocalcin (OC), bone sialoprotein (BSP) and collagen I (Col-1).

Differentiation of mesenchymal progenitor cells into (i) myocytes is under the control of MRFs (myogenic regulatory factors) and MEF2 (myocytes enhancer factor 2), (ii) adipocytes is under the control of C/EBP α , β and δ (CCAAT-enhancer-binding protein) and PPAR γ (peroxisome proliferator activated receptor γ) and (iii) chondrocytes is under the control of Sox 5, 6, and 9 and STAT1 (signal transducers and activator of transcription 1) and express collagen X (Col-X).

Differentiation of mesenchymal progenitors into different cell types is tightly regulated by transcription factors and local growth factors (see Figure 1.2). Mesenchymal progenitor cells differentiate initially into preosteoblasts (which can be identified by positive staining for alkaline phosphatase) but are unable to secrete mineral matrix. Preosteoblasts mature into osteoblasts. Osteoblasts can be identified as cuboidal cells, found in clusters on the bone surface, stain strongly for ALP and secrete mineral matrix. Osteoblasts secrete osteoid, containing type I collagen and noncollagenous proteins, such as osteocalcin and ALP. These are important in the mineralisation of bone matrix. Approximately 50-70% of osteoblasts undergo apoptosis with the remaining cells differentiating into osteocytes or bone lining cells (Bonewald, 2011).

In addition to the production of new bone, osteoblasts secrete factors which are important in the regulation of mineralisation and osteoclast formation. ALP is expressed by osteoblasts and is an important enzyme in the regulation of the mineralisation of bone (addressed in more detail in the section on bone mineralisation) as well as being commonly used as a marker of osteoblast activity. Osteoblasts also express free and cell surface receptor-activator of nuclear factor κ B ligand (RANKL), which is essential for osteoclast maturation and express osteoprotegerin (OPG), which is a decoy receptor that inhibits RANKL binding to receptor-activator of nuclear factor κ B (RANK) (this is addressed in more detail in the section on osteoclasts) (Takahashi et al., 1988). By changing the ratio of RANKL to OPG expressed, osteoblasts are able to regulate osteoclast formation.

Transcription and local growth factors important in osteoblasts

Commitment into the osteoblast lineage occurs under the influence of transcription factors. Two important transcription factors are runt-related transcription factor (Runx 2) and osterix.

Runx 2 appears early on in the progenitor cells and is expressed until osteoblast maturity. It is required for osteoblast differentiation and maturation and Runx 2 knockout mice have early arrested skeletal development with little cartilage or bone. Due to its pivotal role in osteoblast function, Runx 2 is tightly regulated by co-repressors (Westendorf, 2006). Runx 2 stimulates expression of RANKL and M-CSF (Geoffroy et al., 2002, Enomoto et al., 2003, Maruyama et al., 2007), promoting osteoblast driven osteoclastogenesis.

Osterix is expressed by mature osteoblasts, is essential for osteoblast differentiation and regulates the expression of a number of osteoblast related genes, including type 1 Collagen. Osterix knockout mice, similar to Runx 2 knockout mice, lack osteoblasts and have absent embryonic bone

development. Osterix is expressed downstream of Runx 2 and osterix knockout mice express normal levels of Runx 2 and they do not have defects in hypertrophic chondrocytes (Peng et al., 2013).

The number and function of osteoblasts are regulated by a number of extracellular signalling proteins and growth factors. Although there are many signalling pathways which have been identified, there are a few factors that are of particular importance in osteoblasts: bone morphogenic proteins (BMPs), Fibroblast growth factors (FGFs) and Wnts (Miraoui and Marie, 2010).

BMPs were first named because of their ability to induce bone formation and are a group of cytokine signalling molecules belonging to the transforming growth factor (TGF)- β superfamily, which bind to two classes of cell surface receptors, type I and type II. BMPs are important in prenatal bone formation. Binding of BMPs to their receptors activates SMAD and Ras to mitogen activated protein kinase (MAPK) signalling pathways. SMAD 1, 5 and 8 in complex with SMAD 4, translocate into the nucleus and interact with a range of transcription factors such as Runx 2. Clinically, gain of function mutation in BMP type I receptor, ACVR1, results in fibrodysplasia ossificans progressiva where there is dysregulation of bone deposition with extraskeletal ossification (Pignolo et al., 2011).

FGFs and FGF receptors (FGFR) are present in the mesenchyme, chondrocytes and osteoblasts. They are important for cell proliferation, differentiation and apoptosis. Ligand, binding to the extracellular receptor domain, results in dimerisation and autophosphorylation of tyrosine residues in the cytoplasmic domains of the receptor. This then activates downstream signalling cascades via one of three main pathways: phospholipase C γ (PLC γ), signal transducers and activators of transcription (STATs) and MAPK. Downstream signalling pathways may include (Extra cellular signal regulated kinase) ERK1/2, p38 MAPK, Ras-independent phosphoinositide 3-kinase/Akt and Wnt. Many of the signalling pathways activated by FGFs result in an increased expression of genes involved in osteogenesis, such as Runx 2. FGF signalling has been found to be important in the development of bone metastases associated with prostate cancers (Hideshima et al., 2001). Genetic mutations in FGFR result in skeletal dysplasias such as achondroplasia (activating FGFR3 mutation) and craniosynostosis (mutation in FGFR1 or 2) (Miraoui and Marie, 2010).

The canonical Wnt pathway is activated by the binding of Wnt to a cell-surface co-receptor comprising Frizzled (Frz) and a low-density lipoprotein receptor-related protein (Lrp5/6). Wnt inhibits a complex that includes axin, glycogen synthase kinase 3 β (GSK3 β) and adenomatous polyposis coli protein (APC). When Wnt is absent, this complex phosphorylates β -catenin and promotes its degradation by the proteasome. After Wnt binding, axin/GSK3 β /APC is inhibited and β -catenin translocates to the nucleus where it acts with Tcf/Lef to promote gene transcription

(Johnson and Kamel, 2007). The pathway is subject to feedback inhibition - secreted Frz-related proteins act as decoy Wnt receptors, whilst Dickkopf (Dkk) inactivates signalling from Lrp co-receptors (Glass and Karsenty, 2007, Hartmann, 2006). Sclerostin, produced by osteocytes, binds to Lrp5/6 and is an inhibitor of Wnt signalling. Wnt stimulates osteoblast proliferation and inhibits apoptosis *in vivo*, and β -catenin is required for terminal osteoblast differentiation (Day et al., 2005, Hens et al., 2005, Ducky et al., 2000). The canonical pathway also stimulates expression of OPG (Holmen et al., 2005), a decoy receptor for RANKL that inhibits osteoclast differentiation (Glass and Karsenty, 2007). Wnt inhibition therefore leads to reduced β -catenin activity and high bone turnover osteoporosis (Hartmann, 2006). Gain of function mutations in LRP5 cause high bone mass whilst loss of function mutations cause osteoporosis pseudoglioma syndrome.

In summary, osteoblasts are the cells responsible for the production of new bone. They also play important roles in the regulation of both mineralisation and osteoclast function.

1.2.2.1.2 Bone resorbing osteoclasts

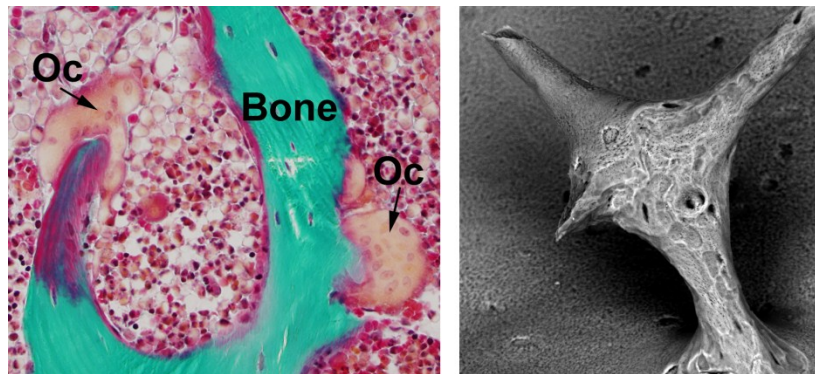


Figure 1.3 Histology image of osteoclast (Oc) resorbing bone and BSE-SEM image of resorbed bone surface.

Osteoclasts are multinucleated cells derived from the monocyte macrophage lineage (Krause, 2008). They are specialised cells that adhere to the mineral surface and secrete acid and enzymes into the extracellular space to resorb mineralised matrix (Figure 1.3). They are found both on the endosteal surface and at the metaphyseal periosteum. Osteoclasts migrate from the bone marrow and become located on the bone surface. They anchor themselves onto the bone surface by foot-like processes known as podosomes and migrate via membrane protrusions called lamellipodia. During the migration phase, the osteoclasts have flattened structures; however, at the resorption site, the cytoskeleton becomes polarised and dome shaped. The cytoplasmic actin becomes organised into a circular structure known as the actin ring. An area of bone, known as the sealing zone, is isolated via attachment of the actin ring by integrin $\alpha\beta3$, in preparation for acidic resorption (see Figure 1.4). The membrane of the osteoclast within the sealing ring, known as the ruffled border, is where HCl and acidic proteases such as cathepsin K and matrix metalloproteinases (MMP) are secreted. HCl breaks down the mineral component of bone (hydroxyapatite) into Ca^+ , HPO_4^{2-} and H_2O . This exposes the organic matrix, composed of collagen and other proteins, which can then be degraded by proteases. Degradation products are exocytosed into the surrounding extracellular matrix (Boyle et al., 2003).

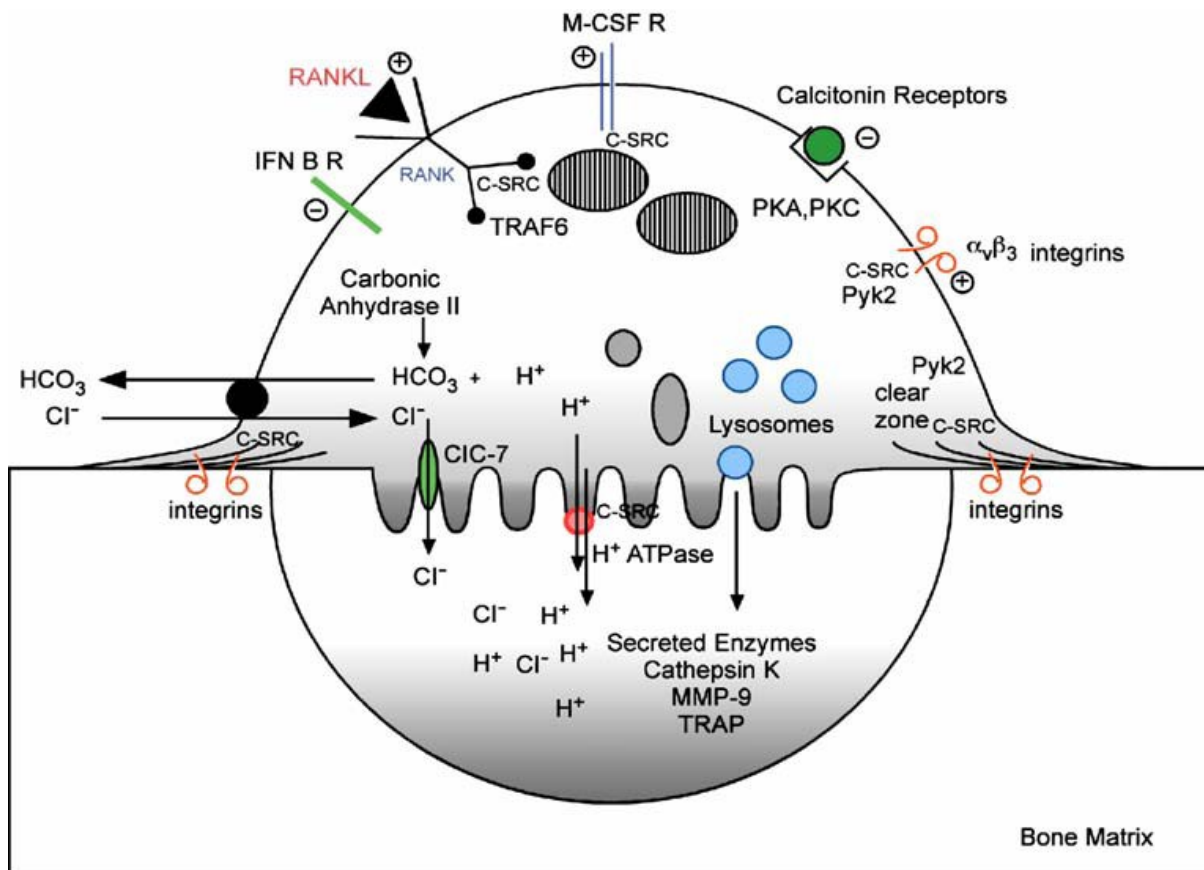


Figure 1.4 Diagram of resorbing osteoclast

Figure reproduced with permission from Bruzzaniti A et al. 2006 (Bruzzaniti and Baron, 2006).

Osteoclasts attach to the bone surface via integrins, creating a sealing zone around the ruffled border. Osteoclast maturation is stimulated by binding of RANKL and M-CSF to their receptors on the cell surface. Osteoclast differentiation is inhibited by binding of calcitonin ligand to its receptors. Carbonic anhydrase converts CO₂ to H⁺ and HCO₃⁻. Chloride enters and bicarbonate leaves the cell via the chloride-bicarbonate exchanger. Hydrochloric acid and acidic proteases are secreted onto the surface of the bone where resorption takes place.

PKA - Protein kinase A, PKC - Protein kinase C, TRAP - Tartrate resistant acid phosphatase, MMP-9 - Matrix metalloproteinase 9

Transcription and local growth factors important in osteoclasts

Osteoclasts are formed by the fusion of macrophage precursors. Commitment to the osteoclast lineage requires two key cytokines - RANKL and M-CSF.

RANK-RANKL-OPG: In 1998, RANK, a member of the tumour necrosis factor superfamily (also known as tumour necrosis factor ligand superfamily member 11), was shown to be essential for osteoclast formation. RANK is a transmembrane molecule found on the surface of osteoclasts and their precursors. Binding of RANK by RANKL results in the commitment of monocytes to the osteoclast lineage and maturation of the osteoclast. RANKL is expressed by many cells in the bone environment, including osteocytes, osteoblasts, T-cells, growth plate chondrocytes and endothelial cells. It can be expressed on cell surfaces or excreted extracellularly. Osteoclasts at the growth plate derive their source of RANKL primarily from chondrocytes, whilst osteoclasts on cancellous bone do so primarily from osteocytes (Nakashima et al., 2011). As a result, chondrocyte and osteocyte defects can adversely affect osteoclastic resorption.

Activation of RANK transduces signals via the TNF receptor-associated factor (TRAF) family of proteins which leads to activation of a cascade of signalling pathways involving NF- κ B, MAPK and phosphoinositide 3 kinase (PI3K), resulting in osteoclast proliferation, cytoskeletal re-organisation, differentiation and cell survival. The binding of RANK to RANKL is inhibited by OPG, a soluble decoy receptor secreted by osteoblasts, which competes with RANKL for the binding to RANK.

The key role of RANKL is highlighted by human mutations in the *TNFSF11* gene (encoding RANKL) which results in autosomal recessive osteopetrosis. This is often a lethal disease characterised by a depletion of osteoclasts and an arrest of skeletal modelling and remodelling. Osteopetrotic *Rankl*^{-/-} mice, treated with RANKL have an improved bone phenotype (Lo Iacono et al., 2012). In humans, autoantibodies to OPG have been reported to result in osteoporosis (Riches et al., 2009), whilst conversely, monoclonal antibodies against RANKL are currently used in the treatment of osteoporosis (Silva-Fernandez et al., 2013).

M-CSF: M-CSF is produced by osteoblasts and stromal cells. M-CSF binds to its receptor colony-stimulating factor-1 receptor (c-fms) in early osteoclast precursors, promoting survival, proliferation and differentiation. Signalling via M-CSF occurs through multiple pathways but experiments in primary macrophages (Ross, 2006) indicate that ERK1/2 and PI3K are the key mediators of signalling. PI3K is important in regulating cell proliferation via the GSK3 β and Forkhead box (FOXO) family of transcription factors. Mice lacking M-CSF or c-fms have an osteopetrotic phenotype and in humans,

mutations in M-CSF can be found in patients with myelodysplastic syndromes and myeloid leukaemia (Rauner et al., 2013).

In summary, osteoclasts are the cells responsible for bone resorption. They respond to signals from osteoblasts, osteocytes and the surrounding bone marrow environment, to direct the timing and direction of bone removal.

1.2.2.1.3 Bone-orchestrating osteocytes

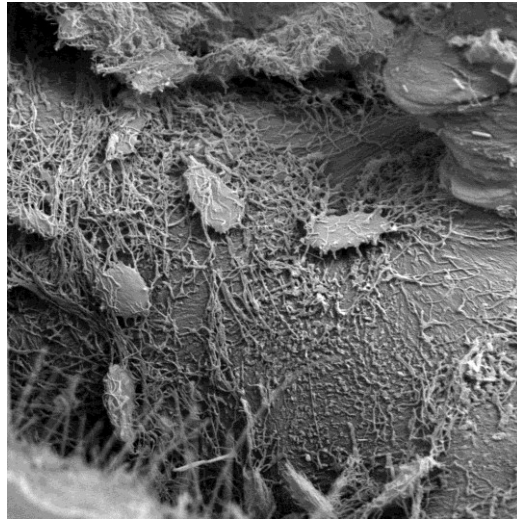


Figure 1.5 Osteocyte lacunae and dendritic processes in cortical bone

BSE-SEM image of acid-etched plastic-embedded murine cortical bone. The dendritic processes are clearly identified, as are the osteocytic lacunae.

Osteocytes make up 90-95% of bone cells and are derived from the MSC lineage via osteoblasts which have become entombed in bone. They differ from osteoblasts morphologically by having long dendritic processes which contact cells on the surface of bone and other embedded osteocytes. They become polarised towards the direction of the mineralising surface.

Osteocytes respond to mechanical strain and send signals through dendritic processes to alter resorption or formation. These signals can negatively regulate osteoblast function and/or activate osteoclastogenesis (Turner and Pavalko, 1998). Osteocytes are the primary source of RANKL for osteoclasts in bone remodelling (Nakashima et al., Xiong et al., 2011). They also highly express DKK1 and sclerostin, which are negative regulators of the Wnt pathway (Moriishi et al., 2012). Mechanical loading reduces sclerostin expression (Robling et al., 2008).

Osteocytic apoptosis occurs with mechanical damage, such as fracture or microcracks. Hypoxia, oestrogen withdrawal, immobilisation and glucocorticoid treatment also promote osteocyte apoptosis (Weinstein et al., 2000, Dodd et al., 1999, Tomkinson et al., 1997, Emerton et al., 2010).

Apoptosed osteocytes result in the release of chemotactic factors (such as RANKL) which are involved in recruiting osteoclasts and initiating resorption.

More recently, it has become clear that osteocytes are important regulators of bone mineralisation and phosphate metabolism. Osteocytes highly express molecules phosphate-regulating neutral endopeptidase, X-linked (PHEX), FGF23 and DMP1, all of which are important in phosphate regulation.

Mutations in osteocyte specific DMP1 result in autosomal recessive hypophosphatemic rickets, patients affected with PHEX mutations have X linked dominant hypophosphatemic rickets and mutations in FGF23 result in autosomal dominant hypophosphatemic rickets (Bergwitz and Juppner, 2010).

In summary, osteocytes are important regulators of bone homeostasis. They are involved in coordinating the activity of osteoclasts and osteoblasts through the release of factors such as RANKL and sclerostin. Osteocytes are also key cells involved in phosphate regulation and, subsequently, bone mineralisation.

1.2.2.1.4 Other cells

Within the bone marrow niche, bone cells are in close proximity to immune cells such as lymphocytes (T-cells and B-cells), granulocytes, monocytes/macrophages, mast cells and megakaryocytes/platelets. Some of these cells have also been shown to modulate the skeleton via cross talk with bone cells.

T-Cells: T-cells express RANKL and so are able to activate RANK on osteoclast precursors. T-cells also produce cytokines such as TNF- α and IL-17, which upregulate RANKL and MMPs in osteoblasts. In contrast, T-helper cells can produce IFN- γ and IL-4, both of which suppress osteoclastogenesis via direct action on osteoclast precursors (Gao et al., 2007b, Bendixen et al., 2001). T-cell deficient mice demonstrate resistance to ovariectomy induced bone loss and further studies suggested that T-cell derived TNF- α is important in bone loss, secondary to ovariectomy (Pacifci, 2007). Consistent with these findings, women with postmenopausal osteoporosis have a greater density of membranous RANKL in marrow T-cells, with greater activation of T-cells. These findings suggests that T-cells play an important role in postmenopausal osteoporosis (Eghbali-Fatourehchi et al., 2003).

Osteomacs: Osteomacs have been relatively recently described and is a term used for resident tissue macrophages which lie in close proximity to periosteal or endosteal surfaces (Kular et al., 2012) (Chang et al., 2008). Osteomacs, often in association with bone lining cells, form a canopy over mature osteoblasts in bone modelling and also above the bone remodelling unit (BRU) (see later section on BRU). They are thought to help regulate bone mineralisation as depletion of osteomacs results in decreased mineralisation. Osteomacs secrete cytokines TGF β and Ephrin B2, which activate osteoclasts and this is potentially one mechanism by which osteomacs help regulate bone remodelling (Pettit et al., 2008).

1.2.2.2 BONE MATRIX AND MINERALISATION

1.2.2.2.1 Bone matrix deposition

Bone is formed when osteoblasts secrete osteoid, which subsequently becomes mineralised by active (primary ossification) and passive (secondary ossification) mechanisms. Osteoid is an organic matrix composed of type I collagen, SIBLING (small integrin-binding ligand, N-linked glycoprotein) proteins (such as osteopontin and bone sialoprotein) and osteocalcin. Type I collagen is a triple helix molecule consisting of two α 1 chains and one α 2 chain.

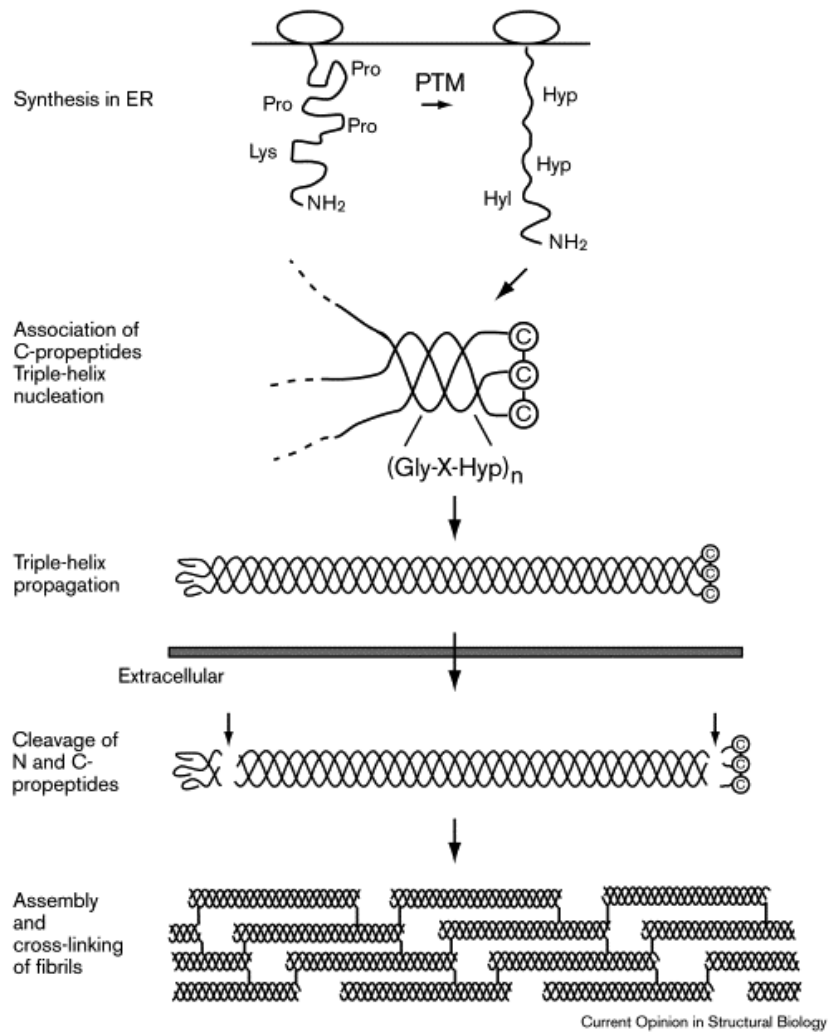


Figure 1.6 Synthesis and structural organisation of type 1 collagen

Figure reproduced with permission Baum, J 1999 (Baum and Brodsky, 1999). Type I collagen molecules are synthesised in the endoplasmic reticulum (ER) of osteoblasts, and after post translational modification (PTM), a triple helix, procollagen, is formed. Procollagen is excreted from the cell, after which the N and C terminals are cleaved before assembly into collagen strands with cross linking of fibrils. Hyp-Hydroxyproline; Gly-Glycine; Pro-Proline; Hyl-Hydroxylysine, Lys- Lysyl.

Type I collagen is initially formed at the endoplasmic reticulum as procollagen, which then undergoes several post translational modifications: hydroxylation of prolyl and lysyl residues, glycosylation of hydroxylysyl, terminal propeptide phosphorylation/glycosylation and formation of covalent cross links between the three strands. After post translational modification, a procollagen triple helix is formed and secreted into the extracellular space. Cleavage of the C and N propeptide terminals of procollagen are removed by proteases, after which the collagen molecules aggregate and cross link to other collagen fibrils (see Figure 1.6). The molecules of collagen are arranged in sheets of unidirectional fibres with each subsequent sheet at a different angle. This allows tight packing of the collagen and also gives the bone tensile strength. These layers give the bone a lamellar structure (see Figure 1.7).

1.2.2.2 Matrix mineralisation

The mineral component of bone, hydroxylapatite ($\text{Ca}_{10}(\text{PO}_4)_5(\text{OH})_2$), is deposited into the spaces in between the organic bone matrix. Mineralisation of matrix is tightly regulated. Osteoblasts maintain a high extracellular concentration of calcium and phosphate via calcium and phosphate pumps, so that the matrix is primed to incorporate mineral. Mineralisation is, however, inhibited by the presence of inorganic pyrophosphate (POP) and it is the ratio of phosphate and POP which regulates the rate of mineralisation. Matrix vesicles bud off the cell membranes of osteoblasts and are released into the premineralised matrix. These vesicles are rich in enzymes such as Nucleotide pyrophosphatase phosphodiesterase1 (NPP1) and tissue nonspecific alkaline phosphatase (TNAP). NPP1 increases extracellular POP concentration and TNAP decreases POP whilst increasing phosphate concentration. The regulation of mineralisation is tightly controlled as excessive mineralisation results in stiff, brittle bones (seen in patients with osteopetrosis) and insufficient mineralisation results in soft, malleable bones (seen in patients with hypophosphataemic rickets).

Mineralisation of matrix in humans initially occurs between 5-10 days after matrix deposition. This is termed 'primary mineralisation'. After this, a slow 'secondary mineralisation' phase takes place which may last up to 30 months and involves up to 50% increased mineral deposition with an increase and augmentation of crystal size (Boivin and Meunier, 2002). Mineral density distribution (also termed material density) can be determined by quantitative backscattered electron microscopy (qBSE-SEM) (Roschger et al., 1998). The degree of bone mineralisation can give some indication of the bone remodelling rate (Boivin and Meunier, 2002), with high turnover bone having a low mineral density distribution and low turnover bone having a high mineral density on qBSE-SEM.

1.2.3 EMBRYONIC DERIVATION OF BONE

Embryonically, the skeleton is derived from mesenchymal progenitor cells which aggregate at the site of the future skeleton. Skeletal patterning is tightly controlled by temporo-spatial expression of genes such as those in the canonical Wnt and Notch pathways (Dequeant et al., 2006). Ossification occurs by two major mechanisms - the flat bones of the body are formed by intramembranous ossification and the long bones are formed by endochondral ossification.

1.2.3.1 INTRAMEMBRANOUS OSSIFICATION

The aggregation of MSCs, known as the ossification centre, becomes highly vascularised and MSCs differentiate into preosteoblasts and then osteoblasts. Osteoblasts secrete an organic mineral matrix which mineralises to form an irregular and disorganised type of bone known as woven bone. Woven bone is then removed and replaced by a highly organised structure known as lamellar bone. Flat bones formed by this mechanism include skull bones, the scapula, mandible and the ilium (Baron, 1999).

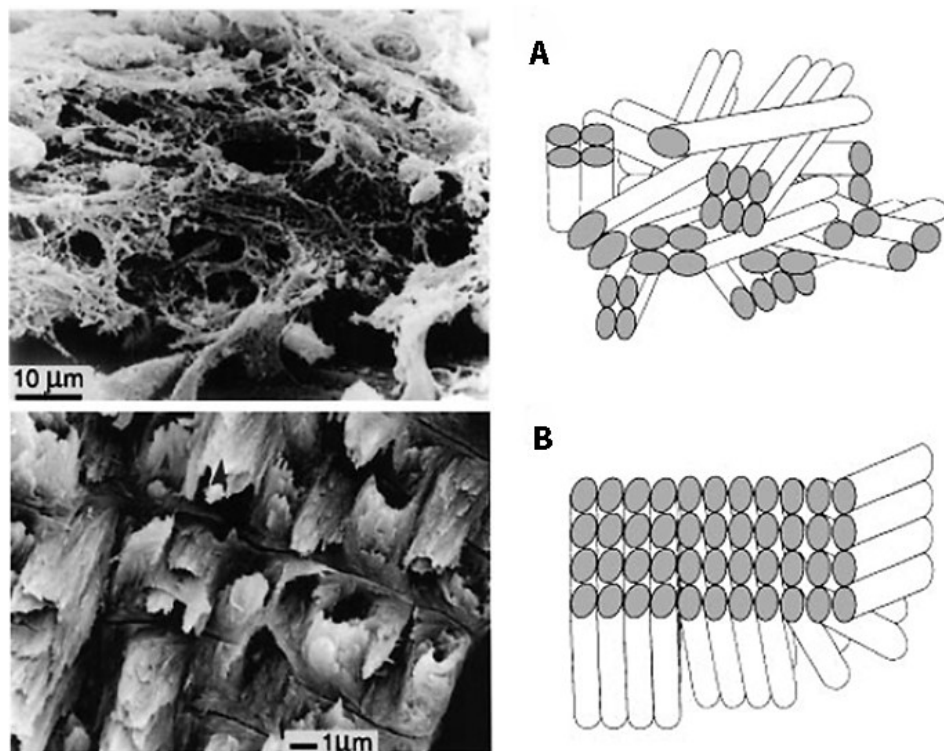


Figure 1.7 Collagen fibrils in woven bone and lamellar bone

Mineralised collagen fibrils are arranged in a random manner in woven bone (A). Woven bone is resorbed and replaced by fibrils arranged in parallel sheets known as lamellar bone (B). Adapted with permission from Weiner S 1998 (Weiner and Wagner, 1998).

1.2.3.2 ENDOCHONDRAL OSSIFICATION

The majority of long bones in the body are formed by endochondral ossification. Embryonic MSCs condense and form a cartilage template (see Figure 1.8). The MSCs differentiate into chondrocytes, which proliferate, release extra cellular matrix (ECM) factors and finally hypertrophy and apoptose.

Ossification of the long bone begins in the middle of the cartilaginous template, where invading blood vessels, and bone marrow containing bone resorbing osteoclasts and bone forming osteoblasts, remove cartilaginous ECM and deposit new bone. From the centre, new bone formation proceeds distally and expands to the distal ends of the cartilaginous template (see Figure 1.8).

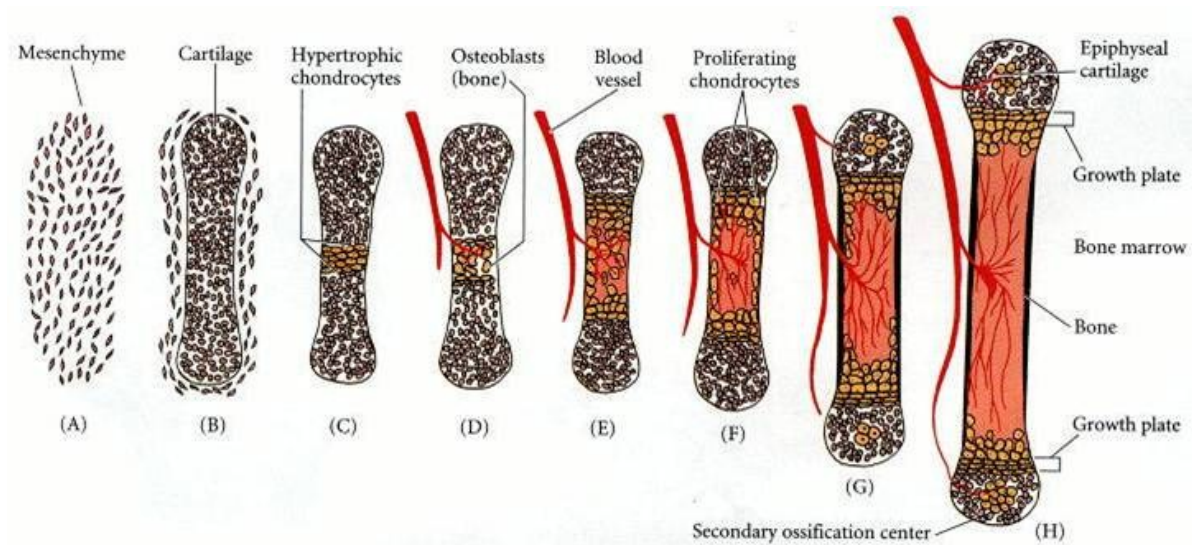


Figure 1.8 Diagram showing the different steps in endochondral ossification.

See text for details

Adapted with permission from Gilbert 2006 (Gilbert, 2006).

At a later stage of development, a secondary centre of ossification commences at the distal ends of the long bones, forming the epiphysis. Where the primary and secondary ossification centres meet, the cartilaginous growth plate remains and is active until the cessation of growth. New bone is formed under the growth plate and in this manner, elongation of long bones occurs (Mackie et al., 2011).

At the epiphyseal end of the growth plate, MSCs differentiate into chondrocytes. Growth plate chondrocytes have a tightly regulated spatial arrangement of columns that lie parallel to the longitudinal axis of the bone (see Figure 1.9). In the distal resting zone, the cells are small and have a low rate of proliferation and matrix secretion. When the chondrocytes enter the proliferative zone (PZ), the cells become ordered into columns, proliferate profusely and express *ColII*. The chondrocytes mature and hypertrophy and express *ColX*, appearing large and round before undergoing apoptosis (Figure 1.11). Before entering the hypertrophic zone, the prehypertrophic chondrocytes produce Indian Hedgehog protein (Ihh). This both increases chondrocyte proliferation and activates the expression of parathyroid related protein (PTHrP) in articular and periarticular chondrocytes. PTHrP, via the G-protein coupled receptor (PTH/PTHrP receptor) PPR, maintains proliferating chondrocytes in the proliferative pool, thereby inhibiting chondrocyte hypertrophy and the production of Ihh (see Figure 1.10). This negative feedback loop regulates the rate of proliferation and hypertrophy of chondrocytes and can be modified by interactions with other signalling molecules such as BMP and FGFs. BMP signalling from hypertrophic chondrocytes promotes Ihh expression and chondrocyte proliferation. Conditional knockout of *BmpRIA* and *BmpRIB* (BMP receptors) in differentiated chondrocytes leads to reduced Ihh expression and reduced chondrocyte proliferation (Kronenberg, 2003). FGFs are highly expressed in the growth plate and, of particular note; FGFR3 inhibits chondrocyte proliferation and hypertrophy through both MAPK signalling pathways and via interactions with the Ihh-PTHrP-BMP pathways. Wnt signalling pathways stimulate chondrocyte terminal differentiation (Wang et al., 2007) (Figure 1.17).

Hypertrophic chondrocytes secrete large quantities of matrix proteins and matrix vesicles. Matrix vesicles contain calcium, phosphates, hydroxyapatite and MMP, all of which function to mineralise the surrounding matrix. Following apoptosis of the chondrocytes, angiogenic factors promote the invasion of blood vessels, which bring osteoblasts and osteoclast progenitors, and the remaining calcified cartilage becomes a scaffold for new bone formation.

Chondrocytes are an important source of the cytokine receptor activator RANKL, which is essential for osteoclast formation and function in the primary spongiosum (Xiong et al., 2011).

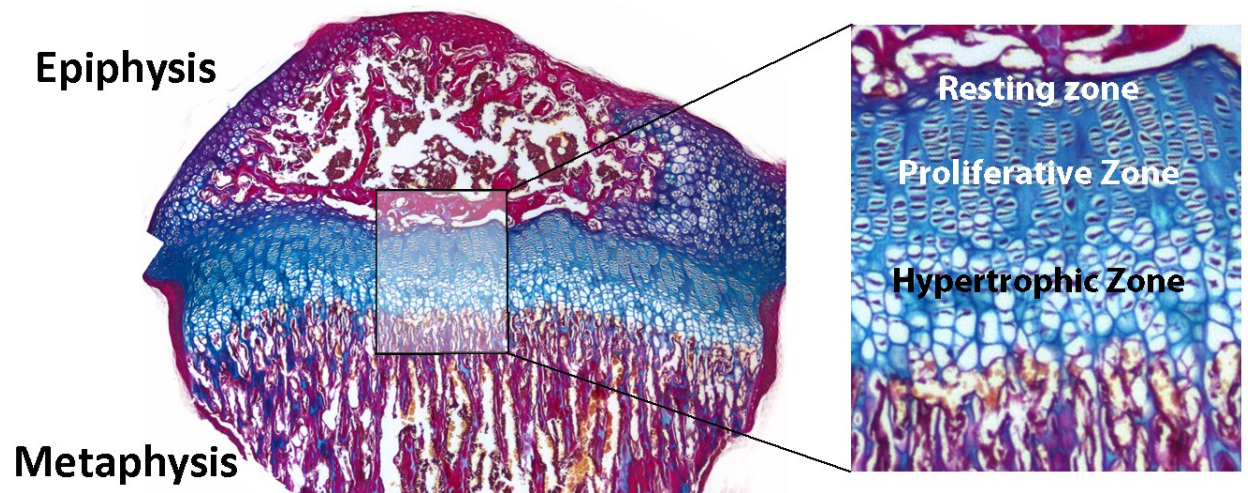


Figure 1.9 Growth plate

Image of tibial growth plate of wild type mouse stained with van Gieson (red for collagen) and alcian blue (blue for cartilage). The growth plate is found between the epiphysis and metaphysis. It consists of matrix embedded chondrocytes arranged in distinct zones. The resting zone chondrocytes are quiescent before becoming organised into columns undergoing proliferation (proliferative zone), differentiation, maturation (hypertrophic zone) and finally undergoing apoptosis.

Slide stained by Y. Liu and raw image taken Dr J. Logan

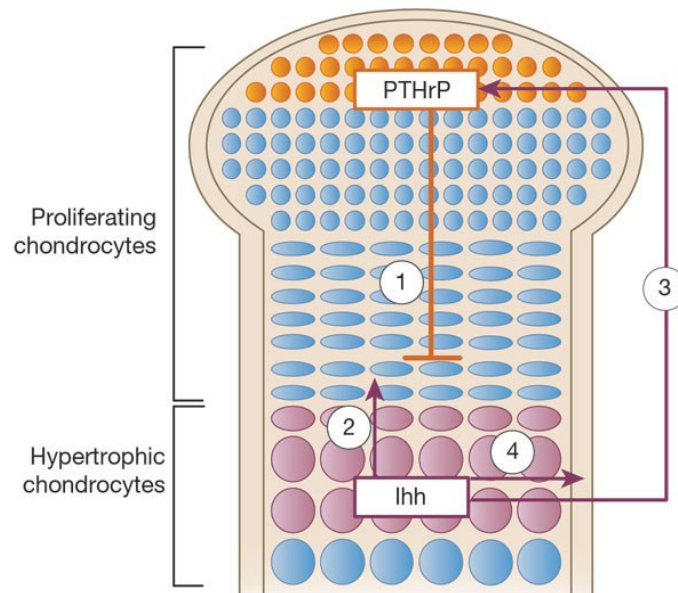


Figure 1.10 Growth plate signalling

Reproduced with permission from Kronenberg Nature 2003 (Kronenberg, 2003).

Chondrocyte proliferation and hypertrophy is regulated by parathyroid related protein (PTHrP) and Ihh. Perichondral cells at the distal end of the bone produce PTHrP, which acts via receptors on proliferating chondrocytes to keep chondrocytes in the proliferative stage (1). When the chondrocytes are far away enough from the source of PTHrP, they differentiate into hypertrophic chondrocytes, which express Ihh (2). Ihh acts to stimulate the production of PTHrP (3) and delay hypertrophy of chondrocytes. Ihh also acts to stimulate the production of osteoblasts in the perichondral cells (4).

1.2.4 REGULATION OF BONE: MODELLING AND REMODELLING

Bone deposition does not occur in a haphazard manner, instead it is directed and shaped during growth (a process known as modelling) and after cessation of growth, bone is continually renewed, replaced and repaired (a process known as remodelling).

1.2.4.1 BONE MODELLING

Long bones increase longitudinally by deposition of bone under the growth plate and increase in diameter by bone deposition under the periosteum. At the metaphysis, bone is removed on the periosteal cortical surface by bone resorbing osteoclasts, resulting in a slender diaphysis. This modelling process is termed metaphyseal inwasting and can be seen to be disrupted when inappropriate doses of osteoclast disrupting bisphosphonates are given during growth, resulting in club shaped bones and in disorders of osteoclasts, such as in osteopetrosis.

Bone is deposited under the periosteum, increasing the external circumference of the diaphysis, whilst bone is also resorbed from the intramedullary cortex. An indication of periosteal bone formation can therefore be gained by assessing the mid shaft diameter of long bones. The cortical thickness of bone results from the difference between periosteal deposition and intramedullary cortical resorption (bone removal).

Disruption of osteoclast function during development would not only result in a decrease in the amount of bone being removed by the BRU, but also in a modelling defect, resulting in club shaped bones. The diameter of the intramedullary cavity and cortical width can also give an indication of osteoclast function.

1.2.4.2 BONE REMODELLING

Bone is renewed and repaired by the BRU, which consists of coordinated teams of osteoclasts and osteoblasts. About 10% of the human adult skeleton is replaced per year with millions of BRUs active at any one time.

The balance of resorption versus deposition determines bone mass and thus is important in bone strength. To maintain the correct balance of bone mass, a tightly regulated process couples the activities of osteoclasts and osteoblasts and disorders in this process result in too little bone (osteopenia, osteoporosis) or excess bone (osteopetrosis, osteosclerosis). In cortical bone, remodelling occurs by osteoclasts removing a cutting zone which is then filled in by layers of bone laid down by invading teams of thousands of osteoblasts. In cortical bone, these BRUs are known as

osteons. In trabecular bone, BRUs are known as hemiosteons, where osteoclasts carve out pits which are then re-filled with bone by invading osteoblasts (Raggatt and Partridge, 2010). The bone remodelling cycle can be divided into several phases (see Figure 1.11) as set out below.

1.2.4.2.1 Activation/Resorption phase

The activation phase is thought to be initiated by the release of local chemotactic factors by osteocytic death (Martin and Burr, 1982) and by signalling by osteocytes in response to mechanical strain (Smit et al., 2002). Hormones such as parathyroid hormone (PTH) also act on osteoblasts and osteocytes to inhibit sclerostin production, and oestrogen (E2) reduces activation of osteoclasts. When the activation phase commences, the lining cells are disrupted, and in preparation for resorption, collagenases and MMPs are produced (Meikle et al., 1992). In addition, osteocytes, lining cells and osteoblasts produce osteoclastogenic factors such as RANKL and M-CSF, which lead to osteoclast precursors being recruited to the site. The osteoclast precursors are recruited either from the bone marrow or via the vasculature which is within the BRU. Osteoclasts bind to the surface of the bone and form an actin ring sealing zone and release HCl and matrix removing enzymes to resorb bone. The activation phase is thought to last about 10 days, after which osteoclasts apoptose and the reversal phase commences.

1.2.4.2.2 Reversal/Formation phase

The activation phase is followed by the reversal phase, where there is inactivation of the osteoclasts which apoptose, and invasion of teams of co-ordinated osteoblasts which differentiate and lay down new bone. Between inactivation of the osteoclasts and the invasion of osteoblasts, a mononuclear reversal cell of undetermined lineage, removes the collagen remnants in preparation for the invasion of osteoblasts. The migration of osteoblast precursors to the site of resorption is likely to be mediated via factors (such as TGF β and insulin like growth factor 1 (IGF1)) which are released when the matrix of bone is broken down. Once they reach the site of newly exposed bone, they lay down layers of osteoid and new bone is formed. The precise mechanism of coupling of breakdown and formation is still unclear but it is likely that osteoclasts produce coupling factors that regulate osteoblasts (Kular et al., 2012).

1.2.4.2.3 Termination phase

The final and longest phase is the termination phase, where osteoblasts lay down matrix and mineralise bone. Osteoblasts secrete type I collagen and non collagenous proteins such as osteocalcin (OCN), osteopontin (OPN), BSP, osteonectin (OSN) and proteoglycans. Primary and secondary mineralisation, as previously described, occurs. Osteoblasts then undergo terminal differentiation and either apoptose, become quiescent lining cells or become buried into bone as osteocytes. The mechanisms by which bone formation is terminated are still unclear, but signalling from the osteocytes via production of sclerostin, may be a mechanism of regulation. This formation phase may last up to 3 months and the bone becomes quiescent until the next BRU is activated.

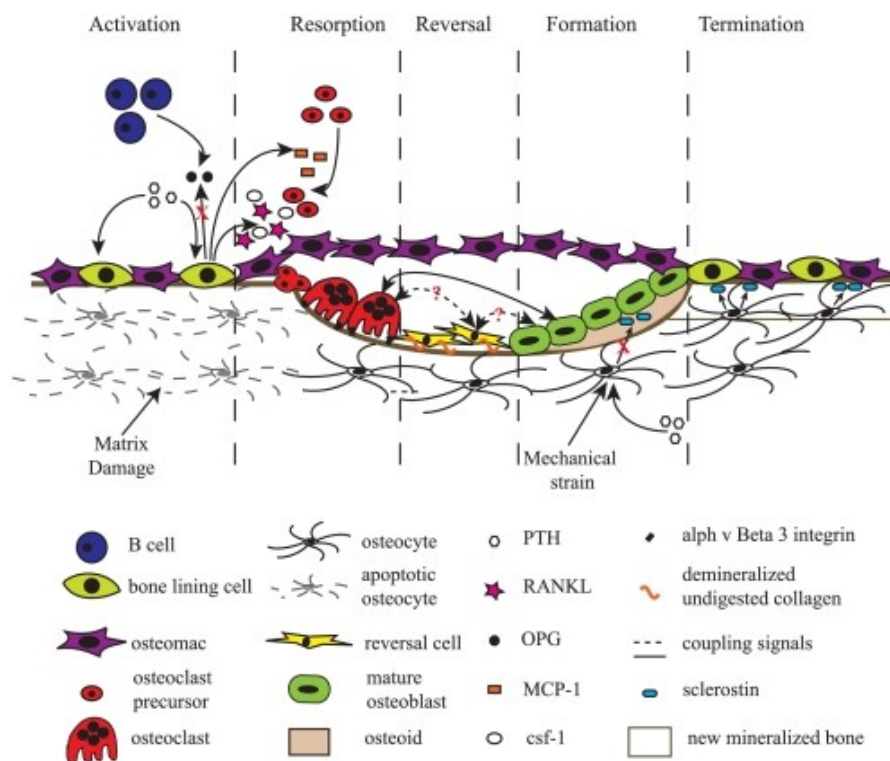


Figure 1.11 Remodelling cycle

Adapted from Raggatt 2010 with permission (Raggatt and Partridge, 2010).

During the activation phase, osteoclasts are recruited, attach to bone and mature, leading to resorption of bone. This is followed by the reversal phase where teams of coordinated osteoblasts are recruited and lay down new bone in orderly sheets. Osteoblasts either apoptose, become quiescent lining cells or become buried and mature into osteocytes that act as mechanosensory regulators, coordinating and directing bone remodelling. As well as osteocytes, cells present in the bone marrow niche such as T and B lymphocytes are also involved in cross communication between osteoblasts and osteoclasts.

1.2.4.3 OTHER MECHANISMS OF REGULATION OF SKELETAL MASS

1.2.4.3.1 Autonomic control

Both the sympathetic (SNS) and parasympathetic (PNS) nervous systems have been shown to influence bone mass. The SNS has been shown to be a negative regulator of bone mass by inhibiting osteoblast proliferation and increasing RANKL expression (Karsenty, 2006), whilst in contrast, the PNS is a positive regulator of bone mass.

Leptin is a neurotransmitter produced by adipocytes, which acts on the hypothalamus to suppress appetite. Recently, it has also been proposed as a key regulator of bone mass, acting via two mechanisms (Ducy et al., 2000). First, leptin acts on the central nervous system, inhibiting the synthesis and release of serotonin, which in turn leads to a decrease in signalling via the hypothalamus, resulting in increased sympathetic output. Sympathetic signals to osteoblasts via adrenergic receptors result in decreased osteoblast proliferation. Second, leptin acts via the hypothalamus to increase expression of a gene called *CART* (cocaine and amphetamine-regulated transcript). *CART* decreases RANKL production from osteoblasts, thus inhibiting bone resorption (Elefteriou et al., 2005). Although these seem to have opposing actions, the combined effect of leptin is the prevention of bone mass accrual via the actions of the SNS and *CART*.

1.3 OSTEOPOROSIS

Osteoporosis is characterised by reduced bone mass, low bone mineral density (BMD), deterioration of bone microarchitecture and an increased susceptibility to fragility fracture. Adult bone mass is determined by the maximum acquisition of bone during growth and the net balance of bone deposition (bone formation) versus bone loss (resorption) thereafter (Seeman and Delmas, 2006).

Established osteoporosis in adults is defined by the World Health Organisation (WHO) as individuals having a BMD measured by dual energy X-ray absorptiometry (DXA) which is more than 2.5 standard deviations below that of a sex-matched young adult (T-score).

Fractures occur when the skeleton is not able to withstand the demands of mechanical stress and is dependent on multiple factors such as bone structure, bone mass and bone quality as well as the stress placed upon the bone. The most common sites of osteoporotic fracture are at the hip, spine and wrist (Seeley et al., 1991).

Estimates for the number of postmenopausal women in the UK with osteoporosis have been predicted to rise from 1.8 million in 2010 to 2.1 million in 2020 (Gauthier et al., 2011). In the UK, the ten year risk of fracture in woman aged 50 years is 0.3% and increases to 8.7% for those aged 80 years. In 50 year old men, the ten year risk of fracture is 0.2%, increasing to 2.9% for those aged 80 years (Karaguzel and Holick, 2010, Harvey et al., 2010). Some estimates state that half of women and a fifth of men over the age of 50 will suffer a fracture. This would equate to over 60,000 hip, 50,000 wrist and over 120,000 vertebral fractures each year in the UK (Harvey et al., 2010).

1.3.1 RISK FACTORS FOR OSTEOPOROSIS

Identifying risk factors has helped medical professionals to diagnose, prevent and treat osteoporosis. Many factors are intrinsic but due to the significant financial burden of osteoporotic fractures, much focus has been placed on the modifiable risk factors.

Age: In adults, age and bone mass are inversely related irrespective of gender (Kanis et al., 2005a). A decline in trabecular bone mass begins around the third decade (Manolagas and Parfitt, 2010, Khosla et al., 2011). Ageing is associated with many disease processes and hormonal changes which together adversely affect bone quality and mass. An increase in reactive oxidative stress (ROS) has been identified as an important mechanism of age related bone loss. This increase in ROS affects both bone forming osteoblasts and bone regulating osteocytes. Increased ROS leads to reduced bone formation by reducing osteoblast lifespan and redirecting progenitors to the adipocyte lineage.

ROS also increases osteocytic apoptosis by reducing autophagy and compromising osteocytic nuclear pore structures (Manolagas, 2010).

Female gender: Women are at greater risk of osteoporosis due to their relatively smaller size and lower total bone mass. Accelerated bone loss after the menopause and comparative longevity increases women's risk of osteoporosis in comparison to men (Khosla et al., 2011).

Family history: A family history of osteoporosis which may include kyphosis or low trauma fractures after the age of 50, is a risk factor for osteoporosis (Soroko et al., 1994). Monozygotic and dizygotic twins studies show a high level of heritability, accounting for 60-80% of variability in BMD and a modest but significant heritability of fracture risk (Dequeker et al., 1987, Pocock et al., 1987). A recent meta-analysis of genome wide association (GWAS) studies has identified 56 loci which are associated with BMD variation susceptibility and 14 that are associated with fragility fractures (Estrada et al., 2012). Further GWAS studies have tried to identify loci associated with trabecular (1 loci identified) versus cortical (4 loci identified) determinants (Paternoster et al., 2013).

Ethnicity: Caucasian women have a 2.5 times greater increased risk of osteoporosis than Afro-Caribbean women (Snelling et al., 2001). This is likely to be due to genetic factors resulting in Afro-Caribbean women having a higher average BMD at all ages and a decreased rate of age related bone loss (Aloia et al., 1996).

Modifiable risk factors: Several studies have shown that body mass index (BMI) is positively associated with BMD and thus low BMI may be a risk factor for osteoporosis (Soroko et al., 1994, Ravn et al., 1999). Other factors have been shown to correlate but it is not clear if these associations are causative.

Smoking is associated with low BMD and increased fracture risk (Kanis et al., 2005b). A meta-analysis of 29 cross sectional studies showed that smokers have a greater rate of post-menopausal bone loss than non-smokers and have a 17% greater risk of fracture at 60 years, 41% at 70 years, 71% at 80 years and 108% at 90 years (Law and Hackshaw, 1997).

Current physical activity levels and physical activity in adolescence have been shown to have a positive correlation with BMD (Rubin et al., 1999); individuals who currently have a sedentary lifestyle and particularly those who were sedentary in adolescence could be at greater risk of osteoporosis. Studies assessing correlation between physical activity and BMD in adults have been conflicting. A study of 580 post-menopausal women in the UK found that brisk walking and stair climbing had a positive correlation with BMD (Coupland et al., 1999). In contrast, an Australian

study of 1075 women and 690 men showed an initially positive correlation between BMD and physical exercise but significance was lost on adjustment for age, BMI, calcium intake and quadriceps strength (Nguyen et al., 2000).

Secondary causes of osteoporosis: Osteoporosis can be secondary to a large number of clinical conditions such as thyrotoxicosis, anorexia nervosa, chronic liver disease, hyperparathyroidism, inflammatory bowel disease, male hypogonadism, renal disease, rheumatological diseases and vitamin D deficiency (Kanis et al., 2005a). Iatrogenic causes include some diuretics, anticonvulsants and corticosteroids (Rizzoli et al., 2012).

Further study of how thyroid and oestrogen hormones interact to maintain bone health is important in understanding how to prevent osteoporosis and fragility fractures.

The next two sections of this Introduction will give background information on thyroid hormone and oestrogen action and what is currently known about their action on bone.

1.4 THYROID HORMONE

In children, thyroid hormone excess (thyrotoxicosis) accelerates growth and advances bone maturation, whereas thyroid hormone deficiency (hypothyroidism) causes growth arrest with delayed skeletal development (Rivkees et al., 1988). Normal thyroid status is essential for acquisition of peak bone mass. In adults, untreated thyrotoxicosis accelerates bone loss and causes osteoporosis (Bassett et al., 2007b). Prospective clinical studies have revealed that even minor or transient disturbances of thyroid status can increase hip and vertebral fracture risk by up to 4-fold (Sambrook and Cooper, 2006, Parle et al., 1993, Murphy and Williams, 2004).

1.4.1 HOMEOSTATIC CONTROL OF THYROID HORMONE

Circulating levels of thyroid hormone are tightly regulated by a classical negative feedback loop in the hypothalamic-pituitary-thyroid (HPT) axis (see Figure 1.12).

Thyrotrophin releasing hormone (TRH) is a peptide hormone which is synthesised by neurons in the hypothalamic paraventricular nucleus (Abel et al., 2001). TRH binding to cell surface TRH receptors on anterior pituitary thyrotrophs stimulates the synthesis and release of the glycoprotein thyroid stimulating hormone (TSH). TSH binding to TSHR, a G protein coupled receptor on the plasma membrane of the thyroid follicular cell, stimulates thyroid hormone production and secretion in the thyroid gland. Transcription of TRH is suppressed by the binding of T3 to thyroid hormone receptor $\beta 2$ which binds to a negative thyroid response element (TRE) in the promoter region of the TRH gene. T3 binding to TR $\beta 2$ in the hypothalamus similarly leads to rapidly decreased transcription of TSH (Forrest et al., 1996).

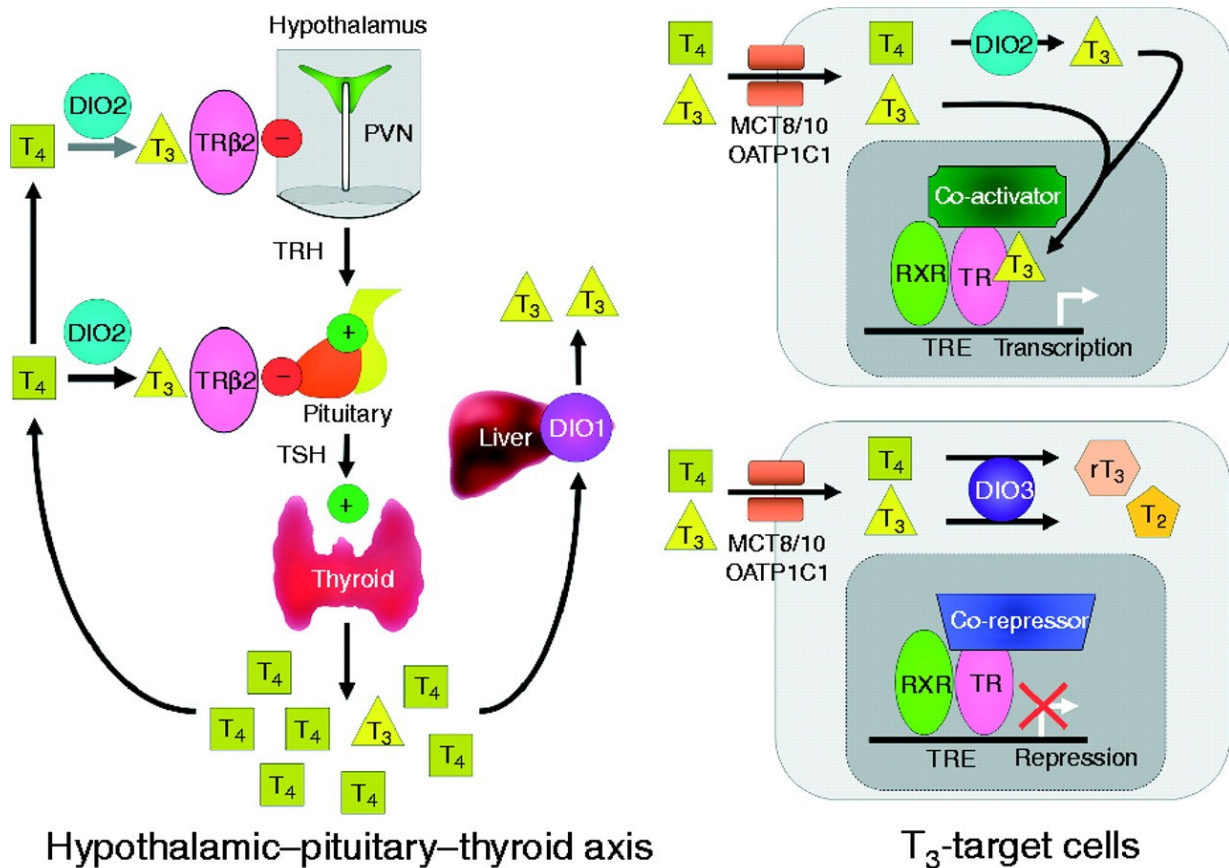


Figure 1.12 Homeostatic control of thyroid hormone

Circulating levels of thyroxine (T₄), the prohormone, are converted to 3,5,3'-L-triiodothyronine (T₃) by the action of deiodinase 2 (D2) in the hypothalamus and pituitary. The active hormone, T₃, inhibits the hypothalamic production of thyroid releasing hormone (TRH) and anterior pituitary production of thyroid stimulating hormone (TSH), via a negative feedback loop. Thus the HPT axis senses circulating levels of mainly T₄. Peripherally, T₄ is converted to T₃ via deiodinase 1 (D1) expressed in the kidney and liver.

Entry into cells is regulated by the transporters MCT8/10 and OATP1C1 on the cell surface. Intracellular T₃ is also regulated by deiodinase type 3, which inactivates T₄ and T₃ to rT₃ and T₂ respectively and D2, which converts T₄ to T₃.

PVN - paraventricular nucleus; TRH - thyrotrophin-releasing hormone; TSH - thyroid-stimulating hormone; DIO1, DIO2 and DIO3, type 1, 2 and 3 deiodinases; MCT8 and MCT10, OATP1C1 - organic acid transporter protein-1C1; TR, thyroid hormone receptor; TRb2, thyroid hormone receptor b2; RXR, retinoid X receptor; T₄ - thyroxine; T₃ - 3,3',5'-triiodothyronine; rT₃ - 3,3',5'-triiodothyronine; T₂ - 3,3'-diiodothyronine.

Reproduced from Nicholls 2012 with permission (Nicholls et al., 2012)

1.4.2 THYROID HORMONE SYNTHESIS

The thyroid gland synthesises the prohormone 3,5,3',5'-L-tetraiodothyronine (thyroxine -T₄) and a small amount of T₃. Iodide is actively taken up and concentrated in the thyroid gland by Na⁺/I⁻ symporters (NIS). Once intracellular, iodide is transported into the lumen of the follicle by a transporter located on the apical surface called pendrin (see Figure 1.13).

Intra luminal iodide is oxidised and incorporated into the tyrosine residues of a large glycoprotein called thyroglobulin (Tg) by the apical membrane enzyme, thyroid peroxidase (TPO). Dual oxidase 2 (DUOX2) is a glycoprotein on the apical membrane and in the presence of the maturation factor dual oxidase maturation factor 2 (DUOXA2), catalyses oxidation of Nicotinamide adenine dinucleotide phosphate (NADPH) from the cytoplasm and releases H₂O₂ into the follicular lumen.

TPO catalyses iodination of specific tyrosine residues on Tg, forming mono-iodotyrosine (MIT) and di-iodotyrosine (DIT) residues. TPO also enzymatically couples MIT and DIT in the presence of H₂O₂. T₃ and T₄ still attached to the Tg backbone is formed and stored in the colloid of the lumen of the thyroid follicle. Secretion of the hormones into the circulation occurs by macropinocytosis and micropinocytosis of vesicles at the apical membranes. Proteolysis by lysosomes releases T₄ and T₃ from Tg into the circulation. Iodotyrosines are rapidly deiodinated by dehalogenase1 in the endoplasmic reticulum and released iodine is recycled. The process of thyroid hormone synthesis and release are stimulated by TSH.

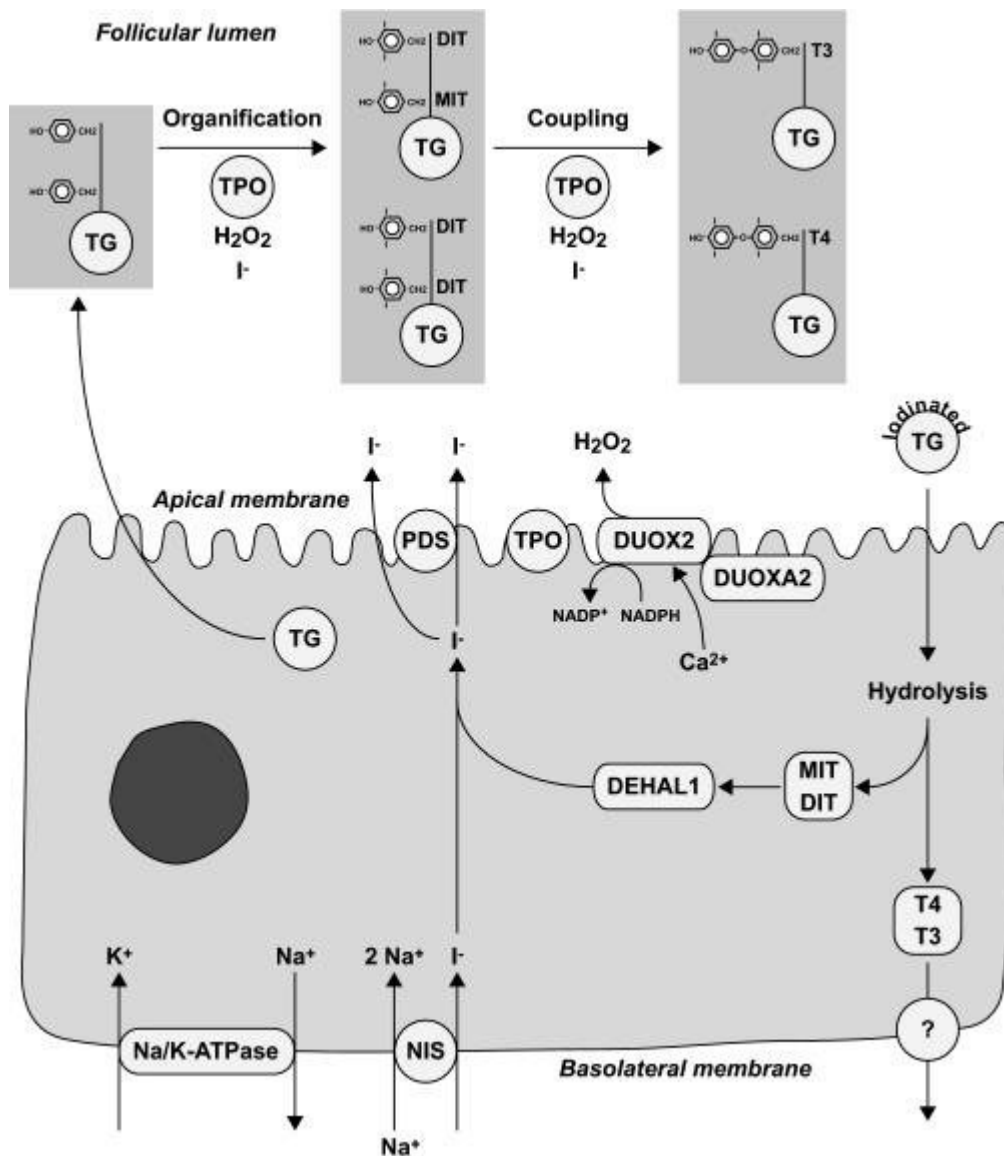


Figure 1.13 Thyroid hormone synthesis

Reproduced with permission from Bizhanova (Bizhanova and Kopp, 2009).

At the basolateral membrane of thyroid follicular cells, NIS transports iodide into thyrocytes after which pendrin further transports the iodide into the follicule lumen. Thyroid follicular cells line the lumen filled with colloid. H_2O_2 is produced in the luman by DUOX2 in the presence of DUOXA2. H_2O_2 is needed for the oxidation by iodide by TPO. Thyroglobulin is secreted into the follicular lumen and MIT and DIT are formed on its tyrosine residues. TPO couples MIT and DIT to form either T3 or T4 and are stored in the follicule until required. When required, thyroglobulin is internalised by pinocytosis. T3 and T4 are released into the bloodstream after thyroglobulin is digested by lysosomes. Any remaining MIT and DIT are deiodinated (by DHAL1) and the iodide recycled.

Na^+/I^- symporters (NIS), pendrin (PDS/SLC26A4), Thyroglobulin (TG), iodotyrosine dehalogenase 1 (DEHAL1),

1.4.3 LOCAL CONTROL OF THYROID HORMONE CONCENTRATIONS

Tissue bioavailability of thyroid hormone is dependent on several modulating factors - serum levels of T3 and T4, transport into the cells, intracellular conversion of prohormone to active hormone, intracellular receptor availability and intracellular inactivation of T3.

1.4.3.1 Serum concentrations of thyroid hormone

The prohormone, T4, is secreted at concentrations approximately 15 times greater than that of the active hormone T3 (130 nmol/l of T4 to 9 nmol of T3). Both hormones are lipophilic and are over 95% protein bound. Free T3 and T4 levels are therefore dependent on the concentration and saturation of transporter proteins, namely thyroxine binding globulin (TBG), transthyretin (TTR) and albumin. 75% of T4 is bound to TBG, 15% bound to albumin and 10% bound to TTR, leaving only about 0.02% non protein bound. Due to higher binding affinities of T4 to transport proteins compared to T3, the circulating free T4 concentration is four-fold greater than free T3. The majority of circulating active T3 hormone (80%) is derived from T4 mono deiodination of its outer ring and is catalysed by the selenocysteine containing deiodinase enzyme type 1 (D1) and deiodinase enzyme type 2 (D2) (Bianco and Kim, 2006).

1.4.3.2 Active transport of thyroid hormones into cells

Despite the lipophilic properties of thyroid hormones, entry to cells by passive diffusion is minimal. Active transporters increase the uptake of tissues by tenfold and regulate intracellular availability. Energy dependent, membrane bound thyroid hormone transporter proteins include monocarboxylate transporter 8 (MCT8), MCT10, organic anion-transporting-polypeptide 1c1 (OATP1c1, OATP14) and non-specific amino acid transporters such as L-type amino acid transporters 1 and 2 (LAT1, LAT2) (Heuer and Visser, 2012, Bianco and Kim, 2006).

1.4.3.3 Intracellular modulation of T3 availability

Intracellular availability of T3 is tightly regulated by deiodinases, a group of selenocysteine containing enzymes. Deiodinase 2 (D2), which has a 700 fold greater catalytic efficiency than D1, converts T4 to T3 in the endoplasmic reticulum near the nucleus. The high catalytic efficiency of D2 is important in protecting the cell against hypothyroidism. D2 is also important in thyroid hormone feedback regulation of TRH and TSH, converting circulating T4 to T3 so that appropriate negative

feedback can take place in proportion to circulating serum levels of thyroid hormone. D2 can be inactivated by ubiquitination, which is triggered by deiodination of T4 (St Germain et al., 2009). Deiodination of T4 exposes lysine residues on D2, which become conjugated to ubiquitin. This complex can be deubiquitinated and reactivated to continue deiodination or can become degraded (Bianco and Kim, 2006, Waung et al., 2012).

Inactivation of T3 and T4 occurs by D3 deiodination to 3, 3'-diiodothyronine (T2) and T4 to 3,3',5'-triiodothyronine (rT3), respectively. Thus, the intracellular availability of thyroid hormone can be fine tuned independently of circulating thyroid levels (see Figure 1.14).

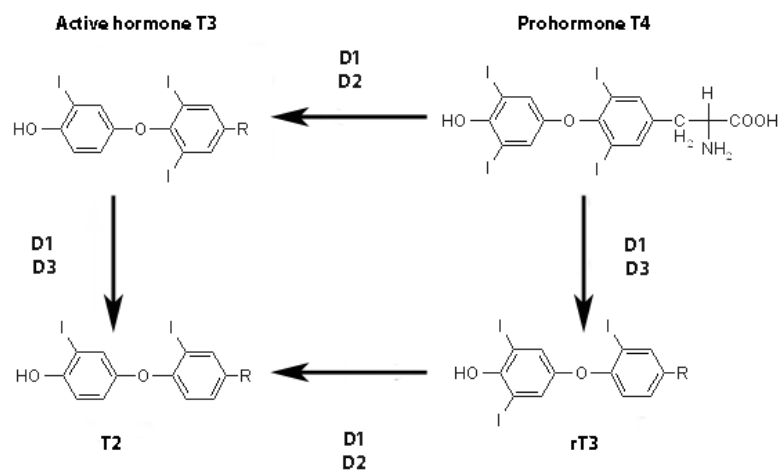


Figure 1.14 Deiodinase activation and inactivation of thyroid hormone

Prohormone T4 is monodeiodinated to either the active hormone T3 or inactive metabolite rT3 by the action of iodothyronine deiodinase 1 and 2 (D1 and D2) or D1 and D3 respectively. T3 or rT3 can be further monodeiodinated to inactive metabolite 3,3'-diiodothyronine (T2).

1.4.4 MOLECULAR MECHANISMS OF THYROID HORMONE ACTION

The principal action of thyroid hormone is via the two nuclear thyroid receptors, thyroid hormone receptor alpha (TR α) and thyroid hormone receptor beta (TR β). Three functional mRNA isoforms exist: TR α 1, TR β 1 and TR β 2 (Cheng, 2000).

Gothe et al compared mice devoid of TR α 1 and all TR β receptors with controls and found that these mice had a phenotype which was more severe (hyperactive pituitary-thyroid axis, poor female fertility, retarded growth and bone maturation) than mice lacking TR α 1 or TR β individually. They concluded that the absence of either TR could be substituted, to a degree, by the other. They also rendered TR α 1^{-/-} and TR β ^{-/-} mice hypothyroid with no detectable change in weight, in contrast to the control mice that lost 7.8% of their weight in 3 weeks. This suggested that TR α 1 and TR β provide the principal means by which thyroid hormone action is mediated (Gothe et al., 1999).

1.4.4.1 Thyroid hormone receptors

Thyroid hormone receptors belong to the nuclear receptor superfamily (Williams and Franklyn, 1994). Other members of this group include sex steroids, adrenal steroids, vitamin D3 and retinoid receptors. These receptors specifically regulate target genes involved in metabolism, development and reproduction. Nuclear receptors are ligand inducible transcription factors which, when bound to hormones, mediate transcriptional response in target genes by binding to hormone response elements in the promoter region of responsive genes. Nuclear receptors have a similar structure consisting of a series of functional domains (Cheng et al., 2010).

The functional domains consist of:

1. Amino-terminal A/B domain which varies highly between isoforms. This is where the N-terminal activation function1 domain (AF) is located.
2. The C domain contains the central DNA binding domain (DBD) which is highly conserved and has two zinc finger subdomains which bind to TREs. This domain also contains motifs important in homo and hetero dimerisation.
3. The hinge domain which contains a nuclear localisation signal, which is involved in transporting the receptor into the nucleus.

4. The E/F domain contains the carboxyl-terminal ligand-binding domain (LBD) which can bind to thyroid hormones, corepressors and coactivators. The E domain contains the AF2 and another nuclear localisation signal.

TRs bind to TREs in DNA both as homodimers and more frequently as heterodimers with retinoid X receptor (RXR). TREs commonly consist of either two half-site sequences (AGGTCA) or a repeat of the half site sequence separated by zero, four or six nucleotides (Lazar, 1993). Binding of the homo or heterodimer is via specific grooves in the two 'zinc fingers' of the DBD. Cofactors and corepressors are recruited and interact with the TR and transcriptional machinery to either result in activation or repression of gene transcription.

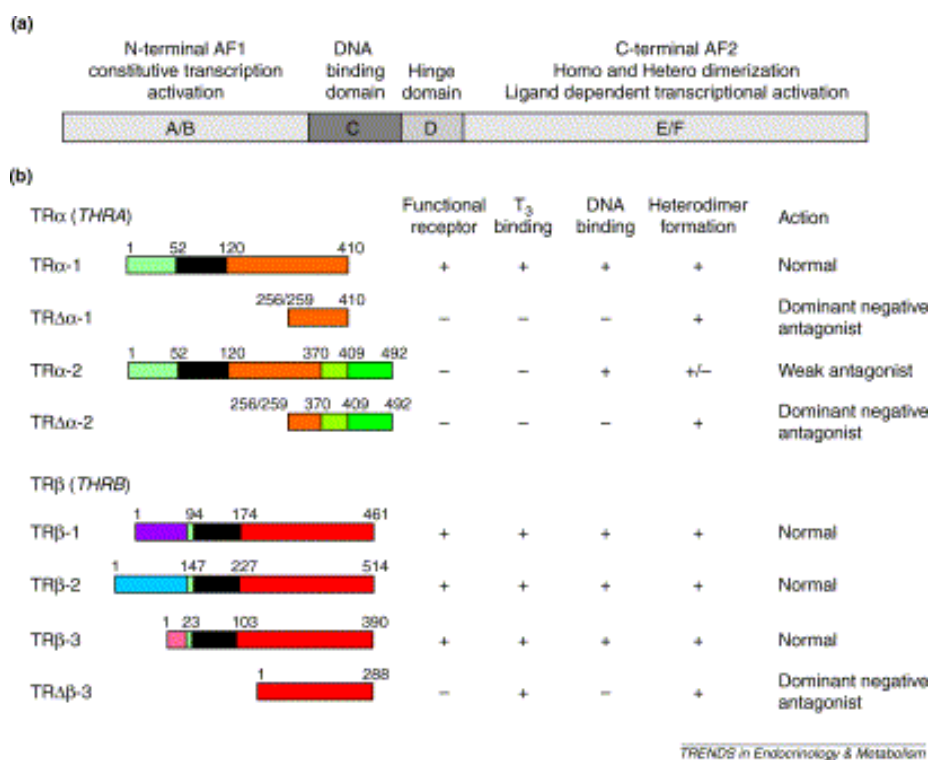


Figure 1.15 Structure of steroid hormone and TR isoforms

- (A) The structure of steroid hormone receptors classically has an A/B domain which is the N-terminal and AF1, the C domain, which is involved in DNA binding, D domain is the hinge domain and E/F domain contains the C-terminal and AF2 and which is important in thyroid hormone binding and co activator and co repressor binding.
- (B) The different isoforms of the receptors are shown with a summary of whether each is a functional receptor, its T₃ binding properties, DNA binding and whether it forms heterodimers.

Taken from Bassett 2003 (Bassett and Williams, 2003).

1.4.4.2 Thyroid receptors are differentially temporally and spatially expressed

Thra and *Thrb* genes on chromosomes 17 and 3 respectively, transcribe three functional mRNA isoforms: TR α 1, TR β 1 and TR β 2 (Cheng et al., 2010).

The TR α locus also encodes TR α 2, TR $\Delta\alpha$ 1 and TR $\Delta\alpha$ 2, which lacks the DNA binding domain of TR α 1. TR α 1 binds T3 and is the predominant thyroid receptor expressed in the brain, heart and bone (Forrest et al., 1990). The delta isoforms TR $\Delta\alpha$ 1 and TR $\Delta\alpha$ 2 are driven by a promoter in intron 7 and lack both a DNA binding domain and part of the ligand binding domain (LBD) (Chassande et al., 1997). They inhibit the actions of TRs *in vitro* (Gauthier et al., 2001) but their role *in vivo* is still uncertain (see Figure 1.15).

TR β 1 is the major receptor in the liver, skeletal muscle, kidney and fat whilst TR β 2 is the predominant receptor expressed in the pituitary, hypothalamus, retina and cochlea. The TR β locus also encodes for TR β 3 and TR $\Delta\beta$ 3 (Williams, 2000); their roles *in vivo* remain unclearly defined.

TRs heterodimerise with RXR and bind to DNA sequences TREs. Heterodimerisation with RXR increases binding of TRs to TRE thus increasing transcriptional activation (Zhang and Kahl, 1993, Cheng, 2000).

1.4.4.3 Coactivators and corepressors

In the absence of T3, unliganded TR/RXR dimers are known as aporeceptors and are bound to DNA along with complexes of co repressors. Co repressors include nuclear receptor co repressor (NCOR) and silencing mediator of retinoid and thyroid hormone receptors (SMRT), which bind to the TR via the C-terminal LBD (see Figure 1.15). Corepressors have chromatin deacetylase activity, which maintains the chromatin in a compact repressed state, thereby blocking access to basal transcriptional machinery (see Figure 1.16). In the absence of T3, aporeceptors therefore mediate repression or silencing of the basal transcription of target genes (Cheng et al., 2010, Chatterjee et al., 1989, Glass et al., 1989).

Liganded TR are known as holoreceptors and in the presence of T3, there is a conformational change in the TR/RXR complex leading to release of co repressors and recruitment of complexes of coactivators such as steroid receptor coactivator-1 (SRC1) and cAMP response element binding protein. Many co-activators belong to the SRC/p160 family, which share approximately 40% homology and have functional properties including DNA binding and dimerisation interaction regions. Other complexes are also present, such as the TR-associated protein, which have

chromatin-free transcriptional enhancing properties and interact with TR in response to T3 (Harvey and Williams, 2002). Coactivators directly or indirectly result in basal transcriptional machinery activation which promotes transcription and histone acetylation. This leads to an open chromatin structure and allows transcriptional activation by nuclear receptors.

The proportion of apo versus holo TRs may be a mechanism of control of T3 action. Furthermore, the repressive effects of apo versus holo TRs serve to augment the amplitude of the transcriptional response to thyroid hormone.

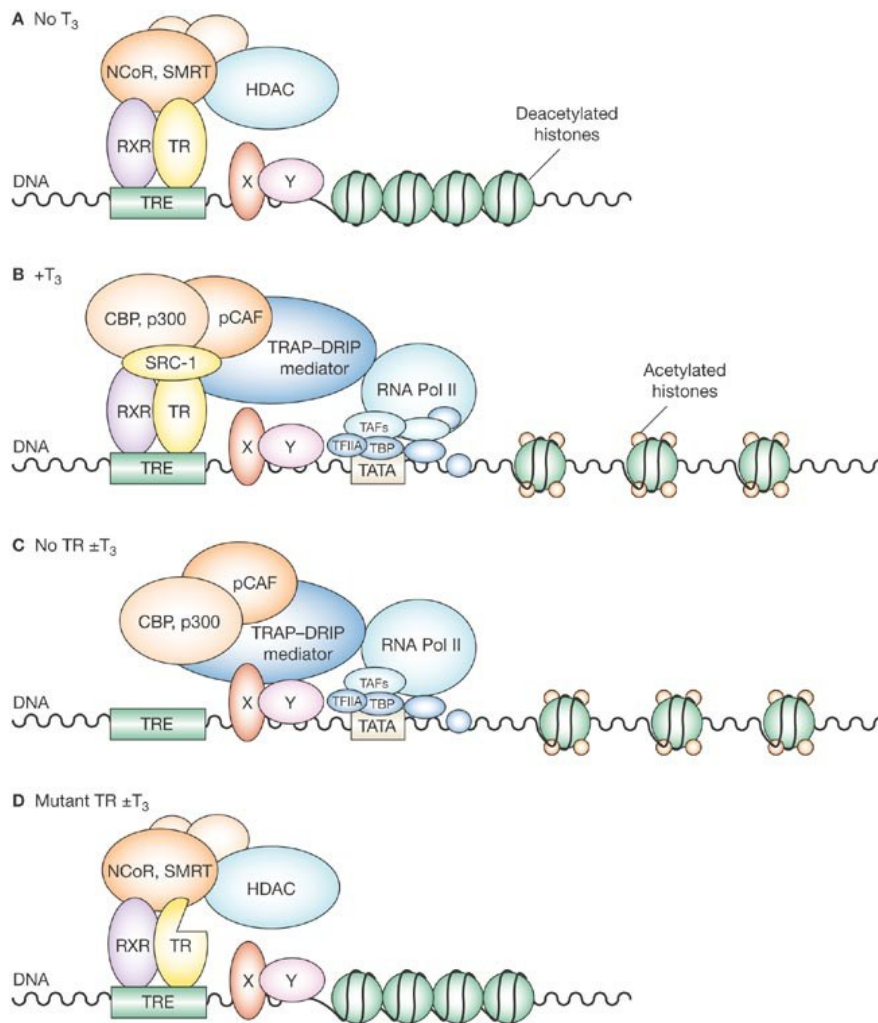


Figure 1.16 TR control of gene expression.

Diagram taken from J. Bernal 2007 with permission (Bernal, 2007).

TR, usually as heterodimers with RXR but also as homodimers, bind to TRE in the regulatory region of target genes. In the absence of hormone binding, the unliganded receptor recruits corepressors such as NCoR and SMRT and histone deacetylases, which maintain the chromatin in a compact repressed state.

- (A) In the presence of T₃ there is a release of corepressors and recruitment of coactivators such as SRC-1, histone acetylases (CBP, p300 and pCAF) and other mediators such as TRAP and DRIP, which facilitate transcriptional machinery access to the promoter.
- (B) In the absence of TR, there is lack of repression and the receptor may facilitate transcription of other transcription factors (basal transcription).
- (C) In the presence of a mutation in the hormone binding domain which blocks T₃ binding but with intact DNA binding, a repressed chromatin state remains.

CBP-CREB-binding protein; DRIP- vitamin D receptor-interacting protein; HDAC- histone deacetylase; NCoR- nuclear receptor corepressor; pCAF- mammalian homologue of the yeast transcriptional activator GCN5; RNA Pol II- RNA polymerase II; RXR- 9-cis retinoic acid receptor; SRC-1- steroid receptor coactivator 1; SMRT- silencing mediator for retinoic and thyroid receptor; TAF- transcription initiation factor; TBP- TATA box binding protein; TFIIA- transcription initiation factor IIA; TR- thyroid hormone receptor; TRE- thyroid hormone response element; TRAP- thyroid-hormone-receptor-associated protein.

1.4.5 THE EFFECTS OF CIRCULATING THYROID HORMONE LEVELS ON THE SKELETON

1.4.5.1 Hypothyroidism in humans

The skeletal effects of hypothyroidism during childhood are characterised by delayed bone age, failure to close fontanelles, epiphyseal dysgenesis and growth arrest. Treatment results in catch up growth with acceleration of bone age and rapid linear growth but may result in compromise of final height (Rivkees et al., 1988). Histomorphometric studies in hypothyroid adults showed reduced osteoid apposition suggesting impaired osteoblast activity, a prolonged period of secondary bone mineralisation and decreased resorption parameters. Despite a reduction in bone remodelling, there is a net positive bone balance resulting in an increased BMD (Eriksen et al., 1986). Population studies suggest that patients with a prior history of hypothyroidism have a 2-3 times increase in relative fracture risk up to 10 years after diagnosis (Vestergaard et al., 2005).

1.4.5.2 Animal models of hypothyroidism

Different animal models have been used to study the effects of hypothyroidism on bone.

1.4.5.2.1 Wild type animals rendered hypothyroid

Several groups have induced hypothyroidism by thyroidectomy (Lanham et al., 2011) or via the administration of drugs such as Propylthiouracil (PTU), methimazole or potassium perchlorate (Allain et al., 1995, Conti et al., 2009).

Adult animals with hypothyroidism develop an increased bone mass. This was demonstrated by an elevated bone volume per tissue volume (BV/TV) (Allain et al., 1995), a higher ash calcium content (Conti et al., 2009) and increased BMD when compared with euthyroid controls.

Histomorphometric parameters were assessed in 18 week old rats which were rendered hypothyroid for 12 weeks (Allain et al., 1995). This resulted in elevated BV/TV accompanied by a marked decrease in osteoid, mineral apposition (MA) and eroded surface per bone surface (BS). These results suggest that the increase in bone was secondary to decreased osteoclast resorption.

Conti et al rendered juvenile 13 week old rats hypothyroid for 10 weeks which resulted in growth retardation with decreased weight and length. They were found to have higher calcium concentration when ashed and higher femoral bone mass. Mechanical properties were assessed and femoral stiffness (elastic modulus) but no other biomechanical parameters of hypothyroid animals were greater than controls (Conti et al., 2009). Lanham et al assessed structural and mechanical properties in ovine fetuses post thyroidectomy and found that there was no change in cortical thickness compared to controls but a decrease in cortical diameter. The trabecular bone had

thicker, more closely spaced trabeculae, despite having a lower BMD. Serum bone markers showed decreased osteocalcin but C-terminal cross-linked telopeptide of type I collagen (CTX) was no different to controls, suggesting that hypothyroidism in utero affects bone formation to a greater extent than resorption. Mechanical testing of hypothyroid foetal femurs compared to controls did not show significant differences in parameters. However, mechanical testing of trabecular bone in hypothyroid animals resulted in a failure at a higher maximum load and higher stiffness and stress than controls (Lanham et al., 2011). Capelo et al rendered pregnant mice hypothyroid and examined the bone development and growth plates of foetal tissue. Their findings suggested that up to embryonic day 16.5, thyroid hormone signalling was kept to a minimum, with little differences compared to controls. Low thyroid hormone signalling was maintained by elevated levels of D3. After this stage, by embryonic day 18.5, D2 expression, which was previously low, was markedly increased (Capelo et al., 2008).

1.4.5.2.2 *Pax8^{-/-}, Hyt/hyt and Duoxa^{-/-} mice*

The skeletal phenotype of some knockout mice with mutations resulting in severe hypothyroidism has been described in detail in the literature.

Pax8^{-/-} mice lack a transcription factor essential for the development of the thyroid gland and have a complete absence of thyroid follicular cells, with a consequent lack of thyroid hormone in post natal life. These mice die at weaning unless treated for a short period with thyroid hormone (Flamant et al., 2002, Mansouri et al., 1998). *Pax8^{-/-}* mice have a skeletal phenotype typical of severe hypothyroidism, including severe delay in growth and ossification, more coarse and plate-like trabeculae and increased connectivity with retention of mineralised calcified cartilage, suggestive of a bone remodelling defect (Bassett et al., 2008).

Hyt/hyt mice have a non functional TSHR and are grossly hypothyroid, exhibiting a skeletal phenotype very similar to that of *Pax8* mice. They exhibit delayed ossification, reduced cortical bone, a trabecular bone remodelling defect and decreased bone mineralisation (Bassett et al., 2008).

Duoxa^{-/-} mice lack DUOX protein (which is critical for the generation of thyroid H₂O₂), have undetectable serum thyroid levels and grossly elevated TSH levels. These mice died if weaned at P21 but if they were weaned at P30, then some of them survived into adulthood. Although the skeletal phenotype for these mice has not been described in detail, mice at P13 exhibit impaired long bone growth, delayed ossification and reduced bone mineralisation (Grasberger et al., 2012).

In summary, animal models of hypothyroidism have similar skeletal findings to those found in human data (Eriksen et al., 1986), indicating that in the hypothyroid mature skeleton, there is an increase in bone mass, which is secondary to decreased osteoclast resorption. Hypothyroidism also depresses osteoblast function, resulting in reduced MA and reduced presence of osteoid. There is also a suggestion that osteocytes may be affected as there is a decrease in secondary mineralisation. Biomechanical animal data suggests that hypothyroidism may result in stronger (higher maximum load) but more stiff bones.

1.4.5.3 Thyrotoxicosis in humans

Hyperthyroidism in childhood results in accelerated growth and bone age, and premature fusion of growth plates leading to short stature and craniosynostosis (Segni et al., 1999).

Thyroid disease occurs 10-fold more frequently in women and its prevalence increases with age. As a result, 3% of the 12 million women over the age of 50 in the UK receive thyroxine (T4) for either primary hypothyroidism or the consequences of surgical or radioiodine treatment for thyrotoxicosis, and more than 20% of them are over-treated (Parle et al., 1993).

In adults, thyrotoxicosis results in osteoporosis and an increased fracture risk (Vestergaard and Mosekilde, 2003). Large population studies in patients with a history of hyperthyroidism have shown a reduced BMD, increased serum bone turnover markers and increased fracture rates (Cheung et al., 2011).

Histomorphometric studies in thyrotoxic patients reveal high bone turnover osteoporosis stemming from increased activation frequency of remodelling units. The reduced duration of the bone remodelling cycle coupled with increased bone resorption parameters results in a net negative bone balance (Eriksen, 1986, Mosekilde and Melsen, 1978).

1.4.5.4 Animal models of hyperthyroidism

1.4.5.4.1 Wild type animals rendered thyrotoxic

Adult mice with hyperthyroidism have decreased bone mass although some studies suggest that this is site specific only. Ongphiphadhanaku et al reported that three weeks of treatment with T4 in rats reduced femoral but not vertebral BMD (Ongphiphadhanakul et al., 1992). No decrease in BV/TV was noted at the vertebral body (Balena et al., 1993, Yamamoto et al., 1993).

Histomorphometric evaluation of adult rats treated with T4 for 3 weeks resulted in a 45% decrease in BV/TV compared to controls, which exhibited a 32% reduction in trabecular number (Tb.N) and a modest but not significant decrease in trabecular thickness (Tb.Th) in the tibia (Balena et al., 1993). This loss in bone mass was secondary to a high turnover osteoporosis. Osteoclast surface (Oc.S) per BS was increased by 40% in the T4 treated tibias. An increase in mineral apposition rate (MAR) and mineral formation rate per BS in thyrotoxic mice compared to controls was reported by Allain et al, with a slight increase in eroded surfaces (Allain et al., 1992).

Mechanical properties of bones from thyrotoxic animals have not been reported in the literature.

In summary, studies in humans and animals demonstrate that thyrotoxicosis results in a high turnover osteoporosis, the effect of which is site specific.

1.4.6 THE ROLE OF THYROID HORMONE TRANSPORTERS AND DEIODINASES IN THE SKELETON

Mutations in genes controlling thyroid hormone transporters and deiodinases provide key information on what role these proteins play in the skeleton.

1.4.6.1 Thyroid hormone transporters

Inactivating mutations in MCT8 lead to a lack of thyroid hormone transport into cells and results in Allan Herndon Dudley Syndrome. Although patients with this syndrome suffer severe global developmental delay (Heuer and Visser, 2012) due to a lack of thyroid hormone transport into neurons, growth in these patients is reportedly unaffected. Based on these observations, Abe et al examined the mRNA expression of several different thyroid hormone transporters in ATDC 5 chondrocyte cell lines and found that MCT10 was the most highly expressed. MCT10 was also found to be highly expressed in the resting growth plate zone, whilst MCT8 and OAT1c1 were minimally expressed (Abe et al., 2012). Capelo et al showed that osteoblasts and MC3T3 osteoblast-like cell lines expressed MCT8, LAT1 and LAT2, but not OATP1 and NTCP. These transporters were up regulated in hypothyroidism and down regulated on treatment with T3. They did not, however, examine the expression of the MCT10 transporter (Capelo et al., 2008). The current data suggests that thyroid hormone transporters are cell type specific, and that in the growth plate, MCT10 is the principal transporter, unlike in neurons, where MCT8 is the most significant thyroid hormone transporter.

1.4.6.2 Thyroid hormone transporter deficient mice

The role of thyroid hormone transporters in bone development has yet to be comprehensively studied but of the published knockout mice that do exist, only growth parameters have been reported. Mice lacking MCT8 (Trajkovic et al., 2007) were noted to have similar growth to that of wild type controls. MCT8 is expressed in ATDC5 and MC3T3 cell lines, primary osteoblasts and primary osteoclasts. *In vitro* studies show that silencing MCT10 in ATDC5 cells reduces the proliferative effects of thyroid hormone (Abe et al., 2012) but studies of mice lacking MCT10 have not been published. Mice deficient in the thyroid hormone transporters *Lat2* and *Oatp1c1* have reportedly normal growth but full skeletal phenotyping is awaited (Braun et al., 2011, Mayerl et al., 2012). Growth preservation in these knockout mice gives us limited information but suggests a degree of compensation within skeletal tissue, with consequent preservation of growth.

1.4.6.3 Deiodinases

In mice, high D3 levels during early foetal bone development results in minimal thyroid hormone signalling. Towards the end of gestation, there is a steep rise in D2 and a decrease in D3, resulting in an acceleration in bone development (Capelo et al., 2008). In adult mice, D2 is present in whole bone and osteoblasts but is absent in chondrocytes and osteoclasts, D3 is present in chondrocytes, osteoblasts and osteoclasts, but D1 is not detectable in any bone cells (Williams and Bassett, 2011, Bassett et al., 2010).

1.4.6.3.1 Deiodinase deficient mice

The role of deiodinase enzymes in the skeleton has been extensively studied in knockout mice. Mice deficient in D2, have a decreased intracellular availability of T3 and affected cells have decreased thyroid signalling, despite normal circulating thyroid hormone status. Growth and development were normal in these mice but adult D2KO mice bones had reduced toughness and were brittle. Bone formation was decreased due to local deficiency of T3 in osteoblasts (Bassett et al., 2010), indicating that D2 in osteoblasts is essential in adult skeletal homeostasis. Studies of D1/D2 double knockout mice have been published and although their skeletal phenotype has not been comprehensively analysed, the weight of the adult mice was lower than controls (Galton et al., 2009). D3 knockout mice have a 35% reduction in body weight at weaning with persistence of severe growth retardation. These global knockout mice have neonatal thyrotoxicosis followed by central hypothyroidism that persists in later life. This extreme thyroid function derangement makes interpretation of the skeletal response complicated (Hernandez et al., 2006).

1.4.7 THE ROLE OF TRS IN THYROID HORMONE SIGNALLING IN THE SKELETON

Changes in TR α and TR β , both in humans and in animal models, provide evidence for the complex interactions of thyroid receptors in the tissue specific regulation of thyroid hormone signalling.

In the skeleton, TR α is expressed in ten-fold greater concentrations than TR β (Bookout et al., 2006, O'Shea et al., 2003). Osteoblasts express TR α 1, TR α 2 and TR β 1 as do reserve and proliferative chondrocytes (Bassett and Williams, 2009). It is not known which receptors are expressed in osteocytes or osteoclasts.

1.4.7.1 Thyroid hormone receptor alpha mutations in humans

Analysis of 19,195 Caucasians did not reveal any associations between a set of 14 polymorphisms in THRA and either BMD or fracture risk (Medici et al., 2012). However, heterozygous human mutations in THRA have been reported in a 6 year old (Bochukova et al., 2012) and a father and daughter, all of whom showed classical features of hypothyroidism (van Mullem et al., 2012, Bochukova et al., 2012). Serum measurements of thyroid hormones showed T4 in the low normal range, elevated T3 and TSH in the normal range. Serum IGF1 levels were reduced. Skeletal radiographs demonstrated patent cranial fontanelles with delayed closure of cranial sutures, multiple wormian bones, delayed tooth eruption, femoral epiphyseal dysgenesis and delayed bone age.

1.4.7.2 TR α knockout mice

Chassande et al generated a TR α knockout mouse (TR α ^{-/-}) but as a result, a previously unknown promoter within intron 7 was discovered, resulting in production of the truncated isoforms $\Delta\alpha$ 1 and $\Delta\alpha$ 2 (Chassande et al., 1997). Consequently, full TR α knockout mice (TR α ^{0/0}) were generated which lack all TR α isoforms (Gauthier et al., 2001, Macchia et al., 2001, Pelletier et al., 2008).

During growth, TR α ^{0/0} mice have normal circulating thyroid hormone levels. Skeletal phenotyping during growth and in adulthood shows divergence. During growth, TR α ^{0/0} mice have a reduced cortical bone diameter compared to wild type mice at P21, delayed endochondral ossification and reduced mineralisation. As adults, TR α ^{0/0} mice have similar cortical bone diameters compared to controls and are osteosclerotic, with increased bone fraction and reduced bone resorption - a phenotype very similar to that of hypothyroid mice (Bassett et al., 2007a).

Accordingly, skeletal expression of the T3 target genes FGFRs 1 and 3 was reduced (Barnard et al., 2005, O'Shea et al., 2003, Stevens et al., 2003), suggesting that skeletal thyroid hormone signalling

was reduced in TR α ^{0/0} mice. As TR α is the predominant receptor in bone, it has been proposed that skeletal thyroid signalling is reduced in TR α ^{0/0} mice (Bassett and Williams, 2009). Although bone formation parameters in TR α ^{0/0} mice have not been published, one would expect them to be reduced, as with hypothyroid mice.

1.4.7.3 Other TR α mutant mouse models

Several dominant negative mutations of TR α have been generated (Kaneshige et al., 2001, Liu et al., 2003, O'Shea et al., 2003, Quignodon et al., 2007, Tinnikov et al., 2002). The different mutations, depending on the location of the mutation, result in varying degrees of dominant negative TR activities. This is clearly evident in the mutant mice and is also likely to be the case in affected humans with mutations in TRs. Mutations in TR α 1^{PV/+} mice (dominant-negative PV mutation was identified based on a mutation in a patient with known severe resistance to thyroid hormone) resulted in severely delayed growth and bone maturation, diminished trabecular mineralisation and reduced cortical thickness. Adult mice have a severe phenotype, with osteosclerosis and greatly increased mineralisation. Dynamic bone formation has not been reported in these mice but osteoclastic bone resorption is decreased (O'Shea et al., 2005). TR α 1^{+/m} mice harbour a milder resistance to thyroid hormone (RTH) mutation than TR α 1^{PV/+} mice, the latter also displaying a transient period of hypothyroidism between P10 and P35. During growth, these mice had delayed endochondral ossification, reduced cortical width and abnormal bone modelling, which remained after the cessation of growth. Trabecular bone was similar to controls during development but increased as adults, where there was increased mineralisation with retention of calcified cartilage. Adult mice had reduced resorption in both cortical and trabecular compartments but dynamic bone formation parameters have not been reported. The skeletal abnormalities seen in these mice were rescued when they were crossed with TR β ^{-/-} mice as the elevated thyroid hormone levels allowed TR α 1^{+/m} to bind to thyroid hormone and activate target genes (Bassett and Williams, 2009).

1.4.7.4 RTH in humans

Dominant negative mutations in TR β genes result in a loss in negative feedback in the hypothalamus and pituitary gland, giving rise to the clinical syndrome RTH (Refetoff, 1993). RTH is characterised by an end organ RTH, leading to elevated levels of T4 or T3, with inappropriately normal or slightly increased serum TSH responsiveness to TRH stimulation. Diagnosis is confirmed on characteristic serum thyroid function tests and a lack of suppression of TSH responsiveness in the presence of

elevated T3. The signs and symptoms of patients with RTH vary widely, with some tissues suggestive of hypothyroidism whilst others suggestive of thyrotoxicosis (Weiss and Refetoff, 2000). The skeletal phenotype of patients with RTH can vary widely. Some may be severely affected, having short stature, advanced bone age, increased bone turnover, osteoporosis, craniofacial abnormalities, osteoporosis and fractures, whilst other patients can have normal stature and development (Weiss and Refetoff, 1996).

Patients with RTH have a disruption of the HPT axis due to tissue insensitivity, resulting in elevated serum thyroid levels but end organ responsiveness in the skeleton and, consequently, increased signalling in the skeleton. Although the skeletal phenotype of these patients has been quite variable, animal models have allowed closer investigation of the role of TR β and its effects on the skeleton.

1.4.7.5 TR β Knockout mice

Two TR β ^{-/-} mice lacking all TR β isoforms have been generated (Forrest et al., 1996, Gauthier et al., 2001, Ng et al., 2001). Heterozygous animals are unaffected but due to the lack of negative feedback on the HPT axis, TR β ^{-/-} mice have elevated circulating TSH and serum T3 and T4 levels. During growth, TR β ^{-/-} mice show advanced skeletal maturation with accelerated chondrocyte differentiation, endochondral ossification and short stature due to premature growth plate quiescence. In maturity, these mice are osteoporotic with reduced micro-mineralisation. Bone resorption is increased as shown by increased osteoclast resorption surfaces and increased number of osteoclasts per BS (Bassett et al., 2007b). Dynamic bone formation parameters and mechanical properties have not been published (Bassett and Williams, 2009).

1.4.7.6 Other TR β mutant mouse models

Mouse models have been generated with dominant negative mutations in TR β , based on a mutation in a patient with known severe RTH (Hashimoto et al., 2001, Kaneshige et al., 2000). These mice have a severe RTH phenotype with 400-fold elevation of TSH and a 15-fold elevation of circulating T4. TR β ^{PV/PV} mice have accelerated in utero ossification and growth. The juvenile mice show a premature cessation of growth, advanced endochondral ossification and increased mineralisation (Bassett et al., 2007a). There is early quiescence of the growth plate by 3 weeks, resulting in shortened bone length and persistent growth retardation. The adult mice have reduced final length

with reduced tibia and ulna length. The complete adult skeletal phenotype has not yet been published.

1.4.7.7 What studies of TR α ^{0/0} and TR β ^{-/-} mice have revealed about the roles of TRs in thyroid signalling

TR α ^{0/0} and TR α 1^{PV} dominant-negative mutant mice are euthyroid but have delayed ossification and reduced bone mineralisation. These changes are consistent with decreased thyroid hormone signalling in the skeleton (Bassett et al., 2007b, Bassett and Williams, 2009). By contrast, TR β ^{-/-} knockout and TR β PV mutant mice have elevated circulating thyroid hormone levels, and display advanced ossification with increased bone mineralisation, features which are consistent with increased thyroid signalling in the skeleton (O'Shea et al., 2003, Bassett and Williams, 2009, Kaneshige et al., 2000). It has been proposed that these opposing phenotypes arise because the pituitary is TR β -responsive, whereas bone is predominantly TR α -responsive. Disrupted TR β function leads to impaired feedback inhibition of TSH in the pituitary (Bassett et al., 2007a, Waung et al.), resulting in elevated T4 and T3 levels, which act via TR α in bone to induce increased thyroid signalling in the skeleton. By contrast, decreased thyroid signalling in the skeleton in TR α mutants may result from impaired TR α function in bone (Bassett and Williams, 2009). Analysis of adult TR α ^{0/0} and TR β ^{-/-} mice is consistent with these findings. Adult trabecular bone in TR α ^{0/0} mice is increased, whereas TR β ^{-/-} mice are osteoporotic. These findings in TR α ^{0/0} mice are also seen in TR α 1^{PV} dominant-negative mice (Kaneshige et al., 2001, Tinnikov et al., 2002). Thus, deletion or mutation of TR α causes an increase in trabecular bone mass in adult mice, suggesting that TR α regulates bone maintenance in adults as well as regulating bone formation and mineralisation during growth. Additionally, the finding that increased TR α activity in adult TR β ^{-/-} mice causes osteoporosis indicates that the level of TR α activity determines acquisition of peak bone mass during growth as well as the efficiency of adult bone maintenance.

1.4.7.8 Double thyroid receptor knockout mice

Mice with absent TR α or TR β transcripts were generated by crossing TR α ^{0/0} with TR β ^{-/-} mice (Gothe et al., 1999, Flamant et al., 2002). Although these mice were viable, they had severely delayed growth, delayed endochondral ossification, impaired chondrocyte differentiation and reduced mineralisation. No dynamic bone formation or osteoclast parameters have been reported in adult TR α ^{0/0}TR β ^{-/-} mice.

1.4.7.9 The role of aporeceptors

Dominant negative mutations in TR α result in a more severely affected skeletal phenotype than in the absence of TR α alone. The mechanism for this was recently explored by Fozzatti et al when they crossed TR $\alpha 1^{PV/+}$ mice with NCOR1 $\Delta ID/\Delta ID$ mice; the latter globally express a mutant NCOR protein leading to an inability to interact with TR or with the PV mutant. NCOR is a protein which mediates transcriptional repression when recruited by unliganded TRs. NCOR1 $\Delta ID/\Delta ID$ mice have increased sensitivity to thyroid hormone and have reduced levels of T3 and T4 but normal levels of TSH. Although the skeletal phenotype of these mice was not comprehensively described, the reduced IGF1 levels in TR $\alpha 1^{PV/+}$ mice were normalised in TR $\alpha 1^{PV/+}$ NCOR1 $\Delta ID/\Delta ID$ mice and the length of femurs was also partially rescued, suggesting that the dominant negative actions of TR $\alpha 1^{PV}$ are in part due to a defective ability of the mutant TR to release the corepressor NCOR1 (Fozzatti et al., 2013).

The most detrimental effects of hypothyroidism are in mice with defects of thyroid gland agenesis such as in Pax8 $^{-/-}$ mice, where they do not survive beyond weaning, and is more severe than in the absence of TR α alone or dominant negative models such as TR $\alpha 1^{PV/PV}$. Flamant et al reported that the severe phenotype of Pax8 $^{-/-}$ mice can be partially rescued by eliminating TR α , suggesting that unliganded TR α (apo TR α) was responsible for the severe phenotype. This suggestion was challenged by Mittag et al who generated Pax8 $^{-/-}$ TR $\alpha 1^{-/-}$ compound mutants, which similar to Pax8 $^{-/-}$ mice, die shortly after weaning (Flamant et al., 2002, Mittag et al., 2005). This may suggest a role for TR $\alpha 2$ which is non DNA binding and has unknown function.

1.4.8 IMPORTANT SIGNALLING PATHWAYS INVOLVED IN THYROID ACTION IN THE SKELETON

The growth plate is extremely sensitive to thyroid hormone dysregulation during growth. Hypothyroidism results in delayed bone age, however this delayed maturation accelerates and corrects on treatment with thyroid hormone if treated early enough but can result in compromised final height (Rivkees et al., 1988). Conversely, thyrotoxicosis results in advanced bone age with premature fusion of the growth plate.

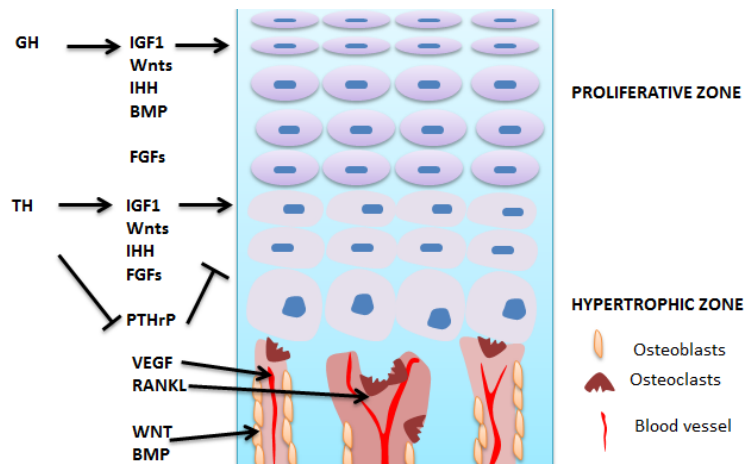


Figure 1.17 Key signalling pathways in the growth plate

This diagram illustrates some of the key signalling pathways in the growth plate. GH and thyroid hormone act on factors secreted by chondrocytes to modify chondrocyte proliferation and hypertrophy. See text for more details.

In 1955, Fell and Mellanby established that thyroid hormone has the direct effect of stimulating chondrocyte maturation *in vitro* by studying the bones of embryonic chicks. Burch et al also demonstrated that porcine scapula and pelvic growth plate cartilage had increased growth and maturation on stimulation with thyroxine *in vitro* (Fell and Mellanby, 1955, Burch and Van Wyk, 1987). Other *in vitro* work looking at markers of chondrocyte differentiation, such as synthesis of type X collagen, AP and cellular hypertrophy, have shown similar effects of thyroid hormone (Burch and Van Wyk, 1987, Ballock and Reddi, 1994, Ohlsson et al., 1992, Quarto et al., 1992).

The relationship between thyroid hormone and the growth hormone/insulin-like growth factor-1 (GH/IGF1) axis was studied using mice with a dominant-negative TR α (TR α 1^{pv/+}) and mice with a dominant-negative TR β (TR β ^{pv/pv}). TR α is the predominant isoform in bone and TR α 1^{pv/+} mice have decreased thyroid signalling in the skeleton whereas TR β is the predominant isoform in the HPT axis and TR β ^{pv/pv} mice have elevated circulating serum thyroid hormone resulting in increased signalling via intact TR α in the skeleton. O'Shea et al demonstrated normal GH production but reduced growth plate chondrocyte GH receptor (GHR) and IGF1 expression in TR α 1^{pv/+} mice. They also demonstrated decreased GH production and increased GHR and IGF1 expression in TR β ^{pv/pv} mice, suggesting that thyroid hormone has a role in the regulation of the GH/IGF1 axis (O'Shea et al., 2006).

The mechanism by which thyroid hormone alters the rate of growth plate maturation is in part via the Ihh/PTHrP axis in the growth plate. PTHrP acts on its receptors in the prehypertrophic

chondrocytes to maintain cells in a proliferative state and prevents maturation of cells into hypertrophic chondrocytes and is therefore important in the Ihh/PTHrP feedback loop (see previous section on chondrocytes). Hypothyroid animals have increased PTHrP mRNA expression in the growth plate (Stevens et al., 2000). Thus, the growth impairment seen in hypothyroidism is likely to be a result of increased expression of PTHrP in the growth plate. In contrast, growth plates of thyrotoxic animals have undetectable expression of mRNA PTHrP receptors. This results in elevated chondrocyte differentiation, thereby resulting in accelerated maturation and early fusion of growth plates (Mackie et al., 2011, Dentice et al., 2005, Stevens et al., 2000).

T3 also acts via FGFRs and there is increased expression of FGFR1 and FGFR3 mRNA and enhanced FGFR2 activation. FGFR3 activation in humans results in acceleration of chondrocyte maturation and achondroplasia. In TR α ^{0/0} mice with decreased skeletal thyroid hormone signalling, there is reduced expression of FGFR3, whilst in TR β ^{-/-} mice with increased skeletal thyroid hormone signalling, there is increased FGFR3 expression, suggesting that FGFR3 may be mediating the action of thyroid hormone on chondrocyte proliferation (Barnard et al., 2005).

In osteoblasts, T3 stimulates cell proliferation, differentiation and apoptosis. Treatment with T3 enhances expression of collagen I, osteocalcin, ALP, MMP9 and MMP13 (Gouveia et al., 2001, Pereira et al., 1999, Varga et al., 2010). *In vitro* osteoblast studies have demonstrated that T3 signals indirectly through the FGFR1 pathway. FGFR1 dependent FGF2 signalling stimulates MAPK in osteoblasts via TR α . Accordingly, Stevens et al showed decreased thyroid hormone signalling in TR α ^{0/0} mice, with osteoblasts and osteocytes having reduced FGFR1 mRNA expression and an absence of T3 stimulated increase in FGFR1 response (Stevens et al., 2003).

Although thyroid hormone clearly increases resorption *in vivo*, the mechanism by which TH acts in osteoclasts is unclear. Osteoclasts express TR α and TR β mRNA but it is unclear if TR proteins are expressed (Abu et al., 2000, Robson et al., 2000). Identifying TR protein expression in skeletal cells is unreliable because available antibodies cannot detect low levels of endogenous TRs expressed in target tissues, even though they are specific and reliable for measurement of TR over-expression *in vitro* or following transfection (Abu et al., 2000, Kanatani et al., 2004, Robson et al., 2000, Stevens et al., 2000, Williams and Franklyn, 1994, Bassett and Williams, 2003, Saraiva et al., 2008). Experimental data as to whether thyroid hormone acts directly or via a secondary cell such as osteoblasts, is conflicting in the literature. Kanatani et al demonstrated that T3 directly stimulates spleen derived osteoclast formation (Kanatani et al., 2004). By contrast, Allain et al reported that the resorptive activity of calvarial derived osteoclasts did not increase with T3, corroborating findings by Miura et al suggesting that thyroid hormone stimulation of osteoclast activity is

secondary to action in osteoblasts (Allain et al., 1992, Miura et al., 2002, Harvey and Williams, 2002). Currently, it is not known if TRs are expressed in osteocytes and further studies are needed to detail the cell specificity and temporal expression of TR.

To summarise, thyroid hormones are essential in the normal development and maintenance of the healthy skeleton. T3 availability is finely controlled on a systemic and cellular level. Disruption to thyroid signalling can result in compromise to skeletal health.

1.4.9 THYROID STIMULATING HORMONE

The catabolic effects of thyrotoxicosis have mostly been attributed to increased genomic action of liganded skeletal thyroid receptors. However, one group proposed that thyrotoxic changes were instead due to a lack of the osteoprotective effects of TSH. Mice with absent TSH receptors (TSHR) and congenital hypothyroidism were treated with thyroid hormone and were found to have high turnover osteoporosis. This finding was interpreted to be due to the lack of TSHR action and was supported with *in vitro* studies showing that TSH inhibits both osteoclast and osteoblast activity (Abe et al., 2003). This data conflicts with clinical data in which patients with TSH antibodies – Graves' disease, for example - have a high turnover osteoporosis and patients with RTH (where there is a mutation in TR β , which gives rise to high circulating TSH and thyroid levels) also have a high turnover osteoporosis. To investigate this relationship, the skeletal phenotypes of two mice with congenital hypothyroidism were compared. Pax8 mice, with a mutation resulting in thyroid follicular cell agenesis, hypothyroidism and 2000-fold elevated TSH were compared with *hyt/hyt* mice, which lacked all TSHR signalling but exhibited hypothyroidism and 2000-fold elevated TSH (Bassett et al., 2007b). Both of these mice types therefore had elevated TSH and hypothyroidism but Pax8 mice had maximum TSH signalling whereas *hyt/hyt* mice had no TSH signalling. The findings of similar skeletal phenotypes indicate that the major HPT axis regulator of skeletal development is thyroid hormone and not TSH. TSH could have a minor role in modulating the skeleton and low doses of TSH were found to prevent ovariectomy induced bone loss (Sun et al., 2008, Sampath et al., 2007).

1.5 OESTROGEN

In adults, oestrogen is important for reproduction, cardiovascular and bone health, and cognition. Oestrogen levels are low prepubertally, when a large proportion of growth takes place indicating that oestrogen is not essential during this phase of development. However, after puberty, oestrogen becomes integral to the maintenance of skeletal integrity. Oestrogen withdrawal in women at the menopause, or earlier where due to ovarian failure, results in an increased turnover and accelerated loss of bone (Clarke and Khosla, 2010a).

Studies have also shown that up to 70% of effects of sex steroids on bone in men are accounted for by oestrogen (Falahati-Nini et al., 2000). Oestrogen deficiency in men can be as a result of aromatase deficiency which leads to diminished oestrogen production or due to a non functional oestrogen receptor (ER) (Khosla et al., 1998, Adler, 2011, Smith et al., 1994).

1.5.1 OESTROGEN SYNTHESIS

Oestrogen is a steroid hormone which is synthesised from cholesterol. There are three main physiological oestrogens: 17 β -estradiol (E2); estrone (E1) and estriol. During the reproductive years, E2 is the major physiological oestrogen. Oestrogens are present in males and females and are synthesised from cholesterol via androgens produced in principal by the ovaries in females, the testes in males but also from the adrenal glands in both sexes. Androgens are converted to oestrogens via aromatase, an enzyme in the cytochrome P450 family. The relative production of oestrogen is target tissue dependent. The ovaries express large amounts of aromatase enzyme and 95% of E2 is therefore secreted by the ovaries in premenopausal women. Post menopause, the majority of oestrogen is derived from the peripheral conversion of adrenal androgens to oestrogens.

1.5.2 HOMEOSTATIC CONTROL OF OESTROGEN

Circulating oestrogen serum concentrations are low in childhood, rise with the onset of puberty (usually around 12.8 y) and decline after the menopause. Premenarchal children have low levels of gonadotrophin releasing hormone (GnRH), luteinising hormone (LH), follicle stimulating hormone (FSH) and E2 but as they approach puberty, the ovaries respond to pulsatile release of FSH and LH from the anterior pituitary gland to begin production of E2. Premenopausal women have a tightly regulated cycle of events leading to ovulation, on average every 28-32 days. Decreased ovarian function in postmenopausal women leads to a decrease in serum E2 levels by 85-90%.

Serum oestrogen levels are regulated by a classical negative feedback loop in the hypothalamic-pituitary-ovarian axis. The menstrual cycle is divided into two phases: the follicular or proliferative phase and the luteal or secretory phase. Ovulation and menstruation separates these two phases (see Figure 1.18).

In premenopausal women, pulsatile GnRH from the hypothalamus stimulates the pituitary to release gonadotrophins FSH and LH, which act by specific membrane receptors in the ovaries to induce oestrogen secretion. At lower concentrations, oestrogen levels negatively feed back to the hypothalamus and pituitary gland to decrease gonadotrophin release. Feedback also occurs via other hormones that are produced by the ovaries such as inhibins, which down regulate FSH synthesis and secretion, and activins, which stimulate FSH synthesis and secretion. Inhibin A begins to be produced in early and mid follicular phase and reaches a peak in the luteal phase. Inhibin B peaks during the follicular phase in response to rising FSH levels and inhibits FSH, resulting in a plateau in the FSH levels in the mid follicular phase.

When concentrations of oestrogen have reached a peak, negative inhibition of GnRH and gonadotrophins reverses and positive feedback results in a surge of GnRH secretion, coupled with an increased responsiveness of the pituitary gland to GnRH. The resultant rise in FSH and LH concentrations induces ovulation. After ovulation, oestrogen levels fall as hypothalamic-pituitary feedback again becomes negative. Progesterone levels, produced by the ovaries, are low during the follicular phase and start to rise and peak just after the FSH/LH peak. The levels then fall, unless the ovum is fertilised.

At the menopause, there is reduced gonadal function with decreased oestrogen secretion, which results in a loss of negative feedback and results in elevation of GnRH, FSH and LH (Clarke and Khosla).

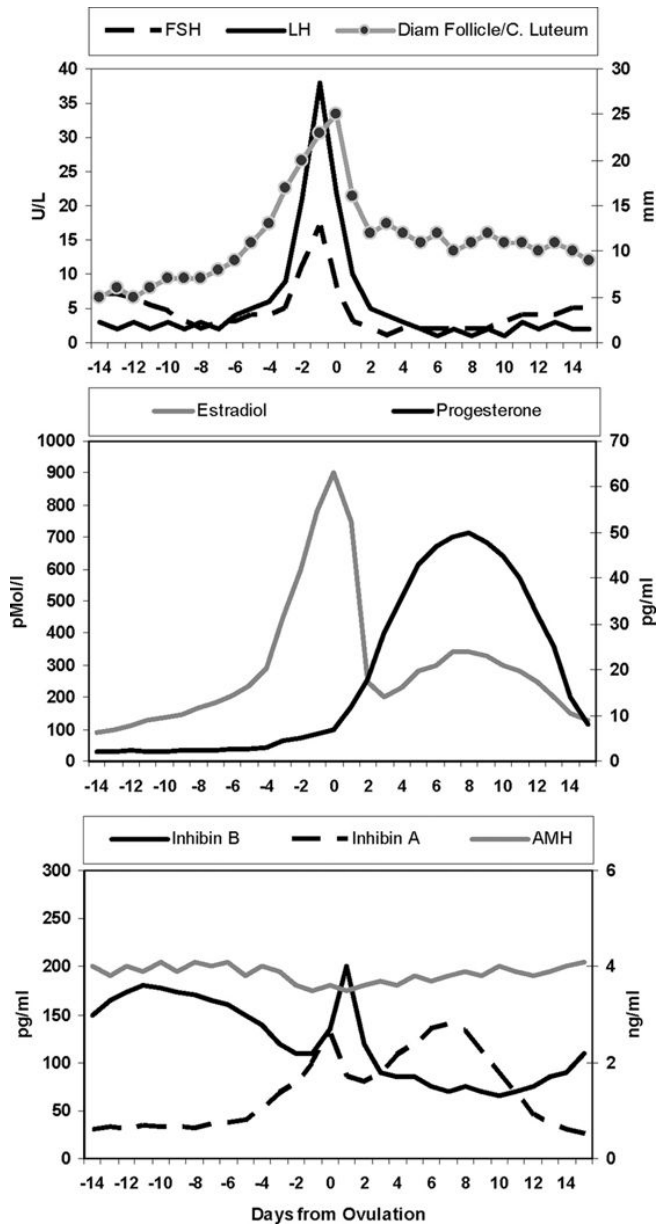


Figure 1.18 Serum hormone concentrations and follicular growth during the menstrual cycle

Taken from Broekmans FJ 2009 with permission (Broekmans et al., 2009).

See text for detail.

1.5.3 LOCAL CONTROL OF OESTROGEN LEVELS

Oestrogen is predominantly bound to sex-hormone-binding globulin (SHBG) and with less affinity to albumin, with 2-3% of the active hormone in the free state. Conversion of androgens to oestrogen is effected via aromatase. Androgens in males are predominantly produced in the testes, the most important being testosterone, however the adrenal cortices also secrete large amounts of dehydroepiandrosterone (DHEA), DHEA sulphate and androstenedione. These androgens can be metabolised to E1, 5 α -dihydrotestosterone (DHT) or testosterone. In the skeleton, enzymes important in the synthesis of oestrogens such as aromatase and biologically active androgens are present, which may contribute to a degree of local control of hormone availability. Currently, there are no known transmembrane transporters of oestrogen and it is thought that oestrogen passively diffuses into cells (Miller, 1979, De Ryck et al., 1985, Muller and Wotiz, 1979).

1.5.4 MOLECULAR MECHANISMS OF OESTROGEN ACTION

The biological effects of oestrogen are mediated via genomic and non genomic pathways. Genomic action involves the binding of oestrogen to ERs and can activate gene transcription either by direct binding to DNA at specific, inverted palindromic sequences known as oestrogen response elements (EREs) or indirectly by associating with transcription factors involved in DNA binding. ERs can also be found bound to the membrane and from there mediate non genomic signalling.

1.5.4.1 Oestrogen receptors

Oestrogen binds to two nuclear receptors: oestrogen receptor alpha (ER α) and oestrogen receptor beta (ER β), mapped to chromosomes 6q25.1 and 14q23-24 respectively. G protein-coupled receptor (GPCR) was reported to be a membrane associated ER, however the status still remains unclear as some studies suggest that it may not be an ER at all (Filardo and Thomas, 2012, Langer et al., 2010, Levin, 2009). ERs like TRs belong to the nuclear hormone receptor family and share a similar structure (see Figure 1.12). They are found in the cytoplasm and nucleus and can shuttle in between the two. They are complexed, in the absence of ligand, to heat shock proteins (eg hsp56, hsp90) which are then released on binding to oestrogen. The liganded ERs bind to DNA hormone response elements as homodimers or ER α -ER β heterodimers (Pettersson et al., 1997, Klinge, 2001). This differs from thyroid receptors which principally bind as heterodimers with RXR.

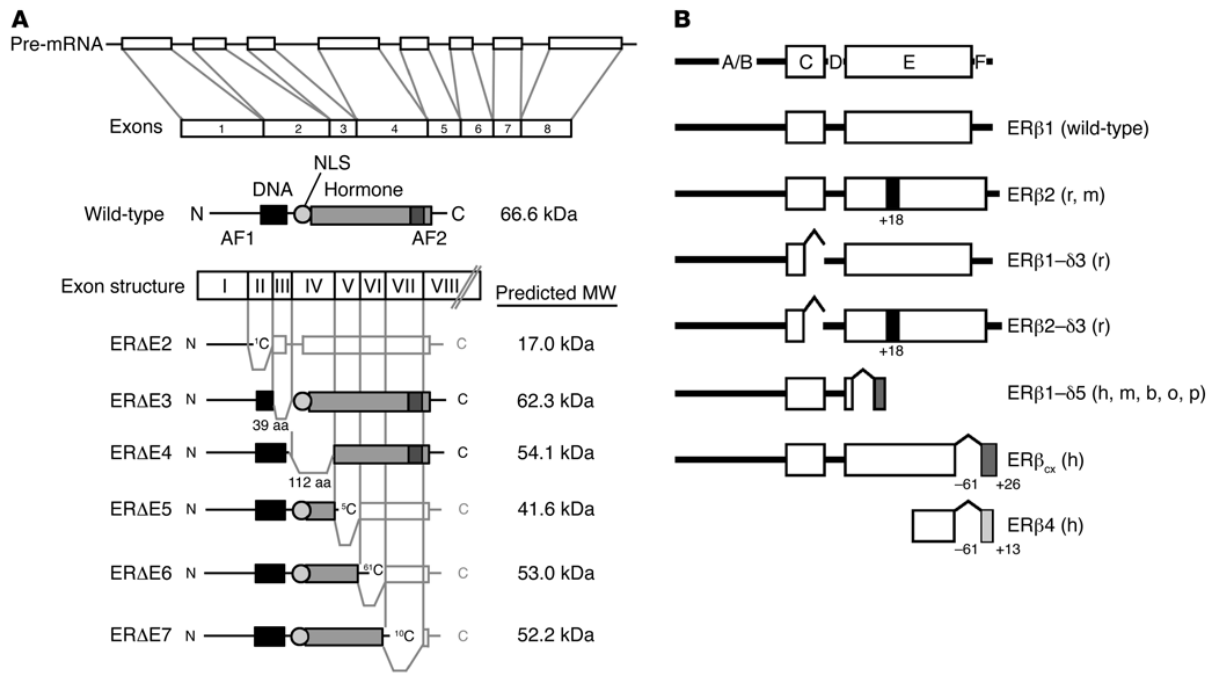


Figure 1.19 ER isoforms

Illustration of the different isoforms of ER α and β and whether they are found in rats (r), mice (m) or humans (h).

Reproduced with permission from Deroo, B 2006 (Deroo and Korach, 2006).

In animals, there have been several isoforms of ERs described. In healthy humans, there have been six characterised alternative splice variants. They all produce a common human ER α protein that is 66 kDa in size (Flouriot et al., 1998). A further, smaller 46kDa ER α protein which does not possess an A/B region had also been identified, which is generated by alternative splicing of the ER α gene and acts as a competitive inhibitor for AF-1 (Flouriot et al., 2000). Other human ER isoform variants have been described in the literature but have been mainly isolated from human cancer cell lines (Vladusic et al., 1998, Pfeffer et al., 1996, Karas et al., 1995). No alternative isoforms of human ER β have been described as yet.

Similar to TRs, ERs have six domains A-F (see Figure 1.19). The N terminus contains a weak ligand-independent transcription activating function-1 (AF-1). The C domain or DNA binding domain contains zinc finger-like motifs that are involved in binding to the EREs. This is the most highly conserved area (>95%) (Pace et al., 1997) between the two receptors and means that ER α and ER β bind to the same DNA sequences. The hinge domain (D region) is important in receptor dimerisation and for binding to heat-shock proteins. The C terminus, containing the LBD and activating function-2 (AF-2), is not well conserved, suggesting that the different isoforms may bind different ER specific ligands.

Er α has five times the affinity for binding to E2 than Er β (Kuiper et al., 1997). Ligand bound ERs undergo conformational change and dimerise as homodimers or Er α -Er β heterodimers. Gene transcription occurs via binding of receptors to EREs in promoter regions of genes. Binding of AF-1 and AF-2 to cofactors results in association with the basal transcriptional machinery to promote gene transcription (Imai et al., 2009).

1.5.4.2 Coactivators and corepressors

Similar to TRs, liganded ER interacts with co-activators to promote gene transcription. Coactivators such as acetyltransferases enable an open chromatin structure and allow transcriptional machinery to access DNA (Klinge et al., 2004).

Unlike TRs, ERs do not typically repress transcription in the absence of hormones, but may have certain repressive functions by interacting with corepressors such as NCOR and SMRT when bound to hormone antagonists such as tamoxifen (Varlakhanova et al., 2010).

1.5.5 THE EFFECTS OF REDUCED OESTROGEN SIGNALLING IN THE SKELETON

1.5.5.1 Postmenopausal osteoporosis

Age related bone loss in women is most pronounced during oestrogen withdrawal at the menopause. Cross sectional and longitudinal population studies have shown a period of rapid bone loss which lasts for about 10 years after the menopause, after which the rate of bone loss becomes similar to that of men (see Figure 1.20) (Clarke and Khosla, 2010a). Bone resorption markers increase by 90% after the menopause but this is only accompanied by a 45% increase in bone formation markers.

Oestrogen withdrawal has the greatest detrimental effect on cortical bone, with density remaining fairly consistent in adults until the menopause. Subsequently, there is an increase in distal forearm fractures around the time of menopause, which plateaus about 15 years after the menopause (Cooper and Melton, 1992). Trabecular bone loss commences at the third decade and continues throughout life with a small acceleration at the menopause (Khosla et al., 2006). There is therefore an increase in the number of vertebral compression fractures at the menopause, a factor which continues to increase throughout the woman's lifespan.

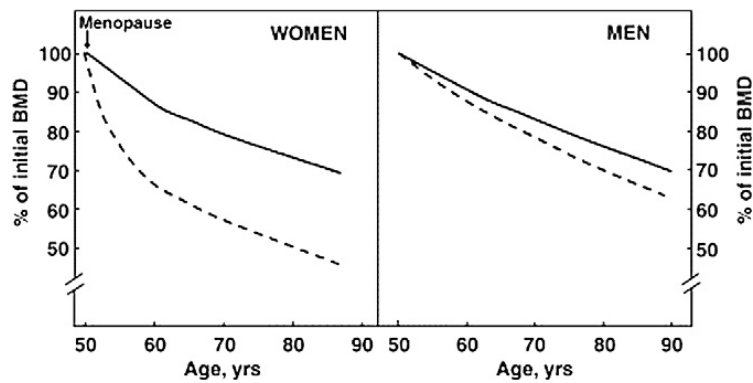


Figure 1.20 Decline in BMD in men and women

Post-menopausal decline in BMD is accelerated for about a decade, after which the rate of bone loss becomes similar to that of men. The dashed lines represent trabecular bone whilst the solid lines represent cortical bone.

Reproduced from Clarke 2010 (Clarke and Khosla, 2010b).

1.5.5.2 Ovariectomy in animal models

The effects of postmenopausal oestrogen withdrawal on the skeleton cannot be adequately recapitulated by ER knockouts (see next section), with these animal models still undergoing ovariectomy induced bone loss. Currently, ovariectomy in rodents is the most widely used model to study the skeletal effects of postmenopausal oestrogen deficiency (Jee and Yao, 2001). Following ovariectomy, rapid loss of cancellous mass consisting of decreased Tb.N and thickness, increase in bone formation, increased resorption and reduction in biomechanical strength recapitulates human menopause or oophorectomy (Egermann et al., 2005). The rat is the established animal model of OVX induced oestrogen deficiency, but the ovariectomised (OVX) mouse model has been the most widely used to understand physiological mechanisms for diseases such as osteoporosis (Iwaniec et al., 2006). Despite widespread use of ovariectomy as a model of oestrogen deficiency, there are various shortcomings of this model. For example, site specific and magnitude responses to ovariectomy are strain/background dependent (Iwaniec et al., 2006). Additionally, small rodents lack osteonal remodelling of cortices, so changes in cortical bone inadequately reflect human responses (Bouxsein et al., 2005, Iwaniec et al., 2006).

1.5.5.3 Aromatase deficiency in humans

Androgens in males and females exert an anabolic effect on bone directly via androgen receptors in bone cells and indirectly via aromatisation to oestrogens. Men with aromatase deficiency such as those with mutations in the CYP19 gene (Bouillon et al., 2004, Gennari et al., 2004, Lanfranco et al.,

2008, Rochira et al., 2007) also have reduced bone mass which improves on treatment with oestrogen therapy but not androgen treatment (Carani et al., 1997). Treatment of children by the use of aromatase inhibitors or GnRh analogues can lead to reduced bone mass (Hero et al., 2005).

1.5.4.4 Aromatase knockout mice

Two different groups, Miyaura et al and Oz et al, studied the effects of targeted disruption of the aromatase gene. These animals had both *in vivo* evidence of oestrogen insufficiency with uterine atrophy and elevated circulating testosterone levels. Female ArKO mice had increased bone turnover and osteopenia, a bone phenotype similar to postmenopausal osteoporosis in humans. The results for males, however, conflicted between the two groups, with Oz et al reporting a decrease in formation and resorption parameters and Miyaura et al reporting elevated formation and resorption parameters. It is evident however that there is a sexually dimorphic response to oestrogen (Miyaura et al., 2001, Oz et al., 2000). Although aromatase knockout mice are oestrogen insufficient, they do not recapitulate the bone phenotype of postmenopausal bone loss as closely as ovariectomy.

1.5.5.5 Oestrogen resistance in humans due to ER mutation

The importance of oestrogen in men's skeletal health was first noted in a report of osteoporosis and delayed bone maturation with unfused growth plates in a 28 year old man with Er α mutation (Smith et al., 1994). Recently, an 18 year old female with a mutation in Er α was reported to have a low bone mass with a Z score of -2.4, a delayed bone age and open epiphyses. She also had elevated osteocalcin, bone ALP and serum C-telopeptide levels, consistent with a high turnover osteoporosis (Quaynor et al., 2013). No patients with Er β have yet been described.

1.5.5.6 ER animal knockout models

Knockout mice of Er α , Er β and of both receptors have been generated. The skeletal phenotypes are not in line with oestrogen deficiency bone loss and are dissimilar to the recently described female patient with an Er α mutation, but they have still provided insights into the molecular role of these receptors in oestrogen signalling.

1.5.5.7 Er α and Er β knockout mice

Global ER α knockout mice (ER α KO) that had no detectable mRNA for Er α were found to be infertile and had elevated circulating levels of oestrogen and androgen (Dupont et al., 2000). Unexpectedly, these mice had decreased, rather than increased, bone turnover. These mice also had increased cortical bone thickness and elevated BMD and trabecular bone volume. Ovariectomy-induced bone loss occurs in ER α KO mice and this can be partially rescued with oestrogen treatment, resulting in an increase in BMD in the trabecular but not cortical compartment (Sims et al., 2003, Windahl et al., 2002).

Two complete Er β KO mice were generated and were shown to have no detectable Er β protein on analysis by immunohistochemistry (Krege et al., 1998, Dupont et al., 2000). Males and females had differing responses to deletion of Er β . Males were unaffected by the deletion whilst females had decreased bone resorption and increased trabecular bone volume but no change in cortical bone thickness (Sims et al., 2002). Circulating oestrogen and androgens were not elevated in Er β KO mice and such mice were not protected against gonadectomy induced bone loss, but similarly to Er α KO mice, could be rescued with oestrogen therapy (Lindberg et al., 2002).

A double knockout of Er α and Er β was generated by crossing Er α KO and Er β KO mice. These mice did not have elevated testosterone or oestrogen levels. Female mice had decreased trabecular bone, associated with a decrease in bone turnover (McCauley et al., 2003, Sims et al., 2002). Ovariectomy in these osteoporotic mice is less clear in the literature, with one group showing no further bone loss (Sims et al., 2002) and another demonstrating OVX induced bone loss (Windahl et al., 2002).

These knockout mouse models were informative as they indicated that in the absence of either ER, the other could at least partially compensate and that the skeletal phenotype was more severe in the double knockout mice.

The literature shows that both Er α KO and Er β KO mouse models were not protected against gonadectomy induced bone loss. Studies also showed that the double knockout mouse model underwent ovariectomy induced bone loss, which suggests one of the following mechanisms was in effect: oestrogen acts via non genomic actions, there is some low affinity binding of oestrogen to other nuclear receptors or bone loss may be indirect such as oestrogen having an effect on the liver or pituitary gland.

Treatment with oestrogen rescued trabecular BMD in wild type and Er β KO ovariectomised mice, but not in Er α KO mice, demonstrating that oestrogen signalling in the trabecular compartment is Er α dependent.

To clarify the effects of oestrogen in osteoclasts, Er α was specifically deleted in these cells by two research groups using cre-lox recombination technology. ER mutant mice have a floxed allele of Er α and deletion occurs following exposure to cre-recombinase, which excises by cutting DNA at loxP sites and recombining the cut loxP sites. Thus, depending on the cre-recombinase used, cell specific gene deletion can be generated.

Nakamura (Nakamura et al., 2007) created a mouse model where cre-recombinase was inserted into the gene locus of *Cathepsin K* (a gene expressed in mature osteoclasts) and crossed these mice with floxed Er α mice to produce animals which had excised Er α only in differentiated osteoclasts (Er $\alpha^{\Delta oc/\Delta oc}$). Likewise, Martin-Millan et al (Martin-Millan et al., 2010) generated a mouse model with restricted Er α in osteoclasts but used a cre recombinase under the control of the promoter of the *LysM* gene, which is expressed in early osteoclast precursors (Er $\alpha_{LysM}^{-/-}$). Both osteoclast specific deletions of Er α resulted in a loss of trabecular bone mass compared to controls, with an increase in osteoclast indices in females. Ovariectomy in these conditional knockout mice did not show the expected increases in trabecular osteoclast indices or a reduction in bone density, but in the Er $\alpha_{LysM}^{-/-}$ mice, there was a loss of cortical bone. Taken together, these results suggest that the osteoprotective action of E2 in the trabecular compartment was via Er α in osteoclasts, whereas this did not appear to be the case in the cortical compartment. Nakamura et al also identified that the proapoptotic effect of oestrogen on osteoclasts was mediated by FasL, which was later confirmed by Krum et al (Krum et al., 2008).

Martin-Millan further created a mouse model with an osteoclast specific knockin of Er α , which prevents binding to DNA (Er $\alpha^{NERKI/-}$), thus leaving any nongenomic actions of Er α intact. These mice responded to ovariectomy in a similar manner to controls, suggesting that the non genomic mechanisms of Er α in osteoclasts are important.

	Er α KO	Er β KO	Er $\alpha\beta$ KO	OcER α KO	OVX
Trabecular BMD	↑	↑	→	↓	↓
Cortical BMD	↓	→	↓	→	↓
BV/TV	↑	↑	↓	↓	↓
Bone formation	↓	→	↓	↑	↑
Bone resorption	↓	↓	→	↑	↑

Table 1.1 Bone phenotype of ER deficient mice

Summary of oestrogen receptor (ER) α , β , $\alpha\beta$ and osteoclast (Oc) specific knockout (KO) bone phenotypes compared to ovariectomy in female mice. ↓ decrease, ↑ increase, → no difference.

In summary, the data from the knockout mice suggest that Er α and Er β are able to compensate for each other but that Er α is the predominant receptor in bone. The bone phenotype of ER knockout mice was less severe than that from ovariectomy induced oestrogen deficient mice, which suggests that the non genomic effects of oestrogen are important in the maintenance of bone health. Whilst these knockout mice provide important insights into the roles of specific ERs, ovariectomy is a more representative animal model of postmenopausal bone loss.

1.5.6 IMPORTANT SIGNALLING PATHWAYS INVOLVED IN OESTROGEN ACTION IN THE SKELETON

Whereas the growth plate is extremely sensitive to thyroid hormone status during growth, the serum levels of oestrogen during growth are minimal, suggesting that during this phase, chondrocyte proliferation and maturation is oestrogen independent. Oestrogen is, however, important during the growth spurt and for the final fusion of the growth plate.

Er α and Er β have been shown to be expressed in all bone cells - osteoblasts, osteocytes and osteoclasts (Bord et al., 2001, Braidman et al., 2001). The relative role of oestrogen on each different cell type in the control of bone mass is not yet completely understood but the effect on osteoclasts has been extensively studied. In contrast to TRs, where the presence of receptors in osteoclasts has not been conclusively established, ERs have been shown to be present in osteoclasts, and studies of osteoclast specific deletions of Er α have demonstrated a decrease in trabecular bone mass (Martin-Millan et al., 2010, Nakamura et al., 2007).

The predominant effects of oestrogen on bone are inhibition of new osteoclast formation, increase in osteoclast apoptosis and inhibition of osteoblast and osteocyte apoptosis (Nakamura et al., 2007). Conversely, oestrogen deficiency results in high bone turnover with increased osteoclast activity, leading to accelerated bone loss and an increased risk of osteoporosis and fracture. In humans, bisphosphonates, with their potent inhibition of osteoclastic bone resorption, are the most commonly used treatment for postmenopausal osteoporosis (Bock and Felsenberg, 2008).

Although there is extensive literature on the downstream pathways important in oestrogen signalling in osteoclasts, it is clear that RANK-RANKL-OPG is a key pathway. *In vivo* and *in vitro* studies have shown that RANKL production is suppressed by E2 in osteoblasts, T lymphocytes and B lymphocytes (Eghbali-Fatourehchi et al., 2003, Clowes et al., 2005, Hsu et al., 1999, Kimble et al., 1996, Onal et al., Pacifici, 2007). E2 increases OPG and TNF β production in osteoblasts (Hofbauer et al., 1999, Shevde et al., 2000), whilst suppressing the production of bone-resorbing cytokines such as IL1, IL6, TNF α , Macrophage colony stimulating factor (M-CSF) and prostaglandins (Riggs, 2002, Lorenzo et al., 1998, Poli et al., 1994). Direct effects of oestrogen attenuate the RANKL pathway via reduction of c-jun and TRAF6, resulting in decreased NF- κ B activation (Huber et al., 2001, Shevde et al., 2000, Srivastava et al., 2001, Robinson et al., 2009).

In osteoblasts, oestrogen deficiency was shown to result in an increase in NF- κ B activity in osteoblasts and inhibition of this activity mitigated ovariectomy induced bone loss (Chang, 1966). Er α is important in osteoblasts for the nuclear translocation of β -catenin in response to strain (Zaman et al., 2000). Studies in premenopausal women and mice suggest that oestrogen deficiency results in a four-fold increase in osteocyte apoptosis (Tomkinson et al., 1997). *In vitro* studies also confirm that oestrogen can prevent induced apoptosis in an osteocyte like cell line (Emerton et al., 2010). In contrast, a study using osteocyte specific DMP1 cre mice, where Er α had been deleted, failed to show any increase in osteocytic apoptosis (Khosla et al., 2012).

1.5.7 FOLLICLE STIMULATING HORMONE

FSH stimulates the ovarian follicles to release oestrogen, which negatively feeds back on the hypothalamic pituitary axis to reduce the production of FSH. Just prior to the menopause, FSH becomes elevated to maintain normal oestrogen levels and bone loss begins. During the perimenopausal phase and prior to complete ovarian dysfunction, oestrogen levels begin to fall. Studies have shown that bone turnover markers correlate more closely to serum FSH levels than to oestrogen levels. Additionally, changes in hip and spine BMD correlated better with longitudinal FSH levels than androgen or oestrogen levels (Ebeling et al., 1996, Sowers et al., 2006). Due to the clinical evidence and the reciprocal relationship between FSH and oestrogen, it was proposed that menopausal related bone loss was secondary to high levels of FSH rather than loss of oestrogen (Sun et al., 2006, Zhu et al.). FSH receptor null (FORKO) mice with gonadal dysfunction had normal bone mass and it was found that FSH but not LH could induce osteoclast formation and function *in vitro*. Furthermore, a FSH blocking antibody injected into ovariectomised FORKO mice inhibited osteoclast resorption and increased bone formation (Sun et al., 2006, Zhu et al.). These results seem to confirm the hypothesis that increases in FSH, and not loss of oestrogen, is the principal hormone implicated in postmenopausal bone loss. However, additional studies showed that androgen levels were elevated in FORKO mice and it was suggested that this factor had led to normal BMD rather than the lack of FSH signalling. When bilateral ovariectomy was performed on these animals, and there was a fall in androgen levels, there was a consequent decrease in bone mass (Gao et al., 2007a).

Clinical studies also examined the hypothesis that rising FSH levels lead to bone loss - postmenopausal women were administered a GnRH agonist to suppress circulating FSH levels and the results were compared to controls. An aromatase inhibitor was also given to both groups to prevent the effects of any oestrogen production from androgen. The results showed that despite the treatment group having low FSH and the control group having very high FSH, there was no difference in bone resorption markers CTX and TRAP5b (Drake et al., 2010) and so concluded that in humans, lack of oestrogen and not elevated FSH was the major contributor to postmenopausal bone loss. There is a degree of controversy surrounding the role of FSH in the skeleton and like TSH, there may be a minor role that FSH contributes to skeletal physiology.

1.6 SIMILARITIES OF OESTROGEN AND THYROID HORMONE ACTION ON BONE

The actions of oestrogen and thyroid hormone are essential for the optimal maintenance of bone mass. Both hormones act via receptors that belong to the nuclear receptor superfamily. Both circulating hormone levels are controlled by negative feedback mechanisms involving the hypothalamic pituitary axis and are transported in the circulation via binding proteins. They bind to hormone specific receptors which act as ligand inducible transcription factors and these receptors bind to hormone response elements on DNA to induce transcription of key genes. Both oestrogen and thyroid hormone receptors dimerise and bind with coactivators. The actions of oestrogen and thyroid hormone have opposing effects on bone. Oestrogen deficiency and thyrotoxicosis both result in a high turnover osteoporosis. A comparison of oestrogen and thyroid hormone actions on bone are summarised in Table 1.2. Based on the evidence demonstrating the similarities in the way oestrogen and thyroid hormone act on bone with balanced but opposing effects, I hypothesised that at the menopause, the actions of thyroid hormone on bone are unopposed following oestrogen withdrawal, leading to accelerated bone loss and fracture.

Table 1.2 Comparison between the actions of thyroid hormone and oestrogen in the skeleton

	Thyroid Hormone	Oestrogen
Control of circulating serum levels	Negative feedback to pituitary and hypothalamus	Negative feedback to pituitary and hypothalamus
Binding proteins	TGB, TTR and Albumin	SHBG, Albumin
Main Receptors	TR α and TR β	ER α and ER β
Dimerisation	Predominantly with RXR but heterodimers or homodimers	Heterodimers with ER α and ER β or homodimers.
Transport into cells	Active via transporters such as MCT8 and 10, LAT1 and 2	Passive
Intracellular modification	Activation or inactivation by deiodinases	Binding to hsp, which is released upon binding to ER
Co regulatory molecules	Co activator and co repressor	Co activator
Repression in absence of hormone	Yes	No
Action on skeleton during growth	Essential and anabolic	Only after puberty
Action on mature skeleton	Catabolic	Anabolic
High turnover osteoporosis	Excess	Deficiency

1.7 EXPERIMENTAL DESIGN

1.7.1 Hypothesis

I hypothesise that at the menopause, the actions of thyroid hormone on bone are unopposed following oestrogen withdrawal, leading to accelerated bone loss and fracture.

1.7.2 Aims

I aim to:

1. Compare the bone phenotypes of TR α ^{0/0} and TR β ^{-/-} mice to hypothyroid and hyperthyroid wild type mice.
2. Establish the effects of altered thyroid status on TR α ^{0/0} and TR β ^{-/-} mice.
3. Characterise the effects of ovariectomy or sham operation on the bone phenotype of thyroid status manipulated wild type, TR α ^{0/0} and TR β ^{-/-} mice.

Chapter 2

Materials and methods

2 MATERIAL AND METHODS

2.1 GENETICALLY MODIFIED MICE

All strains of mice are housed in the registered CBS facility at Imperial College. Breeding, handling and experimental procedures have been followed in accordance with Home Office guidance. Project Licence 70/7188.

2.1.1 TR α ^{0/0} MICE

TR α ^{0/0} mice were obtained from Professor J. Samarut of Ecole Normale Supérieure, 46 allée d'Italie, 69364 Lyon, France. These mice were generated using TR α gene inactivated blastocysts from 129SV mice which were implanted into C57 black6 mothers. The mutant TR α allele contains a deletion extending from the middle part of intron 4 to the beginning of exon 8. These mice are devoid of all known TR α isoforms produced by the TR α locus (Gauthier et al., 2001).

2.1.2 TR β ^{-/-} MICE

TR β ^{-/-} mice were also obtained from Professor J. Samarut. These mice were generated using TR β gene inactivated blastocysts from 129SV mice which were implanted into C57 black6 mothers. The TR β gene was inactivated by targeted insertion of a recombination cassette downstream of exon 3 (Gauthier et al., 1999). TR β ^{-/-} mice are devoid of all known *Thrb* isoforms.

2.2 GENOTYPING OF MOUSE STRAINS

2.2.1 DNA EXTRACTION

Genomic DNA was extracted for genotyping using mouse ear-clip samples using the REDExtract-N-Amp Tissue PCR Kit (Sigma Aldrich, UK). 50 μ l extraction buffer and 12.5 μ l tissue preparation solutions were added to the samples in 1.5ml microtubes and incubated for 15 minutes at 37°C. Samples were then incubated at 95-98°C for 3 minutes and 50 μ l neutralisation solution added prior to removal of remaining tissue and storage at 4°C.

2.2.2 POLYMERASE CHAIN REACTION (PCR)

Genotyping PCR was performed using 2 μ l of DNA solution as template (see Appendix for PCR mix).

PCR primers and conditions were:

Thra

TR α wild type allele

Forward Primer: GAGGAGGCGAAAGGAGGAG

Reverse Primer: TGCCCTGGGCGTTAGTGCTG

TR α mutant allele

Forward primer: ATCGCCTTCTATCGCCTTCTTGACG

Reverse primer: TTCAGGAGGATGATCTGGTCTTCGCAAG

PCR conditions:

95⁰C for 7 mins then 5 cycles of 94⁰C for 20 secs (denaturing), 60⁰C for 20 secs (annealing), 72⁰C for 60 secs (extending) followed by 27 cycles of 94⁰C for 20 secs (denaturing), 56⁰C for 20 secs (annealing), 72⁰C for 60 secs (extending) followed by a final extension at 72⁰C for 10 mins.

Thrb

TR β wild type allele

Forward primer: TGGTGCTGGATGACAGCAAG

Reverse primer: CAGGAATTTCCGCTTCTGCTT

TR β mutant allele

Forward primer: GCCAGAACAATTGCTCTTATTC

Reverse primer: CCTCTTCGCTATTACGCCAG

PCR conditions:

95⁰C for 7 mins followed by 35 cycles of 94⁰C for 30 secs (denaturing), 60⁰C for 30 secs (annealing) and 72⁰C for 30 secs (extending) followed by a final extension at 72⁰C for 10 mins.

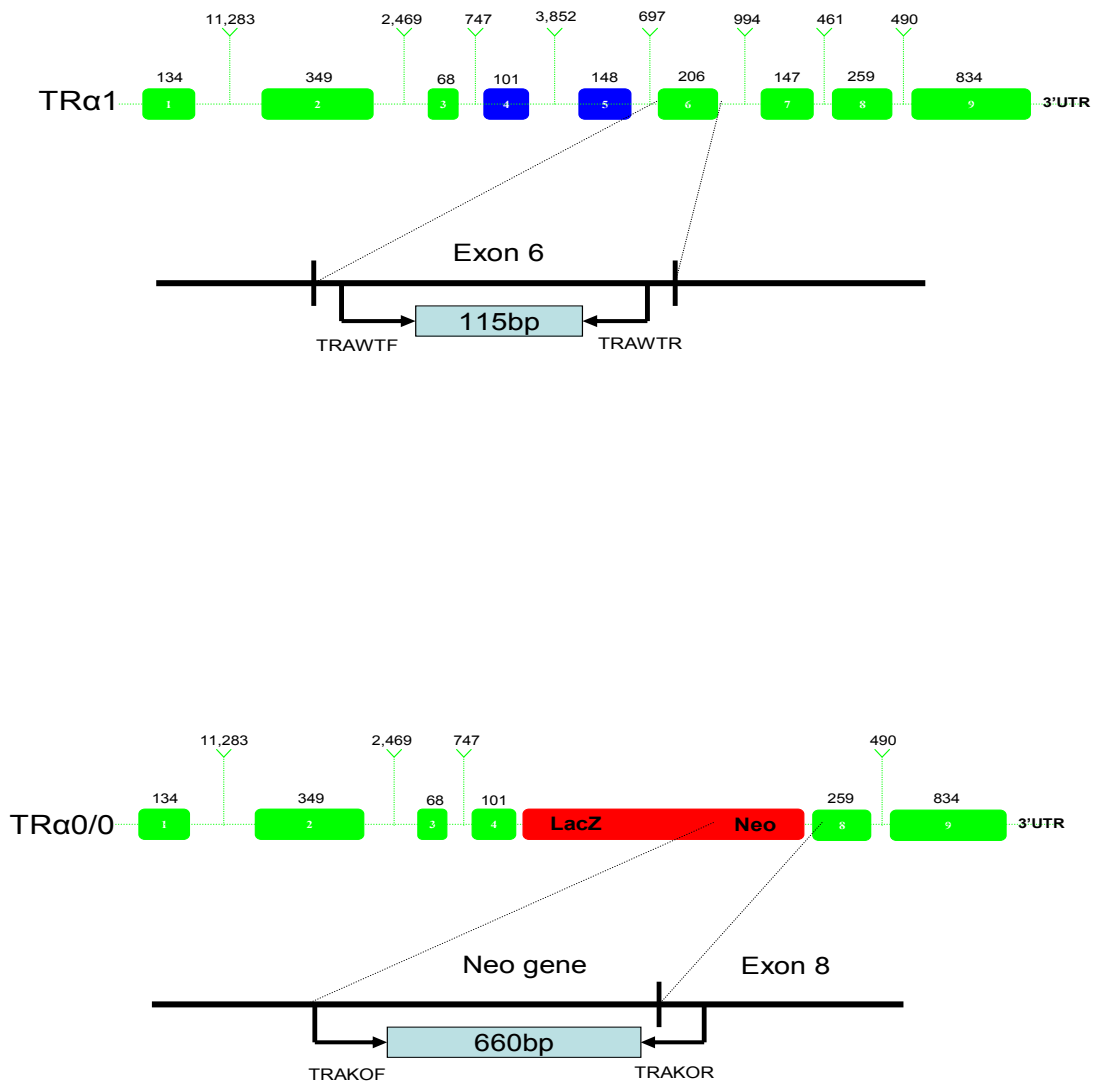


Figure 2.1 Primer locations for identification of wild type and mutant TRα alleles

TRα^{0/0} is constructed from a deletion from intron 4 to 8. Exons are shown as rectangles with the number of base pairs in numerals above. Figures above indicate the position of the primers for the wild type (TRα1) and mutant TRα allele (TRα^{0/0}) and the resultant PCR product size. Illustrations by Dr T. Galliford.

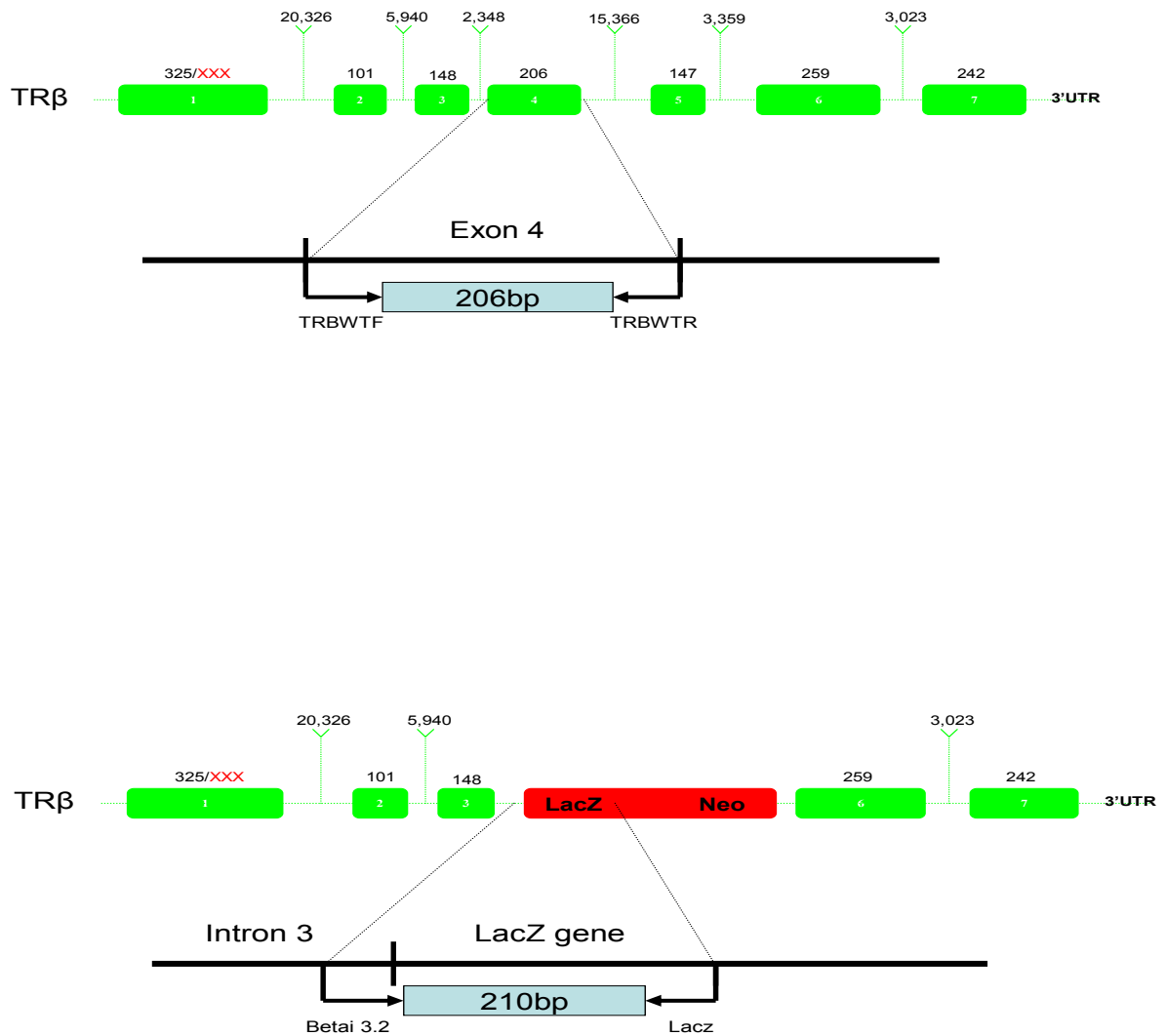


Figure 2.2 Primer locations for identification of wild type and mutant TRβ alleles

The TRβ gene was inactivated by targeted insertion of a recombination cassette downstream of exon 3. Exons are shown as rectangles with the number of base pairs in numerals above. Figures indicate the position of the primers for the wild type and mutant TRβ allele and the resultant PCR product size. Illustrations by Dr T. Galliford.

Agarose gel electrophoresis: PCR products were visualised using a UV transilluminator (Bio-Rad Laboratories Ltd, UK) following electrophoresis in an agarose gel stained with ethidium bromide.

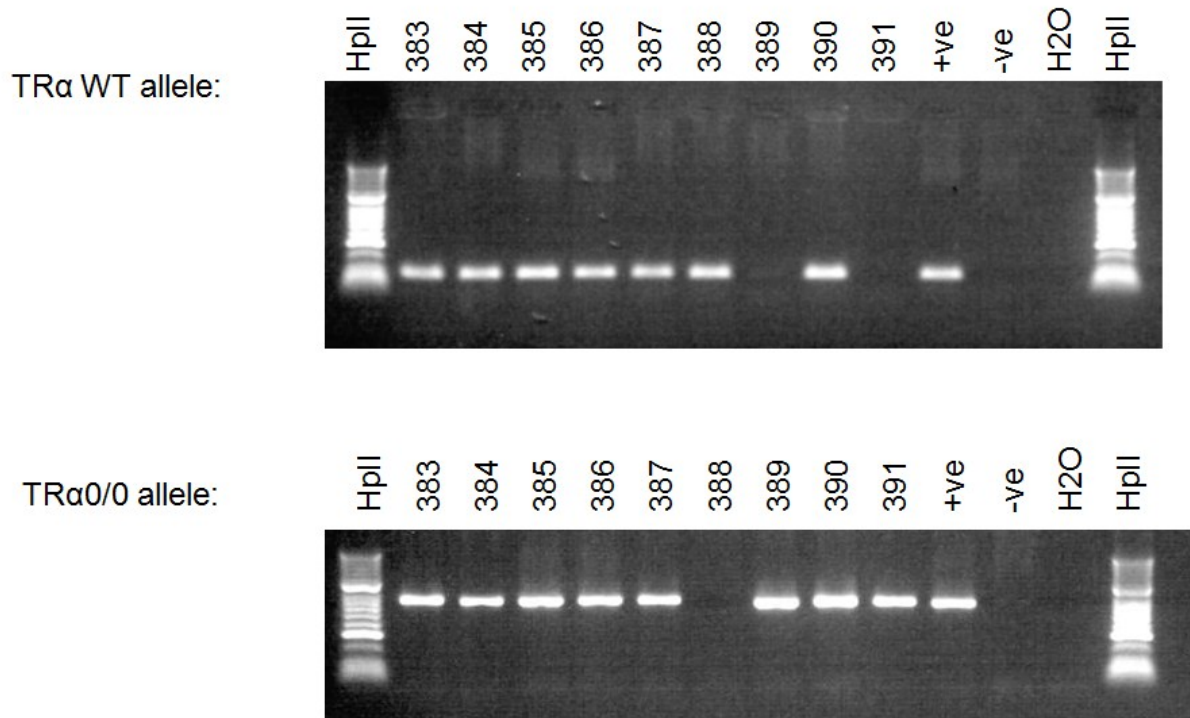
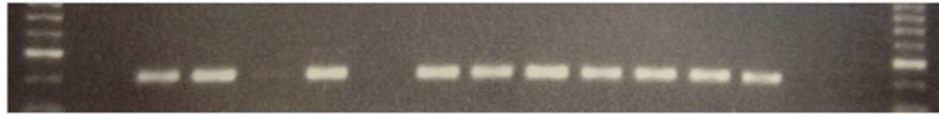


Figure 2.3 Example of PCR gel used for identifying wild type and mutant TRα PCR products

Examples of PCR products run on a 1.5% agarose gel used to identify the genotype of the mice. Mice were categorised into wild type, heterozygous TRα^{0/-} or homozygous TRα^{0/0} dependent on the presence or absence of PCR products. Mouse numbers 383-387 and 390 have both the wild type and mutant PCR products, so are TRα^{0/-} (heterozygous for mutant TRα allele) whilst mice 389 and 391 only show the presence of the mutant PCR product and no wild type PCR product, indicating they are TRα^{0/0} (homozygous for mutant TRα allele). The remaining mice only have wild type PCR products, indicating they are wild type mice. DNA molecular weight marker Hyper II ladder (Bioline reagents Ltd, UK) was used to verify product size; 115 base pairs for wild type and 660 base pairs for mutant TRα PCR products.

TR β WT allele: HYP II 677 678 679 680 681 682 683 684 685 686 687 688 +ve -ve H2O



TR β ^{-/-} allele: HYP II 677 678 679 680 681 682 683 684 685 686 687 688 +ve -ve H2O



Figure 2.4 Example of PCR gel used for identifying wild type and mutant TR β PCR products

Examples of PCR products run on a 1.5% agarose gel used to identify the genotype of TR β ^{-/-} mice. Mouse numbers 679, 683, 685 687 and 688 are wild type mice. Mouse numbers 678, 684 and 686 are TR β ^{+/-} (heterozygous for mutant allele) and mice 677, 680 and 682 are TR β ^{-/-} (homozygous for mutant TR β allele). DNA molecular weight marker Hyper II ladder (Bioline reagents Ltd, UK) was used to verify product size; 206 base pairs for wild type and 210 base pairs for mutant TR β allele.

2.3 OESTROGEN AND THYROID HORMONE MANIPULATION

The effects of altered thyroid status and oestrogen deficiency on adult bone structure and mineralisation was determined in wild-type, TR α ^{0/0} and TR β ^{-/-} female mice. At the time of cessation of growth, post-natal day 70 mice were ovariectomised (OVX) or sham operated and maintained in three groups of 12 mice: (i) euthyroid (n=6 OVX, n=6 sham), (ii) hypothyroid (n=6 OVX, n=6 sham) and (iii) hyperthyroid (n=6 OVX, n=6 sham). Mice were sacrificed and their skeletal phenotypes analysed 6 weeks later at P112. The total number of mice required was 108 (n=3 genotypes, n=3 groups of altered thyroid status, n=12 mice per group).

2.3.1 WILD TYPE AND TR α ^{0/0} MICE

Euthyroid mice were fed a standard diet. Hypothyroid animals were fed a low I2 diet containing 0.15% w/v of the anti-thyroid drug PTU (TD95125 Harlan laboratories, Indianapolis, USA). Hyperthyroid mice were obtained by supplementing their diet with TSH-suppressive doses of T4 (1.2 μ g/ml in drinking water T1775, Sigma Aldrich, UK - see Appendix for solution). Water was changed every three days as T4 slowly degrades following exposure to light. As the mice became thyrotoxic, they drank more and so the concentration of supplemented T4 was adjusted according to intake, in two week cycles, to ensure that the mice did not become markedly thyrotoxic.

2.3.2 TR β ^{-/-} MICE

Euthyroid group: untreated TR β ^{-/-} mice have elevated circulating thyroid hormone concentration so euthyroid status was achieved by a low I2 diet containing PTU and co-administering a physiological replacement dose of T3 (0.05 μ g/ml T2877 Sigma Aldrich, UK - see Appendix for solution) in the drinking water. Treatment with T3 rather than T4 was required because PTU inhibits activity of the D1 which converts T4 to T3. Hypothyroid animals were fed a low I2 diet containing PTU.

Hyperthyroid group: TR β ^{-/-} mice have elevated circulating thyroid hormone concentration and were fed a standard diet.

Genotype	Thyroid status	Treatment
Wild Type	Hyperthyroid	T4 (1.2µg/ml of drinking water)
	Euthyroid	No treatment
	Hypothyroid	Low iodine diet with 0.15% PTU
TRα ^{0/0}	Hyperthyroid	T4 (1.2µg/ml of drinking water)
	Euthyroid	No treatment
	Hypothyroid	Low iodine diet with 0.15% PTU
TRβ ^{-/-}	Hyperthyroid	No treatment
	Euthyroid	Low iodine diet with 0.15% PTU and T3 (0.05µg/ml of drinking water)
	Hypothyroid	Low iodine diet with 0.15% PTU

Table 2.1 Summary of drugs administered to manipulate circulating thyroid status in each group. PTU – propylthiouracil.

2.4 CALCEIN LABELLING

All mice were labelled with 2.5mg/kg of calcein (Sigma CO875), administered by intravenous injection at P107 and P109 prior to sacrifice at P112.

2.5 GROWTH PARAMETERS

Mice were weighed at sacrifice (P112). Tail length was measured immediately prior to sacrifice.

2.6 SERUM SAMPLES

Mice were fasted for 12 hours before sacrifice and blood obtained by cardiac puncture (1ml syringe, 25G needle, Becton Dickinson, UK). Blood samples were incubated at room temperature to allow for coagulation, then spun at 16,000 rpm for 10 mins at 4°C. The pellet was discarded, and the serum supernatant was removed and stored at -80°C.

2.6.1 THYROID HORMONE AND BONE TURNOVER MARKERS

Free T4 and fT3 were measured in chemiluminescence assays (Vitros ECI Immunodiagnostic Systems). Bone formation marker N-terminal propeptide of type 1 procollagen (P1NP) and bone resorption marker CTX concentrations, were determined by enzyme immunoassay using Immunodiagnostic systems (IDS) kit AC-33F1 and AC-06F1. Both assays were carried out in accordance with the manufacturer's instructions (briefly outlined below).

2.6.1.1 P1NP assay IDS AC-33F1

50µl of calibration, control or 5µl of serum sample with 45µl of sample dilutant, were added to antibody coated plate wells. 50µl of P1NP biotin was then added to each of the wells. The plate was placed on a microplate shaker at 500-700 rpm at room temperature, for 1 hour.

The wells were then rinsed with wash solution three times before adding 150µl of enzyme conjugate to each well and incubated for 30 minutes. The wells were then rinsed three times with wash solution and 150µl of TMB solution was added and incubated for 30 minutes. 50µl of HCl was added to all the wells to stop the reactions and the absorbance of each well was measured at 450nm using a microplate reader.

The results of the standards were plotted, creating a standard curve from which sample absorbance values could be read, to determine the serum concentration of P1NP.

2.6.1.2 CTX assay IDS AC-06F1

100µl of biotinylated RatLaps Antigen was added to wells and incubated at room temperature for 30 minutes. The immune strips were washed 5 times with 300µl washing solution. 20 µl of standards,

controls and serum samples were added to each well followed by 100µl of primary antibody. The wells were then sealed and incubated overnight at 4 °C. The following day, the strips were washed 5 times in washing solution and then 100µl of peroxidase conjugated Goat anti-Rabbit IgG Antibody was added to each well and further incubated at 6 mins at room temperature. The wells were again washed 5 times as before and then 100µl of substrate solution was added and incubated for 15 mins in darkness. 100µl of stop solution was added to each well and the absorbance was measured at 450nm. The results of the standards were plotted creating a standard curve and checked against the control. The serum CTX concentration was then determined by reading corresponding absorbance values of samples.

2.7 DISSECTION, FIXATION AND STORAGE OF THE SKELETON

The skeletons of P112 mice were dissected out and all soft tissue removed. The left lower limb, right femur and proximal tail vertebrae were placed in 70% ethanol. The right tibia, lumbar vertebrae and mandible were fixed in 2.5% glutaraldehyde in 0.15M sodium cacodylate buffer (see Appendix for solution) for 18 hours, before storage in 70% ethanol. The left upper limb was fixed in neutral buffered formalin for 18 hours and stored in 70% ethanol. All samples were stored at 4°C.

2.8 BONE IMAGING

2.8.1 FAXITRON POINT PROJECTION MICRORADIOGRAPHIC ANALYSIS

Left lower limb and proximal tail vertebrae digital x-ray images were recorded at 10-µm pixel resolution, using a Qados Faxitron MX20 variable kV point projection x-ray source and digital image system, operating at 26 kV and 5× magnification (Cross Technologies plc). Magnifications were calibrated by imaging a digital micrometre at 15mm. The relative mineral content of calcified tissues was determined by comparison between groups. Each image taken was adjusted according to the following standards included in each image frame: a 1-mm thick steel plate, a 1-mm diameter spectrographically pure aluminium wire, and a 1-mm diameter polyester fibre. 16-bit (2368 × 2340) DICOM images were converted to 8-bit Tiff images using ImageJ, and the histogram stretched from the polyester (grey level 0) to the steel (grey level 255) standards. Decreasing gradations of mineralisation density were represented in 16 equal intervals by a pseudocolor scheme for presentation of digital images. Images of the bones were montaged according to type of bone, genotype and treatment groups. Statistical analyses was performed in an excel spread sheet using

the Kolmogorov-Smirnov test between the grey level distribution of each montage on the cumulative frequencies (CF). The Kolmogorov-Smirnov test is described by Demidenko (<http://www.springerlink.com/content/wpc6c4aw8mpup66g/>).

Femur and tibial lengths were determined on faxitron images using ImageJ 1.41 software (<http://rsb.info.nih.gov/ij/>). Cortical bone thickness and diameter were determined at the mid diaphysis in the mediolateral projection position. A 100 pixel grey box was inserted over the mid diaphysis using Photoshop CSI 5 software. 10 measurements were taken: five between the periosteal surfaces and five between endosteal surfaces (see Figure 2.6). From these measurements, the average cortical thickness was calculated for each bone.



Figure 2.5 Image processing used for determining BMC

A: Faxitron DICOM image of caudal vertebrae and lower limb. Standards: 1-mm thick steel plate (s), a 1-mm diameter spectrographically pure aluminium wire (a), and a 1-mm diameter polyester fibre (p) were imaged with each set of bones. B: The images were standardised by stretching the grey scale histogram from the polyester (grey level 0) to the steel (grey level 255). C: The varying gradations of mineral densities were split into 16 equal intervals and pseudocoloured.



Figure 2.6 Determining cortical thicknesses

Cortical bone thickness was determined by 10 measurements across the mid diaphysis. To optimise accuracy, cortical thickness was determined by measurements of diameter of the external diaphysis (between the white arrows) minus the distance between the internal cortices (between the black arrows). The double headed arrow illustrates measurement of femoral lengths.

2.8.2 MICRO COMPUTED TOMOGRAPHY (CT) ANALYSIS

Femurs were analysed by Skyscan 1172a micro CT at 50kV and 200 μ A using a 0.5mm Al filter and a detection pixel size of 4.3 μ m². Images were taken every 0.7° through 180° rotation of each bone. Reconstruction of scanned images created using Skyscan NRecon software. A 1mm³ volume of trabecular bone, 0.2mm from the growth plate, was selected as the region of interest.

Trabecular bone volume as a proportion of tissue volume (BV/TV), trabecular separation (Tb.Sp, mm), Tb.N, mm⁻¹, Tb.Th, mm and structure model index (SMI) were determined. Images and processing were undertaken by Miss Holly Evans in collaboration with Professor P. Croucher at Sheffield University.



Figure 2.7 Micro CT images of a femur

2.8.3 qBSE-SEM

The distribution of bone micro-mineralisation densities was analysed by qBSE-SEM at cubic micron voxel resolution. Bones were fixed in 2.5% glutaraldehyde in 0.15M sodium cacodylate buffer (see Appendix for solution) and stored in 70% ethanol prior to being embedded in poly-methyl-methacrylate (PMMA). Midline block faces were polished, coated with carbon and analysed using a Zeiss DSM962 digital SEM. Mineralisation densities were determined by comparison with halogenated dimethylacrylate standards: $C_{22}H_{25}O_{10}Br$ (BSE coefficient = 0.1159) to $C_{22}H_{25}O_{10}I$ (BSE coefficient = 0.1519). Increasing gradations of mineralisation density were represented in 8 equal intervals by a pseudocolour scheme for presentation of digital images. Statistical analyses between the distribution of grey levels of each montage were performed on the cumulative frequencies using the Kolmogorov-Smirnov test in an excel spread sheet. Embedding was performed by Maureen Arora and images were taken by Professor Alan Boyde at the Queen Mary, University of London (QMUL). Analysis of images was undertaken by the author.

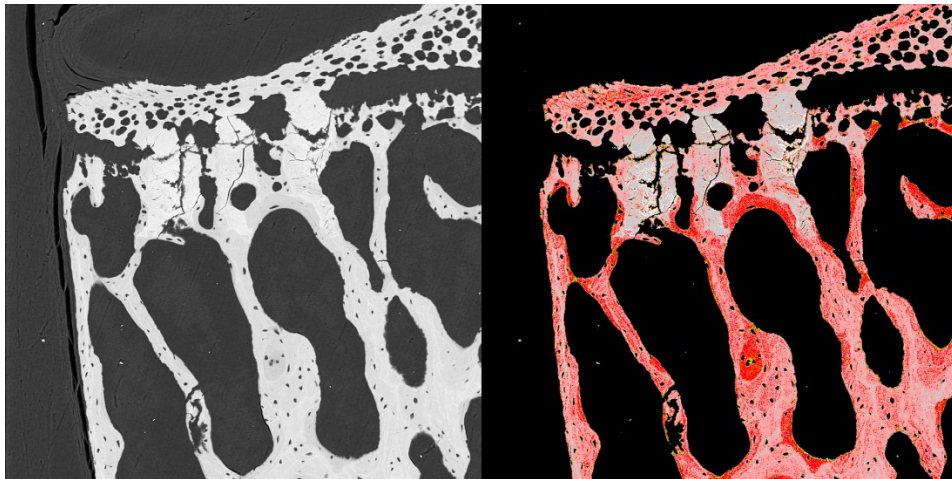


Figure 2.8 Image of lumbar vertebra taken by qBSE

Increasing gradations of mineralisation density were represented in 8 equal intervals by a pseudocolour scheme for presentation of digital images. This image shows the different grey levels represented into 8 equal intervals by a pseudocolour scheme.

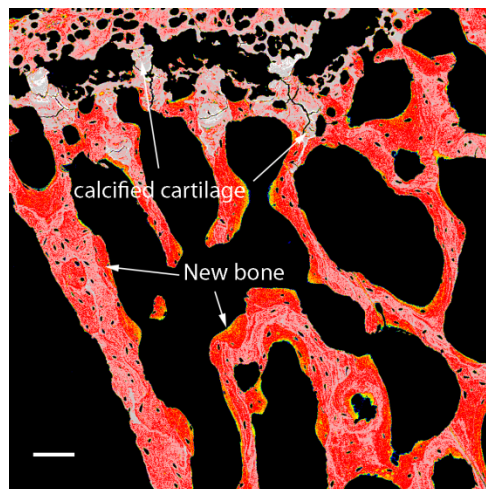


Figure 2.9 Different densities represented in different colours

High density is shown in white and low density in yellow and red. Scale bar is 100 microns. Calcified cartilage is highly mineralised and shown in the areas near the growth plate. New bone is of a lower density where remodelling has occurred.

2.8.4 BSE-SEM

Femurs were opened longitudinally along anatomical curvatures using a fine tungsten carbide milling tool to remove half the cortical bone and medullary trabecular elements. Samples were cleared of cell remnants by maceration with an alkaline bacterial pronase, which also removed unmineralised cartilage. Samples were carbon-coated and imaged using backscattered electrons at 20kV beam potential. The resultant images provided detailed views of bone surfaces and microarchitecture. Endosteal eroded surfaces were quantified using ImageJ. The percentage area of the inner cortex with evident resorption pits was calculated by using a grid of 200 crosses and identifying whether each cross overlaid an area of resorption. Femurs were opened by Professor Alan Boyde. Samples were mounted, imaged and analysed by the author.

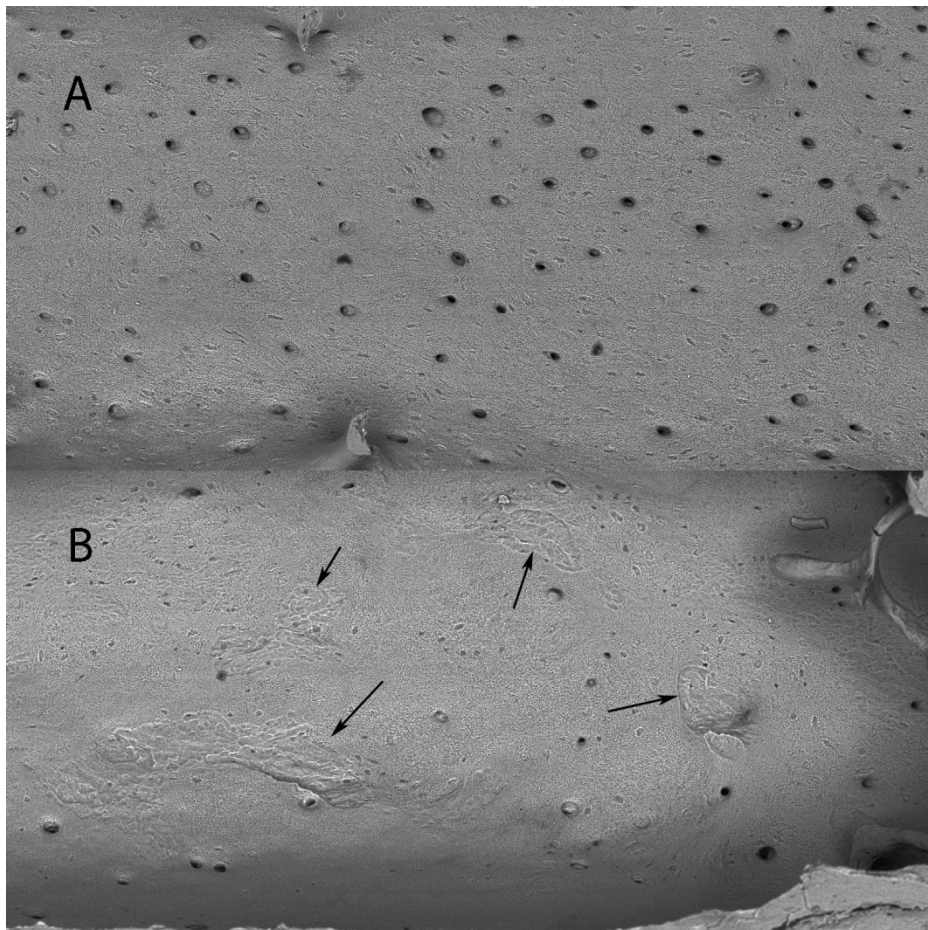


Figure 2.10 BSE-SEM images of the internal cortex of femurs

Image A shows an endocortical surface with very little resorption pits evident. Image B shows an endocortical surface where several areas of resorption are evident (black arrows).

2.8.5 CONFOCAL MICROSCOPY

PMMA embedded lumbar vertebrae were examined by confocal scanning light microscopy (CSLM) to determine the fraction of BS undergoing active bone formation (Doubé et al., 2007). Leica SP2 reflection confocal was utilised, using 488 nm and 543nm excitation and 10x/1.0 and 40x/1.25 objectives. Tissue layers immediately deep to the block surface were visualised to ensure that only fluorescently labelled bone forming surfaces that lie in orthogonal planes were analysed. Montages of overlapping CSLM fields were constructed for each bone using Photoshop CSI 5 software and ImageJ.

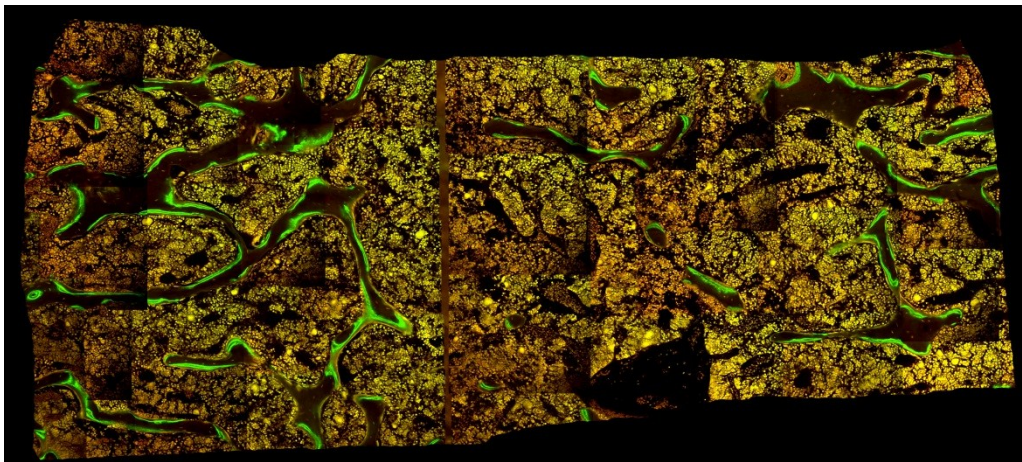


Figure 2.11 Montaged confocal image of a lumbar vertebra

Cortical surfaces and primary spongiosa have been excluded. Trabeculae are identified by their morphology and the presence of identifiable osteocytes. Bright green calcein labelling can be clearly identified and double and single labelled surfaces can be easily defined when viewed in higher magnification.

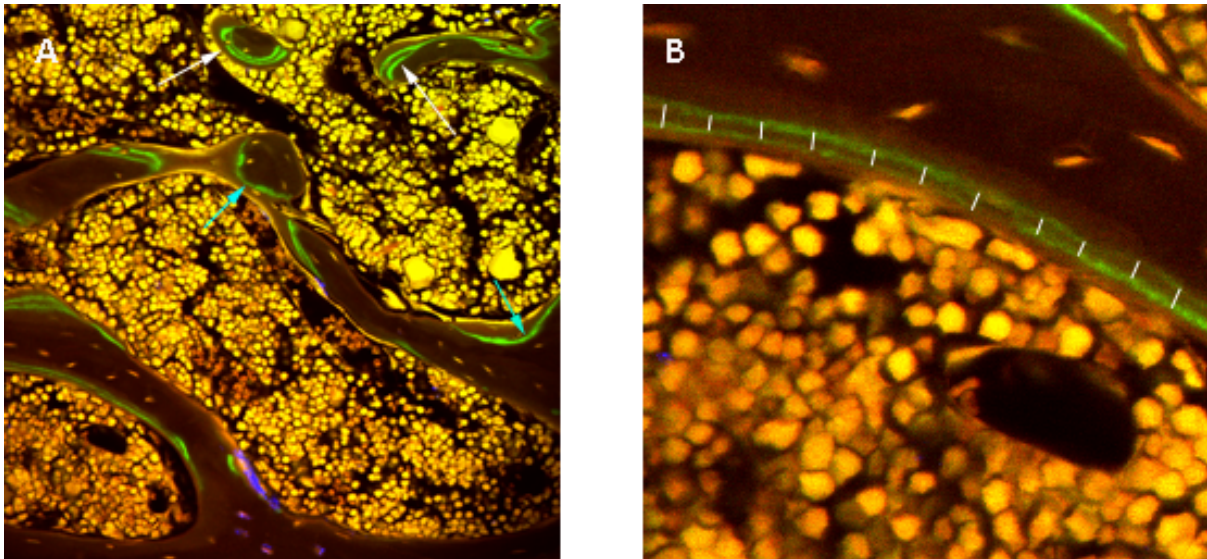


Figure 2.12 Confocal images of double labelling

Confocal image of trabeculae (A). Bone morphology (dark areas with green labels and scattered orange osteocytes) and bone marrow (cellular areas) can be distinctly identified. Calcein labels can be seen in green. Double calcein labels (white arrows) and single calcein labels (blue arrows) can be clearly identified and measured. Mineral apposition is measured as the perpendicular distance between double labels as demonstrated by the white lines (B).

BS was measured using ImageJ software. All the BS, excluding the primary spongiosa just below the growth plate, in a single lumbar vertebra from each mouse were measured. The length of double and single labels was quantified separately. Finally, the multiple distances between all the double labels were measured taking the midpoint of one label and measuring to the midpoint of the label perpendicular to it. Mineralising surface (MS) was determined by adding the length of double labels to half the length of the single labels. MS/BS was calculated by dividing the MS by the total BS. The MAR was determined by the mean separation between double labels. BFR was calculated from the product of MS/BS and MAR.

QBSE-SEM, BSE-SEM and confocal microscopy were undertaken in collaboration with Professor Alan Boyde at QMUL and University College London. Imaging of specimens, manipulation, measurement and analysis of images and parameters was performed by the author.

2.8.6 HISTOMORPHOMETRY

Histomorphometric analysis of osteoclast parameters was performed on decalcified, stained sections of the humerus. After sacrifice, upper limbs were fixed in 10% neutral buffered formalin for 18 hours and then stored in 70% ethanol, following which they were decalcified in 10% EDTA (see Appendix) for three weeks. EDTA was replaced with fresh EDTA once a week and decalcification was verified by faxitron X-ray imaging. Decalcified bones were embedded in paraffin and 3 μ m sections mounted on slides ready for staining with aniline blue to delineate collagen and tartrate resistant acid phosphatase (TRAP) to identify osteoclasts. Paraffin was removed and then the sections rehydrated ready for staining.

The slides were dipped in xylene for 10 mins two times and the samples rehydrated with sequential washes of ethanol at reducing concentrations: 100%, 100%, 80%, 70%, 50% and distilled water. Sections were first stained with TRAP (see Appendix) for 2 hours and the slides were subsequently stained with aniline blue (Aniline Blue 415049 + Phosphotungstic Acid Fluka 79690, both Sigma Aldrich, Dorset, UK) for 20 mins before being washed in water to remove excess stain. The samples were mounted using DPX mountant (Promega, Southampton, UK) and imaged. Sections were photographed using a Leica DM LB2 microscope and DFC320 digital camera and a montage of overlapping fields was constructed for each bone. Analysis was performed with custom software developed by Dr Rob J. van't Hof using the Aphelion Image Analysis tool kit (Adcis SA, Herouville-St Clair, France). Using this software, the tissue area for measurement was first delineated, following which the BS was identified using thresholding of the blue areas. The osteoclasts could then be defined by thresholding of the TRAP stained red areas. Size and location of osteoclasts were individually checked by eye to ensure that those identified were osteoclasts. The software then calculated tissue volume (TV), bone volume (BV), BS, Oc.N and surface (Oc.S). Osteoclast indices could then be normalised to total BS (Oc.N/BS and Oc.S/BS) and compared.

Embedding and sectioning of decalcified samples was performed by Dr Mahrokh Nohadani at Imperial College. Staining, mounting, imaging and analysis all performed by the author. All measurements were performed blind.

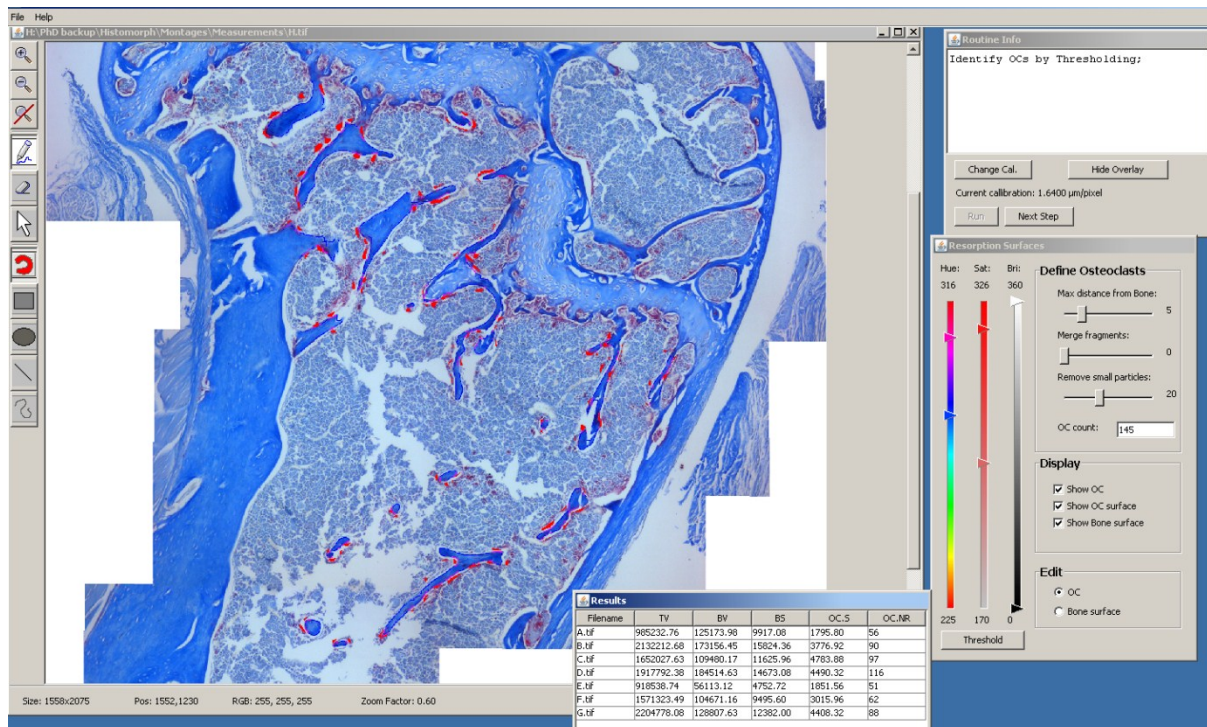


Figure 2.13 Osteoclast parameters analysis

Osteoclast parameters analysis were calculated using custom software developed by Dr Rob J. van't Hof using the Aphelion Image Analysis tool kit. This image demonstrates identification of osteoclasts on the BS by red colour thresholding. The identified osteoclasts were then checked and added or removed as necessary. The software then calculated parameters which were exported onto an excel spread sheet (as seen at the bottom of the image).

2.9 MECHANICAL LOADING AND BONE STRENGTH

Destructive three-point bending tests were performed on tibias using an Instron 5543 load frame (Instron, UK). A load perpendicular to the tibia, at a rate of displacement of 0.03 mm/sec, was applied in the mid diaphysis until fracture. The force applied (load in Newtons) and displacement (in mm) were recorded. Load displacement curves were then generated from the data and recorded on an excel spread sheet to determine yield load (direct measurement), maximum load (direct measurement), fracture load (direct measurement) and stiffness (gradient of the linear part of the graph) of the bone (see Figure 2.14). It can be seen that the bone undergoes elastic deformation in the portion of the graph where there is a linear relationship between load and displacement. The gradient of this section represents the stiffness of the bone - the steeper the gradient the greater the stiffness. The bone undergoes plastic deformation where the relationship between load and displacement is no longer linear after the yield load. The maximum load is the highest load which can be applied to the bone and the fracture load is the load at which the bone breaks.

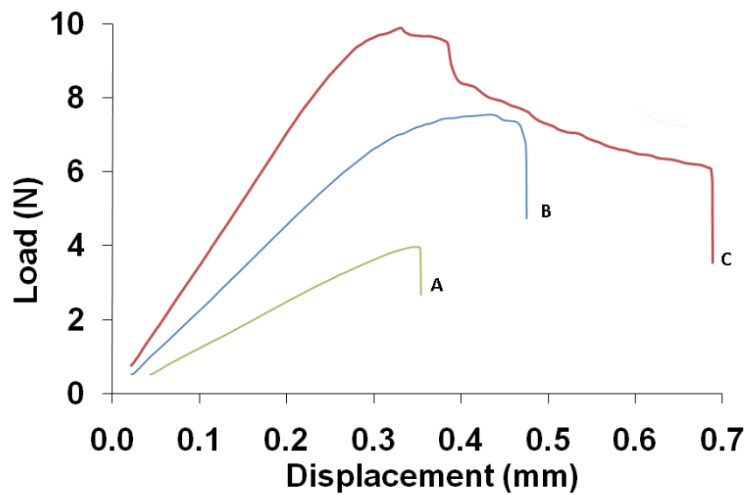
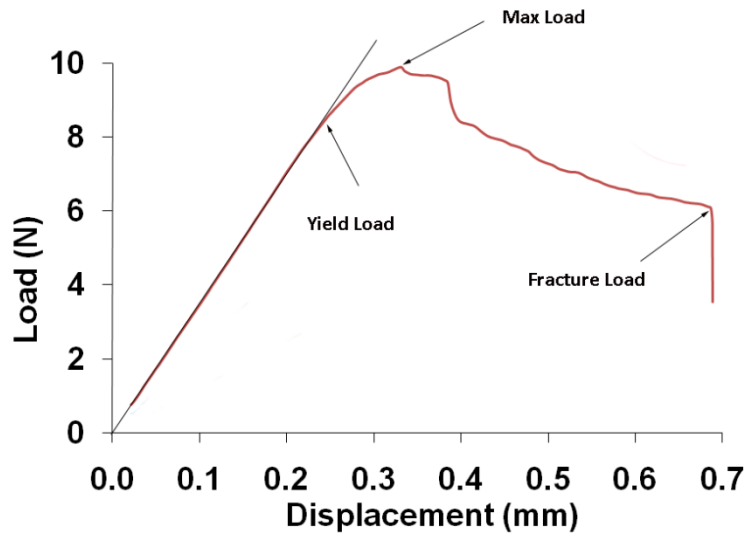


Figure 2.14 Load displacement curves generated from three point bending of femur

The yield load is the point at which the curve no longer shows a linear relationship between load and displacement. The maximum load is the greatest load that can be applied through the bone and the fracture load is the force at which the bone fractures.

These four parameters can be independent. The second graph shows examples of the load displacement of tibias of mice from different genotypes (A-C). Bone A is less stiff (gradient of graph is less steep) and has lower yield, max and fracture loads than that of bones B and C. Bone C has the highest max load of all three bones but the fracture load of bone C is lower than that of bone B.

2.10 STATISTICS

Normally distributed data was analysed using the Student's t-test, or analysis of variance (ANOVA) followed by Tukey's multiple comparison post-hoc test. P values <0.05 were considered significant. Data expressed as mean \pm standard error of mean (SEM).

In Chapter 3, separate ANOVAs were performed in respect of:

- 1) Thyroid status: comparison of hypothyroid (WT Hypo), euthyroid (WT Eu) and hyperthyroid (WT Hyper) groups.
- 2) Genotype: comparison of TR $\alpha^{0/0}$, TR $\beta^{-/-}$ and wild type (WT) groups.

In Chapter 4, separate ANOVAs were performed to compare the effects of thyroid status in 1) TR $\alpha^{0/0}$ and 2) TR $\beta^{-/-}$ groups.

Frequency distributions of bone mineralisation densities obtained by Faxitron and qBSE SEM were compared using the Kolmogorov-Smirnov test, in which P values for the D statistic in 1024 pixel data sets are D = >6.01 P<0.05, D = >7.20 P<0.01, and D = >8.62 P<0.001. The Kolmogorov-Smirnov test is described by Demidenko (<http://www.springerlink.com/content/wpc6c4aw8mpup66g/>).

The software used for statistical analysis was Graph Pad Prism version 4.0.

2.10.1 TYPE I AND TYPE II ERRORS

In Chapter 5, when analysing the different groups, I performed nine independent Student's t-tests for each parameter. Correction for multiple sampling is commonly used when performing several hundred t-tests at the same time; for example when analysing microarrays. Too stringent corrections for multiple testing lead to type II errors, where significant findings are not identified.

I was concerned that any significance that I elicited could be due to chance leading to a type I error. I therefore initially applied two corrections independently, a Bonferroni and then a Sidak's correction ($1-(1-\alpha)^{1/n}$ where α is the significance level and n is the number of tests). However, after applying either of these corrections, there were no significant differences in any of the groups tested. Loss of bone mass has been well documented in mouse models undergoing ovariectomy and the results of my uncorrected Student's t-tests are in line with this. As the number of groups was relatively few at nine, I concluded that applying a correction for multiple testing resulted in a type II error with my analysis. Thus the Student's t-tests performed in Chapter 5 were not corrected for multiple testing.

Chapter 3

Skeletal phenotyping of wild type mice with manipulated thyroid status in comparison to TR α 0/0 and TR β -/- mice

3 SKELETAL PHENOTYPING OF WILD TYPE MICE WITH MANIPULATED THYROID STATUS IN COMPARISON TO TR α ^{0/0} and TR β ^{-/-} MICE

3.1 BACKGROUND

Deletion or mutation of TR α during growth results in delayed endochondral ossification and transient growth retardation with reduced bone mineral deposition. Adult TR α knockout and mutant mice are reported to have osteosclerosis characterised by increased trabecular bone mass, a skeletal remodelling defect and reduced osteoclast numbers and activity (Bassett et al., 2007b, Bassett and Williams, 2009). The features in TR α mutant mice that have been described in the literature to date are characteristic of skeletal responses to hypothyroidism.

By contrast, deletion or mutation of TR β during growth results in accelerated intramembranous and endochondral ossification, with increased bone mineral deposition. Adult TR β knockout and mutant mice are reported to have osteoporosis with reduced bone volume and mineralisation and increased osteoclast numbers and activity (Bassett et al., 2007b, Bassett and Williams, 2009, Forrest et al., 1996). The features in TR β mutant mice are characteristic of skeletal responses to thyrotoxicosis (O'Shea et al., 2003).

Given the data available, it was proposed that the divergent skeletal phenotypes in TR α and TR β mutant mice could be accounted for by consideration of the differing actions of TR α and TR β in bone and on the hypothalamic-pituitary-thyroid axis. TR α is the major TR isoform expressed in bone, whereas TR β predominates in the hypothalamus and pituitary and mediates negative feedback regulation of TSH (Bookout et al., 2006, Forrest et al., 1996, Kaneshige et al., 2000, O'Shea et al., 2003). Consequently, TR β knockout and mutant mice have central RTHs with elevated circulating thyroid hormone concentrations, which lead to increased activation of TR α in bone and a phenotype of increased T3 signalling in the skeleton. By contrast, TR α knockout and mutant mice have absent TR α in bone, leading to reduced T3 signalling in the skeleton despite normal circulating thyroid hormone levels.

The skeletal response to hyperthyroidism includes a reduced bone mass, resulting from both increased bone formation and bone resorption with a net negative balance, whereas the skeletal response to hypothyroidism includes low bone formation, decreased bone resorption and, in animals, an increased bone mass (Mosekilde and Melsen, 1978, Eriksen et al., 1986, Lanham et al., 2011). To date, experimental data which directly compares the skeleton of (i) hypothyroid mice with

TR $\alpha^{0/0}$ mice or (ii) hyperthyroid mice with TR $\beta^{-/-}$ mice is lacking. In particular, dynamic bone formation and biomechanical data in TR $\alpha^{0/0}$ and TR $\beta^{-/-}$ mice, has not been reported in the literature.

In this chapter, I describe the skeletal phenotype of adult wild type mice with manipulated thyroid status mice and compare them with untreated TR $\alpha^{0/0}$ and TR $\beta^{-/-}$ mice.

It should be noted that “WT Eu” and “WT” were the same control group, but labelled differently to reflect the relevant comparison being made.

3.2 RESULTS

3.2.1 CIRCULATING THYROID STATUS OF WILD TYPE, TR α ^{0/0} AND TR β ^{-/-} MICE

The intended thyroid status of treated wild type mice (Table 2.1) was confirmed by analysis of serum total T4 and total T3 levels (Figure 3.1). The hypothyroid group had serum T4 below the limits of detection for the assay and those treated with supplementation of T4 in the drinking water resulted in a 4 fold elevation of serum T4 level. T3 levels in the wild type groups also reflected this trend. TR α ^{0/0} mice were euthyroid, whilst both T3 and T4 were significantly elevated in TR β ^{-/-} mice, to concentrations similar to hyperthyroid wild type mice (T4 concentration 40.8 \pm 10.3pm/l in hyperthyroid wild type mice compared to 43.2 \pm 3.8pm/l in TR β ^{-/-}).

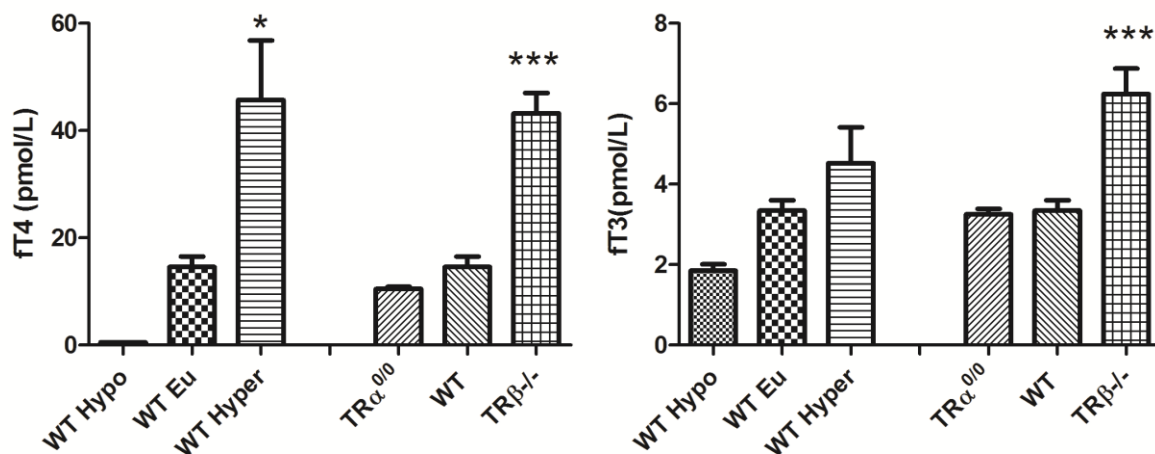


Figure 3.1 Serum free T4 and free T3 levels

Serum free T4 and free T3 concentrations (pmol/litre) at P112 in wild type control mice (WT Eu), wild type mice treated with 1.2 μ g/l of T4 in drinking water for 6 weeks (WT Hyper), wild type mice treated with a low iodine diet containing PTU for 6 weeks (WT Hypo), TR α ^{0/0} and TR β ^{-/-} mice. Data expressed as mean \pm SEM, n=6 per group and analysed by ANOVA and Tukey's Multiple Comparison post hoc test: *, p<0.05; ***, p<0.001 versus euthyroid wild type (WT Eu/WT). Serum free T4 levels for WT Hypo were below lower limit of detection by assay.

3.2.2 ANALYSIS OF BODY WEIGHT AND TAIL LENGTH MEASUREMENTS

There was no difference in body weight or tail length in hypothyroid, euthyroid or hyperthyroid wild type mice. Since both hyperthyroidism and hypothyroidism during development impair growth, this data suggests that the majority of growth was complete upon commencement of thyroid manipulation. $TR\alpha^{0/0}$ mice had similar body weight and tail length to wild type mice whereas $TR\beta^{-/-}$ mice were smaller with a lower body weight and shorter tail length (see Figure 3.2).

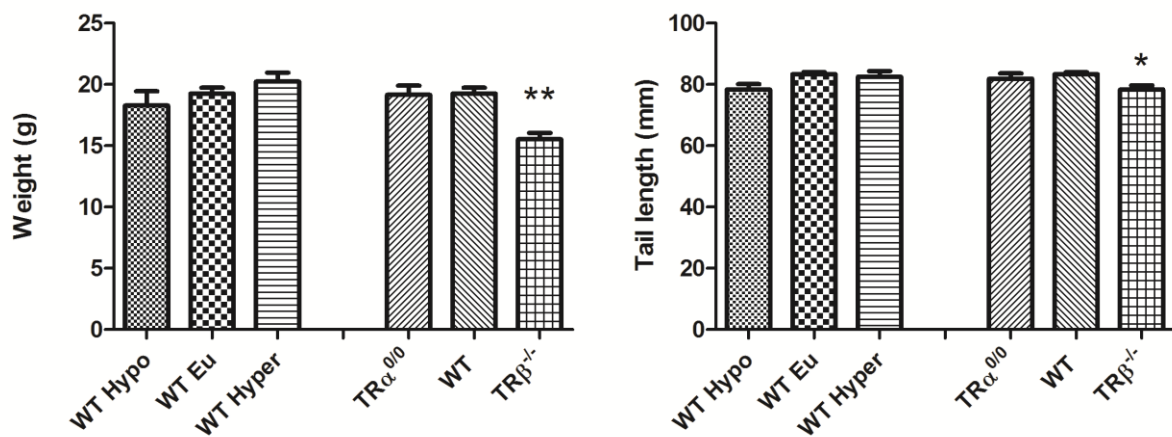


Figure 3.2 Growth parameters

Weight and tail length of P112 mice. Data expressed as mean \pm SEM, n=6 per group. Analysis by ANOVA and Tukey's Multiple Comparison post hoc test: *, $p < 0.05$; **, $p < 0.005$ versus WT.

3.2.3 STRUCTURAL PARAMETERS

3.2.3.1 Analysis of bone length and cortical thickness measurements

Manipulation of thyroid status in adult wild type mice did not alter femur and tibia length or cortical thickness. The femoral and tibial bone lengths, cortical bone diameters and cortical thickness of $TR\alpha^{0/0}$ mice were similar to those of wild type mice. In contrast, $TR\beta^{-/-}$ mice had smaller bones with reduced bone size (femoral and tibial length), cortical bone diameter and cortical thickness when compared with wild type mice (see Figure 3.3).

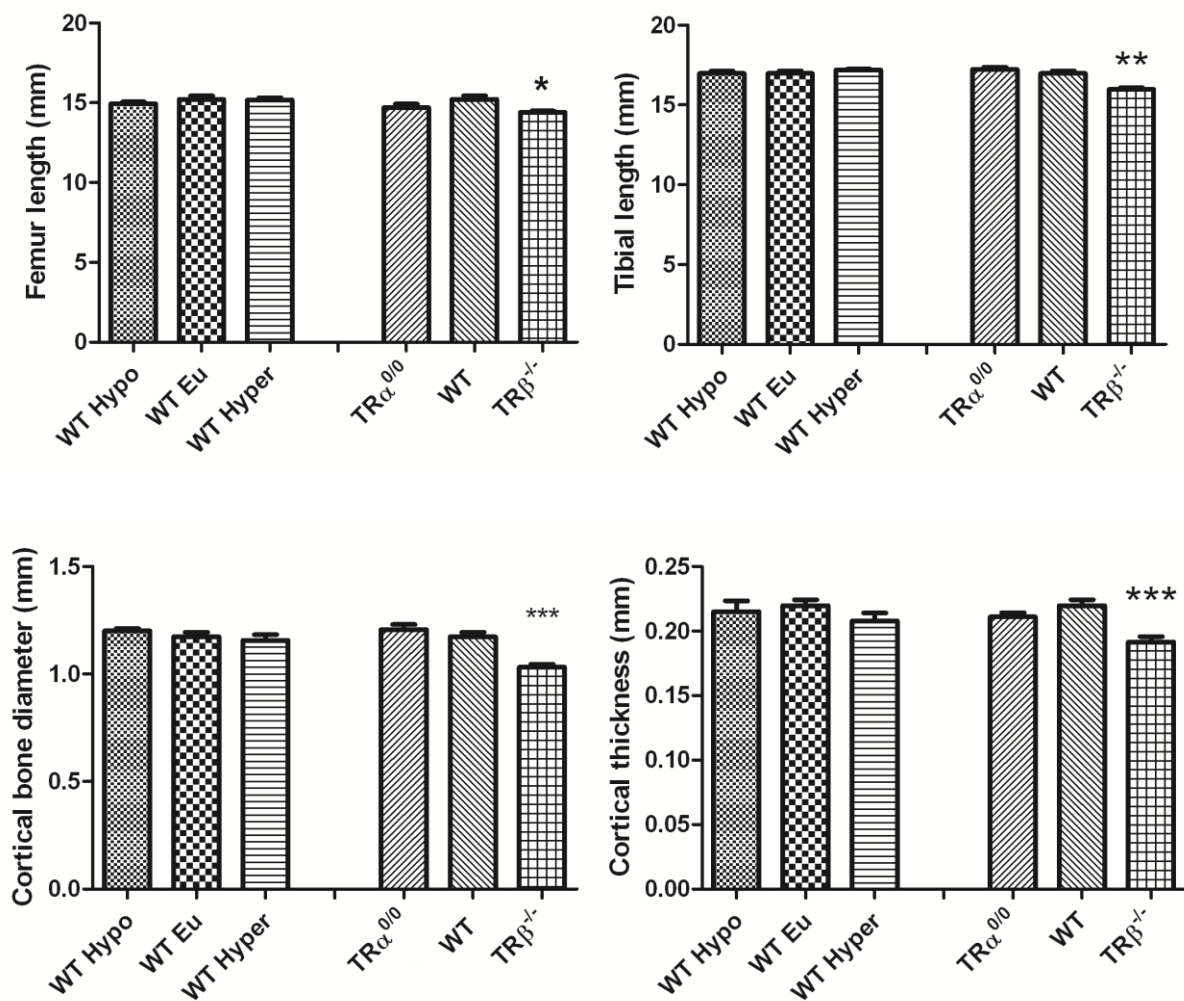


Figure 3.3 Gross structural parameters

Femur length and cortical thickness of P112 mice. Data expressed as mean \pm SEM, n=6 per group and analysed by ANOVA and Tukey's Multiple Comparison post hoc test: *, $p < 0.05$; **, $p < 0.01$; ***, $p < 0.001$ versus WT.

3.2.3.2 Analysis of bone microarchitecture: BSE-SEM and Micro CT

The effect of altered thyroid status on the microarchitecture of bone was investigated with low and high magnification BSE-SEM images and micro CT. Low power BSE-SEM views of distal femurs clearly demonstrate a gain in trabecular bone mass in hypothyroid animals with the trabecular compartment extending up the femoral shaft. Higher magnification images show increased thickness and connectivity of the trabeculae (see Figure 3.4). Similarly, micro CT showed that BV/TV increased by 43% compared to euthyroid mice with significantly increased Tb.Th (see Table 3.1). Hypothyroid and euthyroid mice had similar Tb.Sp, Tb.N and structure module index (SMI) - a measure of how plate-like (score 0) or rod-like (score 3) the trabeculae are.

Conversely, thyrotoxic mice had a loss in trabecular bone mass in the distal femur with a smaller extension up the femoral shaft. High magnification images showed gracile, rod-like trabeculae with low connectivity (see Figure 3.4). Micro CT demonstrated a 42% decrease in BV/TV with significantly increased Tb.Sp, similar Tb.Th and decreased Tb.N. Thyrotoxic mice had a lower mean SMI than euthyroid mice and although this did not reach significance ($p=0.059$), the results suggests that the trabeculae were more rod-like, as in the BSE-SEM images.

TR $\alpha^{0/0}$ mice have substantially increased trabecular bone mass with notable extension of trabeculae up the femoral shaft. High power BSE-SEM images reveal thicker, plate-like trabeculae, with increased connectivity; accordingly, BV/TV was 20% greater than wild type mice and SMI was significantly decreased. Despite a highly significantly increased BV/TV, Tb.Th, spacing and number were not significantly different from wild type mice. This suggests that micro CT is insufficiently precise to determine parameters such as Tb.Th, spacing and number.

In contrast to TR $\alpha^{0/0}$, TR $\beta^{-/-}$ mice have gracile, rod-like trabeculae with low connectivity largely confined to around the growth plate. BV/TV in TR $\beta^{-/-}$ mice was reduced by 22% with increased Tb.Sp. There was no difference in Tb.Th, number or SMI.

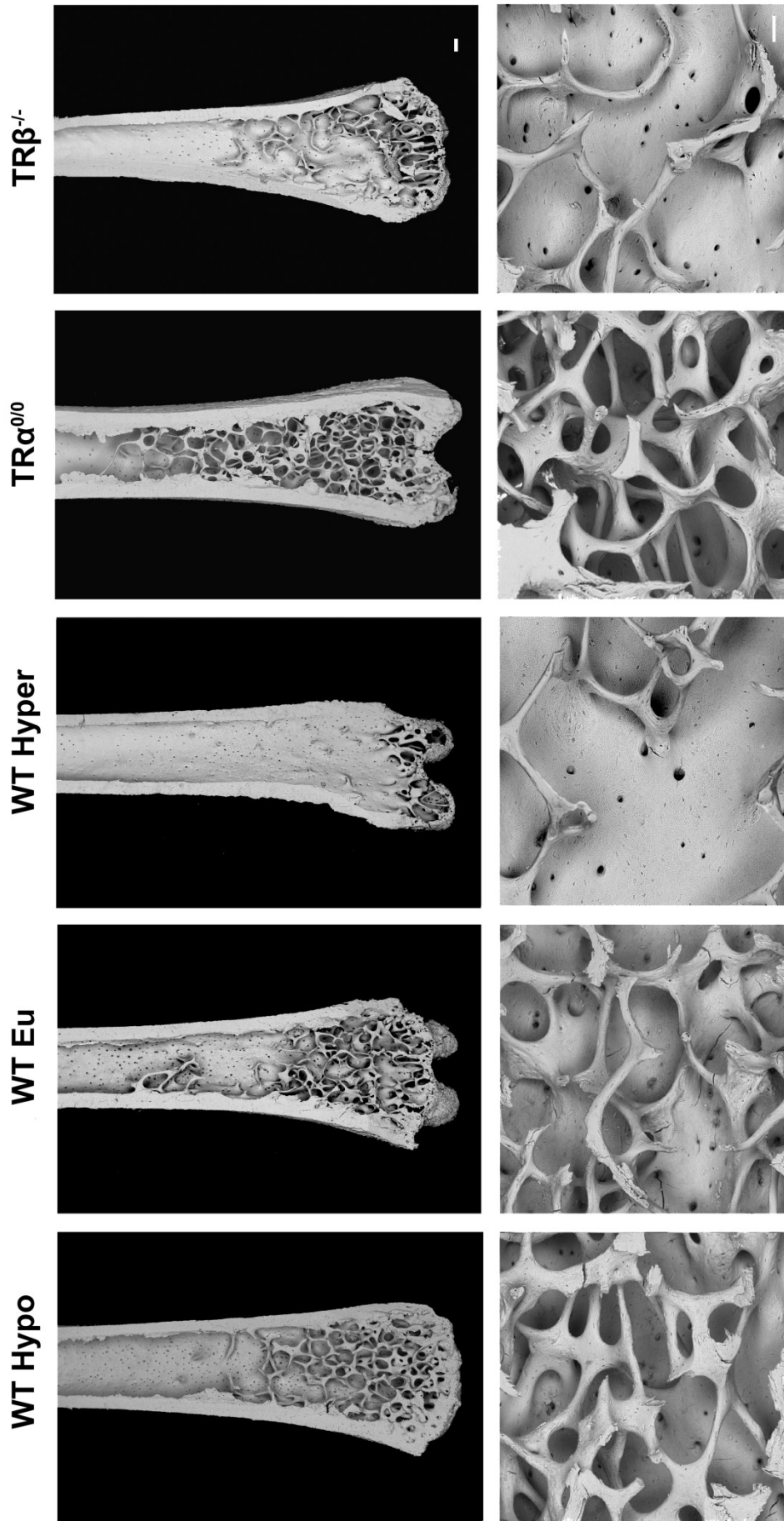


Figure 3.4 BSE-SEM images showing bone micro architecture

BSE-SEM distal femur images from wild type control mice (WT Eu), hyperthyroid wild type mice (WT Hyper), hypothyroid wild type mice (WT Hypo), $TR\alpha^{0/0}$ and $TR\beta^{-/-}$ mice, all at P112. Scale bars, 200 μ m.

	BV/TV (%)	Tb.Th (mm)	Tb.Sp (mm)	Tb.N (mm ²)	SMI
WT hypo	15.6±1.3**	0.05±0.002***	0.20±0.016	3.05±0.15	1.71±0.04
WT Eu	10.9±1.1	0.04±0.003	0.19±0.016	2.74±0.23	1.74±0.09
WT hyper	6.3±0.8*	0.04±0.001	0.25±0.023**	1.68±0.17**	1.99±0.07
TRα^{0/0}	13.1±0.4*	0.04±0.001	0.19±0.006	3.11±0.1	1.64±0.02
TRβ^{-/-}	7.1±0.5*	0.04±0.001	0.23±0.009*	3.24±0.15	1.91±0.05

Table 3.1 Analysis of micro CT data

Quantitative analysis of bone volume (BV/TV), trabecular thickness (Tb.Th), trabecular spacing (Tb.Sp), trabecular number (Tb.N), and structure model index (SMI) determined by micro-CT analysis of distal femur (n=5-6). ANOVA and Tukey's post hoc test. *, p<0.05; **, p<0.01; ***, p<0.001 when compared to euthyroid wild type bones.

3.2.4 BONE MINERAL DENSITY

3.2.4.1 Analysis of bone mineral content

In order to determine bone mineralisation, X-ray microradiography faxitron analysis was utilised to quantify bone mineral content (BMC) in femurs (largely cortical bone) and caudal vertebrae (largely trabecular bone).

In hypothyroid animals, there was a site specific increase in BMC. There was a significantly increased BMC (p<0.001) in femurs whereas the BMC in caudal vertebrae remained unchanged. Thyrotoxic animals were osteopenic with decreased BMC in both femurs (p<0.05) and caudal vertebrae (p<0.001), although the decrease in BMC was more pronounced in the caudal vertebrae, compared to the femurs. TRα^{0/0} mice had increased BMC both in the femurs and in the caudal vertebrae, whilst TRβ^{-/-} mice had reduced BMC in both bone types (see Figures 3.5 and 3.6).

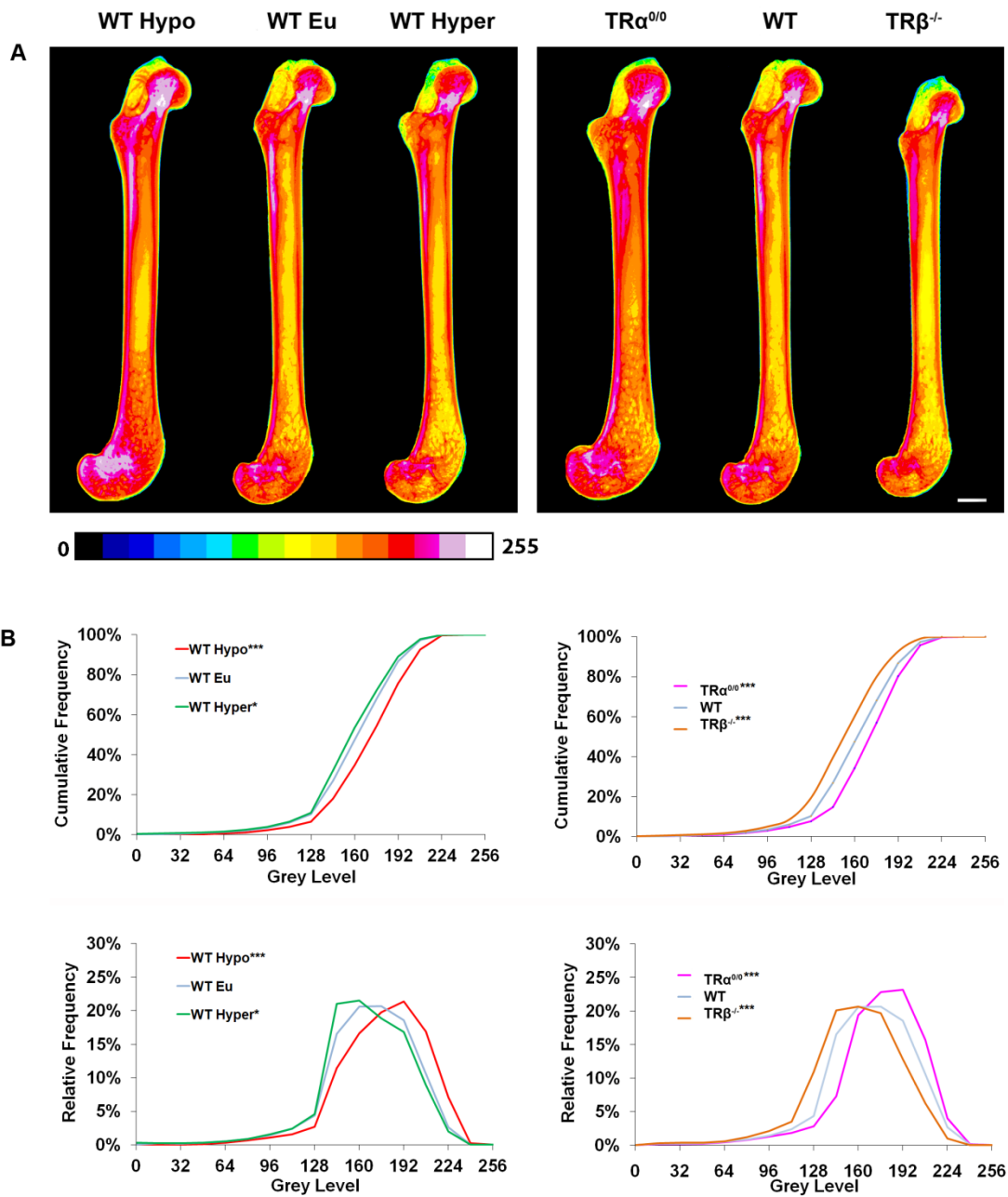


Figure 3.5 Bone mineral content of femurs

Faxitron images of femurs (A) of P112 mice from euthyroid wild type control mice (WT Eu), hyperthyroid wild type mice (WT Hyper), hypothyroid wild type mice (WT Hypo), $TR\alpha^{0/0}$ and $TR\beta^{-/-}$ mice. Scale bar 1mm. (B) Cumulative frequency and relative histograms of bone mineral content for whole femurs. Kolmogorov-Smirnov test; *, $p < 0.05$; **, $p < 0.001$ versus WT Eu/WT.

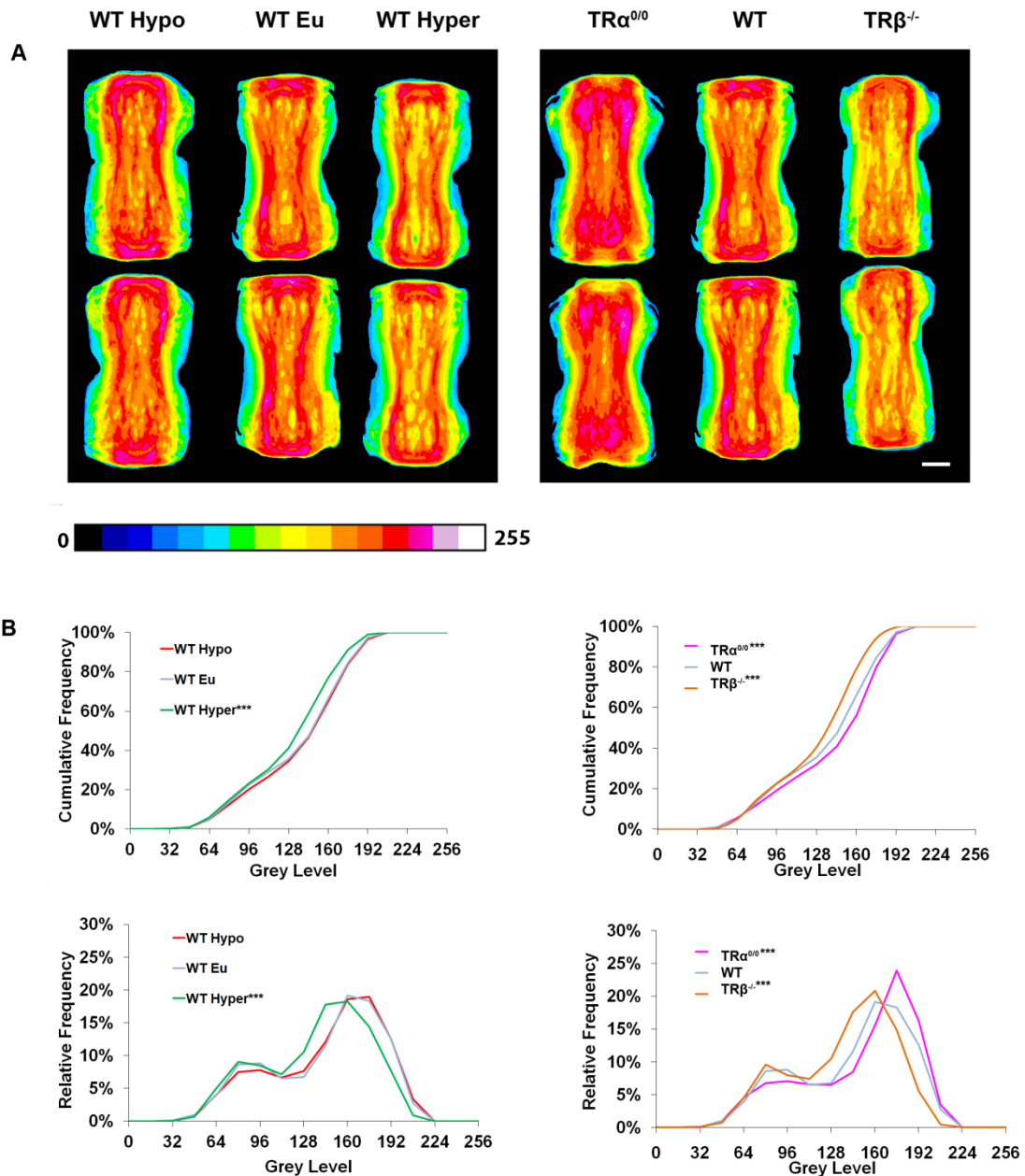


Figure 3.6 Bone mineral content of caudal vertebrae

Faxitron images of caudal vertebrae (A) images of P112 mice from euthyroid wild type control mice (WT Eu), hyperthyroid wild type mice (WT Hyper), hypothyroid wild type mice (WT Hypo), $TR\alpha^{0/0}$ and $TR\beta^{-/-}$ mice. (Scale bar 1mm). (B) Cumulative frequency and relative histograms of mineralisation densities for whole femurs. Kolmogorov-Smirnov test; ***, $p < 0.001$ versus WT Eu/WT.

3.2.4.2 Analysis of qBSE-SEM

Bone micro-mineralisation density was quantified by qBSE-SEM and was assessed in three places: the trabeculae of the lumbar vertebrae; the trabeculae of the proximal tibia and the cortices of the tibia. Hypothyroid and TR $\alpha^{0/0}$ animals had increased micro-mineralisation at all sites. The micro-mineralisation of thyrotoxic mice was similar to wild type mice at all sites assessed. The micro-mineralisation of bone from TR $\beta^{-/-}$ mice was increased in lumbar trabeculae, decreased in the trabeculae of the tibia and similar to wild type controls in the cortical bones (see Figures 3.7-9).

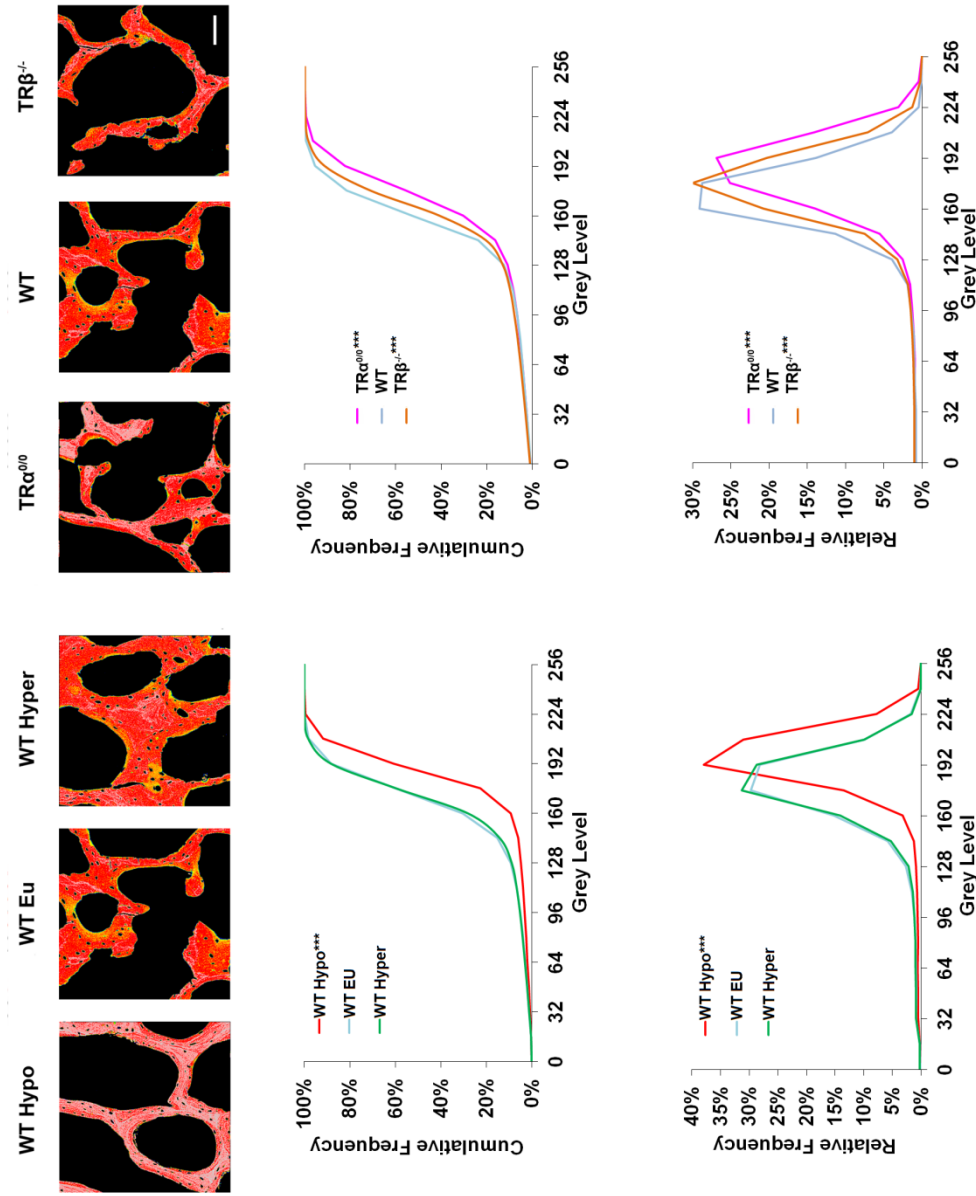


Figure 3.7 Micro-mineralisation of lumbar vertebrae

qBSE-SEM images of lumbar vertebrae from euthyroid wild type control mice (WT Eu), hyperthyroid wild type mice (WT Hyper), hypothyroid wild type mice (WT Hypo), $TR\alpha^{0/0}$ and $TR\beta^{-/-}$ mice (scale bar 100 μ m). Grey scale images were pseudocoloured to an eight colour palette; low mineralisation density is blue and high density is grey. Cumulative frequency histograms were constructed of mineralisation densities. Kolmogorov-Smirnov test; ***, $p < 0.001$ versus euthyroid wild type.

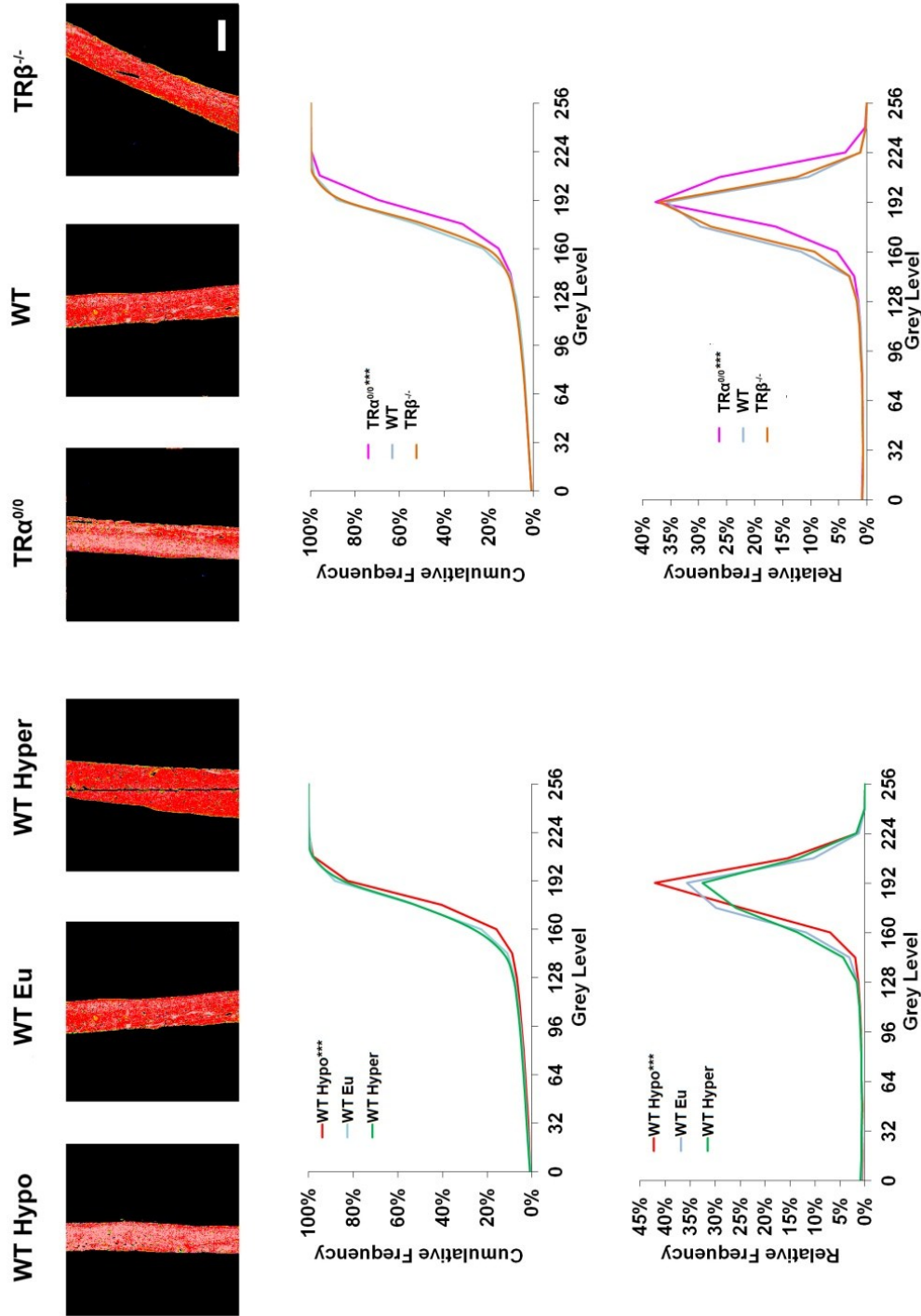


Figure 3.8 Micro-mineralisation of tibial cortical bone

qBSE-SEM images of tibial cortices from euthyroid wild type control mice (WT Eu), hyperthyroid wild type mice (WT Hyper), hypothyroid wild type mice (WT Hypo), $TR\alpha^{0/0}$ and $TR\beta^{-/-}$ mice. (scale bar 100µm). Grey scale images were pseudocoloured to an eight colour palette; low mineralisation density is blue and high density is grey. Cumulative frequency histograms of mineralisation densities. Kolmogorov-Smirnov test; ***, $p < 0.001$ versus euthyroid wild type.

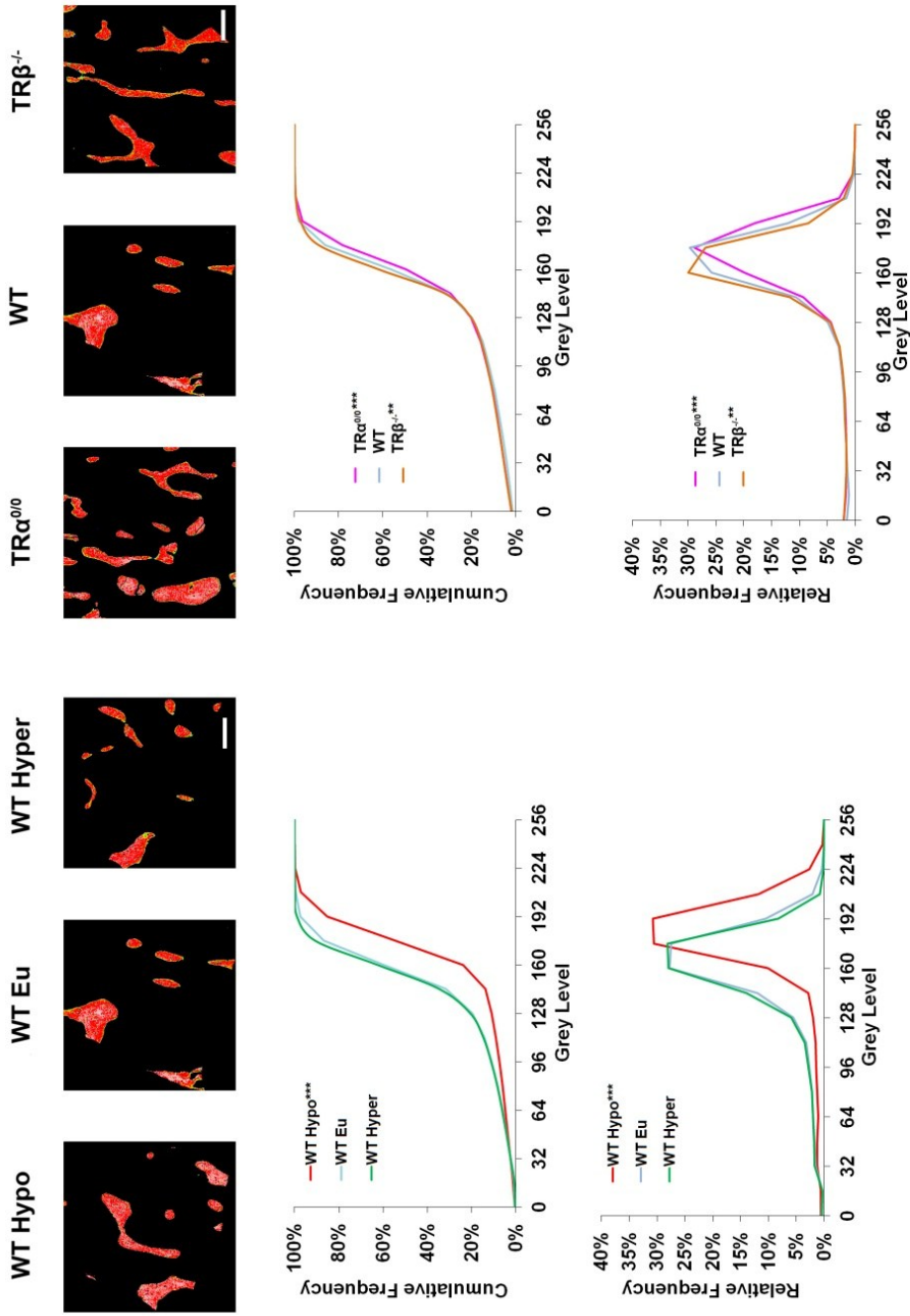


Figure 3.9 Micro-mineralisation of tibial trabeculae

qBSE-SEM images of proximal tibial trabecular bone from euthyroid wild type control mice (WT Eu), hyperthyroid wild type mice (WT Hyper), hypothyroid wild type mice (WT Hypo), TR $\alpha^{0/0}$ and TR $\beta^{-/-}$ mice (scale bar 100 μ m). Grey scale images were pseudocoloured to an eight colour palette; low mineralisation identity is blue and high density is grey. Cumulative frequency histograms of mineralisation densities. Kolmogorov-Smirnov test; **, $p < 0.01$; ***, $p < 0.001$ versus euthyroid wild type.

3.2.5 BONE FORMATION: P1NP AND BFR

The activity of osteoblasts was assessed by quantifying dynamic bone formation parameters and serum bone formation marker P1NP.

Hypothyroid wild type mice had a significantly reduced BFR when compared to euthyroid controls (Figure 3.10). The decreased BFR was due to a reduction in both MA and MS/BS. Calcein labelling in these hypothyroid mice was almost absent as shown in Figure 3.11.

Mean serum P1NP levels in hypothyroid mice, although lower than controls, did not reach significance on statistical analysis. This is likely to be due to the wide variation in P1NP levels in the WT controls.

In hyperthyroid wild type mice, dynamic histomorphometric analysis demonstrated an increased BFR when compared to euthyroid controls. This was predominantly due to an increased MS/BS as the MAR was similar to controls. Analysis of mean serum P1NP levels in hyperthyroid compared to euthyroid controls did not show any statistical difference (see Figure 3.12).

Measurements of dynamic bone formation and serum P1NP parameters were similar in $TR\alpha^{0/0}$ and $TR\beta^{-/-}$ wild type mice, suggesting that changes in bone mass may result from differences in bone resorption.

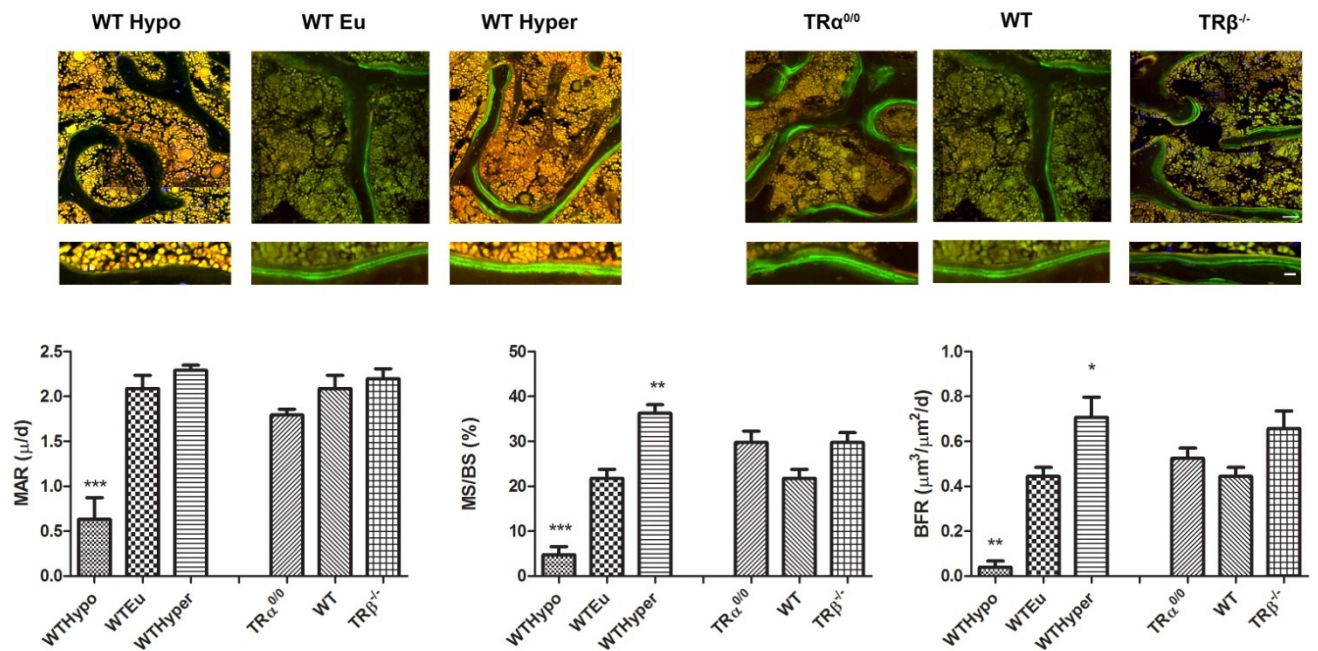


Figure 3.10 Dynamic bone formation parameters

Bone formation in lumbar vertebrae of P112 euthyroid wild type control mice (WT Eu), hyperthyroid wild type mice (WT Hyper), hypothyroid wild type mice (WT Hypo), TR $\alpha^{0/0}$ and TR $\beta^{-/-}$ mice. CSLM views of trabecular bone (scale bar 10 μm). Trabecular bone mineralising surface, MAR and BFR determined by dual calcein labelling. Data expressed as mean \pm SEM, n=4 per group and analysed by ANOVA and Tukey's Multiple Comparison post hoc test: **, p<0.01; ***, p<0.001 versus euthyroid wild type.

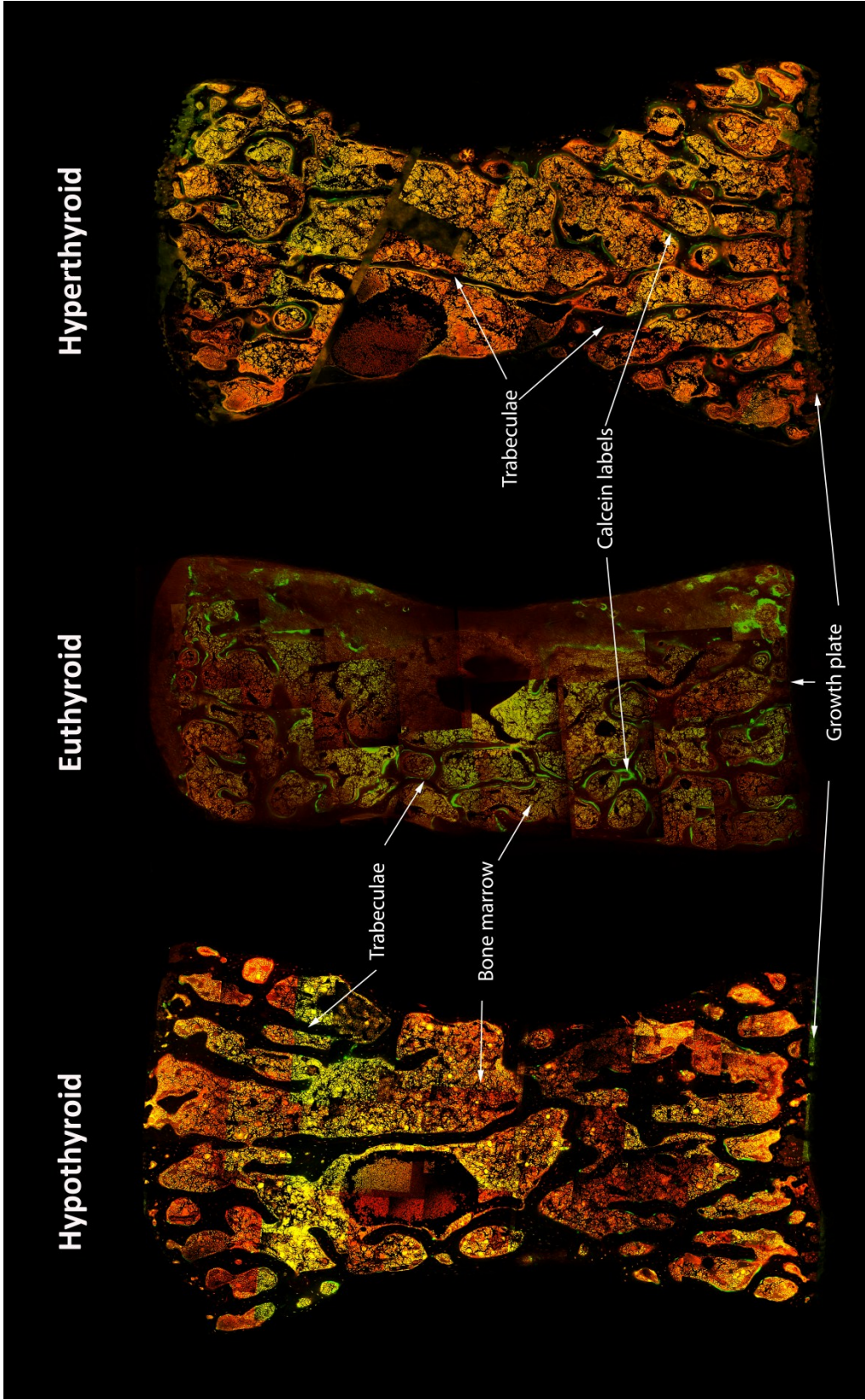


Figure 3.11 Montages of confocal images of lumbar vertebrae of hypothyroid, euthyroid and hyperthyroid wild type mice

Bone formation can be identified by green labelling on the trabecular surfaces. Note how hypothyroid mice have almost absent labelling in contrast to euthyroid and hyperthyroid bones.

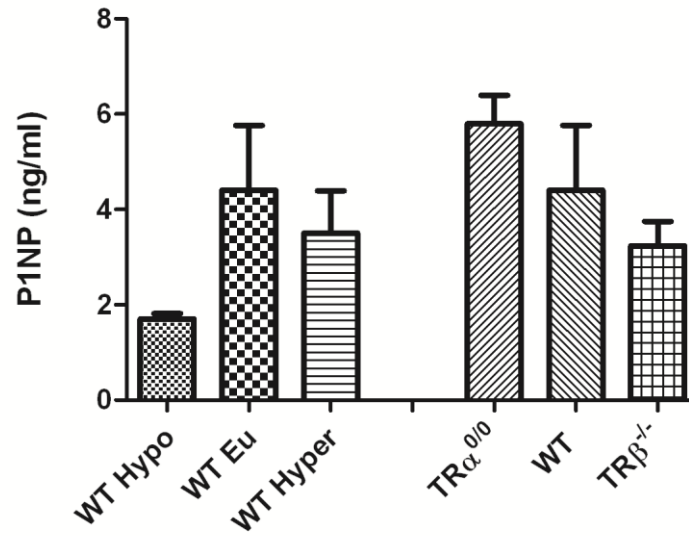


Figure 3.12 Serum P1NP concentrations

Serum samples were obtained from mice at sacrifice and stored at -80°C . N-terminal P1NP was determined by enzyme immunoassay (Immunodiagnostic systems kit AC-33 F1). Data expressed as mean \pm SEM, $n=3-4$ per group and analysed by ANOVA and Tukey's Multiple Comparison post hoc test did not show significant differences between groups compared to wild type.

3.2.6 BONE RESORPTION: CTX, CORTICAL RESORPTION, OSTEOCLAST PARAMETERS

Bone resorption was quantified by serum CTX (which is released into the serum when bone is resorbed and so is an indication of overall resorption), osteoclast histomorphometric parameters and by assessing evidence of bone resorption on the internal (endocortical) cortical surfaces (see Figures 3.13-1.16).

In hypothyroid mice, decreased resorption parameters would be expected in light of an increased bone mass alongside a decreased BFR; this was indeed the case. Decreased osteoclast activity in hypothyroid mice compared to euthyroid controls was evidenced by a serum CTX at the lower limits of the detection range and significantly decreased osteoclast (decreased Oc.N/BS and Oc.N per bone perimeter). Analysis of endocortical resorption pits did not show any significant difference and this is may be due to the presence of resorption pits that remained from before the induction of hypothyroidism.

In hyperthyroid, $TR\alpha^{0/0}$ and $TR\beta^{-/-}$ mice, no difference in serum CTX, endosteal resorption or histomorphometric parameters compared to euthyroid controls was detected.

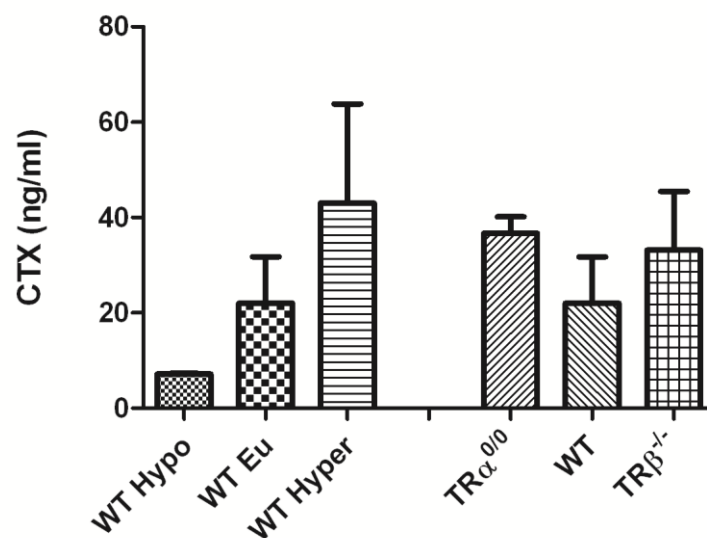


Figure 3.13 Serum bone resorption markers

Serum samples were obtained from mice at sacrifice and stored at -80°C . C-terminal cross-linked telopeptide of type I collagen (CTX) concentrations were determined by enzyme immunoassay. Data expressed as mean \pm SEM, n=3-4 per group and analysed by ANOVA and Tukey's Multiple Comparison post hoc test.

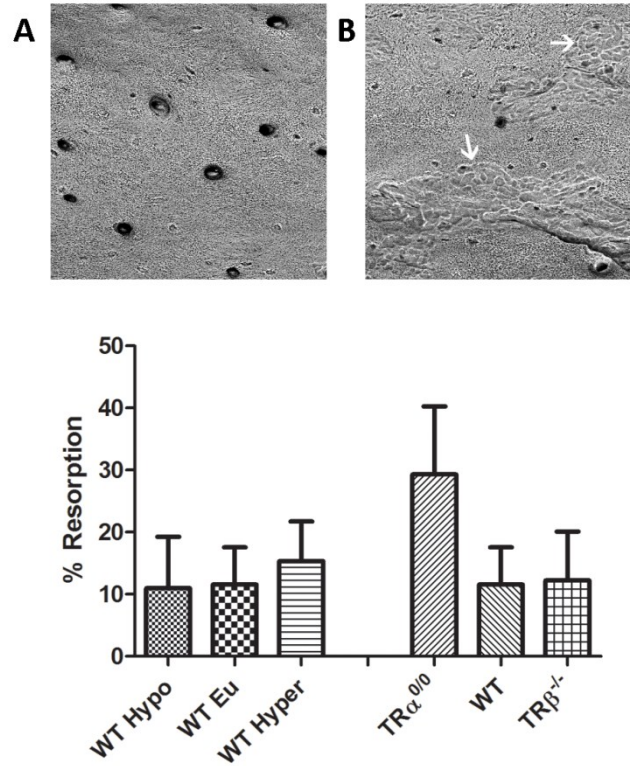


Figure 3.14 Endosteal resorption parameters

Quantitative analysis of endosteal osteoclast resorption surfaces (% of total BS) from P112 euthyroid wild type control mice (WT Eu), hyperthyroid wild type mice (WT Hyper), hypothyroid wild type mice (WT Hypo), TR α ^{0/0} and TR β ^{-/-} mice. Data expressed as mean \pm SEM, n=4 per group and analysed by ANOVA. Images of endosteal surfaces with minimal resorption (A) and with active resorption (B). White arrows illustrate resorption pits.

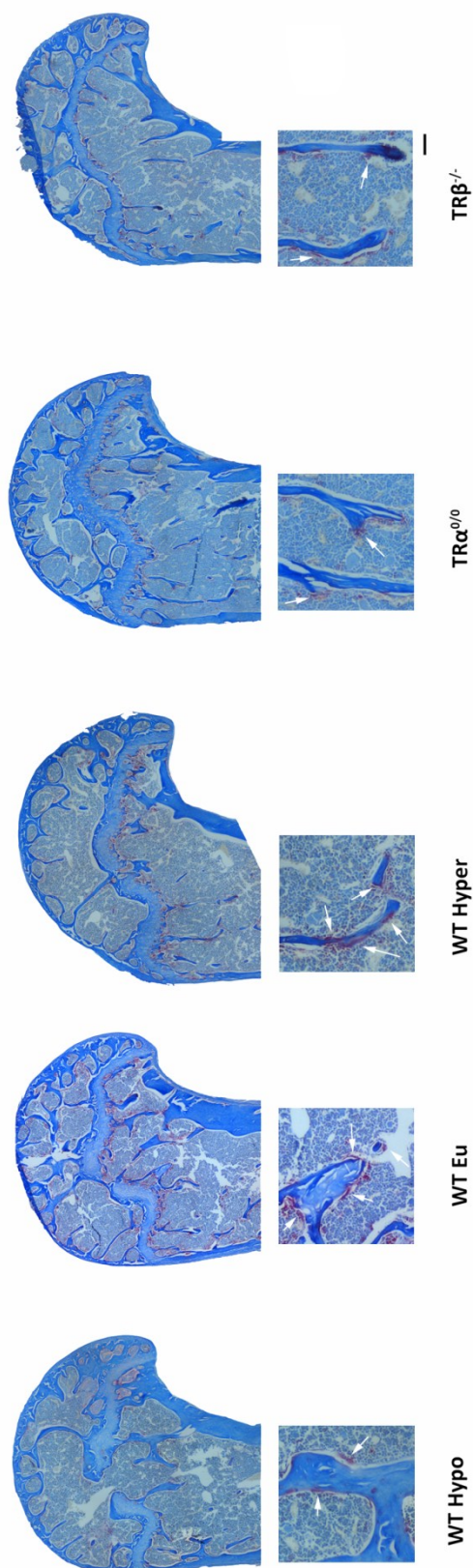


Figure 3.15 Sections of proximal humerus showing TRAP stained osteoclasts in red

Low and high magnification images taken of decalcified specimens of proximal humerus taken by light microscopy. Specimens stained with aniline blue for collagen and osteoclasts are stained red with TRAP staining.

TRAPc stained red osteoclasts are identified by the white arrows. Scale bar is 0.2 mm in image of head of humerus and 0.8mm in high magnification view.

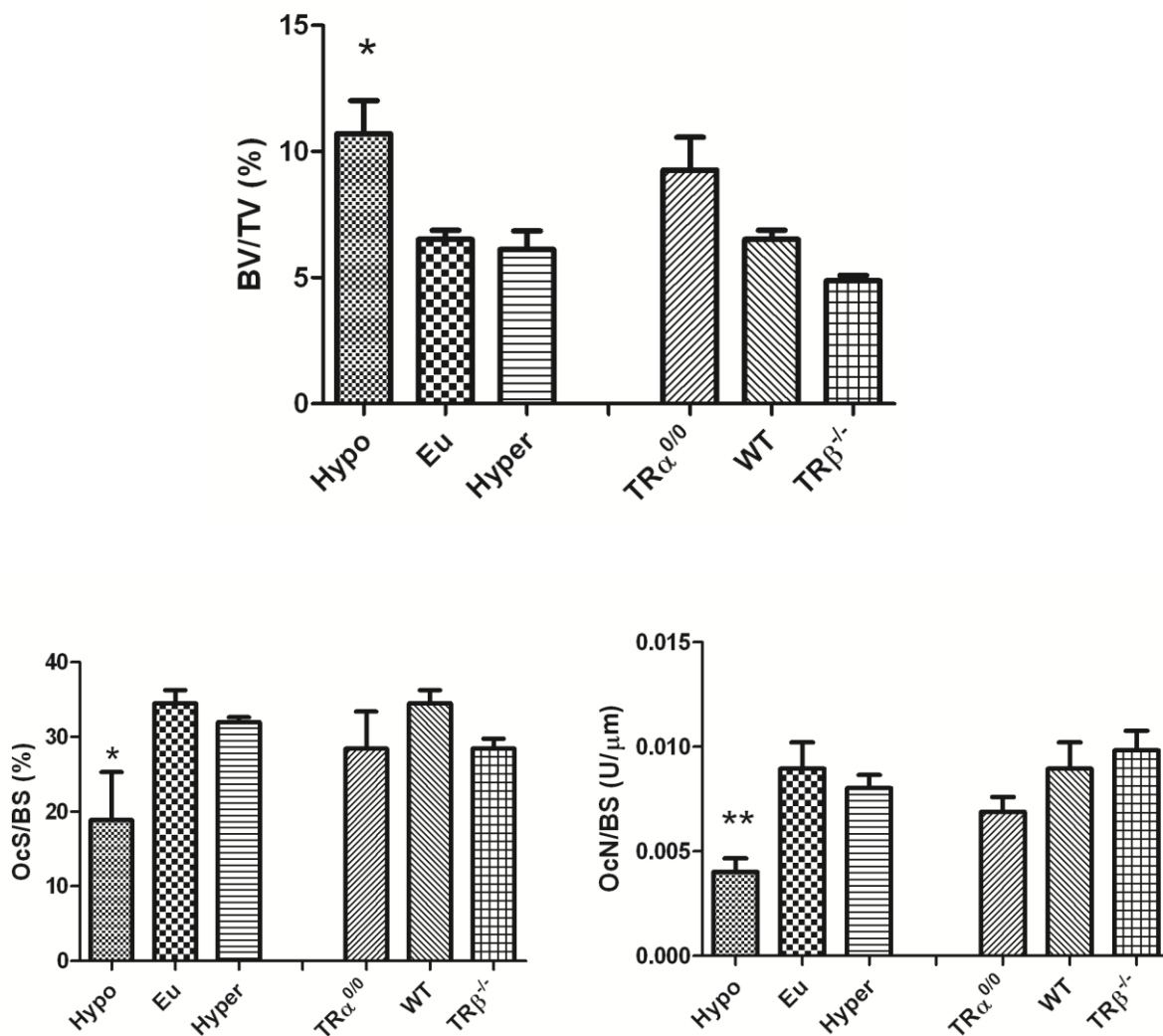


Figure 3.16 Analysis of histomorphometric osteoclast parameters

Bone and osteoclast indices in proximal humerus of P112 euthyroid wild type control mice (Eu), hyperthyroid wild type mice (Hyper), hypothyroid wild type mice (Hypo), TR $\alpha^{0/0}$ and TR $\beta^{-/-}$ mice. BV/TV of the area of analysis is shown. Oc.S/BS and Oc.N/BS graphs are shown. Data expressed as mean \pm SEM, n=4 per group and analysed by ANOVA and Tukey's Multiple Comparison post hoc test: *, p<0.05; **, p<0.001 versus euthyroid wild type mice.

3.2.7 BIOMECHANICAL TESTING

The effects of thyroid status manipulation during adulthood on bone did not significantly alter the mechanical properties of the bones when assessed by three point bending. The TR $\alpha^{0/0}$ mice had similar biomechanical properties as wild type but the long bones of TR $\beta^{-/-}$ mice were weaker with lower stiffness and lower yield, maximum and fracture load (see Figure 3.17).

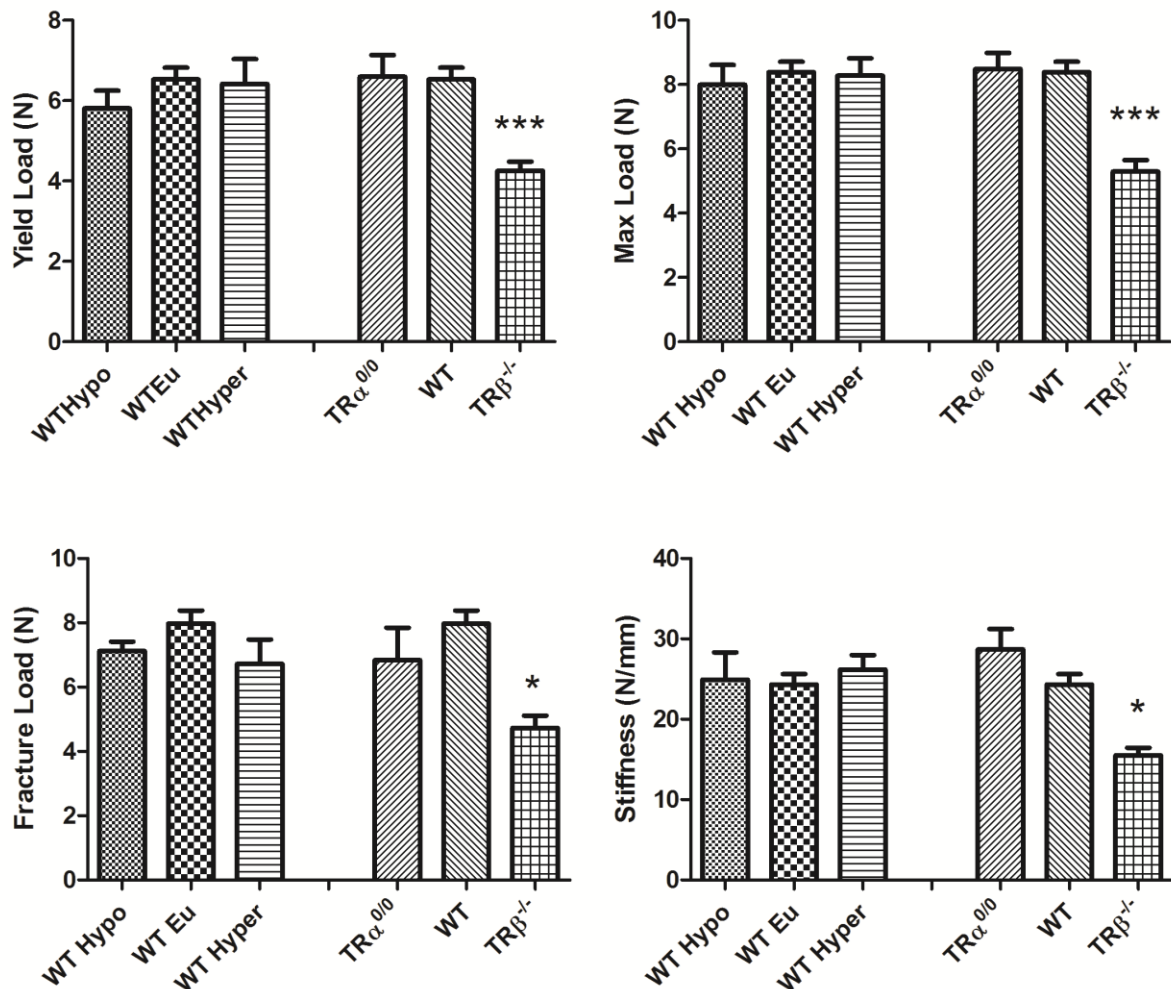


Figure 3.17 Biomechanical properties

Graphs showing yield load, maximum load, fracture load and stiffness in tibias of P112 euthyroid wild type control mice (WT Eu), hyperthyroid wild type mice (WT Hyper), hypothyroid wild type mice (WT Hypo), TR $\alpha^{0/0}$ and TR $\beta^{-/-}$ mice. Data expressed as mean \pm SEM, n=4-6 per group and analysed by ANOVA and Tukey's Multiple Comparison post hoc; *, p<0.05, ***, p<0.001 versus euthyroid wild type mice.

3.3 SUMMARY OF RESULTS

	WT Hypo vs. WT	TR $\alpha^{0/0}$ vs. WT	WT Hyper vs. WT	TR $\beta^{-/-}$ vs. WT
Weight	→	→	→	↓↓
Tail length	→	→	→	↓
Femur length	→	→	→	↓
Tibial length	→	→	→	↓↓
Cortical diameter	→	→	→	↓↓↓
Cortical thickness	→	→	→	↓↓
μ CT BV/TV	↑↑↑	↑	↓	↓
Femoral BMC	↑↑↑	↑↑↑	↓	↓↓↓
Caudal Vert BMC	→	↑↑↑	↓↓↓	↓↓↓
qBSE SEM Lumbar trabeculae	↑↑↑	↑↑↑	→	↑↑↑
qBSE SEM Tibial trabeculae	↑↑↑	↑↑↑	↑↑↑	↓↓
qBSE SEM Tibial cortices	↑↑↑	↑↑↑	↑↑↑	→
BFR	↓↓	→	→	→
MAR	↓↓↓	→	→	→
BS/BS	↓↓↓	→	↑↑↑	→
P1NP	→	→	→	→
CTX	→	→	→	→
Oc.S/BS	↓	→	→	→
N.Oc/B.Pm	↓↓	→	→	→
Resorption	→	→	→	→
Yield Load	→	→	→	↓↓↓
Max Load	→	→	→	↓↓↓
Fracture Load	→	→	→	↓
Stiffness	→	→	→	↓

Table 3.2 Summary of skeletal phenotyping

Results of skeletal phenotyping parameters of hypothyroid (WT hypo), TR $\alpha^{0/0}$, hyperthyroid (WT hyper) and TR $\beta^{-/-}$ mice as compared to (vs) wild type mice controls (WT eu). The level of significant difference of parameters compared to wild type controls are indicated by numbers of arrows: 1 arrow p<0.05, 2 arrows p<0.01, 3 arrows p<0.001 and direction of arrow: up indicates greater than and down indicates lower than control data. → indicates no significant difference.

3.4 DISCUSSION

To date, the published literature has shown that the skeletal phenotypes of TR α ^{0/0} and TR β ^{-/-} mice are similar to those of mice with hypothyroidism and hyperthyroidism respectively. This has led to the hypothesis that TR α ^{0/0} mice have decreased skeletal T3 signalling due to a lack of TR α in skeletal tissue and TR β ^{-/-} mice have increased skeletal T3 signalling due to the increase in circulating thyroid hormones and intact TR α . The results of my experiments suggest that this may only be partially correct.

The skeletal phenotype of TR α ^{0/0} mice analysed in the experiments presented in this chapter, is in agreement with the published literature. However, in addition to what is known, the novel data presented in this chapter provides evidence that TR α ^{0/0} mice, unlike hypothyroid mice, have similar osteoblastic BFRs to those of wild type controls.

This observation suggests that the increased bone mass in TR α ^{0/0} mice is secondary to decreased osteoclast resorption and that there is an uncoupling of bone resorption and formation. Unfortunately, the parameters used, for assessment of bone resorption in these experiments were not sufficiently sensitive to detect any changes in TR α ^{0/0} mice.

TR β ^{-/-} mice have skeletal phenotyping similar to that of mice with thyrotoxicosis, with reduced BMC as a consequence of increased resorption and formation (a high bone turnover osteoporosis) (Bassett and Williams, 2009).

3.4.1 Changes in growth and gross structural parameters may be related to duration of disruption of tissue thyroid status

Serum concentrations of fT4 and fT3 confirmed that manipulation of thyroid status in wild type mice had the desired effect (see Table 2.1). Treatment with T4 in wild type mice was intended to induce hyperthyroidism without extreme thyrotoxicosis and accordingly did not result in a reduction in weight as would be expected in thyrotoxicosis.

During early life and puberty, the skeleton undergoes a period of rapid expansion and remodelling before reaching peak bone mass, after which the skeleton remains in a relatively stable state. In mice, the majority of growth is usually complete by around 10 weeks of age, which is the age at which thyroid status manipulation was commenced in the hypo and thyrotoxic groups.

Both hypothyroid and TR $\alpha^{0/0}$ mice were not growth impaired, and had similar gross structural bone parameters, including femur and tibial length and cortical bone diameter and thickness, when compared with euthyroid controls. Whilst hyperthyroid mice also had similar growth and gross structural parameters as controls, TR $\beta^{-/-}$ mice were lighter, with a shorter tail length, diminished cortical bone diameter and thickness and shorter long bones compared to euthyroid controls.

The differences in growth and gross structural parameters between hyperthyroid and TR $\beta^{-/-}$ mice could have been as a result of either a lack of TR β or the length of time that the mice had been thyrotoxic. TR $\beta^{-/-}$ mice have been thyrotoxic throughout development and normal bone development is already impaired. These mice therefore have a more pronounced phenotype when compared to the wild type mice used in this experiment that have undergone a relatively short duration (6 weeks) of thyroid status manipulation. Further studies that could clarify this hypothesis include skeletal phenotyping of an inducible knockout model where the TR has been knocked out in adult mice for the same amount of time as the wild type mice have been rendered hyper and hypothyroid.

3.4.2 Micro architecture in TR $\alpha^{0/0}$ mice is similar to hypothyroid mice and microarchitecture in TR $\beta^{-/-}$ mice is similar to thyrotoxic mice

Despite the lack of change in bone length and cortical diameter and thickness in wild type hypothyroid and hyperthyroid mice, micro CT and BSE-SEM analysis demonstrate substantial changes in bone microarchitecture. TR $\alpha^{0/0}$ mice are similar to hypothyroid mice, with increased BV/TV and coarse, plate-like trabeculae, whilst TR $\beta^{-/-}$ mice are similar to thyrotoxic mice and show decreased BV/TV with gracile trabeculae.

The micro CT data in TR $\alpha^{0/0}$ mice showed a 20% greater BV/TV than controls but incongruously, no difference in Tb.Th, Tb.Sp or Tb.N. Inconsistencies in micro CT data are also seen in the hypothyroid group, where the data shows a 43% greater BV/TV, with a significantly elevated Tb.Th but with no difference in Tb.N or Tb.Sp. These results are incongruous because an increased Tb.Th with no difference in Tb.N or Tb.Sp should result in a decrease in Tb.Sp. Alternatively, an increased Tb.Th with no difference in Tb.Sp should result in a decrease in Tb.N. These anomalies suggest that some of the micro CT data may not be of sufficient precision and are likely to have arisen due to insufficient resolution. Micro CT is reported to have a detection pixel size of 4.3 μm^3 , which may not be a high enough resolution to detect differences in these parameters. Another possibility is that the real resolution of imaging used for deriving the results is lower than reported. In both cases, the

accuracy of the smaller measures such as Tb.N, Tb.Sp, Tb.N and SMI could have been compromised. The limitations of micro CT, as demonstrated by the data, highlight the importance of using a number of complementary techniques in assessing the skeleton. In this way, an overall picture can be built up that provides a more accurate reflection of the skeletal phenotype.

3.4.3 Changes in bone mineralisation are site specific

Comparisons were further investigated by assessing and comparing bone mineralisation. Hypothyroid animals had an increased BMC, which was highly significant in the femurs but not in the caudal vertebrae. This site specific difference in BMC can be attributed to femurs consisting predominantly of cortical bone whereas caudal vertebrae consist predominantly of cancellous bone. Although the increases in BMC in the femurs are likely to be due to cortical changes, cortical thickness and cortical bone width in hypothyroid mice and euthyroid mice were similar. This suggests that the increase in femoral BMC in the hypothyroid group is likely to be a consequence of increased micro-mineralisation. This was confirmed by qBSE-SEM analysis which showed that micro-mineralisation was significantly increased in all hypothyroid bones assessed. $TR\alpha^{0/0}$ mice showed similar but more pronounced changes in BMD with increased BMC and micro-mineralisation at all skeletal sites evaluated.

The significant increase in micro-mineralisation in hypothyroid mice suggests that thyroid hormone is important in the normal regulation of mineralisation. A potential mechanism for this may be the effects of hypothyroidism on the osteocytes, although this would need further investigation.

Whilst hypothyroidism seems to affect cortical bone predominantly, the effect of hyperthyroidism on BMC is more pronounced in the caudal vertebrae. The decrease in bone mass is a consequence of decreased trabecular volume as shown by the micro CT data rather than a decrease in micro-mineralisation. $TR\beta^{-/-}$ mice having been thyrotoxic throughout development, have a more pronounced phenotype and therefore have lower BMC at both the femur and caudal vertebrae.

Micro-mineralisation in $TR\beta^{-/-}$ mice was higher than controls in the lumbar trabeculae, lower at the tibial trabeculae and no difference in the cortices. These inconsistencies may be as a result of site specific differences in micro-mineralisation, but to draw meaningful conclusions from this data, this finding would ideally be repeated.

3.4.4 Bone formation in TR α ^{0/0} mice is similar to controls

To further assess the mechanism of skeletal changes, bone formation and resorption parameters were evaluated. Bone formation in hypothyroid mice was almost completely absent, however, rather unexpectedly, TR α ^{0/0} mice had bone formation similar to controls. Bone formation in euthyroid TR α ^{0/0} mice has not previously been described in the literature and a divergence in bone formation when compared to hypothyroid animals was unexpected. This indicates that the presence of TR α is not essential for normal bone formation and that in the absence of TR α , thyroid signalling can occur via TR β . This was verified by the results in Chapter 4 which show that when TR α ^{0/0} mice are rendered hypothyroid, the BFR becomes similar to hypothyroid animals, indicating that T3 dependent BFR signalling is occurring via TR β in the absence of TR α . Interestingly, in light of normal bone formation in TR α ^{0/0} mice, the increase in bone mass must therefore be secondary to decreased osteoclastic resorption and due to an uncoupling of the remodelling cycle. These results also indicate that TR α is needed for normal osteoclastic resorption for which TR β cannot be adequately substituted. The role of TR α in osteoclastic resorption is unclear and whether this has a direct or secondary effect on osteoclasts.

BFRs in hyperthyroid and TR β ^{-/-} mice were similar to controls. Unfortunately, there was a wide variation in the measurements of these groups and although the mean BFR in both groups was higher, this was not significantly different from the controls. Hyperthyroid mice, however, did have an elevated MS/BS. Serum P1NP levels also showed a high variability and whilst hypothyroid mice had a serum P1NP at the lower limits of the assay, assessment of bone formation in the other groups did not satisfactorily reflect dynamic bone formation measurements.

Circulating serum levels of bone turnover markers (both formation P1NP and breakdown CTX) exhibit diurnal variation as well as seasonal variation, which may account for the large variability of the results. To minimise the variability of serum bone markers, the mice were fasted and morning blood samples taken. However, there were often a few hours between obtaining the serum samples of the first of a batch of mice compared to the last and the samples were harvested over a period of around 15 months which may have led to some inconsistency in the results. It is also difficult to make direct comparisons between the groups because the bone mass between groups varied widely. Although there is a wide variation in results, hypothyroid mice consistently had a P1NP at the lower limit of detection, whilst P1NP levels in TR α ^{0/0} mice was much higher and similar to dynamic bone formation findings.

3.4.5 Bone resorption

Hypothyroid and TR $\alpha^{0/0}$ mice have increased bone mass with low or normal BFRs. This indicates that the increase in bone mass is likely to be as a result of relatively decreased osteoclast resorption. Conversely, hyperthyroid and TR $\beta^{-/-}$ mice have decreased bone mass with a normal BFR, which indicates that there is likely to be relatively increased bone resorption.

I chose to determine osteoclast activity by assessing three different parameters: serum concentration of bone breakdown marker CTX, percentage of endosteal erosion surfaces and osteoclast histomorphometric parameters (Oc.S/BS (%) and Oc.N/BS). Unlike bone formation assessment by double labelling, there is no method of directly assessing bone resorption and the surrogate measures discriminates differences poorly.

3.4.6 Resorption parameters in hypothyroid and TR $\alpha^{0/0}$ mice

Hypothyroid mice have CTX at the lower limits of the assay and osteoclast surface and number were decreased. The endosteal resorption surfaces were reduced in all but one outlier, which had residual erosion surfaces which were not filled after bone formation was switched off after the induction of hypothyroidism. All these parameters indicate that hypothyroid mice have decreased bone resorption.

Resorption parameters in TR $\alpha^{0/0}$ mice are similar to those in wild type mice but it is important to interpret serum CTX in light of the fact that TR $\alpha^{0/0}$ bones have increased bone volume, so direct comparisons to wild type mice cannot be made. Histomorphometric osteoclast parameters such as Oc.S/BS and N.Oc/B.Pm are not different to controls. CTX and histomorphometric osteoclast parameters are clearly higher than in hypothyroid wild type animals but this data does not indicate whether the osteopetrosis is secondary to dysfunction of osteoclast cells or due to osteoclast inactivity. It is likely that in TR $\alpha^{0/0}$ mice, resorption is impaired but still able to occur as evidenced by adequate modelling of the bones during growth.

3.4.7 Resorption parameters in hyperthyroid and TR $\beta^{-/-}$ mice

Serum CTX, osteoclast parameters and endosteal resorption surfaces were not different compared to controls. Previous studies in rats have shown that thyrotoxicosis results in an increase in resorption and osteoclast parameters but in those studies, the rats had been treated for a longer period and with higher doses of T4 (Ongphiphadhanakul et al., 1992). As seen previously with the densitometry data, the sensitivity of bone to hyperthyroidism is also site specific and thus serum breakdown markers may be more likely to provide a more accurate picture of overall resorption.

TR β ^{-/-} mice have a lower bone mass and although the CTX and mean Oc.N per bone perimeter were higher than controls, they did not reach statistical significance.

3.4.8 Mechanical bone strength

Fracture data shows that changing thyroid status does not impact mechanical bone strength in adult wild type mice. This is likely to be because the thyroid status was manipulated in adult animals and only for a relatively short period of time (6 weeks). TR α ^{0/0} bones have similar mechanical properties to wild type controls, but TR β ^{-/-} bones are less stiff and less strong than wild type controls.

3.4.9 Summary and salient points

In summary, TR α ^{0/0} mice have some similar features to hypothyroid mice, such as increased bone mass and decreased bone resorption. However, unlike in hypothyroidism, TR α ^{0/0} mice have a BFR similar to that of wild type controls, suggesting that there is an uncoupling of bone formation and resorption.

These results suggest that in the absence of TR α , T3 dependent bone formation can continue, compensated for by TR β signalling. Bone resorption, however, is more specifically dependent on T3 signalling through TR α and is impaired in the absence of TR α . It is not clear if TR α dependent osteoclast resorption is a direct or indirect effect of the action of T3 and the molecular mechanism for this process is a potential area of future research. TR β ^{-/-} mice have features of skeletal hyperthyroidism with a high turnover osteoporosis, but, the skeletal phenotype is more pronounced than that of the adult thyrotoxic mice because skeletal hyperthyroidism has been present throughout development. The experiments in this chapter demonstrate that bone remodelling is not dependent on the presence of TR β but the skeletal phenotype is likely to be due to elevated circulating levels of thyroid hormone, signalling through an intact TR α .

The lack of discriminatory osteoclastic resorption parameters is a major short coming of these experiments. The novel findings presented in this chapter highlight the importance of assessing the skeleton using multiple complementary phenotyping techniques (in particular, dynamic bone formation parameters) before determining physiological mechanisms.

Chapter 4

The effects of differing thyroid status on the skeletal phenotype of TR α 0/0 and TR β -/- mice

4 THE EFFECTS OF DIFFERING THYROID STATUS ON THE SKELETAL PHENOTYPE OF TR α ^{0/0} AND TR β ^{-/-} MICE

4.1 BACKGROUND

The effects of excess thyroid hormone on the developing skeleton are anabolic, stimulating bone formation and resulting in increased linear growth and bone mass. In adults, the effects of excess thyroid hormone are catabolic, stimulating bone turnover (particularly by increasing osteoclastic bone resorption and bone loss) and resulting in osteoporosis (Mosekilde and Melsen, 1978). Conversely, insufficient thyroid hormone during development results in delayed bone maturation, lower bone mass and decreased linear growth. In adults, one of the primary effects of hypothyroidism is decreased bone turnover, particularly due to decreased osteoclastic bone resorption (Eriksen et al., 1986). The skeletal phenotyping of wild type hypo and hyperthyroid mice presented in Chapter 3 is in line with what is currently known in the literature.

The role of TR α and TR β in mediating the effects of thyroid hormone in skeletal tissue remains unclear.

Previous studies of TR α ^{0/0} and TR β ^{-/-} mice from Professor Graham Williams' lab, led to the proposal that differences in bone phenotype are accounted for by the differences in action of TR α and TR β in the skeleton and in the HPT axis (Bassett and Williams, 2009). It was hypothesised that TR α ^{0/0} mice, despite having normal circulating thyroid hormone levels, have reduced skeletal T3 signalling due to the absence of TR α , the predominant receptor in bone. TR β ^{-/-} mice have RTH and have elevated circulating thyroid hormone levels, which result in increased T3 signalling in the skeleton through an intact TR α .

The normal BFR in TR α ^{0/0} mice, as shown in Chapter 3, suggests that thyroid hormone signalling is not reduced in the osteoblasts of these mice and that in the absence of TR α , TR β is able to compensate. The elevated bone mass in TR α ^{0/0} mice, however, suggests that bone osteoclastic resorption is impaired and therefore TR α dependent.

Another group, Monfoulet *et al*, proposed that the acute effects of changes in thyroid status were mediated by TR β and that the long term chronic effects were mediated by TR α (Monfoulet et al., 2011). This group reached this conclusion after comparing the skeletal effects of hypothyroidism and thyrotoxicosis in TR α ^{0/0} and TR β ^{-/-} mice. They found that after two weeks of thyroid manipulation, hypothyroid TR α ^{0/0} mice had an increased BV/TV and bone density, and reduced

serum osteocalcin and CTX levels when compared to thyrotoxic TR $\alpha^{0/0}$ mice. Conversely, after two weeks of treatment, hypothyroid TR $\beta^{-/-}$ mice showed no differences in BV/TV, bone density or serum turnover parameters when compared to hyperthyroid mice. They then extended thyroid status manipulation in TR $\beta^{-/-}$ mice to five weeks and found a significantly higher BV/TV and lower MS/BS and Oc.S/BS in hypothyroid TR $\beta^{-/-}$ mice. The data presented by Monfoulet *et al*, however, has a number of limitations. For example, data for the skeletal phenotypes of euthyroid TR $\alpha^{0/0}$ and TR $\beta^{-/-}$ mice was not provided, so the individual effects of hyperthyroidism versus hypothyroidism on the skeleton are not clear. Micro CT with a resolution of 16 μ m was used to measure differences in trabecular parameters such as Tb.N and thickness. However, given the scan resolution, the reported significant differences in Tb.Th of less than 10 μ m are unlikely to be accurate. Additionally, the authors were surprised to find that double labelling in T4 treated mice was 54% lower than in untreated mice. They then also noted that there was considerable fragmentation of the double labels and therefore surmised that MAR and BFR could not be reliably measured. Despite the observation that double labelling measurements were unreliable, they continued to use MS/BS data to support their conclusions. These limitations in data analysis have led to controversies in the interpretation of the data.

In this chapter, I describe the effects of hypothyroid, euthyroid and hyperthyroid status on the skeletal phenotype of adult TR $\alpha^{0/0}$ and TR $\beta^{-/-}$ mice in order to clarify the role of liganded and unliganded TR α and TR β in the skeleton. I have used a number of techniques to verify the skeletal phenotype. Of particular note, micro CT analysis was performed on images with 4.3 μ m resolutions giving greater accuracy to measurement and calcein double labels were administered intravenously with a short interlabel interval to increase accuracy of measurements. The data obtained and presented in this chapter provides important new information about the effects of increased thyroid hormone signalling through each receptor and the effects of unliganded receptors on the skeleton.

4.2 RESULTS

4.2.1 CIRCULATING THYROID HORMONE STATUS

Thyroid manipulation to induce hypothyroidism with low iodine diet and PTU was effective with serum levels of fT4 below the limits of detection in all groups of treated mice (Figure 4.1). For hyperthyroid groups, TR $\alpha^{0/0}$ mice were treated with 1.2 ml/l of T4 which resulted in a significantly elevated serum T4, whilst TR $\beta^{-/-}$ mice remained untreated but had significantly elevated circulating T3 and T4 compared to euthyroid wild type mice (see data in Chapter 3). For the euthyroid group,

$TR\alpha^{0/0}$ mice remained untreated and had a normal circulating thyroid hormone status, whilst $TR\beta^{-/-}$ mice were rendered euthyroid by administering a low iodine diet with PTU alongside physiological concentrations of T3 (block and replace). T3, and not T4, was required to render the mice euthyroid because PTU has actions to block deiodinase 1 activity and so prevents the conversion of prohormone T4 to T3. Serum T3 levels in treated $TR\beta^{-/-}$ mice were not significantly different to euthyroid wild type mice, confirming euthyroid circulating thyroid hormone status (Figure 4.1).

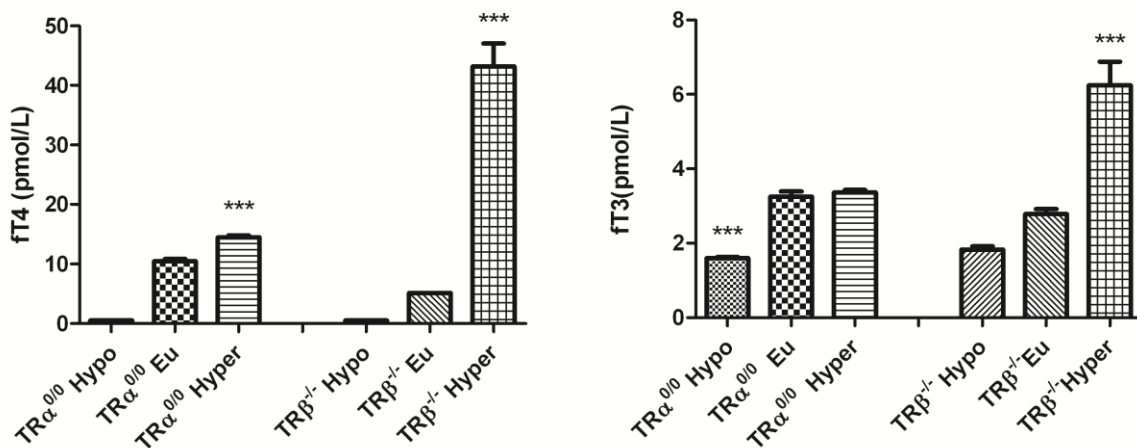


Figure 4.1 Circulating thyroid hormone status

Serum free T4 and free T3 concentrations (pmol/litre) in P112 mice.

Data expressed as mean \pm SEM, n=6 per group and analysed by ANOVA and Tukey's Multiple Comparison post hoc test: ***, p<0.001 versus euthyroid animals in the same groups. Serum free T4 levels for Hypo groups were below the lower limit of detection of the assay.

4.2.2 GROWTH

4.2.2.1 Body weight and tail length measurements

Manipulation of thyroid status in adult $TR\alpha^{0/0}$ and $TR\beta^{-/-}$ mice did not have a significant impact on weight or tail length. This is likely to be because the majority of growth was complete at the onset of thyroid status manipulation and so change in thyroid status was predominantly affecting remodelling and not modelling (see Figure 4.2).

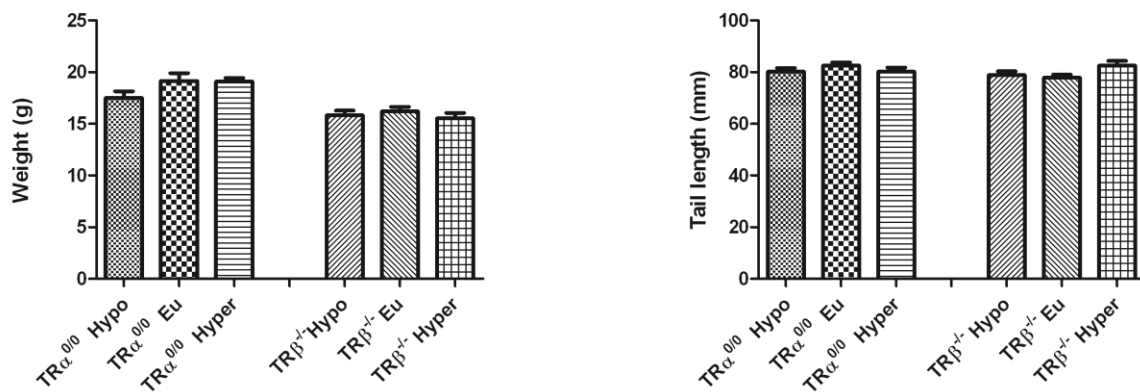


Figure 4.2 Growth parameters

Weight and tail length of P112 mice. Data expressed as mean \pm SEM, n=6 per group and analysed by ANOVA and Tukey's Multiple Comparison post hoc test: no significant difference in any group when compared to euthyroid mice.

4.2.3 STRUCTURAL PARAMETERS

4.2.3.1 Bone length and cortical measurements

There was no difference in femur or tibial length in adult $TR\alpha^{0/0}$ and $TR\beta^{-/-}$ mice as a result of change in thyroid status (Figure 4.3). However, rendering $TR\alpha^{0/0}$ mice thyrotoxic resulted in a reduction in cortical thickness without any change in cortical bone diameter (Figure 4.3). Alterations in thyroid status did not result in changes in bone length or cortical measurements in $TR\beta^{-/-}$ mice.

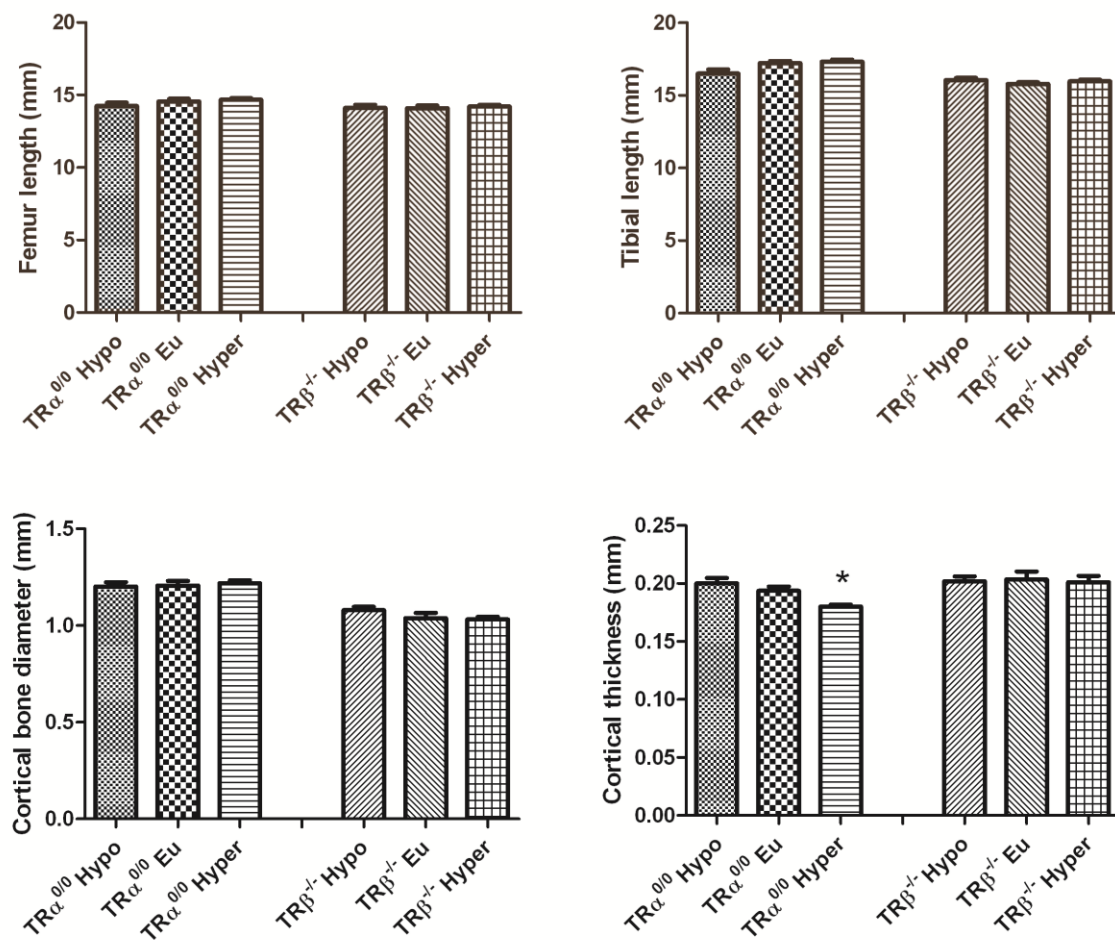


Figure 4.3 Gross structural parameters

Femur length and cortical thickness of P112 mice. Data expressed as mean \pm SEM, n=6 per group and analysed by ANOVA and Tukey's Multiple Comparison post hoc test: *, p<0.05; versus euthyroid group.

4.2.3.2 Bone microarchitecture: BSE-SEM and micro CT

Micro CT measurements of trabecular bone were analysed in the region above the growth plate of the distal femur. The results for adult TR $\alpha^{0/0}$ and TR $\beta^{-/-}$ mice with differing thyroid status are set out in Table 4.1. BV/TV was similar in hypothyroid and euthyroid TR $\alpha^{0/0}$ mice (14.7 \pm 1.9% versus 13.1 \pm 0.4% respectively). Trabeculae of hypothyroid and euthyroid TR $\alpha^{0/0}$ femurs looked very similar in SEM images (see Figure 4.4). SEM images of distal femoral trabeculae in hyperthyroid TR $\alpha^{0/0}$ mice appear similar to those of euthyroid TR $\alpha^{0/0}$ mice near the growth plate but are less coarse and less closely spaced further up the shaft of the femur (Figure 4.4). The micro CT BV/TV parameters in hyperthyroid TR $\alpha^{0/0}$ mice are lower but not significantly different to euthyroid and hypothyroid TR $\alpha^{0/0}$ mice (ANOVA and Tukey's post hoc test not significant).

In TR $\beta^{-/-}$ mice, there was a 63% increase in BV/TV in hypothyroid versus euthyroid groups (Table 4.1), which may be the result of an apoTR α effect. There was no difference in BV/TV when hyperthyroid TR $\beta^{-/-}$ mice were rendered euthyroid. SEM images of the distal femurs also reflected the micro CT indices, suggesting more plate-like and coarse trabeculae in the hypothyroid TR $\beta^{-/-}$ femur and scanty, gracile trabeculae in the euthyroid and hyperthyroid bones (Figure 4.4).

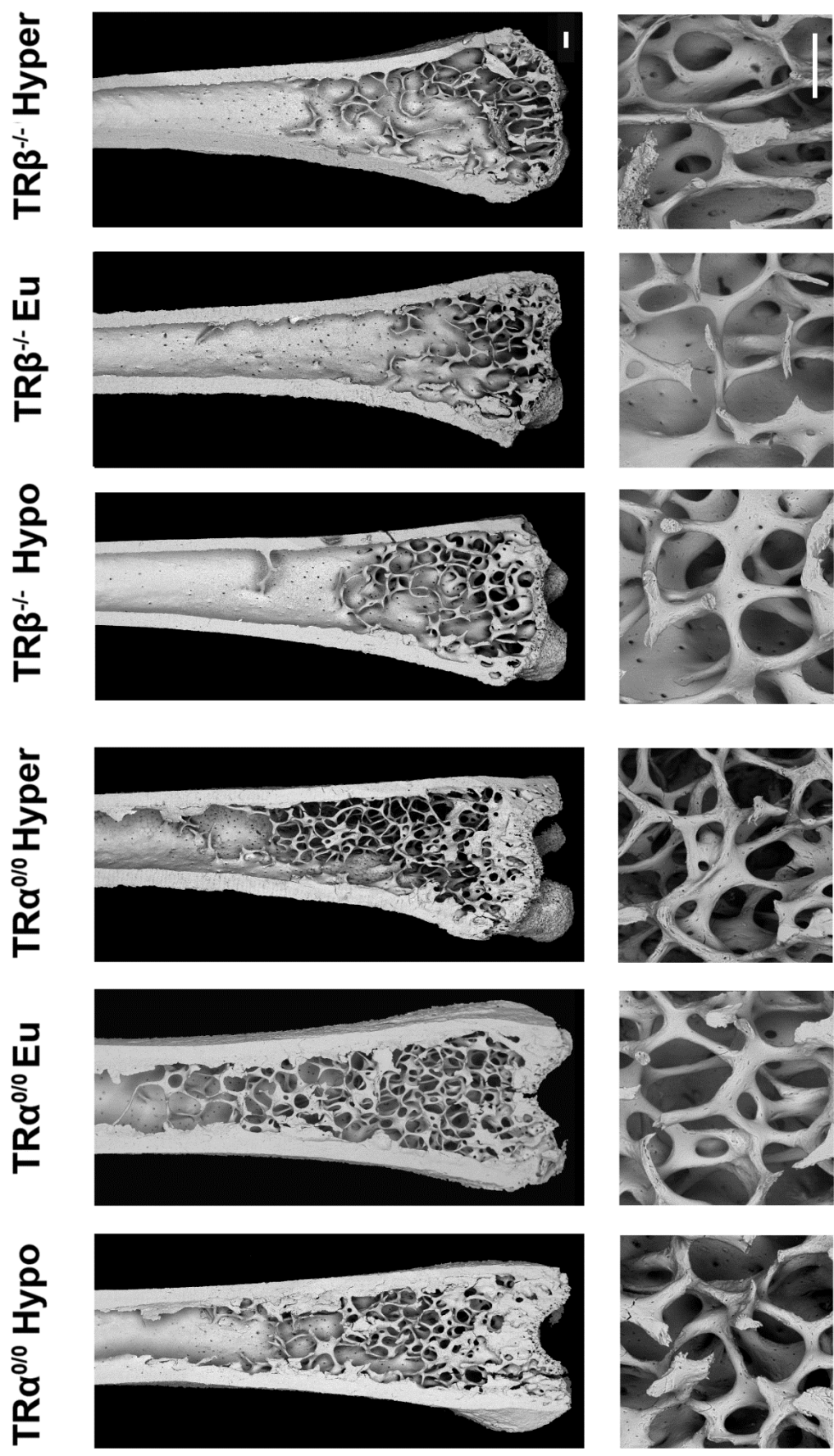


Figure 4.4 SEM images showing bone micro architecture
 BSE-SEM distal femur images of P112 mice. Scale bars, 200 μ m.

	BV/TV (%)	Tb.Th(mm)	Tb.Sp (mm)	Tb.N (mm ²)	SMI
TRα^{0/0} Hypo	14.7±1.9	0.05±0.001	0.18±0.009	3.16±0.29	0.83±0.08
TRα^{0/0} Eu	13.1±0.4	0.04±0.001	0.19±0.006	3.11±0.1	1.64±0.02
TRα^{0/0} Hyper	11.8±0.4	0.04±0.001	0.18±0.005	2.96±0.22	1.75±0.09
TRβ^{-/-} Hypo	12.6±1.1**	0.05±0.002**	0.21±0.006	2.59±0.17*	1.87±0.06
TRβ^{-/-} Eu	7.7±0.8	0.04±0.001	0.22±0.005	1.96±0.16	2.06±0.07
TRβ^{-/-} Hyper	7.1±0.5	0.04±0.001	0.23±0.009	3.24±0.15***	1.91±0.05

Table 4.1 Analysis of micro CT data

Quantitative analysis of bone volume (BV/TV), Trabecular thickness (Tb.Th), trabecular spacing (Tb.Sp), trabecular number (Tb.N), and structure model index (SMI) determined by micro CT analysis of distal femur (n=5-6). ANOVA and Tukey's post hoc test. *, P<0.05; **, P<0.01; ***, P<0.001 when compared to euthyroid bones of the same genotype.

4.2.4 BONE MINERAL DENSITY

4.2.4.1 BMC: Faxitron Analysis

Cumulative and relative histograms of mineralisation density for femurs and caudal vertebrae are shown in Figures 4.5 and 4.6. BMC is unchanged in both the femur and the caudal vertebrae in hypothyroid TRα^{0/0} mice compared to the euthyroid group, but significantly reduced BMC when the mice are rendered hyperthyroid. Conversely, TRβ^{-/-} mice have significantly increased BMC in both the femur and caudal vertebrae when rendered hypothyroid but similar BMC when euthyroid and hyperthyroid groups are compared (Figures 4.5 and 4.6). Unlike wild type mice, the changes to BMC are similar in both the femur and caudal vertebrae (see Chapter 3).

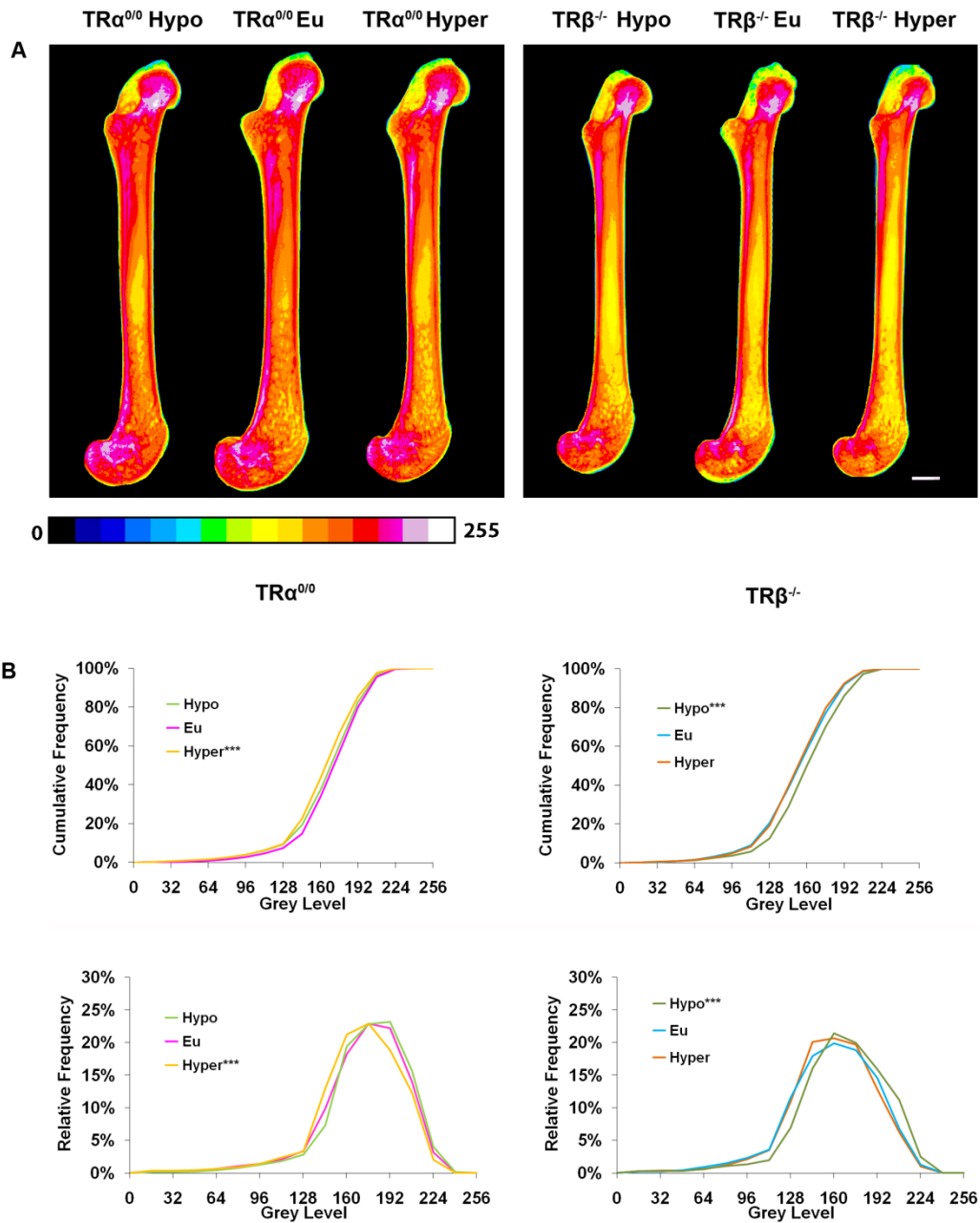


Figure 4.5 Bone mineral content of femurs

Faxitron images of femurs of P112 mice. Grey scale images were pseudocoloured with a 16 colour palette where low mineralisation density is black and high density is white. (Scale bar 1mm). Cumulative frequency histograms of mineralisation densities for whole femurs. Kolmogorov-Smirnov test ***, $p < 0.001$ versus euthyroid wild type mice.

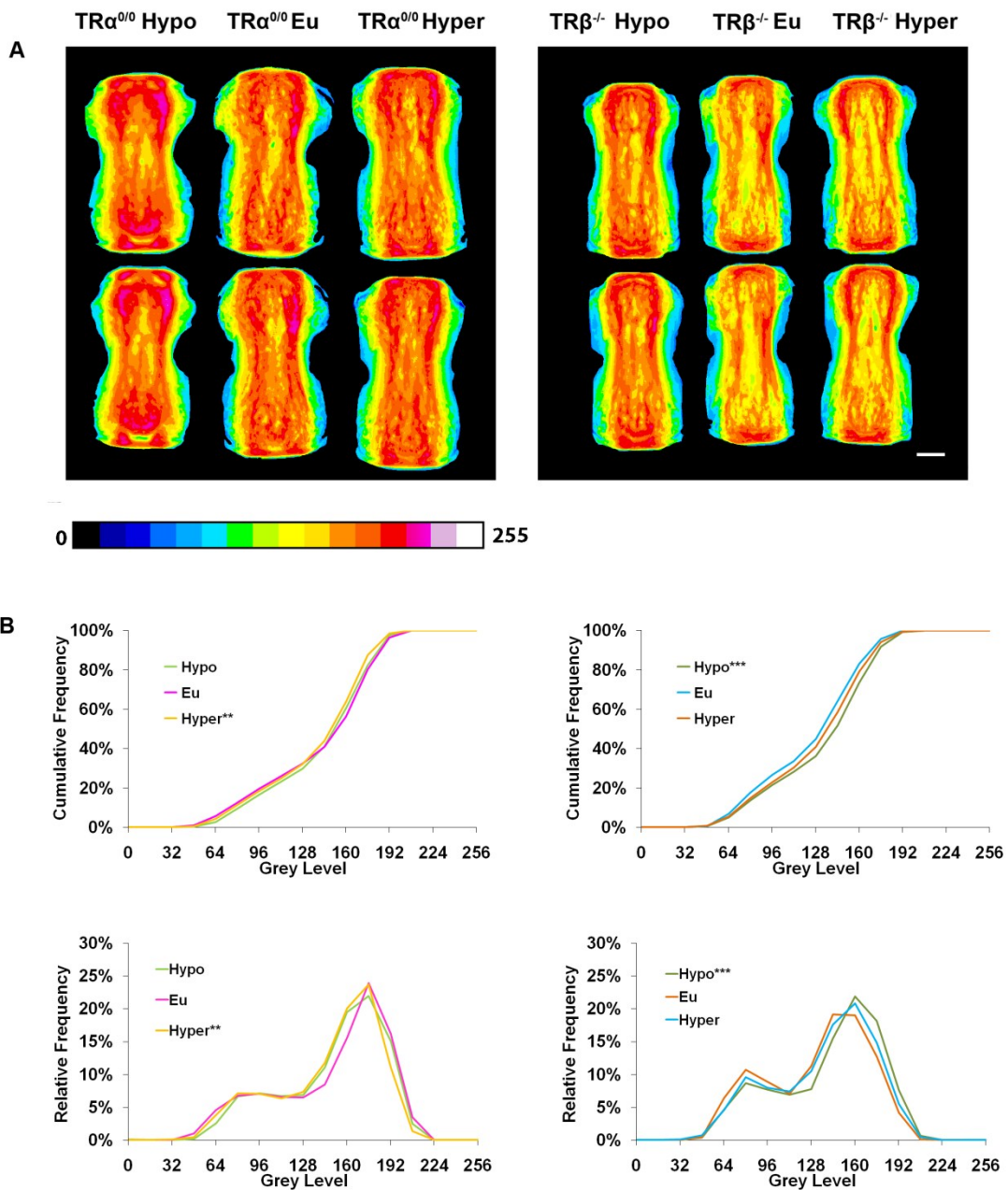


Figure 4.6 Bone mineral content of caudal vertebrae

Faxitron images of caudal vertebrae (A) of P112 mice. Grey scale images were pseudocoloured with a 16 colour palette where low mineralisation density is black and high density is white. (Scale bar 1mm). Cumulative frequency histograms (B) of mineralisation densities for whole femurs. Kolmogorov-Smirnov test; **, $p < 0.01$; ***, $p < 0.001$ versus euthyroid wild type mice.

4.2.4.2 Micro-mineralisation: qBSE-SEM

Cumulative and relative histograms of micro-mineralisation of the lumbar vertebrae are shown in Figure 4.7. Micro-mineralisation is increased in hypothyroid and decreased in hyperthyroid TR $\alpha^{0/0}$ mice at the lumbar vertebrae, when compared to euthyroid TR $\alpha^{0/0}$ mice. Unexpectedly, micro-mineralisation in the lumbar vertebrae of TR $\beta^{-/-}$ mice was highest in the euthyroid group when compared to either hypothyroid or hyperthyroid TR $\beta^{-/-}$ mice. To verify this finding, micro-mineralisation was repeated in the tibia (Figure 4.8). There was decreased micro-mineralisation in the hyperthyroid mice and increased micro-mineralisation in hypothyroid TR $\beta^{-/-}$ mice at the tibial trabeculae. The results of micro-mineralisation analysis in the cortices showed a similar pattern of results as the lumbar vertebrae, with increased micro-mineralisation in both the hyper and hypothyroid TR $\beta^{-/-}$ mice, when compared to euthyroid mice.

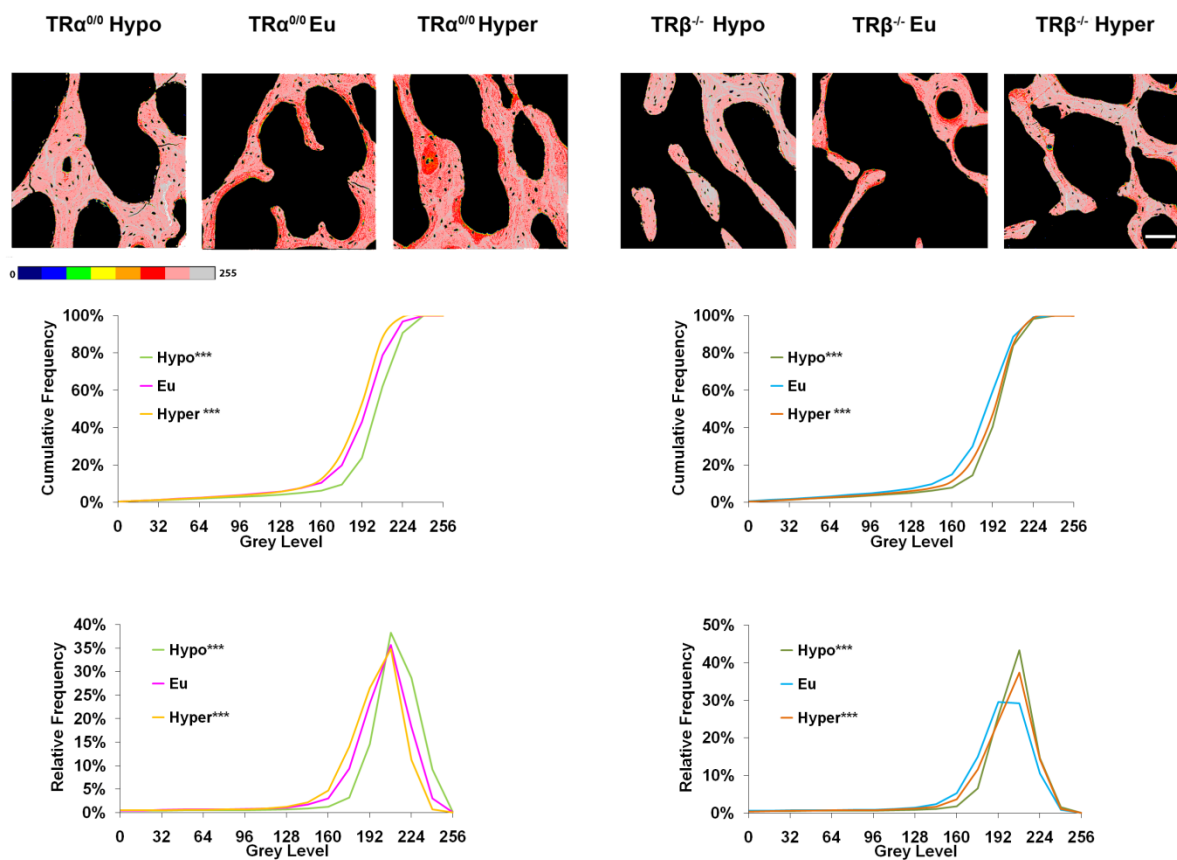


Figure 4.7 Micro-mineralisation of lumbar vertebrae

qBSE-SEM images of lumbar vertebrae P112 mice of $TR\alpha^{0/0}$ and $TR\beta^{-/-}$ mice. Grey scale images were pseudocoloured to an eight colour palette; low mineralisation is blue and high density is grey. Cumulative frequency histograms of mineralisation densities. Kolmogorov-Smirnov test; ***, $p < 0.001$ versus euthyroid wild type mice.

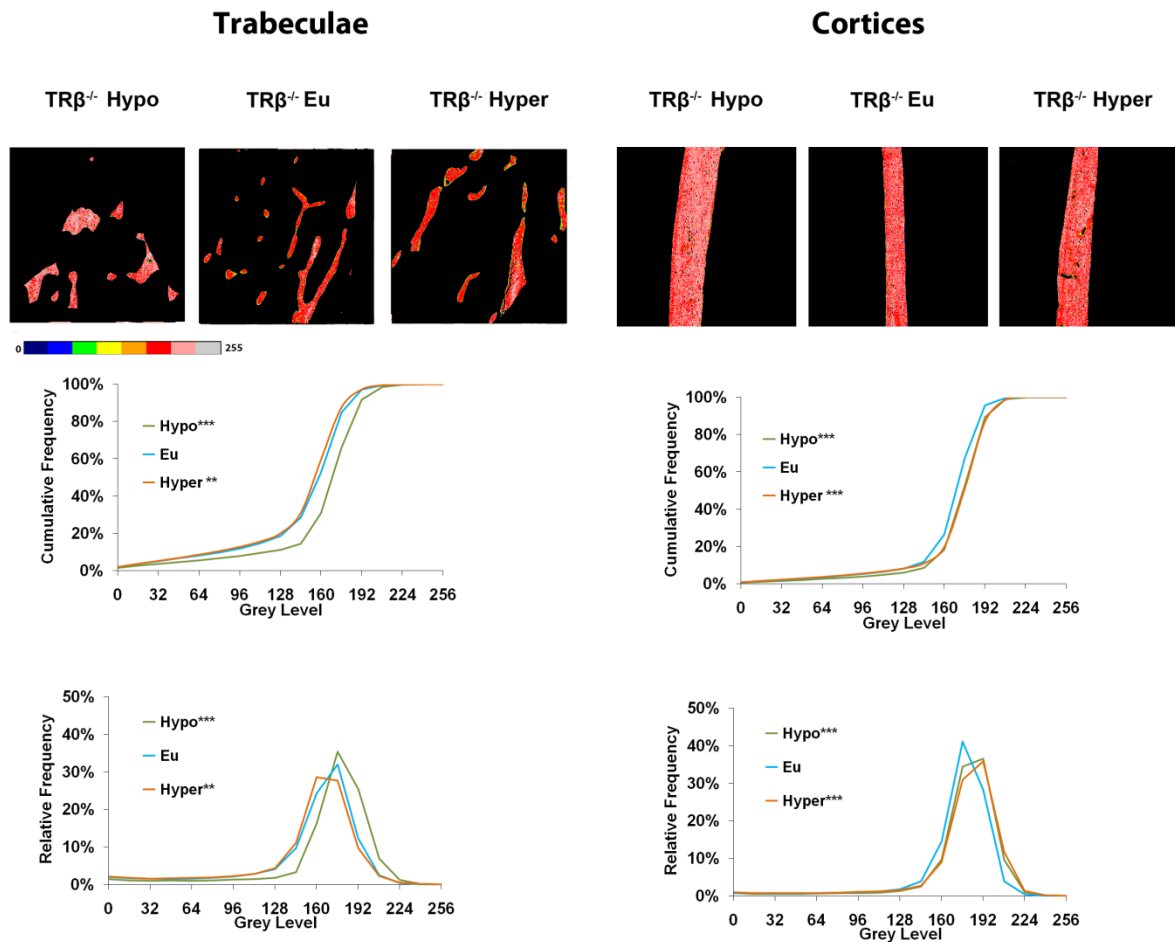


Figure 4.8 Micro-mineralisation of tibial trabeculae and cortical bone

qBSE-SEM images of trabeculae and cortices of P112 $TR\beta^{-/-}$ mice with manipulated thyroid status. Grey scale images were pseudocoloured with an eight colour palette; low mineralisation density is blue and high density is grey. Cumulative frequency histograms of mineralisation densities. Kolmogorov-Smirnov test; **, $p < 0.01$; ***, $p < 0.001$ versus euthyroid wild type mice.

4.2.5 BONE FORMATION: P1NP AND BFR

Bone formation was assessed by both serum markers for P1NP (Figure 4.9) and dynamic bone formation (Figure 4.10). In hypothyroid $TR\alpha^{0/0}$ mice, serum P1NP and BFR are significantly lower than in euthyroid $TR\alpha^{0/0}$ mice. This indicates that thyroid hormone is important in bone formation in $TR\alpha^{0/0}$ mice. Hypothyroid $TR\beta^{-/-}$ mice also have reduced MS/BS and BFR compared to the euthyroid group but P1NP was not different between the groups. Of particular note, when comparing the bone formation of hypothyroid wild type (results in Chapter 3), hypothyroid $TR\alpha^{0/0}$ and hypothyroid $TR\beta^{-/-}$ mice, bone formation is fourfold greater in hypothyroid $TR\alpha^{0/0}$ mice and significantly higher ($p < 0.05$, ANOVA and Tukey's Multiple Comparison post hoc test) when compared to hypothyroid wild type or hypothyroid $TR\beta^{-/-}$ mice. Hyperthyroid $TR\alpha^{0/0}$ mice had similar serum P1NP and dynamic bone formation indices to euthyroid $TR\alpha^{0/0}$ mice. Hyperthyroid $TR\beta^{-/-}$ mice had significantly higher BS/MS and BFR compared to euthyroid $TR\beta^{-/-}$ mice, although serum P1NP was not significantly different.

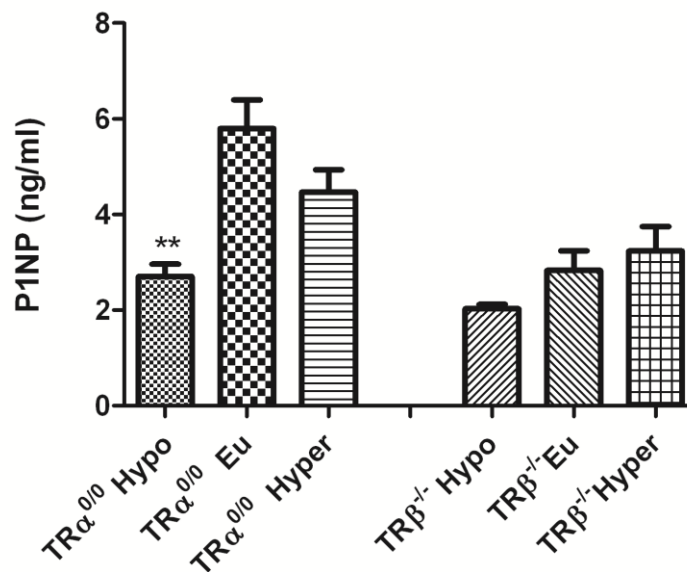


Figure 4.9 Serum P1NP concentrations

Serum samples were obtained from mice at sacrifice and stored at -80°C . P1NP concentrations were determined by enzyme immunoassay (Immunodiagnostic systems kit AC-33 F1). Data expressed as mean \pm SEM, $n=3-4$ per group and analysed by ANOVA and Tukey's Multiple Comparison post hoc test: **, $p < 0.005$; versus euthyroid wild type mice.

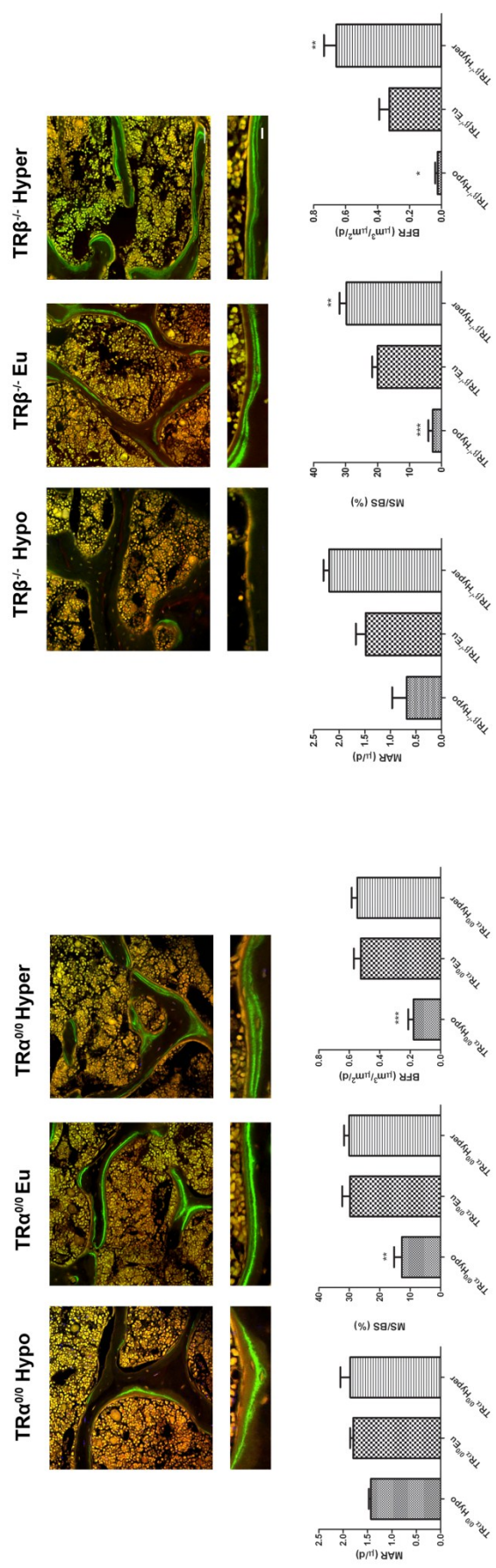


Figure 4.10 Dynamic bone formation parameters

Bone formation in lumbar vertebrae of P112. CSLM views of trabecular bone (scale bar 10 μm). Trabecular bone mineralising surface, MAR and BFR determined by dual calcein labelling. Data expressed as mean ± SEM, n=4 per group and analysed by ANOVA and Tukey's Multiple Comparison post hoc test: *, p<0.05; **, p<0.005; ***, p<0.001 versus euthyroid wild type mice.

4.2.6 BONE RESORPTION: CTX AND ENDOCORTICAL RESORPTION

Serum levels of bone resorption marker CTX (Figure 4.11) and endocortical resorption (Figure 4.12), as assessed by percentage of surface covered with resorption pits, was higher in hyperthyroid TR $\alpha^{0/0}$ mice when compared to euthyroid controls.

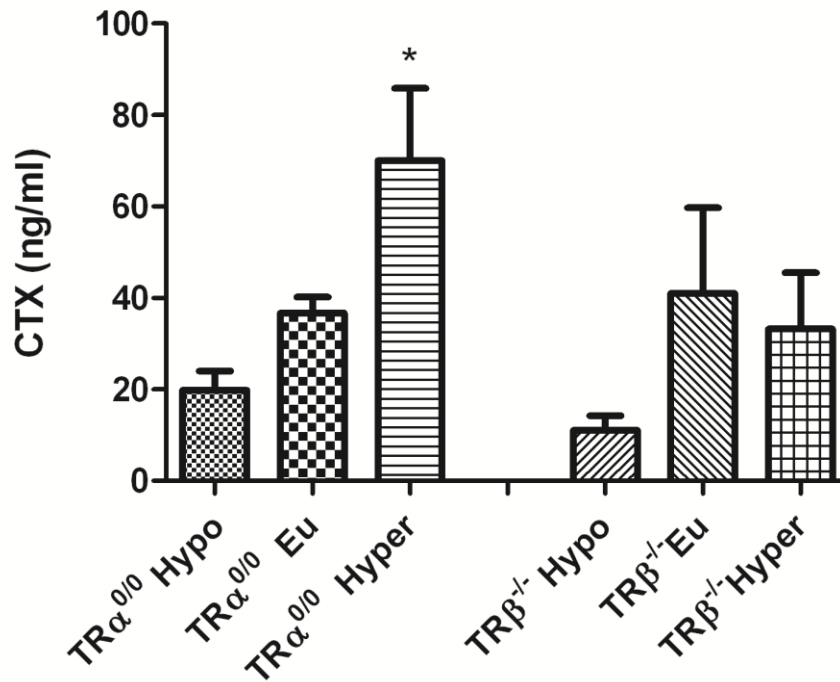


Figure 4.11 Serum bone resorption markers

Serum samples were obtained from mice at sacrifice and stored at -80°C . C-terminal cross-linked telopeptide of type I collagen (CTX) concentrations were determined by enzyme immunoassay (AC06F1). Data expressed as mean \pm SEM, $n=3-4$ per group and analysed by ANOVA and Tukey's Multiple Comparison post hoc test: *, $p<0.05$ versus euthyroid type mice in respective genotypes.

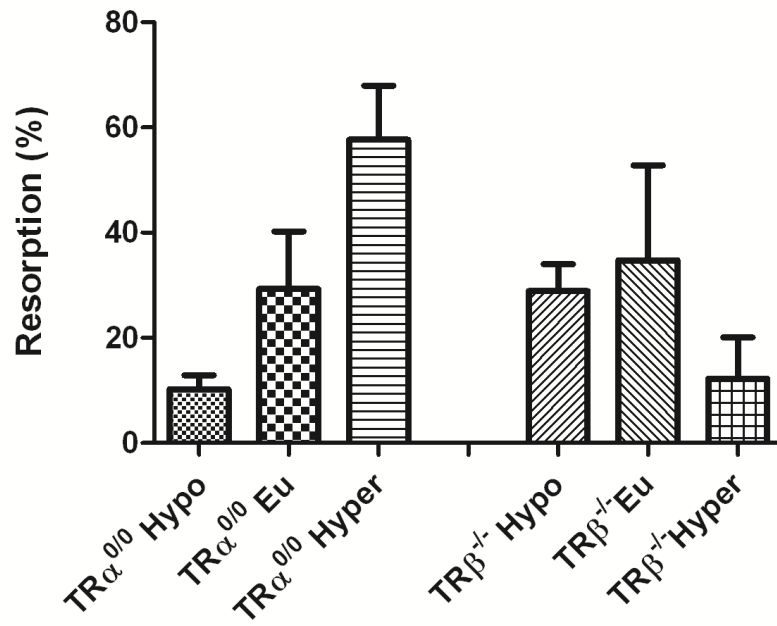


Figure 4.12 Bone resorption parameters

Quantitative analysis of endosteal osteoclast resorption surfaces from BSE-SEM images (% of total BS) of P112 mice. Data expressed as mean \pm SEM, n=3-4 per group and analysed by ANOVA and Tukey's Multiple Comparison post hoc test: no groups were significantly different.

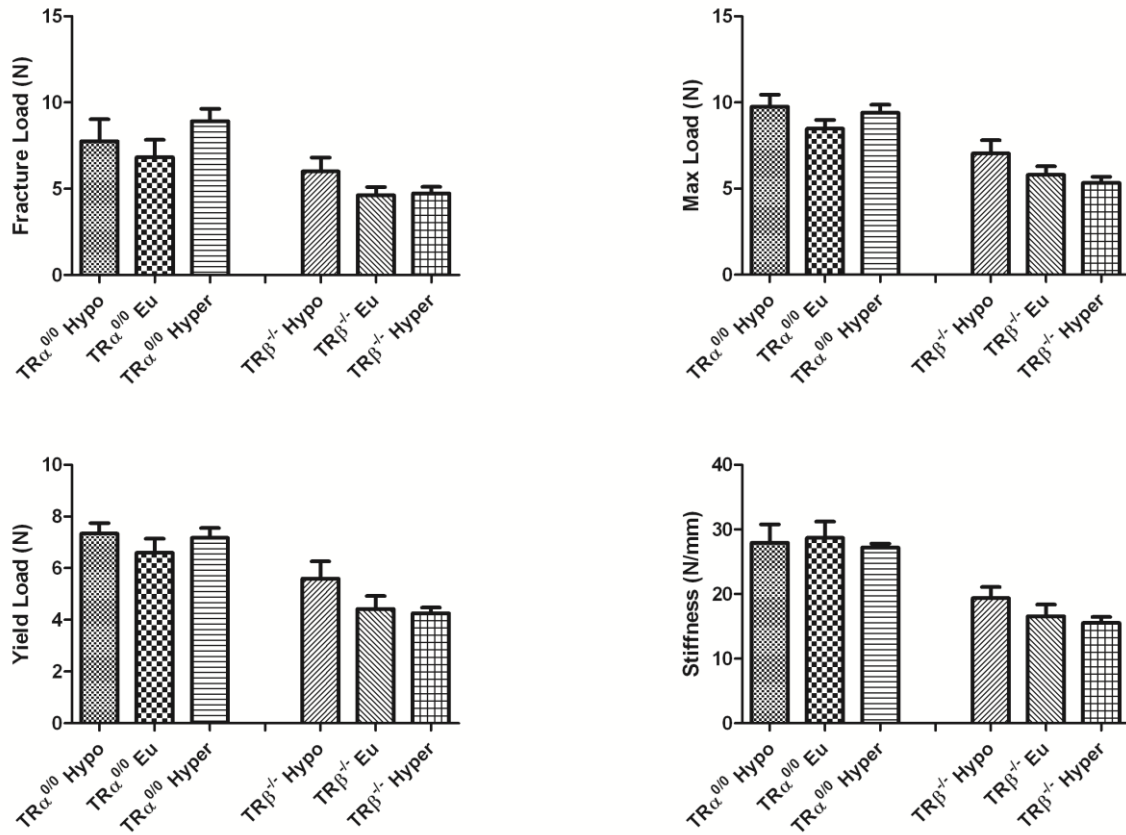


Figure 4.13 Mechanical properties

Graphs showing yield load, maximum load, fracture load and stiffness in tibias of P112 mice. Data expressed as mean \pm SEM, n=4-6 per group and analysed by ANOVA and Tukey's Multiple Comparison post hoc test: in no groups did altering thyroid status significantly affect mechanical properties.

4.2.7 BIOMECHANICAL TESTING

Mechanical testing of tibias by three point bending assessed for differences in yield load, fracture load, maximum load and stiffness. Although there was no significant change in the mechanical properties that could be statistically detected (Figure 4.13), TR β ^{+/-} mice showed an inverse non-significant trend in all parameters to thyroid hormone levels.

4.3 SUMMARY OF RESULTS

	WT			TR $\alpha^{0/0}$			TR $\beta^{-/-}$	
	Hypo	Hyper		Hypo	Hyper		Hypo	Hyper
Weight	→	→		→	→		→	→
Tail length	→	→		→	→		→	→
Femur length	→	→		→	→		→	→
Tibial length	→	→		→	→		→	→
Cortical diameter	→	→		→	→		→	→
Cortical thickness	→	→		→	↓		→	→
μ CT BV/TV	↑↑	↓		→	→		↑↑	→
Femoral BMC	↑↑↑	→		→	↓↓↓		↑↑↑	→
Vert BMC	→	↓↓↓		→	↓↓↓		↑↑↑	→
qBSE SEM Lumbar vertebral trabeculae	↑↑↑	→		↑↑↑	↓↓↓		↑↑↑	↑↑↑
qBSE SEM Tibial trabeculae							↑↑↑	↓↓
qBSE SEM Tibial cortices							↑↑↑	↑↑↑
BFR	↓↓	→		↓↓↓	→		↓	↑↑
MAR	↓↓↓	→		→	→		→	→
BS/BS	↓↓↓	↑↑		↓↓	→		↓↓↓	↑↑
P1NP	→	→		↓↓	→		→	→
CTX	→	→		↑	→		→	→
Oc.S/BS	↓	→						
N.Oc/B.Pm	↓↓	→						
% Resorption	↓	→		→	→		→	→

Table 4.2 Summary of effects of alteration in thyroid status in TR $\alpha^{0/0}$ and TR $\beta^{-/-}$ mice compared to euthyroid status in respective genotype

→ No significant difference, ↑ significant increase, ↓ significant decrease. Number of arrows indicates significance level: 1 arrow p<0.05, 2 arrows p<0.01, 3 arrows p<0.001.

4.4 DISCUSSION

During development, thyroid hormones stimulate bone formation, mineral deposition and linear growth. These effects are anabolic. By contrast, in adults, thyroid hormones stimulate bone turnover, particularly increasing osteoclastic bone resorption and bone loss, resulting in osteoporosis. These effects are catabolic. The age at which changes in thyroid hormone status occurs can therefore result in either anabolic effects or catabolic effects. The severity to which circulating thyroid hormone status is altered is likely to be important to the degree of effect on bone and as to whether such effects can be detected by phenotyping.

Changes to the skeleton are influenced by the pre-existing bone structure – in the case of TR α ^{0/0} and TR β ^{-/-} mice, changes to the skeleton have been present throughout growth.

To be able to understand to the effects of thyroid status manipulation on the skeleton, it is therefore critically important to consider three points:

1. The age at which thyroid status is being manipulated.
2. The degree and length of thyroid manipulation prior to skeletal phenotyping.
3. Whether the skeletal phenotype was affected during growth and development prior to manipulation of thyroid status.

The experiments in this thesis were performed when the mice were adults (P70-P112). Manipulation of thyroid hormone in these experiments rendered mice severely hypothyroid but only mildly hyperthyroid. This was demonstrated by the very low serum thyroid hormone levels in all the hypothyroid groups and only mildly elevated thyroid hormone levels in hyperthyroid TR α ^{0/0} and wild type mice (untreated TR β ^{-/-} mice are very thyrotoxic).

It is important to note that untreated skeletal phenotypes of TR α ^{0/0} and TR β ^{-/-} mice are significantly different from those of wild type mice both during development and in adulthood. Therefore, comparisons need to be made to the euthyroid skeleton of the corresponding genotype, rather than against wild type mice, in order to elicit any changes to the skeletal phenotype resulting from altered thyroid status.

Type 2 deiodinase in target cells is regulated by the concentration of T4, which maintains a constant supply of T3 to the nucleus over a range of circulating hormone concentrations. This regulatory mechanism is only overridden at the extremes of hypothyroidism, as was the case in the mice used in the experiments presented in this thesis. The manipulation of thyroid hormone status in mice lacking TR α and TR β provides important information regarding the roles of liganded and unliganded

thyroid hormone receptors in bone. The presence of liganded or unliganded receptors is summarised in Table 4.3.

		Wild Type	TR $\alpha^{0/0}$	TR $\beta^{-/-}$
Hyperthyroid	TR α	Liganded	Absent	Liganded
	TR β	Liganded	Liganded	Absent
Euthyroid	TR α	Liganded	Absent	Liganded
	TR β	Liganded	Liganded	Absent
Hypothyroid	TR α	Unliganded	Absent	Unliganded
	TR β	Unliganded	Unliganded	Absent

Table 4.3 Table showing the presence of liganded or unliganded TR α and TR β in the different treatment groups

4.4.1 Skeletal effects of thyroid status in TR $\alpha^{0/0}$ mice

Euthyroid TR $\alpha^{0/0}$ mice have similar bone formation to wild type mice but have increased BMC as a result of decreased osteoclast resorption (see results Chapter 3). Rendering TR $\alpha^{0/0}$ mice hypothyroid decreases bone formation, suggesting that thyroid hormone is important in bone formation but also demonstrates that bone formation is not dependent on the presence of TR α , and that in its absence, TR β can compensate.

Rendering adult TR $\alpha^{0/0}$ mice hypothyroid had no effect on bone length, cortical measures, BMC or femoral BV/TV when compared to euthyroid TR $\alpha^{0/0}$ mice. This is likely to be because TR $\alpha^{0/0}$ mice may already have decreased osteoclast resorption which could account for most of the acute changes in bone structure (as seen in the comparison between TR $\alpha^{0/0}$ and wild type skeletal phenotypes – see results Chapter 3). Reduction in bone formation probably has a smaller role in changing the aforementioned elements of the adult skeletal phenotype.

Low turnover bone which is not removed quickly has more time for secondary or passive mineralisation to occur, which results in increased micro-mineralisation (Boivin and Meunier, 2002). Hypothyroid TR $\alpha^{0/0}$ mice had decreased bone formation and resorption and in line with this, had elevated micro-mineralisation.

When TR $\alpha^{0/0}$ mice were rendered hyperthyroid, there was a decrease in cortical thickness, lower BMC at both the femur and caudal vertebrae and a decrease in micro-mineralisation. These effects are due to an uncoupling of bone formation and resorption, with BFR being unaffected by higher circulating thyroid hormone levels but resorption being elevated, resulting in a net negative balance and significant bone loss.

As TR $\alpha^{0/0}$ mice lack all TR α receptors, the observed effects of hypothyroidism are likely to be due to a loss of liganded TR β mediated action. Thus, although TR α is the predominant receptor found in bone, it appears that TR β also can have a compensatory role in the absence of TR α . Unexpectedly, there was no increase in BFR in hyperthyroid mice compared to euthyroid TR $\alpha^{0/0}$ mice. Reasons for this may include: (i) increases in osteoblastic bone formation are a TR α dependent process, (ii) thyroid hormone signalling in the skeleton is maximal in euthyroid animals (i.e. all the available TR β are saturated - see Table 4.3) so increased amounts of free hormone should have no effect and (iii) that the because the hyperthyroidism was mild, small changes in BFR were not detected.

The data in this chapter corroborates previous data showing that BV/TV decreases (Bassett and Williams, 2009, Monfoulet et al., 2011) upon rendering TR $\alpha^{0/0}$ mice hyperthyroid and concurs with a significant increase in resorption parameters. MS/BS is significantly higher in hyperthyroid compared to hypothyroid TR $\alpha^{0/0}$ mice, which is in contrast to the data from Monfoulet et al showing a decrease in MS/BS in hyperthyroid compared to hypothyroid TR $\alpha^{0/0}$ mice (Monfoulet et al., 2011). It is not clear why this is, however the bone formation data in the Monfoulet paper, as previously discussed was suboptimal.

4.4.2 Skeletal effects of thyroid status in TR $\beta^{-/-}$ mice

The response to hypothyroidism is similar in TR $\beta^{-/-}$ mice and wild type mice. Hypothyroid TR $\beta^{-/-}$ mice have significantly greater BMC (both in femurs and caudal vertebrae), BV/TV and micro-mineralisation when compared to euthyroid TR $\beta^{-/-}$ mice. Bone formation is nearly completely absent with a BFR similar to that of hypothyroid wild type mice. As the increase in bone volume and BMC is not secondary to increased bone formation, it must therefore be as a result of decreased bone resorption. Unfortunately, the parameters used to assess bone resorption in this thesis were not

able to detect this decrease as there was a large variation in the measurements. Future work could include assessment of osteoclast parameters by quantitative histomorphometry.

The lack of difference between euthyroid and hyperthyroid TR β ^{-/-} mice in cortical parameters, BMC and BV/TV was unexpected, but it is important to consider that these mice were hyperthyroid throughout development and therefore both smaller and osteoporotic as adults before intervention was commenced. To render them euthyroid, they were made hypothyroid and given physiological replacement T3 (block and replace). To observe an increase in bone mass, there would need to be either increased bone formation and/or decreased bone resorption. As the TR β ^{-/-} mice are osteoporotic, the surface area (scaffold) upon which osteoblasts can lay down new bone is small, making it more difficult initially to accrue bone mass. Six weeks of treatment may not have been insufficient time to observe a difference in the aforementioned parameters.

Analysis of qBSE-SEM results showed lower micro-mineralisation in euthyroid TR β ^{-/-} mice when compared to the hyperthyroid or hypothyroid groups. Previous published data (Bassett et al., 2007b) has shown that T4 treatment in TR β ^{-/-} mice did not alter micro-mineralisation in the trabeculae or cortices of proximal femurs. Lower micro-mineralisation in euthyroid compared to hyperthyroid mice was surprising and to try to rule out any technical or processing factors, the assessment of micro-mineralisation was repeated in the tibia, where both cortical and trabecular bone were analysed.

Micro-mineralisation of the tibial cortices was similar to that in lumbar vertebrae, with the euthyroid mice having reduced micro-mineralisation when compared to either hyperthyroid or hypothyroid mice. However, the tibial trabeculae showed a significantly increased micro-mineralisation in hypothyroid TR β ^{-/-} mice and decreased micro-mineralisation in hyperthyroid TR β ^{-/-} mice. As the cortices and the trabecular bone were embedded in the same block and processed in exactly the same manner, it suggests that an artefact of processing was unlikely to be responsible for affecting results and that there may be a real site specific difference in micro-mineralisation. Physiologically, micro-mineralisation is affected by both the age of the bone (secondary mineralisation) and controlled by embedded osteocytes. The mechanism for control of micro-mineralisation is likely to be different in the cortices compared to the trabeculae due to the different strains put on the compartments as well as the differing osteocyte alignment. Trabeculae in the lumbar vertebrae are derived from both cortical bone and from the growth plate; hence, the osteocytic control of micro-mineralisation in the lumbar vertebrae may be a combination of the mechanisms in the two different types of bone.

4.4.3 Changes in BMC in response to alteration in thyroid status in different genotypes

The increase in BMC upon rendering mice hypothyroid compared to euthyroid mice was most pronounced in $TR\beta^{-/-}$ mice, with changes in both the femurs and caudal vertebrae, intermediate in wild type mice (see Chapter 3), where the BMC was only increased in the femurs but not the caudal vertebrae and least in $TR\alpha^{0/0}$ mice where BMC remained unchanged at both sites.

Conversely, the decrease in BMC upon rendering mice hyperthyroid was most pronounced in $TR\alpha^{0/0}$ mice, with changes in both the femurs and caudal vertebrae, intermediate in wild type mice where the BMC was only decreased in the caudal vertebrae but not the femurs (see Chapter 3) and least in $TR\beta^{-/-}$ mice, where BMC remained unchanged at both sites.

		WT		$TR\alpha^{0/0}$		$TR\beta^{-/-}$	
		Hypo	Hyper	Hypo	Hyper	Hypo	Hyper
FAXITRON BMC	Femur	↑↑↑	↓	→	↓↓↓	↑↑↑	→
	Caudal Vert	→	↓↓↓	→	↓↓	↑↑↑	→

Table 4.4 Summary of changes in BMC in femurs and caudal vertebrae of wild type, $TR\alpha^{0/0}$ and $TR\beta^{-/-}$ mice with differing thyroid status

The reason for these responses may not just be a thyroid receptor specific response but could also be explained by the different genotypes having a different setpoint at which changes in BMD occur. $TR\alpha^{0/0}$ mice are osteosclerotic so to increase their BMC would need a relatively large change in bone remodelling. However, to render them osteoporotic should be relatively simple. $TR\beta^{-/-}$ mice are thyrotoxic and osteoporotic, so when rendering them euthyroid, the changes in BMC may not initially be great. However, when rendering them hypothyroid, the changes are much more pronounced. This is demonstrated in a model where thyroid status and BMC are correlated in sigmoid curve distribution which is shifted in $TR\alpha^{0/0}$ and $TR\beta^{-/-}$ mice (see Figure 4.14).

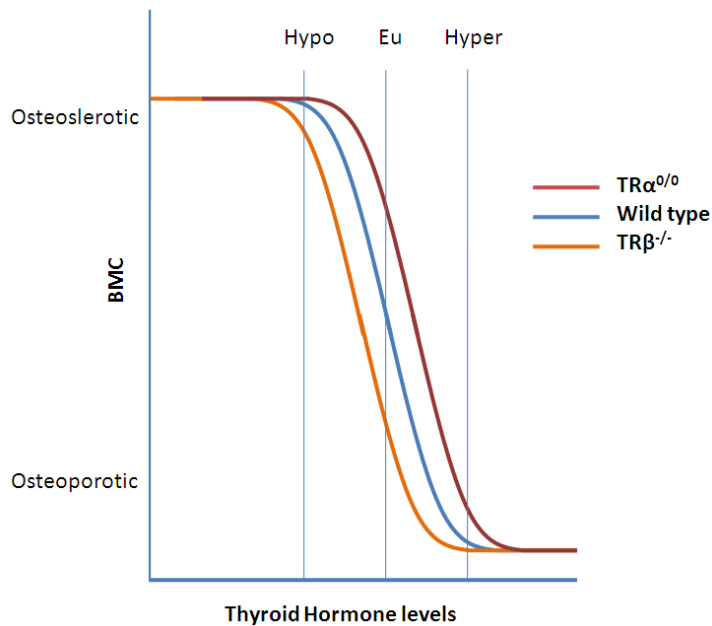


Figure 4.14 Proposed model of thyroid hormone induced bone changes in differing genotypes

Graph illustrating changes in BMC in response to differing circulating thyroid hormone levels in wild type, TR $\alpha^{0/0}$ and TR $\beta^{-/-}$ mice. Levels of hypothyroidism (Hypo) and hyperthyroidism (Hyper) are suggested on the graph alongside when such bones are osteoporotic or osteosclerotic. Each genotype has a different setpoint around which changes in BMC occur.

Thyroid status appeared to have a direct relationship with bone formation in wild type and TR $\beta^{-/-}$ mice, but was blunted in TR $\alpha^{0/0}$ mice. It is likely that thyroid hormone directly regulates bone formation by osteoblasts via TR α a mechanism which can be partially compensated for by TR β in its absence.

Hypothyroid wild type and TR $\beta^{-/-}$ mice have an almost complete absence of bone formation but by comparison, hypothyroid TR $\alpha^{0/0}$ mice have four-fold greater BFR (Table 4.6). This suggests that although bone formation is decreased in the absence of thyroid hormone, a basal rate of bone formation remains, which is inhibited by unliganded TR α (apo TR α). Evidence for this includes the growth retarded but viable skeleton of double knock out TR $\alpha\beta$ mice, despite the absence of both thyroid hormone receptors (Gothe et al., 1999).

		Wild Type	TR $\alpha^{0/0}$	TR $\beta^{-/-}$
BFR $\mu\text{m}^3/\mu\text{m}^2/\text{d}$		0.03	0.18* ^{###}	0.04
Hypothyroid	TR α	Unliganded	Absent	Unliganded
	TR β	Unliganded	Unliganded	Absent

Table 4.5 Table summarising the BFR in each genotype which are hypothyroid and whether each TR is liganded or not

BFR of hypothyroid TR $\alpha^{0/0}$ is significantly higher than wild type * ($p < 0.05$) or TR $\beta^{-/-}$ ^{###} ($p < 0.01$) analysed by ANOVA and Tukey's Multiple Comparison post hoc test.

4.4.4 Summary and salient points

Manipulation of thyroid status in TR $\alpha^{0/0}$ and TR $\beta^{-/-}$ mice has provided important insights into the individual roles of TRs in bone. Whilst TR $\beta^{-/-}$ mice are thyrotoxic due to central RTH, they respond to hypothyroidism in a similar way to wild type mice. TR $\alpha^{0/0}$ mice, however, are euthyroid but are osteopetrotic and whilst they have features of hypothyroidism during development, the picture is mixed, and such mice have uncoupled bone remodelling with normal bone formation and reduced bone resorption. Hypothyroid wild type, TR $\alpha^{0/0}$ and TR $\beta^{-/-}$ mice all have decreased bone formation, indicating that normal thyroid status is essential for normal bone development. The decrease in bone formation in hypothyroid TR $\alpha^{0/0}$ mice indicates that TR β can play a compensatory role in the skeleton in the absence of TR α . The data showing wild type and TR $\beta^{-/-}$ mice having an almost complete absence of bone formation in contrast to TR $\alpha^{0/0}$ mice, which have a fourfold greater BFR, suggests that unliganded TR α has a repressive role on bone formation in the skeleton.

Chapter 5

Effects of oestrogen and thyroid hormone interactions in the regulation of bone mass

5 EFFECTS OF OESTROGEN AND THYROID HORMONE INTERACTIONS IN THE REGULATION OF BONE MASS

5.1 BACKGROUND

Thyroid hormone and oestrogen both which act via intranuclear receptors to activate response elements and stimulate gene transcription. However, oestrogen and thyroid hormone have opposing actions on adult bone and I hypothesise that accelerated bone loss at the menopause is due to unopposed actions of thyroid hormone on the skeleton. To date, no *in vivo* experiments have investigated interactions between the two hormones in the skeleton. In the previous two results chapters, I have described, in detail, the effects of thyroid status on the skeleton of wild type, TR α ^{0/0} and TR β ^{-/-} mice. In this chapter I now describe the effects of oestrogen deficiency on the skeleton in each group.

5.2 RESULTS

5.2.1 GROWTH

5.2.1.1 Body weight and bone length parameters

To evaluate the effects of oestrogen deficiency on growth in each group, detailed weight and bone measurements were taken. Ovariectomy resulted in a 10 and 13.5% weight gain in euthyroid wild type and hyperthyroid TR β ^{-/-} mice, respectively, but tail length remained similar in all groups (Figure 5.1).

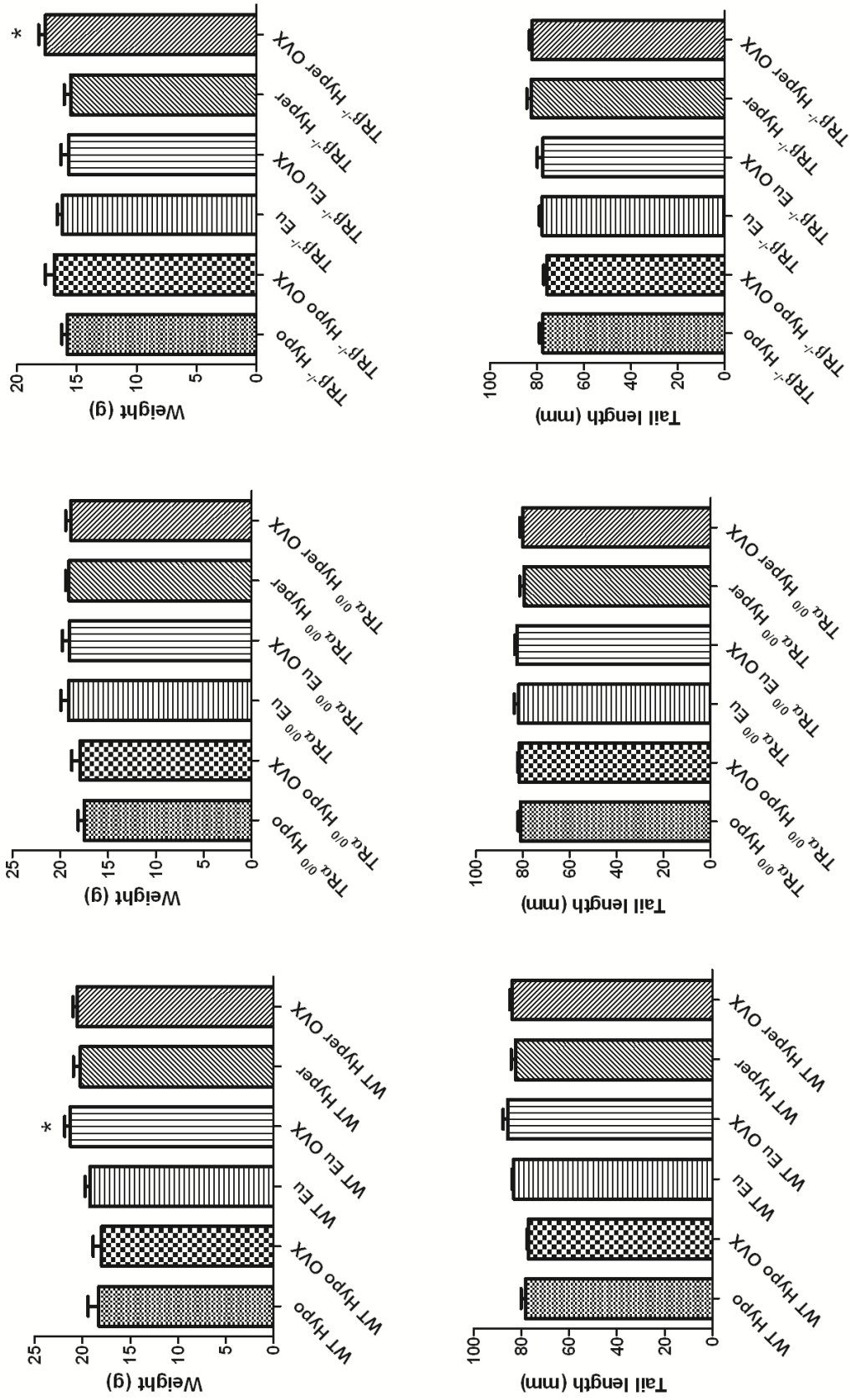


Figure 5.1 Growth parameters

Weight and tail length of P112 mice. Data expressed as mean \pm SEM, n=6 per group and analysed by Student's t-test *, $p < 0.05$; ovariectomised groups versus sham operated controls.

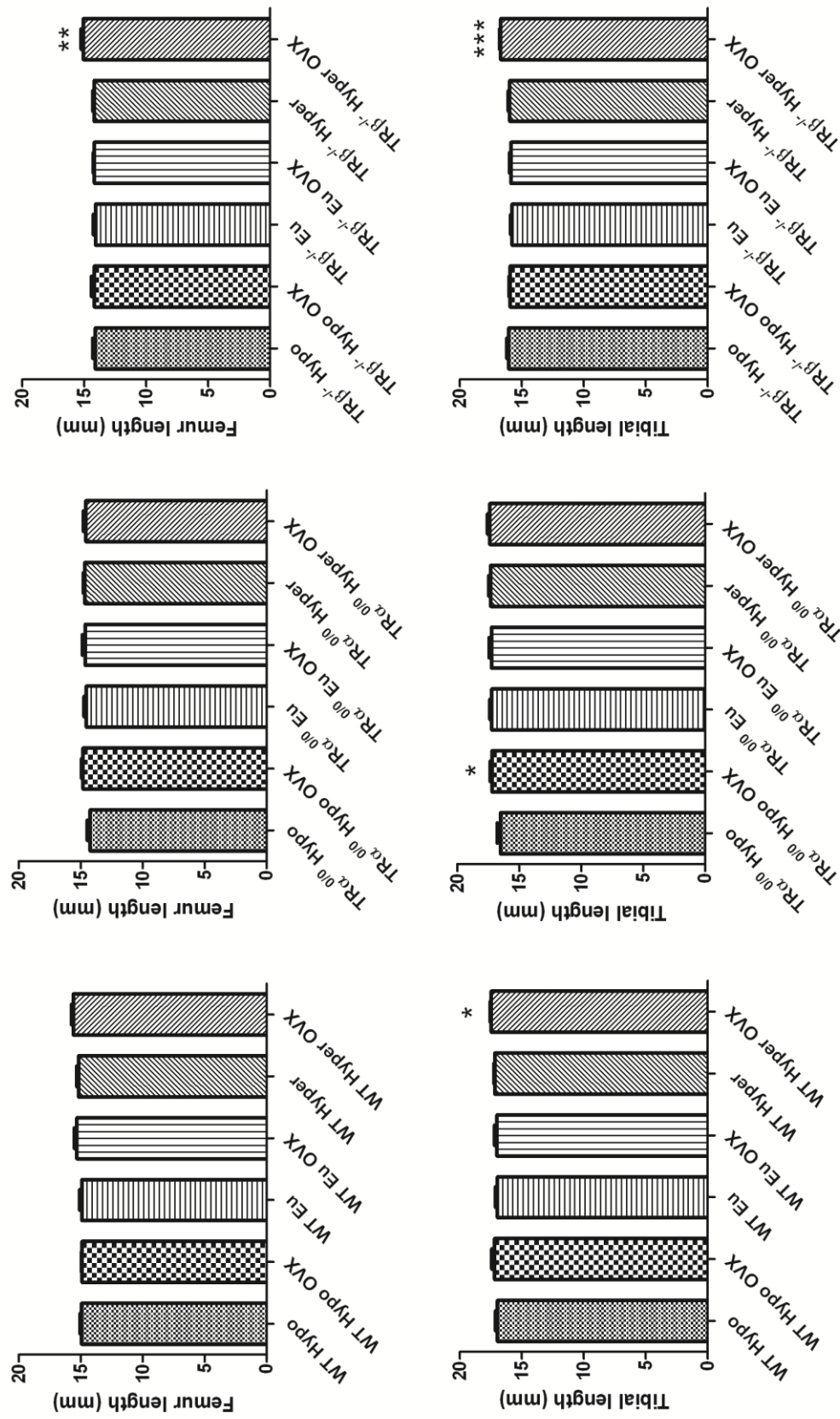


Figure 5.2 Bone length

Femur and tibial length of P112 mice. Data expressed as mean \pm SEM, n=6 per group and analysed by Student's t-test: *, p<0.05; **, p<0.01; ***, p<0.001; ovariectomised groups versus sham operated controls.

5.2.3 STRUCTURAL PARAMETERS

5.2.3.1 Bone length and cortical measurements

Femur lengths were significantly longer in the hyperthyroid TR $\beta^{-/-}$ group only post ovariectomy. Tibial bone lengths were longer in hyperthyroid TR $\beta^{-/-}$, hyperthyroid wild type and hypothyroid TR $\alpha^{0/0}$ groups post ovariectomy (Figure 5.2). The results of the bone length measurements seem to indicate that the tibia is more sensitive to changes in oestrogen status than the femur.

Cortical bone diameter is an indirect measure of periosteal apposition on the external cortical surface. Cortical thickness results from the net balance between external cortical periosteal apposition by osteoblasts and internal cortical resorption by osteoclasts.

Oestrogen deficiency did not result in changes to cortical bone diameter in any of the groups (Figure 5.3). There was a decrease in cortical thickness in euthyroid wild type mice and euthyroid and hyperthyroid TR $\alpha^{0/0}$ mice post ovariectomy, indicating increased endocortical resorption in these groups.

The data suggests that TR $\beta^{-/-}$ mice may be protected from oestrogen deficient endocortical bone loss (by the presence of TR α) and there is even an increase in cortical thickness in hypothyroid TR $\beta^{-/-}$ mice (8% increase) post ovariectomy.

Thyroid hormone replete TR $\alpha^{0/0}$ mice have the most significant decrease in cortical thickness in response to oestrogen deficiency (Figure 5.3, 8.2% decrease in Eu TR $\alpha^{0/0}$ and 13.7% decrease in Hyper TR $\alpha^{0/0}$ post ovariectomy) which also suggests that TR α has an osteoprotective effect against oestrogen deficiency bone loss.

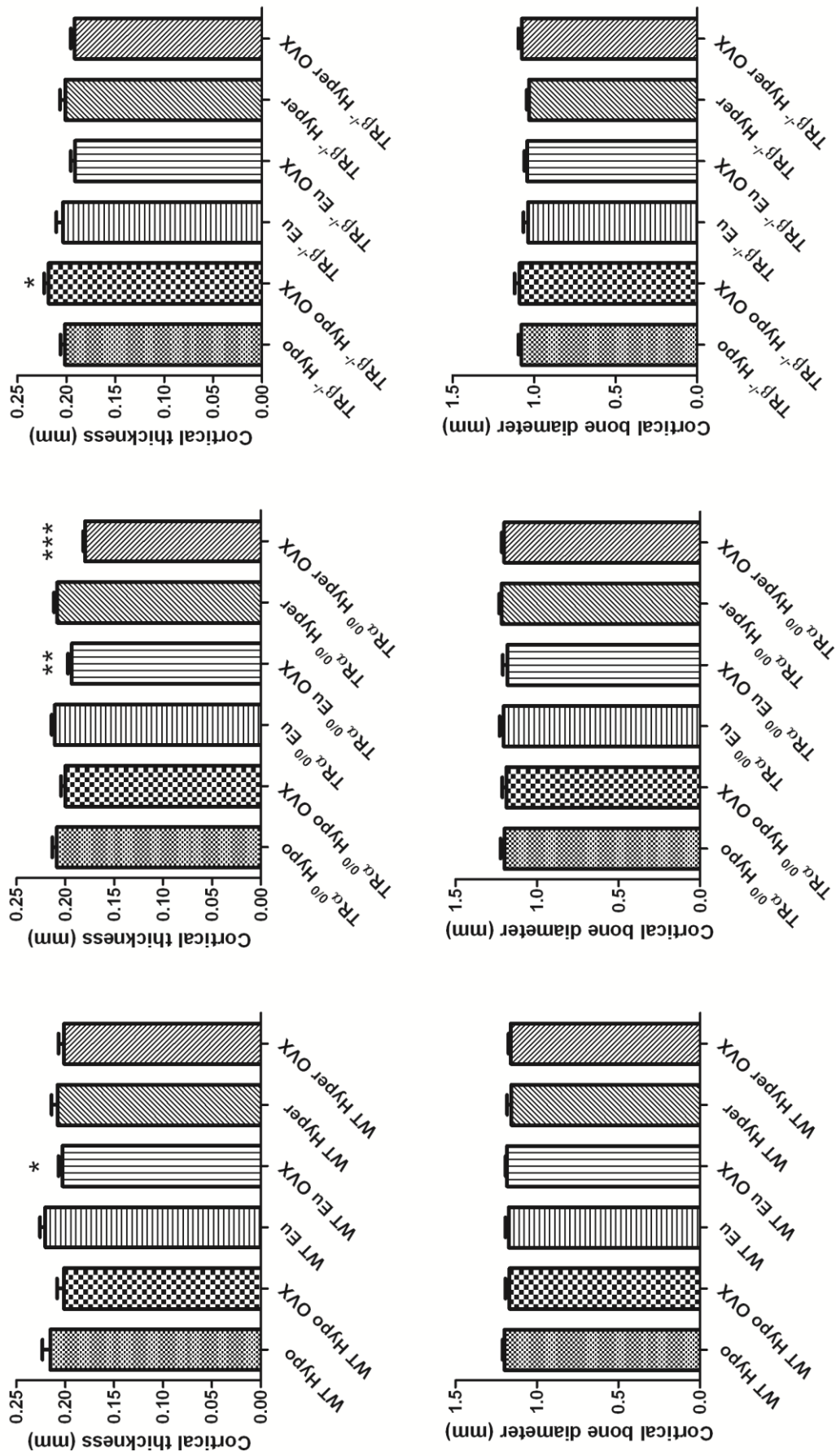


Figure 5.3 Cortical parameters

Cortical parameters of P112 mice (cortical thickness and cortical bone diameter). Data expressed as mean \pm SEM, n=6 per group and analysed by Student's t-test:***, p<0.001; ovarioectomised groups versus sham operated controls.

5.2.3.2 Bone microarchitecture: BSE-SEM and micro CT

In almost all of the femur BSE-SEM images, the trabecular compartments in the ovariectomised groups occupy a smaller endocortical area than the sham operated groups. The trabeculae appeared more gracile and less numerous (see Figure 5.5).

Micro CT analysis showed that wild type mice have decreased BV/TV post ovariectomy in hypothyroid but not euthyroid or hyperthyroid groups (Figure 5.4 and Table 5.1). TR α ^{0/0} mice were found to have a 40-60% reduction in BV/TV in response to oestrogen deficiency, regardless of thyroid status. BV/TV in hypothyroid and hyperthyroid TR β ^{-/-} mice was unaffected by ovariectomy, but there was a 20% decrease in BV/TV in the euthyroid group. These results suggest that genotype is important (with TR α being osteoprotective) in determining trabecular bone loss in response to oestrogen deficiency.

The micro CT data suggests that trabecular bone loss due to oestrogen deficiency (BV/TV) at the distal femur is largely secondary to a decrease in Tb.N (and correspondingly to an increase in Tb.Sp) and, to a lesser degree, to the thickness of the trabeculae (see Table 5.1). This is the case in all of the TR α ^{0/0} groups, regardless of thyroid status, and also in euthyroid TR β ^{-/-} mice. The SMI (trabecular morphology is graded into 0=plate-like and 3=rod-like) was highly significantly elevated in all TR α ^{0/0} groups ($p < 0.001$), indicating that the trabeculae were more gracile and rod-like post ovariectomy.

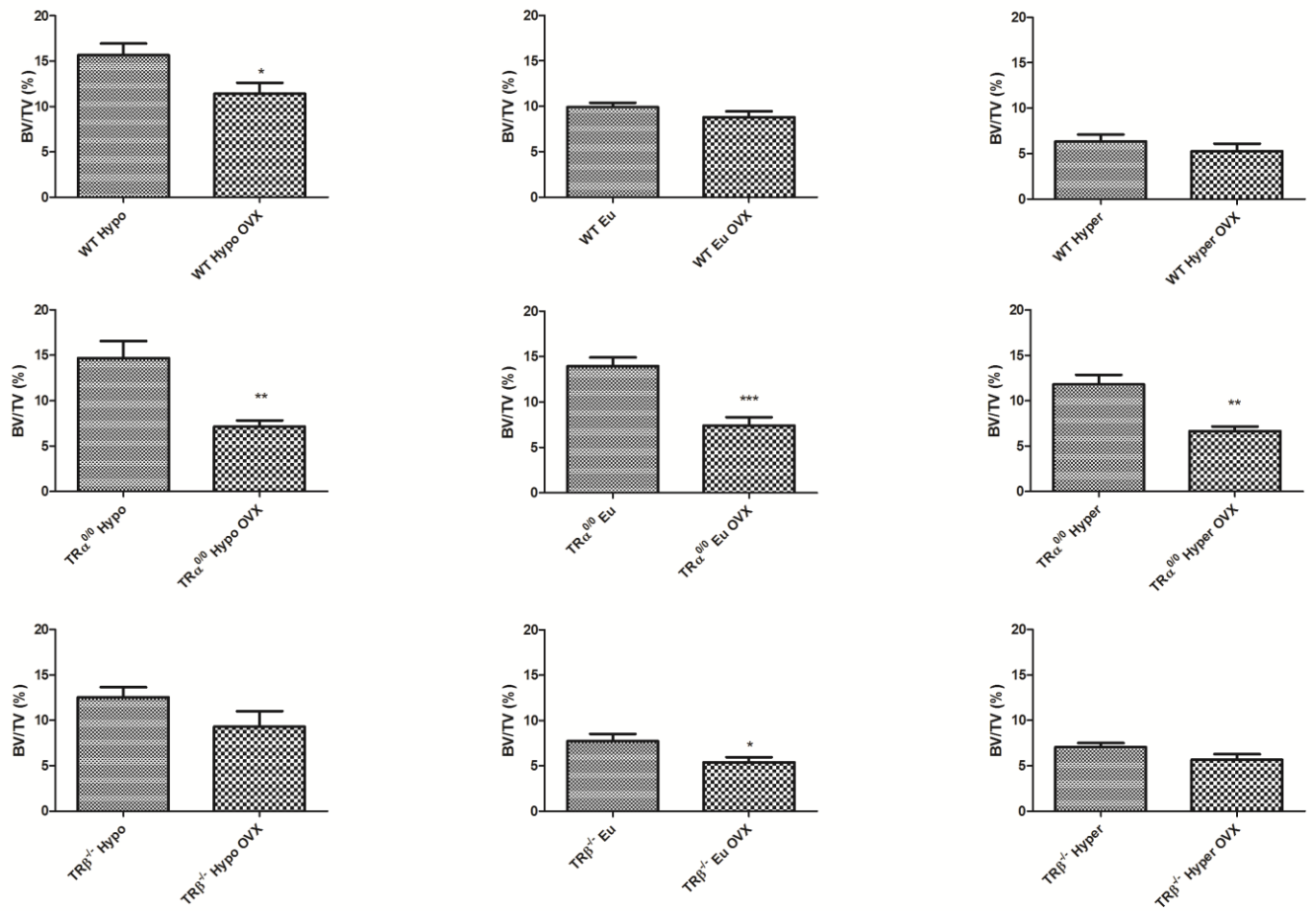


Figure 5.4 Micro CT assessment of BV/TV

Bone volume (BV/TV), determined by micro CT analysis of distal femur (n=5-6). Data expressed as mean \pm SEM, n=6 per group and analysed by Student's t-test: *, p<0.05, **, p<0.01, ***, p<0.001; versus non ovariectomised group of the same genotype and thyroid status.

	BV/TV (%)	Tb.Th(mm)	Tb.Sp (mm)	Tb.N (mm ²)	SMI
WT Hypo	15.6±1.3	0.051±0.002	0.20±0.006	3.05±0.15	1.71±0.04
WT Hypo OVX	11.4±1.2*	0.045±0.001	0.21±0.008	2.53± 0.23	1.83± 0.09
WT Eu	10.9±1.1	0.040±0.003	0.19±0.006	2.74±0.23	1.74±0.09
WT Eu OVX	8.8±0.6	0.040±0.001	0.23±0.010*	2.18±0.17	1.88 ± 0.08
WT Hyper	6.3±0.8	0.037±0.001	0.25±0.010	1.68±0.17	1.99±0.07
WT Hyper OVX	5.3±0.8	0.043±0.001**	0.29±0.018	1.23±0.20	2.30±0.09*
TRα^{0/0} Hypo	14.7±1.9	0.046±0.001	0.18±0.009	3.16±0.29	0.83±0.08
TRα^{0/0} Hypo OVX	7.1±0.7**	0.040±0.001**	0.23±0.073**	1.68±0.15**	2.20± 0.07**
TRα^{0/0} Eu	13.1±0.4	0.042±0.001	0.19±0.006	3.11±0.10	1.64±0.02
TRα^{0/0} Eu OVX	7.4±0.9***	0.040±0.001	0.23±0.009**	1.85 ± 0.18***	2.10 ± 0.06***
TRα^{0/0} Hyper	11.8±0.4	0.039±0.001	0.18±0.005	2.96±0.22	1.75±0.09
TRα^{0/0} Hyper OVX	6.7±0.5**	0.039±0.0005	0.24±0.008***	1.73 ± 0.13**	2.12± 0.07*
TRβ^{-/-} Hypo	12.6±1.1	0.048±0.002	0.21±0.006	2.59±0.17	1.87±0.06
TRβ^{-/-} Hypo OVX	9.3±1.7	0.045±0.002	0.22±0.012	2.27± 0.32	1.96± 0.10
TRβ^{-/-} Eu	7.7±0.8	0.040±0.001	0.22±0.005	1.96±0.16	2.06±0.07
TRβ^{-/-} Eu OVX	5.4±1.0*	0.038±0.001	0.26±0.022**	1.40 ± 0.14*	2.11± 0.07
TRβ^{-/-} Hyper	7.1±0.5	0.036±0.004	0.23±0.009	3.24±0.15	1.91±0.05
TRβ^{-/-} Hyper OVX	5.7±0.6	0.038±0.001	0.28±0.019*	1.50±0.17***	2.04± 0.063

Table 5.1 Analysis of micro CT data. Quantitative analysis of bone volume (BV/TV), trabecular thickness (Tb.Th), trabecular spacing (Tb.Sp), trabecular number (Tb.N), and structure model index (SMI) determined by micro CT analysis of distal femur (n=5-6). Data expressed as mean ± SEM, analysed by Student's t-test:*, p<0.05, **, p<0.01, ***, p<0.001; versus non ovariectomised group of the same genotype and thyroid status.

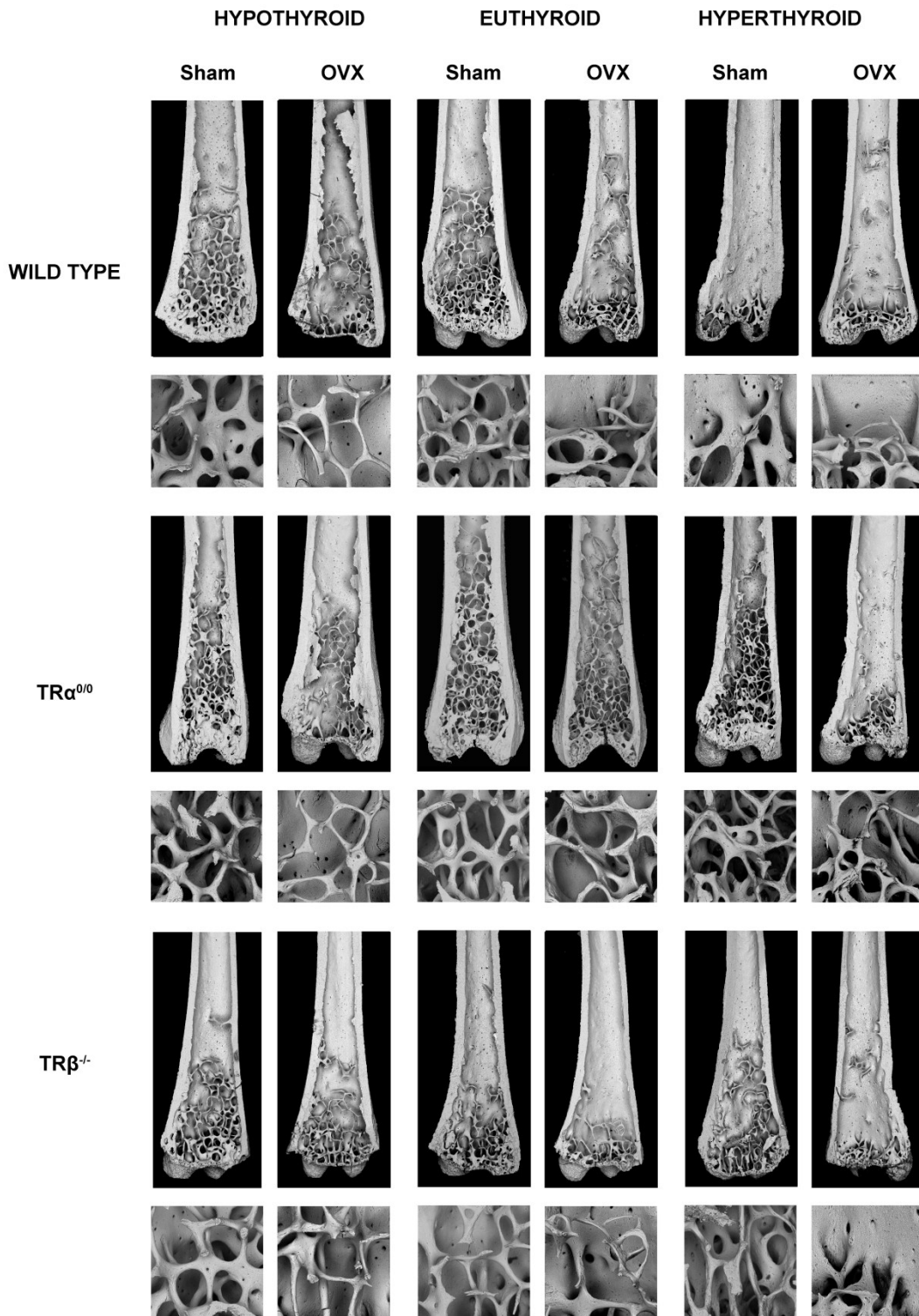


Figure 5.5 SEM images showing bone micro architecture

BSE-SEM images of distal femurs from hypothyroid, euthyroid and hyperthyroid wild type (WT), TR α ^{0/0} and TR β ^{-/-} genotypes. Images of femurs from sham operated and ovariectomised mice from all groups are demonstrated.

5.2.4 BONE MINERAL DENSITY

5.2.4.1 BMC

The effects of oestrogen and thyroid hormone interaction on BMC were assessed by faxitron analysis of femurs and caudal vertebrae (Figures 5.6 and 5.7).

In wild type mice, femurs were more sensitive to oestrogen deficiency bone loss than the caudal vertebrae (Figures 5.6 and 5.7). There was a significant decrease in femoral BMC in hypothyroid and euthyroid, but not hyperthyroid wild type mice, post ovariectomy. No change in BMC was observed in the caudal vertebrae of wild type mice post ovariectomy, regardless of the thyroid hormone status.

There were highly significant decreases in BMC post ovariectomy, in both femurs and caudal vertebrae of euthyroid and hyperthyroid TR α ^{0/0} mice, but in contrast to wild type mice, no difference in BMC in the hypothyroid group (Figures 5.6 and 5.7).

TR β ^{-/-} mice showed no change in femoral or caudal BMC in response to ovariectomy, regardless of thyroid status.

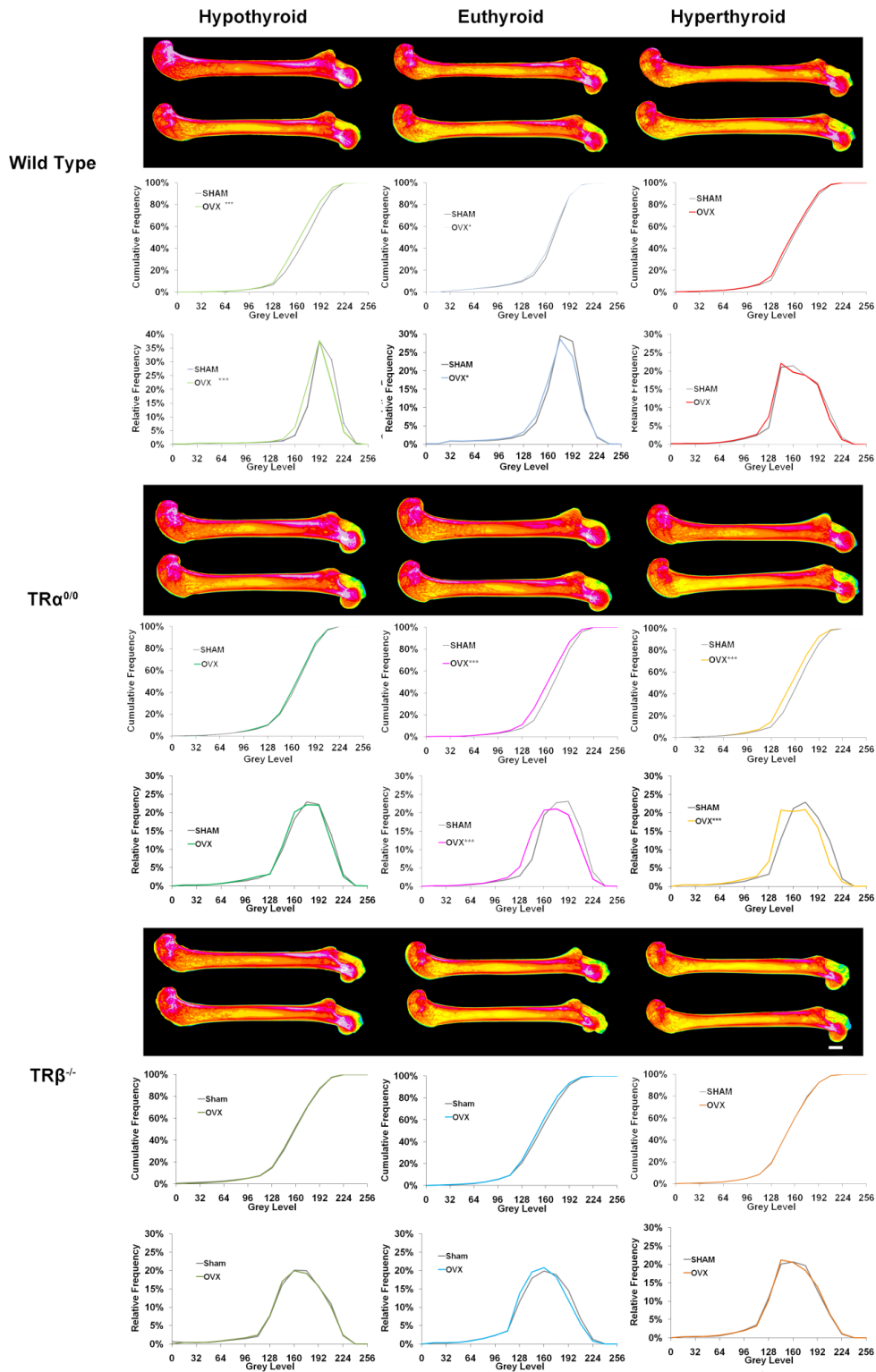


Figure 5.6 Bone mineral content of femurs

Faxitron images of femurs of P112 mice. Grey scale images were pseudocoloured with a 16 colour palette where low mineralisation density is black and high density is white. Images of femurs from sham operated groups are on top whilst the bone from ovariectomised group is shown underneath (scale bar 1mm). Cumulative and relative frequency histograms of mineralisation densities for whole femurs. Kolmogorov-Smirnov test; *, $p < 0.05$; ***, $p < 0.001$ Sham operated versus OVX.

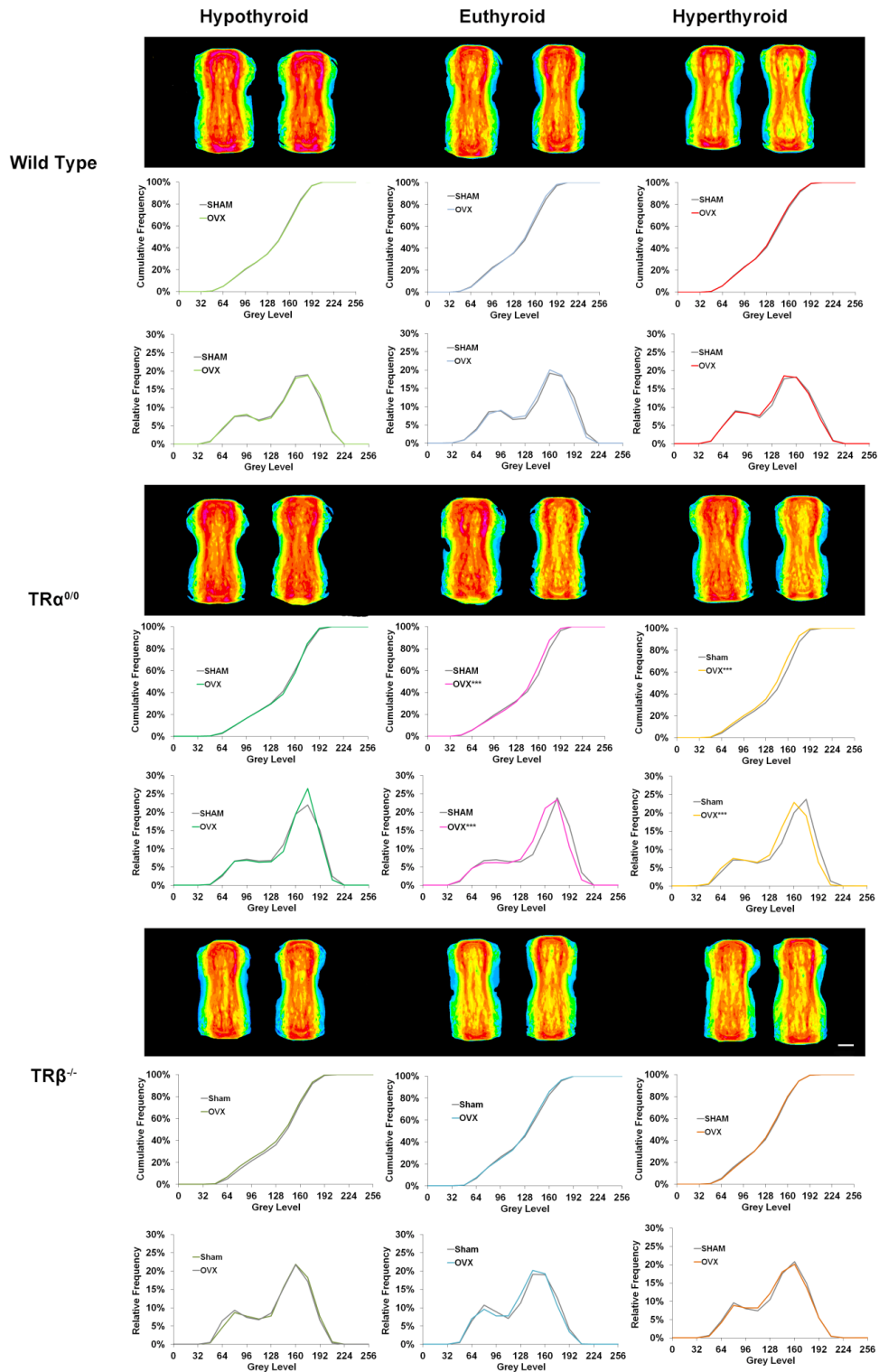


Figure 5.7 Bone mineral content of caudal vertebrae

Faxitron images of caudal vertebrae of P112 mice. Grey scale images were pseudocoloured with a 16 colour palette where low mineralisation density is black and high density is white (scale bar 1mm). Images of caudal vertebrae of sham operated mice shown on left with ovariectomy group on right. Cumulative and relative frequency histograms of mineralisation densities for vertebrae shown. Kolmogorov-Smirnov test; ***, $p < 0.001$ Sham operated versus OVX.

5.2.3.2 Micro-mineralisation: qBSE-SEM

qBSE-SEM analysis (Figure 5.8) demonstrated that oestrogen deficiency resulted in significantly decreased micro-mineralisation in all groups of wild type mice, regardless of thyroid status. These findings are in line with a high turnover osteoporosis with decreased mineralisation resulting from removal of older, more mineralised, bone and deposition of newer, less mineralised bone.

The TR α ^{0/0} mice had a significant reduction in micro-mineralisation post ovariectomy in all groups. This was particularly pronounced in the hypothyroid group but also highly significant in the euthyroid and hyperthyroid groups. This suggests that the deletion of TR α increases susceptibility to oestrogen deficient bone loss and increases its magnitude.

The TR β ^{-/-} mice showed a reduction in micro-mineralisation in the hypothyroid group post ovariectomy but not in the euthyroid or hyperthyroid groups. This suggests that the presence of liganded TR α mitigates the effect of ovariectomy on bone.

Of particular note, the qBSE-SEM and BMC results show that hypothyroidism does not protect against oestrogen deficiency bone changes in any of the genotypes tested in these experiments, disproving my original hypothesis.

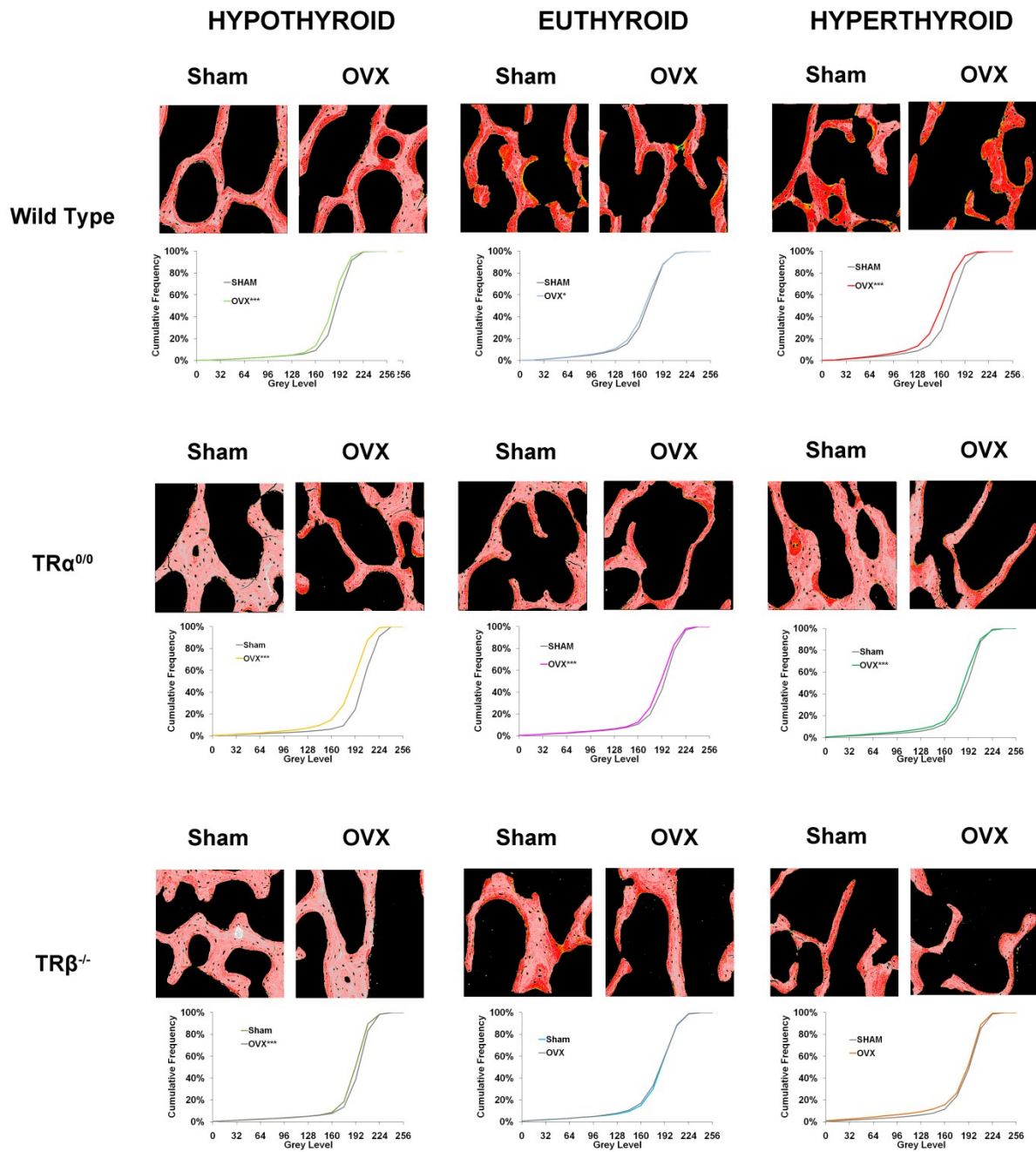


Figure 5.8 Micro-mineralisation of lumbar vertebrae

qBSE-SEM images of lumbar vertebrae from wild type, TR $\alpha^{0/0}$ and TR $\beta^{-/-}$ mice with differing thyroid status. (scale bar 100 μ m). Grey scale images were pseudocoloured with an eight colour palette; low mineralisation density is blue and high density is grey. Cumulative frequency histograms of mineralisation densities. Kolmogorov-Smirnov test; *, $p < 0.05$; ***, $p < 0.001$ for sham versus ovariectomy.

5.2.5 BONE FORMATION: P1NP AND BFR

Bone formation was assessed by histomorphometry (Table 5.2) and serum formation marker P1NP concentrations (Figure 5.9). There was a significant decrease in P1NP concentrations post ovariectomy in euthyroid and hyperthyroid $TR\alpha^{0/0}$ mice compared to sham operated mice.

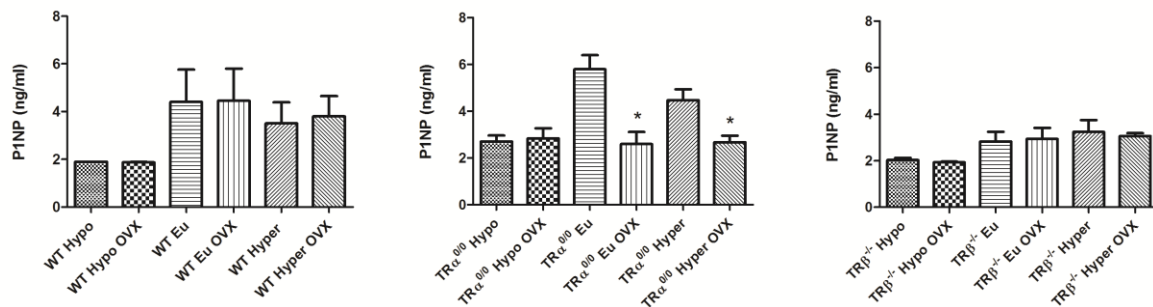


Figure 5.9 Serum P1NP from wild type, $TR\alpha^{0/0}$ and $TR\beta^{-/-}$ mice with differing thyroid status

N=3 per group and analysed by Student's t-test. No groups were significantly different when ovariectomised and sham operated comparisons were made.

Dynamic BFRs in lumbar vertebrae were assessed and compared in each group and the results are summarised in Figure 5.10.

In wild type mice, BFR post ovariectomy was elevated (secondary to an increase in MA) in the euthyroid group as expected, but remained unchanged in hypothyroid or hyperthyroid groups.

Hypothyroid $TR\alpha^{0/0}$ mice had a 2.6 fold greater BFR (as a result of increased MS/BS – Table 5.2) in ovariectomised mice when compared to sham operated mice. There was no change in BFR in euthyroid or hyperthyroid $TR\alpha^{0/0}$ mice.

This data suggests that a reduction of bone formation, which is secondary to hypothyroidism, can be overcome by oestrogen deficiency.

Hypothyroid $TR\alpha^{0/0}$ mice had similar BMC post ovariectomy versus sham (Figure 5.5), but in light of the data showing an increased BFR, it can be concluded that this was as a result of equal and

balanced increases in bone resorption and formation. This conclusion is also supported by the qBSE-SEM data which showed a decreased micro-mineralisation in hypothyroid TR α ^{0/0} mice post ovariectomy (Figure 5.9).

Hypo and euthyroid TR β ^{-/-} mice had increased BFRs with elevated MS/BS in the ovariectomised group. Ovariectomy had no effect on bone formation in the hyperthyroid animals of all three genotypes, suggesting that the increase in bone formation following oestrogen deficiency is attenuated by hyperthyroidism. This may be due to the fact that bone formation is already at a maximal rate in hyperthyroidism.

	BFR	MA	MS/BS
WT Hypo	0.04 ± 0.03	0.63 ± 0.24	4.62 ± 1.83
WT Hypo OVX	0.11 ± 0.02	0.93 ± 0.11	11.49 ± 2.46
WT Eu	0.44 ± 0.04	2.09 ± 0.15	21.50 ± 1.98
WT Eu OVX	1.06 ± 0.22*	2.98 ± 0.31*	35.56 ± 5.84
WT Hyper	0.71 ± 0.09	2.29 ± 0.06	30.70 ± 3.40
WT Hyper OVX	0.85 ± 0.07	2.35 ± 0.12	36.10 ± 1.86
TRα^{0/0} Hypo	0.18 ± 0.04	1.43 ± 0.04	12.59 ± 2.58
TRα^{0/0} Hypo OVX	0.54 ± 0.08**	1.80 ± 0.16	29.07 ± 2.07**
TRα^{0/0} Eu	0.53 ± 0.04	1.80 ± 0.06	29.52 ± 2.59
TRα^{0/0} Eu OVX	0.70 ± 0.09	1.91 ± 0.16	36.94 ± 3.45
TRα^{0/0} Hyper	0.55 ± 0.04	1.86 ± 0.20	30.02 ± 1.64
TRα^{0/0} Hyper OVX	0.47 ± 0.06	1.71 ± 0.14	27.68 ± 3.17
TRβ^{-/-} Hypo	0.03 ± 0.01	0.68 ± 0.29	2.76 ± 1.26
TRβ^{-/-} Hypo OVX	0.11 ± 0.03*	1.23 ± 0.18	8.14 ± 1.63*
TRβ^{-/-} Eu	0.33 ± 0.06	1.49 ± 0.19	20.25 ± 1.60
TRβ^{-/-} Eu OVX	0.57 ± 0.05*	1.58 ± 0.03	35.83 ± 3.49**
TRβ^{-/-} Hyper	0.66 ± 0.08	2.20 ± 0.11	29.70 ± 2.27
TRβ^{-/-} Hyper OVX	0.61 ± 0.09	1.70 ± 0.21	35.38 ± 2.00

Table 5.2 Analysis of dynamic bone formation parameters

BFR, Mineral MA and mineralising surface per BS (MS/BS). Data expressed as mean ± SEM, n=4 per group and analysed by Student's t-test:*, p<0.05, **, p<0.01, ***, p<0.001 versus non ovariectomised group of the same genotype and thyroid status.

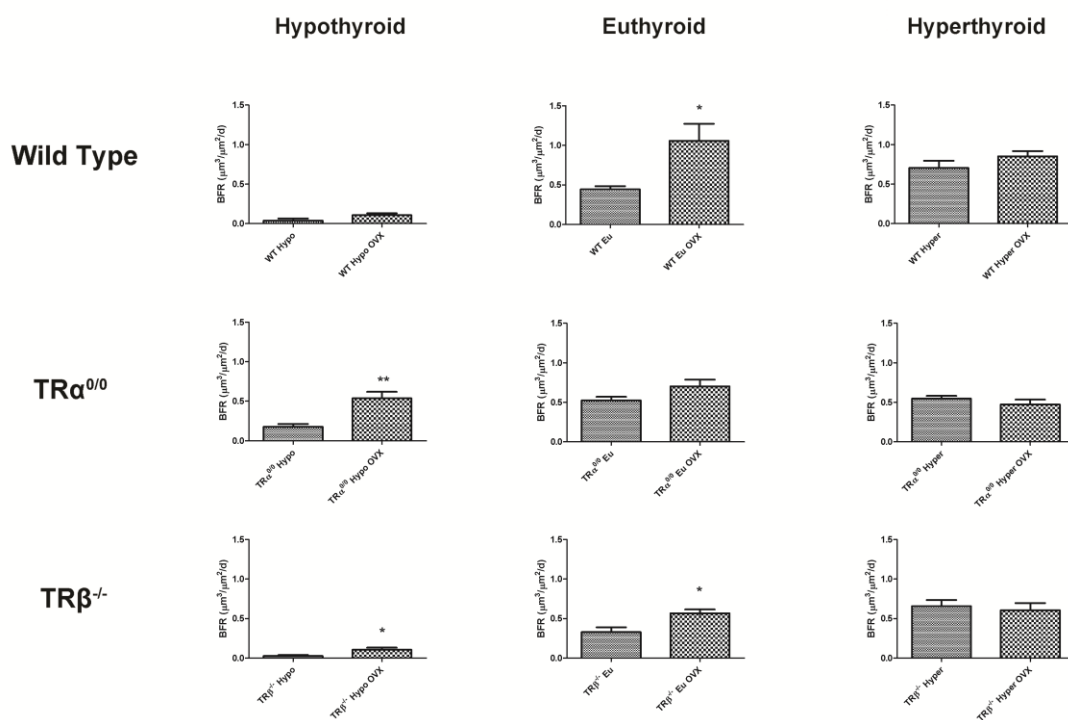


Figure 5.10 Graphical representation of BFR

Data expressed as mean ± SEM, n=4 per group and analysed by Student's t-test: *, p<0.05, **, p<0.01, versus non ovariectomised group of the same genotype and thyroid status.

5.2.6 BONE RESORPTION: CTX AND CORTICAL RESORPTION

Serum bone resorption markers CTX and endocortical surface resorption analysis (shown in Figure 5.11) show a wide variation in measurements and therefore do not provide discriminatory information. Given that oestrogen deficiency results in increased bone formation and has not been documented to decrease bone formation, it can be concluded that groups which have a decreased bone mass (BMC or BV/TV) probably have increased osteoclastic resorption. This derived result would include hypothyroid and euthyroid wild type mice, all TR α ^{0/0} mice and hypothyroid and euthyroid TR β ^{-/-} mice which have undergone ovariectomy.

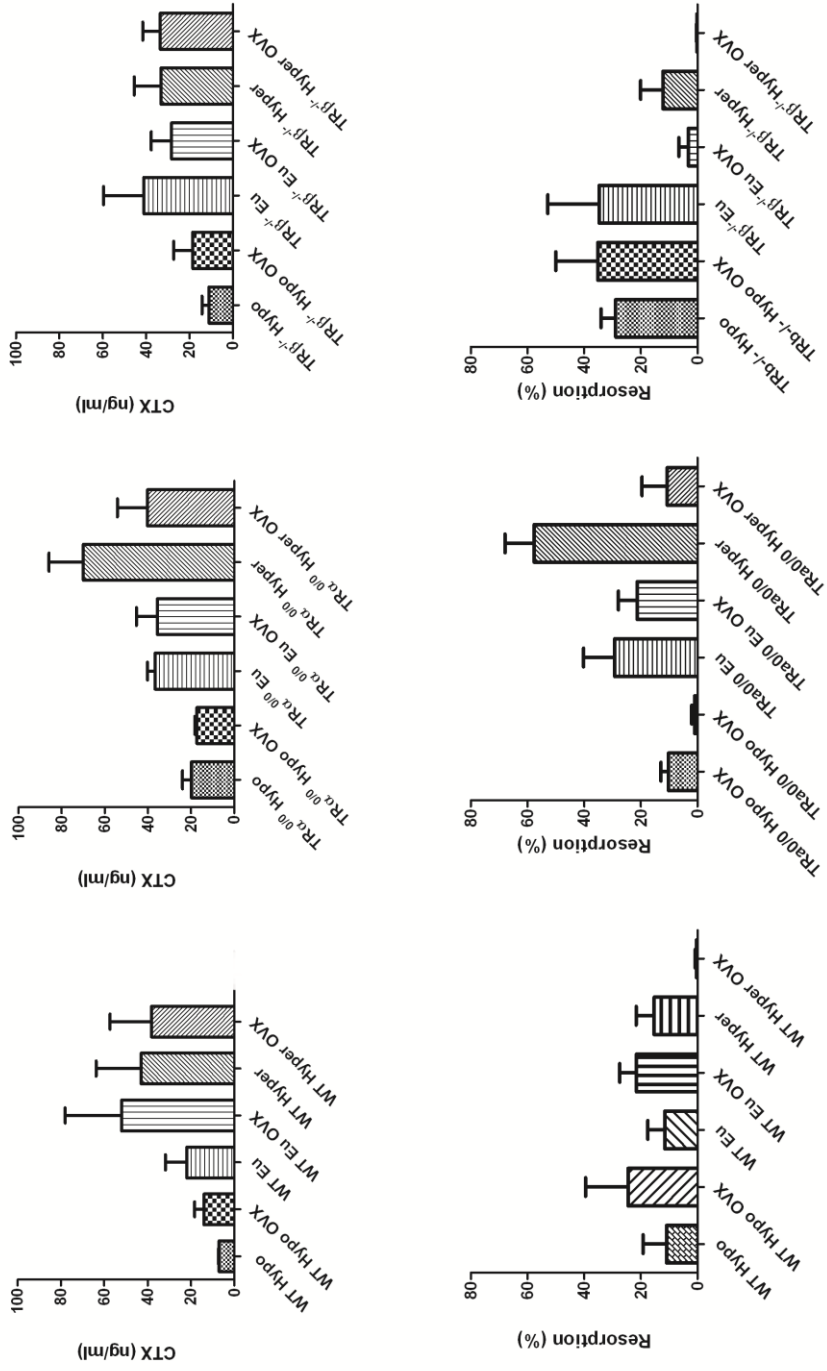


Figure 5.11 Serum bone resorption markers

Serum samples were obtained from mice at sacrifice and stored at -80°C. C-terminal cross-linked telopeptide of type I collagen (CTX) concentrations were determined by enzyme immunoassay (AC06F1). Data expressed as mean ± SEM, n=3-4 per group, sham versus ovariectomy. Quantitative analysis of endosteal osteoclast resorption surfaces (% of total BS) from P112 euthyroid wild type, TRα^{0/0} and TRβ^{-/-} mice with differing oestrogen and thyroid status. Data expressed as mean ± SEM, n=4 per group and analysed by Student's t-test. Sham operated versus ovariectomy.

5.2.7 BIOMECHANICAL TESTING

Mechanical properties of strength and load bearing were studied using destructive three point bending. Yield, maximum and fracture loads as well as stiffness, were measured and compared in ovariectomised and sham operated mice.

Figure 5.12 shows that in wild type mice, ovariectomy did not significantly alter the yield load, maximal load or the fracture load, regardless of the thyroid status.

Despite a quite significant reduction in cortical thickness, BV/TV and BMC in euthyroid and hyperthyroid TR α ^{0/0} mice post ovariectomy, there was no difference in the mechanical properties tested for any of the compared groups.

Oestrogen deficiency for a six week time period made little difference to the mechanical properties of the tibia of adult mice. Only euthyroid TR β ^{-/-} mice had a decrease in fracture load in mice with oestrogen deficiency compared to controls. There was no difference in yield load, maximum load or stiffness.

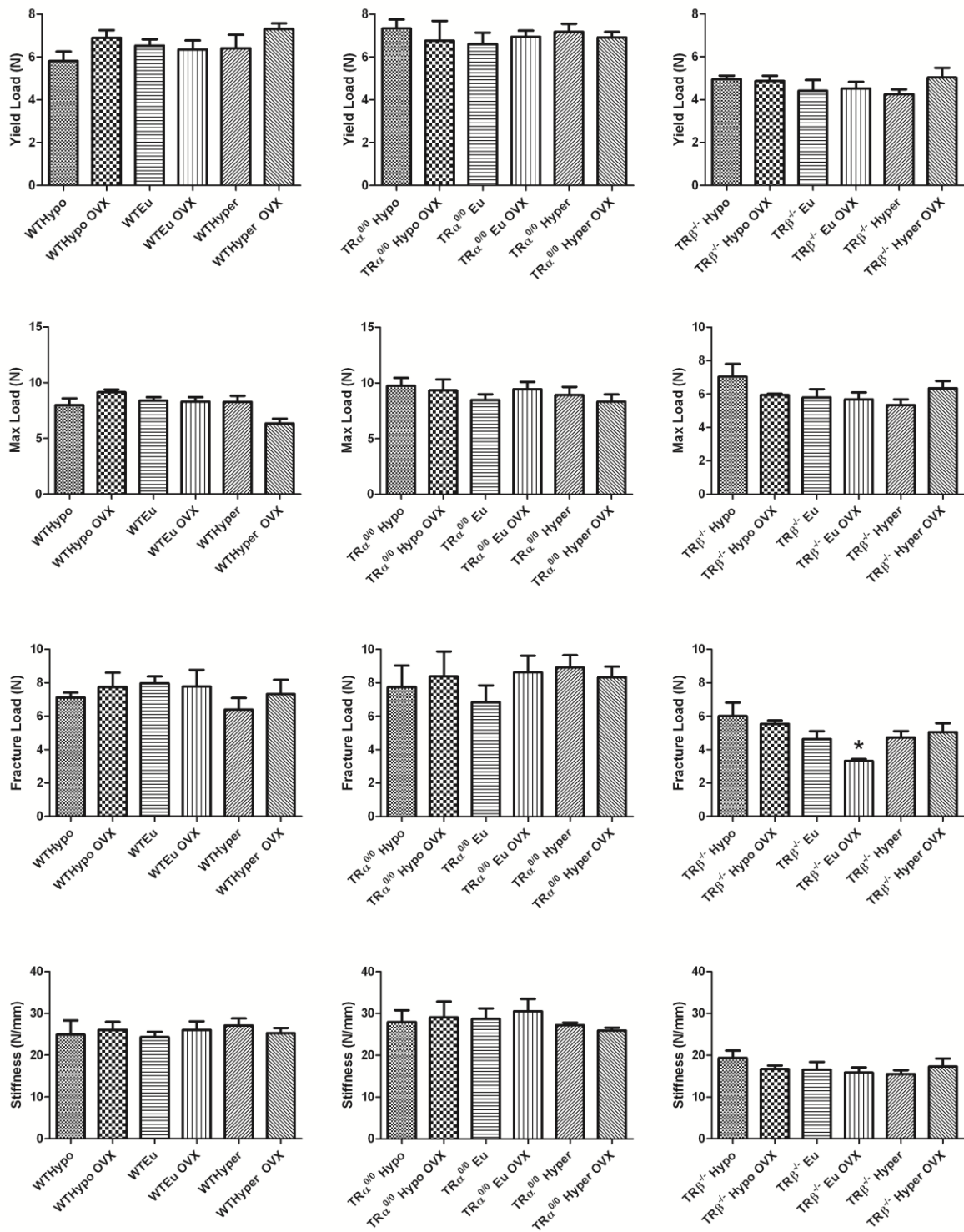


Figure 5.12 Mechanical properties

Graphs showing yield, maximum and fracture load and stiffness in tibias of P112 wild type, TR $\alpha^{0/0}$ and TR $\beta^{-/-}$ mice with differing oestrogen and thyroid status. Data expressed as mean \pm SEM, n=4-6 per group and analysed by Student's t-test.

5.3 SUMMARY OF RESULTS

	Wild type			TR $\alpha^{0/0}$			TR $\beta^{-/-}$		
	Hypo	Eu	Hyper	Hypo	Eu	Hyper	Hypo	Eu	Hyper
Weight	→	↑	→	→	→	→	→	→	↑
Tail length	→	→	→	→	→	→	→	→	→
Femoral length	→	→	→	→	→	→	→	→	↑↑
Tibial length	→	→	↑	↑	→	→	→	→	↑↑↑
Cortical diameter	→	→	→	→	→	→	→	→	→
Cortical thickness	→	↓	→	→	↓↓	↓↓↓	↑	→	→
μ CT BV/TV	↓	→	→	↓↓	↓↓↓	↓↓	→	↓	→
Femoral BMC	↓↓↓	↓	→	→	↓↓↓	↓↓↓	→	→	→
Vert BMC	→	→	→	→	↓↓↓	↓↓↓	→	→	→
qBSE SEM Lumbar Vertebrae	↓	↓	↓	↓	↓	↓	↓	→	→
BFR	→	↑	→	↑↑	→	→	↑	↑	→
MAR BS/BS	→	↑	→	→	→	→	→	→	→
	→	→	→	↑↑	→	→	↑	↑↑	→
P1NP	→	→	→	→	↓	↓	→	→	→
CTX	→	→	→	→	→	→	→	→	→
Resorption	→	→	→	→	→	→	→	→	→

Table 5.3 Summary of effects of ovariectomy on the skeletal phenotype of wild type, TR $\alpha^{0/0}$ and TR $\beta^{-/-}$ mice with differing thyroid status

Table is grouped according to genotype. → No significant difference, ↑ significant increase, ↓ significant decrease. Number of arrows indicates significance level: 1 arrow p<0.05, 2 arrows p<0.005, 3 arrows p<0.001.

	Hypothyroid			Euthyroid			Hyperthyroid		
	Wild type	TR α ^{0/0}	TR β ^{-/-}	Wild type	TR α ^{0/0}	TR β ^{-/-}	Wild type	TR α ^{0/0}	TR β ^{-/-}
Weight	→	→	→	↑	→	→	→	→	↑
Tail length	→	→	→	→	→	→	→	→	→
Femoral length	→	→	→	→	→	→	→	→	↑↑
Tibial Length	→	↑	→	→	→	→	↑	→	↑↑↑
Cortical diameter	→	→	→	→	→	→	→	→	→
Cortical thickness	→	→	↑	↓	↓↓	→	→	↓↓↓	→
μCT BV/TV	↓	↓↓	→	→	↓↓↓	↓	→	↓↓	→
Femoral BMC	↓↓↓	→	→	↓	↓↓↓	→	→	↓↓↓	→
Vert BMC	→	→	→	→	↓↓↓	→	→	↓↓↓	→
qBSE SEM Lumbar vertebrae	↓	↓	↓	↓	↓	→	↓	↓	→
BFR	→	↑↑	↑	↑	→	↑	→	→	→
MAR BS/BS	→	→	→	↑	→	→	→	→	→
	→	↑↑	↑	→	→	↑↑	→	→	→
P1NP	→	→	→	→	↓	→	→	↓	→
CTX	→	→	→	→	→	→	→	→	→
Resorption	→	→	→	→	→	→	→	→	→

Table 5.4 Summary of effects of ovariectomy on the skeletal phenotype of hypo, eu and hyperthyroid mice in different genotypes

Table is grouped according to thyroid status. → No significant difference, ↑ significant increase, ↓ significant decrease. Number of arrows indicates significance level: 1 arrow p<0.05, 2 arrows p<0.005, 3 arrows p<0.001.

5.4 DISCUSSION

These studies demonstrate that oestrogen deficiency bone loss was greater in hypothyroid compared to hyperthyroid mice. This indicates that accelerated bone loss following oestrogen withdrawal cannot result from the unopposed actions of thyroid hormones and thus disproves my hypothesis. These studies also demonstrate the complex oestrogen and thyroid hormone receptor interactions in the regulation of bone mass.

5.4.1 TR α has an osteoprotective effect on oestrogen deficiency bone loss

The most prominent finding of the experiments in this chapter is that TR α has an osteoprotective effect against oestrogen deficiency bone loss. This is apparent because in the absence of TR α (i.e. in TR α ^{0/0} mice), there is a greater susceptibility to ovariectomy induced bone loss, which is mitigated in wild type and TR β ^{-/-} mice.

The results of multiple techniques used in evaluating the various skeletal phenotypes supported this finding and are listed:

- 1 There was a highly significant reduction in cortical thickness in euthyroid and hyperthyroid TR α ^{0/0} mice, in response to ovariectomy.
- 2 Micro CT analysis showed that TR α ^{0/0} mice had a 40-60% reduction in BV/TV in response to ovariectomy, regardless of thyroid status, with these changes in bone microarchitecture also being clearly visible on BSE-SEM images.
- 3 Ovariectomy resulted in highly significantly decreased BMC at the femur and vertebrae in euthyroid and hyperthyroid TR α ^{0/0} mice. Although ovariectomised hypothyroid TR α ^{0/0} mice had a similar BMC to sham operated mice, there was a significantly elevated BFR in this group, suggesting that to maintain normal BMC, there was also likely to have been an increase in bone resorption.
- 4 Analysis of qBSE-SEM results showed a significant reduction in micro-mineralisation in all TR α ^{0/0} mice in response to ovariectomy, regardless of thyroid status.

Unfortunately, parameters used to assess bone resorption were not sufficiently sensitive to detect any changes. However, a decrease in bone mass in conjunction with normal or raised bone formation in TR α ^{0/0} mice, suggests that ovariectomy induced bone loss is secondary to increased bone resorption.

Ovariectomy induced bone loss in TR α ^{0/0} mice is reduced or mitigated in the presence of TR α and this is demonstrated in the skeletal response of TR β ^{-/-} and wild type mice to ovariectomy.

The finding that TR α is osteoprotective against ovariectomy induced bone loss is novel and contrary to my initial hypothesis that in the absence of oestrogen, bone loss results from the unopposed actions of thyroid hormone. The molecular signalling pathways responsible for this finding are an area for possible future research.

5.4.2 Oestrogen withdrawal associated with increased weight and bone length

Oestrogen deficiency has been associated with increased central fat distribution in postmenopausal women when compared to premenopausal women (Toth et al., 2000). Likewise, in oestrogen deficient mice, increased weight is found in euthyroid wild type and hyperthyroid TR β ^{-/-} groups.

Hyperthyroid TR β ^{-/-} mice, which had the greatest increase in weight, also had a highly significant increase in femoral and tibial length. This was unexpected, as hyperthyroid TR β ^{-/-} mice have advanced growth plate maturation with diminished final height and would have reached skeletal maturity before the other groups (Bassett et al., 2007a). The growth plates in these mice at P70 would have been quiescent before manipulation of oestrogen and thyroid status and must have undergone reactivation, resulting in increased bone length. It would appear that tibias are more sensitive to changes in bone length than femurs after oestrogen deficiency growth plate reactivation. This may be because the reactivated growth plates of the tibia and femur have different sensitivities to thyroid hormone induced growth. This observation is in line with findings in patients with TR α mutations have rhizomelia (Bochukova et al., 2012). There is a small increase in tibial, but not femoral length, in hyperthyroid wild type and hypothyroid TR α ^{0/0} mice. Unlike humans, mice continue to grow slowly and their growth plates do not completely fuse. This data suggests that in the presence of TR α and excess thyroid hormone, oestrogen withdrawal reactivates the growth plate, resulting in an increase in long bone length. An increase in bone length and growth plate thickness post ovariectomy has been described in rats (Gevers et al., 1995) (van der Eerden et al., 2003). This effect has been attributed to the direct action of oestrogen on chondrocytes (van der Eerden et al., 2002) or to the secondary action of oestrogen on GH/IGF and vascular endothelial growth factor (VEGF) (Borjesson et al., 2010, Juul, 2001, Emons et al., 2010). It would be interesting to investigate this further by assessing growth plate width and evaluating GH and IGF1 levels in the serum and at the growth plate.

5.4.3 Oestrogen withdrawal in hypothyroid mice is associated with increased resorption on cancellous surfaces but not endocortical surfaces

Oestrogen withdrawal does not result in any change in cortical diameter in any group, so any changes in cortical thickness must result from an increase in endocortical resorption. Although there is a significant reduction in cortical thickness in wild type and euthyroid and hyperthyroid TR α ^{0/0} groups, there is no decrease in cortical thickness in any of the hypothyroid groups in response to oestrogen deficiency. There is even an increase in cortical thickness in hypothyroid TR β ^{-/-} mice, all of which suggests that hypothyroidism is associated with reduced endocortical resorption in response to oestrogen deficiency. This is particularly evident in the TR α ^{0/0} group, where there is a highly significant decrease in cortical thickness in euthyroid and hyperthyroid groups but none in the hypothyroid group.

It was surprising that the measurements of percentage of endocortical resorption pits (Figure 5.11) did not confirm these findings. This is likely to be because evaluation of endocortical resorption pits, in mice rendered hypothyroid, still reflects the resorption that was occurring at the time of being rendered hypothyroid and not at the time of sacrifice.

Despite the lack of endocortical resorption, there is evidence for active resorption of the trabeculae. Hypothyroid mice have a significant decrease in BV/TV in response to oestrogen deficiency, as measured by micro CT, in wild type and TR α ^{0/0} groups. There is also a highly significant decrease in femoral BMC in hypothyroid wild type mice in response to ovariectomy.

5.4.4 Hyperthyroid mice do not demonstrate oestrogen deficiency elevation in bone formation

Hyperthyroid mice in all genotypes do not respond to oestrogen deficiency by an increase in BFR. This data may indicate that a similar mechanism of action or pathway to increase osteoblastic bone formation may be shared by thyroid excess and oestrogen deficiency. This pathway may be saturated in hyperthyroid mice and so no further increases in BFR are detected on oestrogen withdrawal.

5.4.5 Decreased bone formation associated with presence of oestrogen and unliganded TR α

The presence of oestrogen decreases osteoblastic bone formation and data in Chapter 4 also suggests that unliganded TR α has a similar effect. Thus, in hypothyroid ovariectomised TR α ^{0/0} mice, where there is an absence of oestrogen and no apoTRAs, the BFR is significantly higher when

compared to sham operated mice. The BFR of these mice is similar to euthyroid wild type mice. Interestingly, in ovariectomised TR α ^{0/0} mice, only the hypothyroid group had a BFR comparable to euthyroid wild type mice, which suggests that hypothyroid induced suppression of bone resorption can be overcome with oestrogen deficiency.

5.4.6 Bone remodelling uncoupled in ovariectomised TR α ^{0/0} mice

In Chapter 3, euthyroid TR α ^{0/0} mice were shown to have uncoupled remodelling, with normal bone formation and reduced bone resorption, resulting in increased bone mass. Resorption increased when the TR α ^{0/0} mice were rendered hyperthyroid and increased further in response to oestrogen deficiency. Although both hyperthyroidism and oestrogen withdrawal increase resorption, there is no corresponding increase in BFR, evidencing uncoupling of remodelling in euthyroid and hyperthyroid TR α ^{0/0} mice. This data suggests that thyroid hormone may play an important role in osteoblast-osteoclast coupling. The presence of TR α seems to be osteoprotective, but in its absence, the effects of thyroid hormone and oestrogen deficiency on osteoclast function appear to be independent.

Chapter 6

General discussion

6 DISCUSSIONS AND CONCLUSIONS

The novel findings presented in this thesis provide further insight into how thyroid hormone and its receptors affect the skeleton and also suggest complex interactions between oestrogen and thyroid hormone in the regulation of bone mass.

6.1 Effects on the skeleton of oestrogen and thyroid hormone interactions

The bone phenotype of TR $\alpha^{0/0}$ mice is very similar to that of hypothyroid mice (both show increased bone mass and decreased resorption compared with controls) but dynamic bone formation measurements uncover a divergence between these two groups when comparing bone formation. Hypothyroid wild type mice have almost absent bone formation whereas TR $\alpha^{0/0}$ mice have a BFR similar to that of wild type controls. Thus, although it has previously been hypothesised that TR $\alpha^{0/0}$ mice have decreased thyroid hormone signalling in the skeleton, the picture is likely to be more heterogeneous than one would expect. It is possible that a lack of T3 liganded TR α action impairs chondrocyte and osteoclast function but there is no evidence of a similar effect on osteoblast function.

The role of TR α in the skeleton is very evident when comparisons are made between the effects of hypothyroidism on wild type TR $\alpha^{0/0}$ and TR $\beta^{-/-}$ mice. Bone formation is radically reduced as a response to a lack of thyroid hormone but in the absence of unliganded TR α , bone formation is partially rescued with four times the BFR, suggesting that unliganded TR α , but not TR β , has a repressive effect on bone formation. This finding is in agreement with data from Flamant 2002, who generated congenitally hypothyroid pax8 $^{-/-}$ mice, which were lethal, but could be rescued by crossing them with TR $\alpha^{0/0}$ mice to generate double knockout pax8 $^{-/-}$ TR $\alpha^{0/0}$ mice. Double knockout pax8 $^{-/-}$ TR $\beta^{-/-}$ mice, however, were similar to pax8 $^{-/-}$ mice, resulting in early lethality before weaning. From this data, the authors noted that TR α was the predominant receptor in bone and that unliganded TR α had a repressive effect on bone development. My data adds to these findings by showing that apo TR α has a repressive effect specifically on osteoblastic bone formation. The data from my experiments suggests that thyroid hormone has a direct incremental effect on bone formation via TR α , and additionally, that in the absence of TR α , TR β has an important compensatory role in bone formation, as evidenced by the highly significant decrease in BFR when TR $\alpha^{0/0}$ mice are rendered hypothyroid.

Comparing the effects of thyroid hormones and oestrogen deficiency on different genotypes is highly complex and these experiments have demonstrated that it is important to assess the skeleton via a number of methods before conclusions can be drawn. It is particularly difficult to assess responses to thyroid or oestrogen status across genotypes where bone development has been compromised. Monfoulet *et al* assessed the response of thyroid status in wild type, TR α ^{0/0} and TR β ^{-/-} mice and found that TR α ^{0/0} mice had a significant response to elevated thyroid hormone (much like with my data) but that TR β ^{-/-} mice only had a significant response after prolonged exposure to excess thyroid hormone. They concluded that TR β mediates the acute effects of thyroid hormone, whilst TR α mediates the long term effects. However, as discussed in Chapter 4, the data from that study did not include adequate bone formation parameters and no data for the euthyroid groups was given, making it difficult to assess the full picture.

The skeletal phenotyping in this thesis has provided a more comprehensive picture. Rather than TR β mediating the acute effects of thyroid hormone and TR α mediating the long term effects, it is more likely that TR β ^{-/-} mice (which are osteoporotic at baseline) are more resistant to excess thyroid hormone and TR α ^{0/0} mice (which have a higher bone mass at baseline) are more sensitive to the effects of excess thyroid hormone.

The skeletal response to oestrogen withdrawal differs not only with thyroid status and the presence of TR α , but is also dependent on which skeletal site is being assessed. Intramedullary cortical resorption appears to be highly sensitive to hypothyroidism, in contrast to resorption in the cancellous compartment, which is less sensitive.

The most significant ovariectomy induced decrease in bone resorption, regardless of thyroid status, was in the TR α ^{0/0} group, which suggests that the presence of TR α has an osteoprotective effect against oestrogen deficiency bone loss. The molecular mechanism behind this osteoprotective effect, is a potential area for future research.

6.2 Bone biology

As a result of the observations made in this thesis, I also now hypothesise that bone response differs according to pre-existing bone mass setpoints. These setpoints may have been determined during growth or according to mutation. This hypothesis would account for the differing responses of bone mass in wild type, TR α ^{0/0} and TR β ^{-/-} mice to changes in thyroid status. Adult TR β ^{-/-} mice are osteoporotic and a pre-existing low bone mass setpoint would account for the minimal differences

between euthyroid and hyperthyroid bone mass in these mice, a factor which can be overcome when the mice are rendered hypothyroid. Adult TR $\alpha^{0/0}$ mice are osteosclerotic with a higher bone mass setpoint, so when rendered hyperthyroid, they showed a significant reduction in bone mass, but conversely, there was minimal change in bone mass when these mice were rendered hypothyroid.

Surprisingly, given the literature, TR $\alpha^{0/0}$ mice had normal bone formation but decreased resorption, resulting in a net positive balance and a greatly increased bone mass. Osteoblast and osteoclast function are usually highly coupled and the one directly affects the other. For example, in bisphosphonate therapy, which renders osteoclasts apoptotic or dysfunctional (Russell, 2011), osteoblast function is also impaired, as evidenced by decreased bone formation rate and a reduction in other osteoblast indices (Munns et al., 2005). Very few therapeutic interventions are able to uncouple bone formation and resorption and the finding in this thesis that uncoupling occurs in TR $\alpha^{0/0}$ mice is therefore of significance. Further comprehension of the molecular mechanisms regulating bone formation in the skeleton of TR $\alpha^{0/0}$ mice could assist in developing therapeutic interventions for osteoporosis.

6.3 Future research and ongoing experiments

The experiments in this thesis contribute novel data to the published literature on both the role of thyroid receptors in bone and the interactions between thyroid hormone and oestrogen.

Additional work for these experiments

Bones from each mouse used in these experiments have been snap frozen and maintained in liquid Nitrogen for RNA extraction at a later date. These samples could be used to assess the relative expression of RANK/RANKL/OPG, mRNAs or other important bone signalling pathways in the different mouse groups. These experiments are due to be undertaken by other members of the laboratory, who will continue the work started in this thesis.

Future experiments

As with much research, the results of the experiments presented in this thesis lead to further questions, some of which have already started to be addressed in the laboratory.

1. In vivo studies addressing cell specific effects of thyroid hormone

The role of thyroid hormone signalling in specific bone cells has begun to be investigated using mice which harbour floxed constructs for the conditional overexpression of the Dio3 enzyme. These mice can be crossed with lines that selectively express cre recombinase. This results in mice with conditional overexpression of Dio3, resulting in cell specific hypothyroidism. Thyroid hormone regulation of bone is currently being investigated in chondrocytes, osteoblasts and osteoclasts using this technique. The results of these further experiments should provide insight into whether the effects of hypothyroidism on decreased osteoclast activity are direct or indirect, and which other bone cell types may be involved in this process.

2. In vitro osteoclast studies

It is clear from my experiments that osteoclast function is TR α dependent. To investigate if the action of T3 in osteoclasts is direct or mediated via TR α in another cell type, *in vitro* studies could be used. The direct effects of T3 on osteoclasts can be assessed using cultures of wild type, TR $\alpha^{0/0}$ and TR $\beta^{-/-}$ osteoclasts to study osteoclast survival and activity. Cell co-culture studies could then be used to assess the effect of T3 on the interactions between osteoblasts, or another cell type, and osteoclasts from wild type, TR $\alpha^{0/0}$ and TR $\beta^{-/-}$ mice.

3. Investigation of cellular mechanism to establish why TR α is osteoprotective against oestrogen deficiency bone loss

Further research in respect of molecular signalling would include looking at the downstream signalling pathways involved in the changes seen in the skeleton as a result of oestrogen and thyroid hormone interactions. Key pathways that could be investigated include the RANK/RANKL/OPG and Wnt pathways using techniques such as qRT-PCR, Western blots and immunoprecipitation. Understanding the molecular mechanisms behind the osteoprotective nature of TR α could lead to potential therapies for osteoporosis.

APPENDIX

Solutions used in this thesis

T4: Sigma T1775

Stock solution: 60mg to 10ml of dH₂O

Working solution: 20ul stock to 100mls of drinking water (final concentration of 1.2ug/ml)

T3: Sigma T2877

Stock solution: 5mg of T3 in 0.25ml of 1M NaOH and made up to 5ml with dH₂O to make stock concentration of 1mg/ml

Working solution: 12.5µl of stock to 250ml water to make final concentration of 0.05mg/ml

Calcein: Sigma CO875

Working solution: 5mg dissolved in 10mls of warmed pbs and administered at 5mls/kg iv

Cacodylate: Agar R1103

Stock solution: Dissolve 21.4gm sodium cacodylate in dH₂O and adjust pH to 7.4 by adding 9.5ml of 1M HCl. Make up to 500mls with distilled H₂O to make 0.2M sodium cacodylate solution

2.5% Glutaraldehyde Fixative: Agar R1012

1ml of 25% glutaraldehyde

1.5ml dH₂O

7.5mls of 0.2M sodium cacodylate buffer

Histology staining

Aniline Blue and Phosphotungstic Acid: Sigma 415049 and Fluka 79690:

0.166g Aniline Blue

3g Phosphotungstic Acid

500ml H₂O

Acetate Buffer: 0.82g Sodium Acetate Anhydrous

100ml dH₂O

pH adjusted to 5.2 using 100% Glacial Acetic Acid

TRAP stain:

350mg Naphthol AS-TR Phosphate

1250µl N-NDimethyl formamide

250ml 0.2M Sodium Acetate Buffer

575mg Sodium Tartrate dehydrate

350mg Fast Red Salt TR

Page Number	Type of work: text, figure, map, etc.	Source work	Copyright holder & year	Permission to re-use
Page 26	figure	Nature (2003), vol 423, p349-355	© 2003, Nature publishing group	✓
Page 31	figure	Reviews in Endocrine and Metabolic Disorders (2006) vol 7, p123-139	© 2006, Springer	✓
Page 37	figure	Current Opinion in Structural Biology (1999) vol 9, p122-128	© 1999 Elsevier	✓
Page 39	figure	Annual Review of Materials Science (1998) vol 28, p271-298	© 1998 Annual Review of Materials Science	✓
Page 40	figure	Developmental Biology, 8 ed Gilbert 2006	©2006 Sinauer	✓
Page 43	figure	Nature (2003) vol 423 p332-336	© 2003 Nature publishing group	✓
Page 46	figure	Journal of Biological Chemistry (2010) Vol 258, p25103-8	© 2013 American Society for Biochemistry and Molecular Biology	✓
Page 52	figure	The Journal of Endocrinology (2012) vol 213(3) 209-21	©2013 Bioscientifica	✓
Page 54	figure	Endocrinology (2009) vol 150 p1084-1090	© 2009 Annual Review of Materials Science	✓
Page 58	figure	Molecular and Cellular Endocrinology (2013) vol 213 p1-11	©2013 Elsevier	✓
Page 61	figure	Nature Reviews Endocrinology (2007), vol 3, p249-259	© 2007 Nature publishing group	✓
Page 77	figure	Endocrine Reviews (2009), vol 30, p465	© Annual Review of Materials Science	✓
Page 79	figure	The Journal of Clinical Investigation (2006) Vol 116(3) p561-570	© Annual Review of Materials Science	✓
Page 81	figure	Radiologic Clinics of North America (2010), 48(3), p483-95	© 2010 Elsevier	✓

**NATURE PUBLISHING GROUP LICENSE
TERMS AND CONDITIONS**

Nov 18, 2013

This is a License Agreement between Moira Cheung ("You") and Nature Publishing Group ("Nature Publishing Group") provided by Copyright Clearance Center ("CCC"). The license consists of your order details, the terms and conditions provided by Nature Publishing Group, and the payment terms and conditions.

All payments must be made in full to CCC. For payment instructions, please see information listed at the bottom of this form.

License Number	3271860110827
License date	Nov 18, 2013
Licensed content publisher	Nature Publishing Group
Licensed content publication	Nature
Licensed content title	Control of osteoblast function and regulation of bone mass
Licensed content author	Shun-ichi Harada and Gideon A. Rodan
Licensed content date	May 15, 2003
Volume number	423
Issue number	6937
Type of Use	reuse in a dissertation / thesis
Requestor type	academic/educational
Format	electronic
Portion	figures/tables/illustrations
Number of figures/tables/illustrations	1
High-res required	no
Figures	figure 3
Author of this NPG article	no
Your reference number	fig 1.2 mesencymal progenitor differentiation
Title of your thesis / dissertation	oestrogen and thyroid hormone interactions in the regulation of bone mass
Expected completion date	Dec 2013
Estimated size (number of pages)	250
Total	0.00 GBP
Terms and Conditions	

Terms and Conditions for Permissions

Nature Publishing Group hereby grants you a non-exclusive license to reproduce this material for this purpose, and for no other use, subject to the conditions below:

1. NPG warrants that it has, to the best of its knowledge, the rights to license reuse of this material. However, you should ensure that the material you are requesting is original to Nature Publishing Group and does not carry the copyright of another entity (as credited in

<https://s100.copyright.com/App/PrintableLicenseFrame.jsp?publisherID=52&pu...> 18/11/2013

**SPRINGER LICENSE
TERMS AND CONDITIONS**

Nov 18, 2013

This is a License Agreement between Moira Cheung ("You") and Springer ("Springer") provided by Copyright Clearance Center ("CCC"). The license consists of your order details, the terms and conditions provided by Springer, and the payment terms and conditions.

All payments must be made in full to CCC. For payment instructions, please see information listed at the bottom of this form.

License Number	3210340744737
License date	Aug 15, 2013
Licensed content publisher	Springer
Licensed content publication	Reviews in Endocrine & Metabolic Disorders
Licensed content title	Molecular regulation of osteoclast activity
Licensed content author	Angela Bruzzaniti
Licensed content date	Jan 1, 2006
Volume number	7
Issue number	1
Type of Use	Thesis/Dissertation
Portion	Figures
Author of this Springer article	No
Order reference number	
Title of your thesis / dissertation	oestrogen and thyroid hormone interactions in the regulation of bone mass
Expected completion date	Aug 2013
Estimated size(pages)	250
Total	0.00 GBP

Terms and Conditions

Introduction

The publisher for this copyrighted material is Springer Science + Business Media. By clicking "accept" in connection with completing this licensing transaction, you agree that the following terms and conditions apply to this transaction (along with the Billing and Payment terms and conditions established by Copyright Clearance Center, Inc. ("CCC"), at the time that you opened your Rightslink account and that are available at any time at <http://myaccount.copyright.com>).

Limited License

With reference to your request to reprint in your thesis material on which Springer Science and Business Media control the copyright, permission is granted, free of charge, for the use indicated in your enquiry.

Licenses are for one-time use only with a maximum distribution equal to the number that you identified in the licensing process.

<https://s100.copyright.com/CustomAdmin/PLF.jsp?ref=06864d05-3afd-4a40-8fbc-3...> 18/11/2013

**ELSEVIER LICENSE
TERMS AND CONDITIONS**

Nov 18, 2013

This is a License Agreement between Moira Cheung ("You") and Elsevier ("Elsevier") provided by Copyright Clearance Center ("CCC"). The license consists of your order details, the terms and conditions provided by Elsevier, and the payment terms and conditions.

All payments must be made in full to CCC. For payment instructions, please see information listed at the bottom of this form.

Supplier	Elsevier Limited The Boulevard, Langford Lane Kidlington, Oxford, OX5 1GB, UK
Registered Company Number	1982084
Customer name	Moira Cheung
Customer address	52 Perrers Road London, W6 0EZ
License number	3271860696961
License date	Nov 18, 2013
Licensed content publisher	Elsevier
Licensed content publication	Current Opinion in Structural Biology
Licensed content title	Folding of peptide models of collagen and misfolding in disease
Licensed content author	Jean Baum, Barbara Brodsky
Licensed content date	1 February 1999
Licensed content volume number	9
Licensed content issue number	1
Number of pages	7
Start Page	122
End Page	128
Type of Use	reuse in a thesis/dissertation
Intended publisher of new work	other
Portion	figures/tables/illustrations
Number of figures/tables/illustrations	1
Format	electronic
Are you the author of this Elsevier article?	No
Will you be translating?	No
Title of your thesis/dissertation	oestrogen and thyroid hormone interactions in the regulation of bone mass
Expected completion date	Dec 2013

<https://s100.copyright.com/App/PrintableLicenseFrame.jsp?publisherID=70&pu...> 18/11/2013

Estimated size (number of pages)	250
Elsevier VAT number	GB 494 6272 12
Permissions price	0.00 GBP
VAT/Local Sales Tax	0.00 GBP / 0.00 GBP
Total	0.00 GBP
Terms and Conditions	

INTRODUCTION

1. The publisher for this copyrighted material is Elsevier. By clicking "accept" in connection with completing this licensing transaction, you agree that the following terms and conditions apply to this transaction (along with the Billing and Payment terms and conditions established by Copyright Clearance Center, Inc. ("CCC"), at the time that you opened your Rightslink account and that are available at any time at <http://myaccount.copyright.com>).

GENERAL TERMS

2. Elsevier hereby grants you permission to reproduce the aforementioned material subject to the terms and conditions indicated.

3. Acknowledgement: If any part of the material to be used (for example, figures) has appeared in our publication with credit or acknowledgement to another source, permission must also be sought from that source. If such permission is not obtained then that material may not be included in your publication/copies. Suitable acknowledgement to the source must be made, either as a footnote or in a reference list at the end of your publication, as follows:

“Reprinted from Publication title, Vol /edition number, Author(s), Title of article / title of chapter, Pages No., Copyright (Year), with permission from Elsevier [OR APPLICABLE SOCIETY COPYRIGHT OWNER].” Also Lancet special credit - “Reprinted from The Lancet, Vol. number, Author(s), Title of article, Pages No., Copyright (Year), with permission from Elsevier.”

4. Reproduction of this material is confined to the purpose and/or media for which permission is hereby given.

5. Altering/Modifying Material: Not Permitted. However figures and illustrations may be altered/adapted minimally to serve your work. Any other abbreviations, additions, deletions and/or any other alterations shall be made only with prior written authorization of Elsevier Ltd. (Please contact Elsevier at permissions@elsevier.com)

6. If the permission fee for the requested use of our material is waived in this instance, please be advised that your future requests for Elsevier materials may attract a fee.

7. Reservation of Rights: Publisher reserves all rights not specifically granted in the combination of (i) the license details provided by you and accepted in the course of this licensing transaction, (ii) these terms and conditions and (iii) CCC's Billing and Payment terms and conditions.

8. License Contingent Upon Payment: While you may exercise the rights licensed immediately upon issuance of the license at the end of the licensing process for the



1
PAYMENT
2
REVIEW
3
CONFIRMATION

Step 3: Order Confirmation

Thank you for your order! A confirmation for your order will be sent to your account email address. If you have questions about your order, you can call us at +1.877.239.3415 Toll Free, M-F between 3:00 AM and 6:00 PM (Eastern), or write to us at info@copyright.com. This is not an invoice.

Confirmation Number: 11138528
Order Date: 11/18/2013

If you paid by credit card, your order will be finalized and your card will be charged within 24 hours. If you choose to be invoiced, you can change or cancel your order until the invoice is generated.

Payment Information

Moira Cheung
moira_cheung@doctors.org.uk
+44 2087413045
Payment Method: n/a

Order Details

ANNUAL REVIEW OF MATERIALS SCIENCE

<p>Order detail ID: 64157935 Order License Id: 3271870311318 ISSN: 0084-6600 Publication Type: Monographic Series Volume: Issue: Start page: Publisher: ANNUAL REVIEWS, INC.</p>	<p>Permission Status: ✔ Granted Permission type: Republish or display content Type of use: Republish in a thesis/dissertation</p>
	Requestor type: Academic institution
	Format: Electronic
	Portion: chart/graph/table/figure
	Number of charts/graphs/tables/figures: 1
	Title or numeric reference of the portion (s): Figure 6
	Title of the article or chapter the portion is from: NA
	Editor of portion(s): NA
	Author of portion(s): NA
	Volume of serial or monograph: NA
	Issue, if republishing an article from a serial: 28
	Page range of portion: p284

<https://www.copyright.com/printCoiConfirmPurchase.do?operation=defaultOperation...> 18/11/2013

Publication date of portion	Dec 2013
Rights for	Main product
Duration of use	Current edition and up to 5 years
Creation of copies for the disabled	no
With minor editing privileges	no
For distribution to	U.K. and Commonwealth (excluding Canada)
In the following language(s)	Original language of publication
With incidental promotional use	no
Lifetime unit quantity of new product	0 to 499
Made available in the following markets	education
The requesting person/organization	Dr Moira Cheung, Imperial
Order reference number	fig1.7
Author/Editor	Dr Moira Cheung
The standard identifier	thesis
Title	Oestrogen and thyroid hormone interactions in the regulation of bone mass
Publisher	Imperial college
Expected publication date	Dec 2013
Estimated size (pages)	250

Note: This item will be invoiced or charged separately through CCC's **RightsLink** service. [More info](#) **\$ 0.00**

Total order items: 1

This is not an invoice.

Order Total: \$ 0.00



SINAUER ASSOCIATES, Inc. • Publishers • P.O. Box 407 • Sunderland, MA 01375-0407

Telephone: (413) 549-4300
Fax: (413) 549-1118
E-mail: orders@sinauer.com

PERMISSIONS AGREEMENT

November 18, 2013

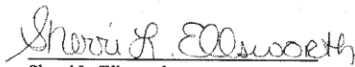
Permission granted to:
Maira Cheung
52 Perrers Road
London W6 0EZ
UNITED KINGDOM

Email: moiracheung@gmail.com

Material to be reproduced:
Gilbert: *Developmental Biology, Eighth Edition*
Figure 14.14, page 456

To be reproduced in the work:
Maira Cheung's PhD Thesis entitled "Oestrogen and thyroid hormone interaction in the regulation of bone mass" to be published by Imperial College (print and electronic)

Sinauer Associates owns copyright to the material described above and hereby grants permission for the one-time use of the material as specified, and for nonexclusive world rights provided that full and appropriate credit is given to the original source and that the work is for NON-COMMERCIAL use only. Please request permission for further use in subsequent editions, translations, or revisions of the work.


Sherri L. Ellsworth
Permissions Coordinator

Nov. 18, 2013
Date

Please acknowledge your acceptance of these terms by signing one copy of this form and returning it to Sinauer Associates. Permission Agreement is not valid until signed by applicant and received by Sinauer Associates.


Signature of Applicant

Nov 20 2013
Date

NATURE PUBLISHING GROUP LICENSE
TERMS AND CONDITIONS
Feb 27, 2014


This is a License Agreement between Moira Cheung ("You") and Nature Publishing Group ("Nature Publishing Group") provided by Copyright Clearance Center ("CCC"). The license consists of your order details, the terms and conditions provided by Nature Publishing Group, and the payment terms and conditions.

All payments must be made in full to CCC. For payment instructions, please see information listed at the bottom of this form.

License Number	3271880315993
License date	Nov 18, 2013
Licensed content publisher	Nature Publishing Group
Licensed content publication	Nature
Licensed content title	Developmental regulation of the growth plate
Licensed content author	Henry M. Kronenberg
Licensed content date	May 15, 2003
Volume number	423
Issue number	6937
Type of Use	reuse in a dissertation / thesis
Requestor type	academic/educational
Format	electronic
Portion	figures/tables/illustrations
Number of figures/tables/illustrations	1
High-res required	no
Figures	Growth plate signalling
Author of this NPG article	no
Your reference number	Fig 1.10
Title of your thesis / dissertation	oestrogen and thyroid hormone interactions in the regulation of bone mass
Expected completion date	Dec 2013
Estimated size (number of pages)	250
Total	0.00 GBP
Terms and Conditions	

Terms and Conditions for Permissions

Nature Publishing Group hereby grants you a non-exclusive license to reproduce this material for this purpose,

	
Confirmation Number: 11115682 Order Date: 08/15/2013	
Customer Information	
Customer: Moira Cheung Account Number: 3000685895 Organization: Moira Cheung Email: moira_cheung@doctors.org.uk Phone: +44 2087413045 Payment Method: Invoice	
This not an invoice	
Order Details	
ANNUAL REVIEW OF MATERIALS SCIENCE	
Order detail ID: 63898172 ISSN: 0084-6600 Publication Type: Monographic Series Volume: Issue: Start page: Publisher: ANNUAL REVIEWS, INC.	Permission Status: <input checked="" type="checkbox"/> Granted Permission type: Republish or display content Type of use: Republish in a thesis/dissertation Order License Id: 3210360929805 Order ref number: 1
	Billing Status: N/A
	Requestor type: Academic institution Format: Print, Electronic Portion: image/photo Number of images/photos requested: 1 Title or numeric reference of the portion (s): Figure 1 Title of the article or chapter the portion is from: The sodium Iodide symporter Editor of portion(s): N/A Author of portion(s): N/A Volume of serial or monograph: N/A Issue, if republishing an article from a serial: 1 Page range of portion: NK Publication date of portion: 2009 Rights for: Main product Duration of use: Current edition and up to 5 years Creation of copies for the disabled: no With minor editing privileges: no For distribution to: U.K. and Commonwealth (excluding Canada) In the following language(s): Original language of publication With incidental promotional use: no Lifetime unit quantity of new product: 0 to 499 Made available in the following markets: education Moira Cheung

**ELSEVIER LICENSE
TERMS AND CONDITIONS**

Nov 18, 2013

This is a License Agreement between Moira Cheung ("You") and Elsevier ("Elsevier") provided by Copyright Clearance Center ("CCC"). The license consists of your order details, the terms and conditions provided by Elsevier, and the payment terms and conditions.

All payments must be made in full to CCC. For payment instructions, please see information listed at the bottom of this form.

Supplier	Elsevier Limited The Boulevard, Langford Lane Kidlington, Oxford, OX5 1GB, UK
Registered Company Number	1982084
Customer name	Moira Cheung
Customer address	52 Perrers Road London, W6 0EZ
License number	3271910477712
License date	Nov 18, 2013
Licensed content publisher	Elsevier
Licensed content publication	Molecular and Cellular Endocrinology
Licensed content title	Mechanisms of thyroid hormone receptor-specific nuclear and extra nuclear actions
Licensed content author	J.H. Duncan Bassett, Clare B. Harvey, Graham R. Williams
Licensed content date	31 December 2003
Licensed content volume number	213
Licensed content issue number	1
Number of pages	11
Start Page	1
End Page	11
Type of Use	reuse in a thesis/dissertation
Intended publisher of new work	other
Portion	figures/tables/illustrations
Number of figures/tables/illustrations	1
Format	electronic
Are you the author of this Elsevier article?	No
Will you be translating?	No
Order reference number	fig 1.15
Title of your	oestrogen and thyroid hormone interactions in the regulation of

<https://s100.copyright.com/App/PrintableLicenseFrame.jsp?publisherID=70&pu...> 18/11/2013



[My Orders](#) [My Library](#) [My Profile](#)

Welcome moira_cheung@doctors.org.uk [Log out](#) | [Help](#)

[My Orders](#) > [Orders](#) > All Orders

License Details


This is a License Agreement between Moira Cheung ("You") and Nature Publishing Group ("Nature Publishing Group"). The license consists of your order details, the terms and conditions provided by Nature Publishing Group, and the [payment terms and conditions](#).

[Get the printable license.](#)

License Number	3271910903366
License date	Nov 18, 2013
Licensed content publisher	Nature Publishing Group
Licensed content publication	Nature Reviews Endocrinology
Licensed content title	Thyroid hormone receptors in brain development and function
Licensed content author	Juan Bernal
Licensed content date	Mar 1, 2007
Type of Use	reuse in a dissertation / thesis
Volume number	3
Issue number	3
Requestor type	academic/educational
Format	electronic
Portion	figures/tables/illustrations
Number of figures/tables/illustrations	1
High-res required	no
Figures	Figure 1
Author of this NPG article	no
Your reference number	Fig 1.16
Title of your thesis / dissertation	oestrogen and thyroid hormone interactions in the regulation of bone mass
Expected completion date	Dec 2013
Estimated size (number of pages)	250
Total	0.00 GBP

[← Back](#)

Copyright © 2013 Copyright Clearance Center, Inc. All Rights Reserved. [Privacy statement](#) . Comments? We would like to hear from you. E-mail us at customercare@copyright.com

	
Confirmation Number: 11115698 Order Date: 08/15/2013	
Customer Information	
Customer: Moira Cheung Account Number: 3000685895 Organization: Moira Cheung Email: moira_cheung@doctors.org.uk Phone: +44 2087413045 Payment Method: Invoice	
This not an invoice	
Order Details	
ANNUAL REVIEW OF MATERIALS SCIENCE	
Order detail ID: 63898258 ISSN: 0084-6600 Publication Type: Monographic Series Volume: Issue: Start page: Publisher: ANNUAL REVIEWS, INC.	Permission Status: <input checked="" type="checkbox"/> Granted Permission type: Republish or display content Type of use: Republish in a thesis/dissertation Order License Id: 3210370952591 Requestor type: Academic institution Format: Print, Electronic Portion: image/photo Number of images/photos requested: 1 Title or numeric reference of the portion (s): Figure 8 Title of the article or chapter the portion is from: Ovarian aging: Mechanisms Editor of portion(s): N/A Author of portion(s): N/A Volume of serial or monograph: N/A Issue, if republishing an article from a serial: N/A Page range of portion: N/A Publication date of portion: august 2014 Rights for: Main product Duration of use: Current edition and up to 5 years Creation of copies for the disabled: no With minor editing privileges: no For distribution to: U.K. and Commonwealth (excluding Canada) In the following language(s): Original language of publication With incidental promotional use: no Lifetime unit quantity of new product: 0 to 499 Made available in the following markets: education The requesting person/organization: Moira Cheung
	Billing Status: N/A



1
PAYMENT
2
REVIEW
3
CONFIRMATION

Step 3: Order Confirmation

Thank you for your order! A confirmation for your order will be sent to your account email address. If you have questions about your order, you can call us at +1.877.239.3415 Toll Free, M-F between 3:00 AM and 6:00 PM (Eastern), or write to us at info@copyright.com. This is not an invoice.

Confirmation Number: 11138540
Order Date: 11/18/2013

If you paid by credit card, your order will be finalized and your card will be charged within 24 hours. If you choose to be invoiced, you can change or cancel your order until the invoice is generated.

Payment Information

Moira Cheung
moira_cheung@doctors.org.uk
+44 2087413045
Payment Method: n/a

Order Details

JOURNAL OF CLINICAL INVESTIGATION. ONLINE

<p>Order detail ID: 64157964 Order License Id: 3271930237100 ISSN: 1558-8238 Publication Type: e-Journal Volume: Issue: Start page: Publisher: AMERICAN SOCIETY FOR CLINICAL INVESTIGATION</p>	<p>Permission Status: ✔ Granted Permission type: Republish or display content Type of use: Republish in a thesis/dissertation</p> <p>Requestor type: Academic institution</p> <p>Format: Electronic</p> <p>Portion: chart/graph/table/figure</p> <p>Number of charts/graphs/tables/figures: 1</p> <p>Title or numeric reference of the portion (s): Figure 2</p> <p>Title of the article or chapter the portion is from: Estrogen receptors and human disease</p> <p>Editor of portion(s): NA</p> <p>Author of portion(s): NA</p> <p>Volume of serial or monograph: NA</p> <p>Issue, if republishing an article from a serial: NA</p> <p>Page range of portion: 561-570</p>
--	---

<https://www.copyright.com/printCoiConfirmPurchase.do?operation=defaultOperation...> 18/11/2013

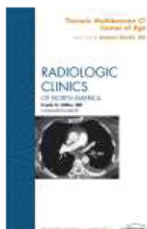


RightsLink®

Home

Account
Info

Help



Title: Physiology of Bone Loss
Author: Bart L. Clarke, Sundeep Khosla
Publication: Radiologic Clinics of North America
Publisher: Elsevier
Date: May 2010
 Copyright © 2010, Elsevier

Logged in as:
 Moira Cheung
 Account #: 3000685895

LOGOUT

Order Completed

Thank you very much for your order.

This is a License Agreement between Moira Cheung ("You") and Elsevier ("Elsevier"). The license consists of your order details, the terms and conditions provided by Elsevier, and the [payment terms and conditions](#).

[Get the printable license.](#)

License Number	3271920404148
License date	Nov 18, 2013
Licensed content publisher	Elsevier
Licensed content publication	Radiologic Clinics of North America
Licensed content title	Physiology of Bone Loss
Licensed content author	Bart L. Clarke, Sundeep Khosla
Licensed content date	May 2010
Licensed content volume number	48
Licensed content issue number	3
Number of pages	13
Type of Use	reuse in a thesis/dissertation
Portion	figures/tables/illustrations
Number of figures/tables/illustrations	1
Format	electronic
Are you the author of this Elsevier article?	No
Will you be translating?	No
Order reference number	Fig 1.2
Title of your thesis/dissertation	oestrogen and thyroid hormone interactions in the regulation of bone mass
Expected completion date	Dec 2013
Estimated size (number of pages)	250
Elsevier VAT number	GB 494 6272 12
Permissions price	0.00 GBP
VAT/Local Sales Tax	0.00 GBP / 0.00 GBP
Total	0.00 GBP

ORDER MORE...

CLOSE WINDOW

Copyright © 2013 Copyright Clearance Center, Inc. All Rights Reserved. [Privacy statement](#).
 Comments? We would like to hear from you. E-mail us at customercare@copyright.com

REFERENCES

- ABE, E., MARIANS, R. C., YU, W., WU, X. B., ANDO, T., LI, Y., IQBAL, J., ELDEIRY, L., RAJENDREN, G., BLAIR, H. C., DAVIES, T. F. & ZAIDI, M. (2003) TSH is a negative regulator of skeletal remodeling. *Cell*, 115, 151-62.
- ABE, S., NAMBA, N., ABE, M., FUJIWARA, M., AIKAWA, T., KOGO, M. & OZONO, K. (2012) Monocarboxylate transporter 10 functions as a thyroid hormone transporter in chondrocytes. *Endocrinology*, 153, 4049-58.
- ABEL, E. D., AHIMA, R. S., BOERS, M. E., ELMQUIST, J. K. & WONDISFORD, F. E. (2001) Critical role for thyroid hormone receptor beta2 in the regulation of paraventricular thyrotropin-releasing hormone neurons. *J Clin Invest*, 107, 1017-23.
- ABU, E. O., HORNER, A., TETI, A., CHATTERJEE, V. K. & COMPSTON, J. E. (2000) The localization of thyroid hormone receptor mRNAs in human bone. *Thyroid*, 10, 287-93.
- ADLER, R. A. (2011) Osteoporosis in men: insights for the clinician. *Ther Adv Musculoskelet Dis*, 3, 191-200.
- ALLAIN, T. J., CHAMBERS, T. J., FLANAGAN, A. M. & MCGREGOR, A. M. (1992) Tri-iodothyronine stimulates rat osteoclastic bone resorption by an indirect effect. *J Endocrinol*, 133, 327-31.
- ALLAIN, T. J., THOMAS, M. R., MCGREGOR, A. M. & SALISBURY, J. R. (1995) A histomorphometric study of bone changes in thyroid dysfunction in rats. *Bone*, 16, 505-9.
- ALOIA, J. F., VASWANI, A., YEH, J. K. & FLASTER, E. (1996) Risk for osteoporosis in black women. *Calcif Tissue Int*, 59, 415-23.
- BALENA, R., MARKATOS, A., GENTILE, M., MASARACHIA, P., SEEDOR, J. G., RODAN, G. A. & YAMAMOTO, M. (1993) The aminobisphosphonate alendronate inhibits bone loss induced by thyroid hormone in the rat. Comparison between effects on tibiae and vertebrae. *Bone*, 14, 499-504.
- BALLOCK, R. T. & REDDI, A. H. (1994) Thyroxine is the serum factor that regulates morphogenesis of columnar cartilage from isolated chondrocytes in chemically defined medium. *J Cell Biol*, 126, 1311-8.
- BARNARD, J. C., WILLIAMS, A. J., RABIER, B., CHASSANDE, O., SAMARUT, J., CHENG, S. Y., BASSETT, J. H. & WILLIAMS, G. R. (2005) Thyroid hormones regulate fibroblast growth factor receptor signaling during chondrogenesis. *Endocrinology*, 146, 5568-80.
- BARON, R. (1999) Anatomy and Ultrastructure of Bone. IN ROSEN, C. J. (Ed.) *Primer on the Metabolic Bone Diseases and Disorders of Mineral Metabolism*. Fourth ed., American Society for Bone and Mineral Research.
- BASSETT, J. H., BOYDE, A., HOWELL, P. G., BASSETT, R. H., GALLIFORD, T. M., ARCHANCO, M., EVANS, H., LAWSON, M. A., CROUCHER, P., ST GERMAIN, D. L., GALTON, V. A. & WILLIAMS, G. R. (2010) Optimal bone strength and mineralization requires the type 2 iodothyronine deiodinase in osteoblasts. *Proc Natl Acad Sci U S A*, 107, 7604-9.
- BASSETT, J. H., NORDSTROM, K., BOYDE, A., HOWELL, P. G., KELLY, S., VENNSTROM, B. & WILLIAMS, G. R. (2007a) Thyroid status during skeletal development determines adult bone structure and mineralization. *Mol Endocrinol*, 21, 1893-904.
- BASSETT, J. H., O'SHEA, P. J., SRISKANTHARAJAH, S., RABIER, B., BOYDE, A., HOWELL, P. G., WEISS, R. E., ROUX, J. P., MALAVAL, L., CLEMENT-LACROIX, P., SAMARUT, J., CHASSANDE, O. & WILLIAMS, G. R. (2007b) Thyroid hormone excess rather than thyrotropin deficiency induces osteoporosis in hyperthyroidism. *Mol Endocrinol*, 21, 1095-107.
- BASSETT, J. H., WILLIAMS, A. J., MURPHY, E., BOYDE, A., HOWELL, P. G., SWINHOE, R., ARCHANCO, M., FLAMANT, F., SAMARUT, J., COSTAGLIOLA, S., VASSART, G., WEISS, R. E., REFETOFF, S. & WILLIAMS, G. R. (2008) A lack of thyroid hormones rather than excess thyrotropin causes abnormal skeletal development in hypothyroidism. *Mol Endocrinol*, 22, 501-12.

-
- BASSETT, J. H. & WILLIAMS, G. R. (2003) The molecular actions of thyroid hormone in bone. *Trends Endocrinol Metab*, 14, 356-64.
- BASSETT, J. H. & WILLIAMS, G. R. (2009) The skeletal phenotypes of TRalpha and TRbeta mutant mice. *J Mol Endocrinol*, 42, 269-82.
- BAUM, J. & BRODSKY, B. (1999) Folding of peptide models of collagen and misfolding in disease. *Curr Opin Struct Biol*, 9, 122-8.
- BENDIXEN, A. C., SHEVDE, N. K., DIENGER, K. M., WILLSON, T. M., FUNK, C. D. & PIKE, J. W. (2001) IL-4 inhibits osteoclast formation through a direct action on osteoclast precursors via peroxisome proliferator-activated receptor gamma 1. *Proc Natl Acad Sci U S A*, 98, 2443-8.
- BERGWITZ, C. & JUPPNER, H. (2010) Regulation of phosphate homeostasis by PTH, vitamin D, and FGF23. *Annu Rev Med*, 61, 91-104.
- BERNAL, J. (2007) Thyroid hormone receptors in brain development and function. *Nat Clin Pract Endocrinol Metab*, 3, 249-59.
- BIANCO, A. C. & KIM, B. W. (2006) Deiodinases: implications of the local control of thyroid hormone action. *J Clin Invest*, 116, 2571-9.
- BIZHANOVA, A. & KOPP, P. (2009) Minireview: The sodium-iodide symporter NIS and pendrin in iodide homeostasis of the thyroid. *Endocrinology*, 150, 1084-90.
- BOCHUKOVA, E., SCHOENMAKERS, N., AGOSTINI, M., SCHOENMAKERS, E., RAJANAYAGAM, O., KEOGH, J. M., HENNING, E., REINEMUND, J., GEVERS, E., SARRI, M., DOWNES, K., OFFIAH, A., ALBANESE, A., HALSALL, D., SCHWABE, J. W., BAIN, M., LINDLEY, K., MUNTONI, F., KHADEM, F. V., DATTANI, M., FAROOQI, I. S., GURNELL, M. & CHATTERJEE, K. (2012) A mutation in the thyroid hormone receptor alpha gene. *N Engl J Med*, 366, 243-9.
- BOCK, O. & FELSENBERG, D. (2008) Bisphosphonates in the management of postmenopausal osteoporosis--optimizing efficacy in clinical practice. *Clin Interv Aging*, 3, 279-97.
- BOIVIN, G. & MEUNIER, P. J. (2002) Changes in bone remodeling rate influence the degree of mineralization of bone. *Connect Tissue Res*, 43, 535-7.
- BONEWALD, L. F. (2011) The amazing osteocyte. *J Bone Miner Res*, 26, 229-38.
- BOOKOUT, A. L., JEONG, Y., DOWNES, M., YU, R. T., EVANS, R. M. & MANGELSDORF, D. J. (2006) Anatomical profiling of nuclear receptor expression reveals a hierarchical transcriptional network. *Cell*, 126, 789-99.
- BORD, S., HORNER, A., BEAVAN, S. & COMPSTON, J. (2001) Estrogen receptors alpha and beta are differentially expressed in developing human bone. *J Clin Endocrinol Metab*, 86, 2309-14.
- BORJESSON, A. E., LAGERQUIST, M. K., LIU, C., SHAO, R., WINDAHL, S. H., KARLSSON, C., SJOGREN, K., MOVERARE-SKRTIC, S., ANTAL, M. C., KRUST, A., MOHAN, S., CHAMBON, P., SAVENDAHL, L. & OHLSSON, C. (2010) The role of estrogen receptor alpha in growth plate cartilage for longitudinal bone growth. *J Bone Miner Res*, 25, 2690-700.
- BOUILLON, R., BEX, M., VANDERSCHUEREN, D. & BOONEN, S. (2004) Estrogens are essential for male pubertal periosteal bone expansion. *J Clin Endocrinol Metab*, 89, 6025-9.
- BOUXSEIN, M. L., MYERS, K. S., SHULTZ, K. L., DONAHUE, L. R., ROSEN, C. J. & BEAMER, W. G. (2005) Ovariectomy-induced bone loss varies among inbred strains of mice. *J Bone Miner Res*, 20, 1085-92.
- BOYLE, W. J., SIMONET, W. S. & LACEY, D. L. (2003) Osteoclast differentiation and activation. *Nature*, 423, 337-42.
- BRAIDMAN, I. P., HOYLAND, J. A. & SELBY, P. (2001) Comment on "estrogen receptors alpha and beta are differentially expressed in developing bone". *J Clin Endocrinol Metab*, 86, 5640.
- BRAUN, D., WIRTH, E. K., WOHLGEMUTH, F., REIX, N., KLEIN, M. O., GRUTERS, A., KOHRLE, J. & SCHWEIZER, U. (2011) Aminoaciduria, but normal thyroid hormone levels and signalling, in mice lacking the amino acid and thyroid hormone transporter Slc7a8. *Biochem J*, 439, 249-55.
- BROEKMANS, F. J., SOULES, M. R. & FAUSER, B. C. (2009) Ovarian aging: mechanisms and clinical consequences. *Endocr Rev*, 30, 465-93.

-
- BRUZZANITI, A. & BARON, R. (2006) Molecular regulation of osteoclast activity. *Rev Endocr Metab Disord*, 7, 123-39.
- BURCH, W. M. & VAN WYK, J. J. (1987) Triiodothyronine stimulates cartilage growth and maturation by different mechanisms. *Am J Physiol*, 252, E176-82.
- CAPELO, L. P., BEBER, E. H., HUANG, S. A., ZORN, T. M., BIANCO, A. C. & GOUVEIA, C. H. (2008) Deiodinase-mediated thyroid hormone inactivation minimizes thyroid hormone signaling in the early development of fetal skeleton. *Bone*, 43, 921-30.
- CARANI, C., QIN, K., SIMONI, M., FAUSTINI-FUSTINI, M., SERPENTE, S., BOYD, J., KORACH, K. S. & SIMPSON, E. R. (1997) Effect of testosterone and estradiol in a man with aromatase deficiency. *N Engl J Med*, 337, 91-5.
- CHANG, M. C. (1966) Transport of eggs from the fallopian tube to the uterus as a function of oestrogen. *Nature*, 212, 1048-9.
- CHANG, M. K., RAGGATT, L. J., ALEXANDER, K. A., KULIWABA, J. S., FAZZALARI, N. L., SCHRODER, K., MAYLIN, E. R., RIPOLL, V. M., HUME, D. A. & PETTIT, A. R. (2008) Osteal tissue macrophages are intercalated throughout human and mouse bone lining tissues and regulate osteoblast function in vitro and in vivo. *J Immunol*, 181, 1232-44.
- CHASSANDE, O., FRAICHARD, A., GAUTHIER, K., FLAMANT, F., LEGRAND, C., SAVATIER, P., LAUDET, V. & SAMARUT, J. (1997) Identification of transcripts initiated from an internal promoter in the c-erbA alpha locus that encode inhibitors of retinoic acid receptor-alpha and triiodothyronine receptor activities. *Mol Endocrinol*, 11, 1278-90.
- CHATTERJEE, V. K., LEE, J. K., RENTOUMIS, A. & JAMESON, J. L. (1989) Negative regulation of the thyroid-stimulating hormone alpha gene by thyroid hormone: receptor interaction adjacent to the TATA box. *Proc Natl Acad Sci U S A*, 86, 9114-8.
- CHENG, S. Y. (2000) Multiple mechanisms for regulation of the transcriptional activity of thyroid hormone receptors. *Rev Endocr Metab Disord*, 1, 9-18.
- CHENG, S. Y., LEONARD, J. L. & DAVIS, P. J. (2010) Molecular aspects of thyroid hormone actions. *Endocr Rev*, 31, 139-70.
- CHEUNG, M. S., AGOGAKOS, A. I., BASSETT, J. H. & WILLIAMS, G. R. (2011) Thyroid disorders and bone disease. IN J.A.H., W. & STEWART, P. M. (Eds.) *Oxford Textbook of Endocrinology and Diabetes*. Second ed.
- CLARKE, B. L. & KHOSLA, S. (2010a) Female reproductive system and bone. *Arch Biochem Biophys*, 503, 118-28.
- CLARKE, B. L. & KHOSLA, S. (2010b) Physiology of bone loss. *Radiol Clin North Am*, 48, 483-95.
- CLOWES, J. A., RIGGS, B. L. & KHOSLA, S. (2005) The role of the immune system in the pathophysiology of osteoporosis. *Immunol Rev*, 208, 207-27.
- CONTI, M. I., MARTINEZ, M. P., OLIVERA, M. I., BOZZINI, C., MANDALUNIS, P., BOZZINI, C. E. & ALIPPI, R. M. (2009) Biomechanical performance of diaphyseal shafts and bone tissue of femurs from hypothyroid rats. *Endocrine*, 36, 291-8.
- COOPER, C. & MELTON, L. J., 3RD (1992) Epidemiology of osteoporosis. *Trends Endocrinol Metab*, 3, 224-9.
- COUPLAND, C. A., CLIFFE, S. J., BASSEY, E. J., GRAINGE, M. J., HOSKING, D. J. & CHILVERS, C. E. (1999) Habitual physical activity and bone mineral density in postmenopausal women in England. *Int J Epidemiol*, 28, 241-6.
- DAY, T. F., GUO, X., GARRETT-BEAL, L. & YANG, Y. (2005) Wnt/beta-catenin signaling in mesenchymal progenitors controls osteoblast and chondrocyte differentiation during vertebrate skeletogenesis. *Dev Cell*, 8, 739-50.
- DE RYCK, L. M., ROSS, J. B., PETRA, P. H. & GURPIDE, E. (1985) Estradiol entry into endometrial cells in suspension. *J Steroid Biochem*, 23, 145-52.
- DENNISON, E. & COOPER, C. (2011) Osteoporosis in 2010: building bones and (safely) preventing breaks. *Nat Rev Rheumatol*, 7, 80-2.

-
- DENTICE, M., BANDYOPADHYAY, A., GEREBEN, B., CALLEBAUT, I., CHRISTOFFOLETE, M. A., KIM, B. W., NISSIM, S., MORNON, J. P., ZAVACKI, A. M., ZEOLD, A., CAPELO, L. P., CURCIO-MORELLI, C., RIBEIRO, R., HARNEY, J. W., TABIN, C. J. & BIANCO, A. C. (2005) The Hedgehog-inducible ubiquitin ligase subunit WSB-1 modulates thyroid hormone activation and PTHrP secretion in the developing growth plate. *Nat Cell Biol*, 7, 698-705.
- DEQUEANT, M. L., GLYNN, E., GAUDENZ, K., WAHL, M., CHEN, J., MUSHEGIAN, A. & POURQUIE, O. (2006) A complex oscillating network of signaling genes underlies the mouse segmentation clock. *Science*, 314, 1595-8.
- DEQUEKER, J., NIJS, J., VERSTRAETEN, A., GEUSENS, P. & GEVERS, G. (1987) Genetic determinants of bone mineral content at the spine and radius: a twin study. *Bone*, 8, 207-9.
- DEROO, B. J. & KORACH, K. S. (2006) Estrogen receptors and human disease. *J Clin Invest*, 116, 561-70.
- DODD, J. S., RALEIGH, J. A. & GROSS, T. S. (1999) Osteocyte hypoxia: a novel mechanotransduction pathway. *Am J Physiol*, 277, C598-602.
- DOUBE, M., FIRTH, E. C. & BOYDE, A. (2007) Variations in articular calcified cartilage by site and exercise in the 18-month-old equine distal metacarpal condyle. *Osteoarthritis Cartilage*, 15, 1283-92.
- DRAKE, M. T., MCCREADY, L. K., HOEY, K. A., ATKINSON, E. J. & KHOSLA, S. (2010) Effects of suppression of follicle-stimulating hormone secretion on bone resorption markers in postmenopausal women. *J Clin Endocrinol Metab*, 95, 5063-8.
- DUCY, P., AMLING, M., TAKEDA, S., PRIEMEL, M., SCHILLING, A. F., BEIL, F. T., SHEN, J., VINSON, C., RUEGER, J. M. & KARSENTY, G. (2000) Leptin inhibits bone formation through a hypothalamic relay: a central control of bone mass. *Cell*, 100, 197-207.
- DUPONT, S., KRUST, A., GANSMULLER, A., DIERICH, A., CHAMBON, P. & MARK, M. (2000) Effect of single and compound knockouts of estrogen receptors alpha (ERalpha) and beta (ERbeta) on mouse reproductive phenotypes. *Development*, 127, 4277-91.
- EBELING, P. R., ATLEY, L. M., GUTHRIE, J. R., BURGER, H. G., DENNERSTEIN, L., HOPPER, J. L. & WARK, J. D. (1996) Bone turnover markers and bone density across the menopausal transition. *J Clin Endocrinol Metab*, 81, 3366-71.
- EGERMANN, M., GOLDHAHN, J. & SCHNEIDER, E. (2005) Animal models for fracture treatment in osteoporosis. *Osteoporos Int*, 16 Suppl 2, S129-38.
- EGHBALI-FATOURECHI, G., KHOSLA, S., SANYAL, A., BOYLE, W. J., LACEY, D. L. & RIGGS, B. L. (2003) Role of RANK ligand in mediating increased bone resorption in early postmenopausal women. *J Clin Invest*, 111, 1221-30.
- ELEFTERIOU, F., AHN, J. D., TAKEDA, S., STARBUCK, M., YANG, X., LIU, X., KONDO, H., RICHARDS, W. G., BANNON, T. W., NODA, M., CLEMENT, K., VAISSE, C. & KARSENTY, G. (2005) Leptin regulation of bone resorption by the sympathetic nervous system and CART. *Nature*, 434, 514-20.
- EMERTON, K. B., HU, B., WOO, A. A., SINOFSKY, A., HERNANDEZ, C., MAJESKA, R. J., JEPSEN, K. J. & SCHAFFLER, M. B. (2010) Osteocyte apoptosis and control of bone resorption following ovariectomy in mice. *Bone*, 46, 577-83.
- EMONS, J., CHAGIN, A. S., MALMLOF, T., LEKMAN, M., TIVESTEN, A., OHLSSON, C., WIT, J. M., KARPARIEN, M. & SAVENDAHL, L. (2010) Expression of vascular endothelial growth factor in the growth plate is stimulated by estradiol and increases during pubertal development. *J Endocrinol*, 205, 61-8.
- ENOMOTO, H., SHIOJIRI, S., HOSHI, K., FURUICHI, T., FUKUYAMA, R., YOSHIDA, C. A., KANATANI, N., NAKAMURA, R., MIZUNO, A., ZANMA, A., YANO, K., YASUDA, H., HIGASHIO, K., TAKADA, K. & KOMORI, T. (2003) Induction of osteoclast differentiation by Runx2 through receptor activator of nuclear factor-kappa B ligand (RANKL) and osteoprotegerin regulation and partial rescue of osteoclastogenesis in Runx2^{-/-} mice by RANKL transgene. *J Biol Chem*, 278, 23971-7.

-
- ERIKSEN, E. F. (1986) Normal and pathological remodeling of human trabecular bone: three dimensional reconstruction of the remodeling sequence in normals and in metabolic bone disease. *Endocr Rev*, 7, 379-408.
- ERIKSEN, E. F., MOSEKILDE, L. & MELSEN, F. (1986) Kinetics of trabecular bone resorption and formation in hypothyroidism: evidence for a positive balance per remodeling cycle. *Bone*, 7, 101-8.
- ESTRADA, K., STYRKARSDOTTIR, U., EVANGELOU, E., HSU, Y. H., DUNCAN, E. L., NTZANI, E. E., OEI, L., ALBAGHA, O. M., AMIN, N., KEMP, J. P., KOLLER, D. L., LI, G., LIU, C. T., MINSTER, R. L., MOAYYERI, A., VANDENPUT, L., WILLNER, D., XIAO, S. M., YERGES-ARMSTRONG, L. M., ZHENG, H. F., ALONSO, N., ERIKSSON, J., KAMMERER, C. M., KAPTOGE, S. K., LEO, P. J., THORLEIFSSON, G., WILSON, S. G., WILSON, J. F., AALTO, V., ALEN, M., ARAGAKI, A. K., ASPELUND, T., CENTER, J. R., DAILIANA, Z., DUGGAN, D. J., GARCIA, M., GARCIA-GIRALT, N., GIROUX, S., HALLMANS, G., HOCKING, L. J., HUSTED, L. B., JAMESON, K. A., KHUSAINOVA, R., KIM, G. S., KOOPERBERG, C., KOROMILA, T., KRUK, M., LAAKSONEN, M., LACROIX, A. Z., LEE, S. H., LEUNG, P. C., LEWIS, J. R., MASI, L., MENCEJ-BEDRAC, S., NGUYEN, T. V., NOGUES, X., PATEL, M. S., PREZELJ, J., ROSE, L. M., SCOLLEN, S., SIGGEIRSDOTTIR, K., SMITH, A. V., SVENSSON, O., TROMPET, S., TRUMMER, O., VAN SCHOOR, N. M., WOO, J., ZHU, K., BALCELLS, S., BRANDI, M. L., BUCKLEY, B. M., CHENG, S., CHRISTIANSEN, C., COOPER, C., DEDOISSIS, G., FORD, I., FROST, M., GOLTZMAN, D., GONZALEZ-MACIAS, J., KAHONEN, M., KARLSSON, M., KHUSNUTDINOVA, E., KOH, J. M., KOLLIA, P., LANGDAHL, B. L., LESLIE, W. D., LIPS, P., LJUNGGREN, O., LORENC, R. S., MARC, J., MELLSTROM, D., OBERMAYER-PIETSCH, B., OLMOS, J. M., PETERSSON-KYMMER, U., REID, D. M., RIANCHO, J. A., RIDKER, P. M., ROUSSEAU, F., SLAGBOOM, P. E., TANG, N. L., et al. (2012) Genome-wide meta-analysis identifies 56 bone mineral density loci and reveals 14 loci associated with risk of fracture. *Nat Genet*, 44, 491-501.
- FALAHATI-NINI, A., RIGGS, B. L., ATKINSON, E. J., O'FALLON, W. M., EASTELL, R. & KHOSLA, S. (2000) Relative contributions of testosterone and estrogen in regulating bone resorption and formation in normal elderly men. *J Clin Invest*, 106, 1553-60.
- FELL, H. B. & MELLANBY, E. (1955) The biological action of thyroxine on embryonic bones grown in tissue culture. *J Physiol*, 127, 427-47.
- FILARDO, E. J. & THOMAS, P. (2012) Minireview: G protein-coupled estrogen receptor-1, GPER-1: its mechanism of action and role in female reproductive cancer, renal and vascular physiology. *Endocrinology*, 153, 2953-62.
- FLAMANT, F., POGUET, A. L., PLATEROTI, M., CHASSANDE, O., GAUTHIER, K., STREICHENBERGER, N., MANSOURI, A. & SAMARUT, J. (2002) Congenital hypothyroid Pax8(-/-) mutant mice can be rescued by inactivating the TRalpha gene. *Mol Endocrinol*, 16, 24-32.
- FLOURIOT, G., BRAND, H., DENGEL, S., METIVIER, R., KOS, M., REID, G., SONNTAG-BUCK, V. & GANNON, F. (2000) Identification of a new isoform of the human estrogen receptor-alpha (hER-alpha) that is encoded by distinct transcripts and that is able to repress hER-alpha activation function 1. *Embo J*, 19, 4688-700.
- FLOURIOT, G., GRIFFIN, C., KENEALY, M., SONNTAG-BUCK, V. & GANNON, F. (1998) Differentially expressed messenger RNA isoforms of the human estrogen receptor-alpha gene are generated by alternative splicing and promoter usage. *Mol Endocrinol*, 12, 1939-54.
- FORREST, D., HANEBUTH, E., SMEYNE, R. J., EVERDS, N., STEWART, C. L., WEHNER, J. M. & CURRAN, T. (1996) Recessive resistance to thyroid hormone in mice lacking thyroid hormone receptor beta: evidence for tissue-specific modulation of receptor function. *Embo J*, 15, 3006-15.
- FORREST, D., SJOBERG, M. & VENNSTROM, B. (1990) Contrasting developmental and tissue-specific expression of alpha and beta thyroid hormone receptor genes. *Embo J*, 9, 1519-28.
- FOZZATTI, L., KIM, D. W., PARK, J. W., WILLINGHAM, M. C., HOLLENBERG, A. N. & CHENG, S. Y. (2013) Nuclear receptor corepressor (NCOR1) regulates in vivo actions of a mutated thyroid hormone receptor alpha. *Proc Natl Acad Sci U S A*, 110, 7850-5.

-
- GALTON, V. A., SCHNEIDER, M. J., CLARK, A. S. & ST GERMAIN, D. L. (2009) Life without thyroxine to 3,5,3'-triiodothyronine conversion: studies in mice devoid of the 5'-deiodinases. *Endocrinology*, 150, 2957-63.
- GAO, J., TIWARI-PANDEY, R., SAMADFAM, R., YANG, Y., MIAO, D., KARAPLIS, A. C., SAIRAM, M. R. & GOLTZMAN, D. (2007a) Altered ovarian function affects skeletal homeostasis independent of the action of follicle-stimulating hormone. *Endocrinology*, 148, 2613-21.
- GAO, Y., GRASSI, F., RYAN, M. R., TERAUCHI, M., PAGE, K., YANG, X., WEITZMANN, M. N. & PACIFICI, R. (2007b) IFN-gamma stimulates osteoclast formation and bone loss in vivo via antigen-driven T cell activation. *J Clin Invest*, 117, 122-32.
- GAUTHIER, A., KANIS, J. A., JIANG, Y., MARTIN, M., COMPSTON, J. E., BORGSTROM, F., COOPER, C. & MCCLOSKEY, E. V. (2011) Epidemiological burden of postmenopausal osteoporosis in the UK from 2010 to 2021: estimations from a disease model. *Arch Osteoporos*, 6, 179-88.
- GAUTHIER, K., CHASSANDE, O., PLATEROTI, M., ROUX, J. P., LEGRAND, C., PAIN, B., ROUSSET, B., WEISS, R., TROUILLAS, J. & SAMARUT, J. (1999) Different functions for the thyroid hormone receptors TRalpha and TRbeta in the control of thyroid hormone production and post-natal development. *Embo J*, 18, 623-31.
- GAUTHIER, K., PLATEROTI, M., HARVEY, C. B., WILLIAMS, G. R., WEISS, R. E., REFETTOFF, S., WILLOTT, J. F., SUNDIN, V., ROUX, J. P., MALAVAL, L., HARA, M., SAMARUT, J. & CHASSANDE, O. (2001) Genetic analysis reveals different functions for the products of the thyroid hormone receptor alpha locus. *Mol Cell Biol*, 21, 4748-60.
- GENNARI, L., MASI, L., MERLOTTI, D., PICARIELLO, L., FALCHETTI, A., TANINI, A., MAVILIA, C., DEL MONTE, F., GONNELLI, S., LUCANI, B., GENNARI, C. & BRANDI, M. L. (2004) A polymorphic CYP19 TTTA repeat influences aromatase activity and estrogen levels in elderly men: effects on bone metabolism. *J Clin Endocrinol Metab*, 89, 2803-10.
- GEOFFROY, V., KNEISSEL, M., FOURNIER, B., BOYDE, A. & MATTHIAS, P. (2002) High bone resorption in adult aging transgenic mice overexpressing cbfa1/runx2 in cells of the osteoblastic lineage. *Mol Cell Biol*, 22, 6222-33.
- GEVERS, E. F., WIT, J. M. & ROBINSON, I. C. (1995) Effect of gonadectomy on growth and GH responsiveness in dwarf rats. *J Endocrinol*, 145, 69-79.
- GILBERT (2006) *Developmental Biology*, Sinauer.
- GLASS, C. K., LIPKIN, S. M., DEVARY, O. V. & ROSENFELD, M. G. (1989) Positive and negative regulation of gene transcription by a retinoic acid-thyroid hormone receptor heterodimer. *Cell*, 59, 697-708.
- GLASS, D. A., 2ND & KARSENTY, G. (2007) In vivo analysis of Wnt signaling in bone. *Endocrinology*, 148, 2630-4.
- GOTHE, S., WANG, Z., NG, L., KINDBLOM, J. M., BARROS, A. C., OHLSSON, C., VENNSTROM, B. & FORREST, D. (1999) Mice devoid of all known thyroid hormone receptors are viable but exhibit disorders of the pituitary-thyroid axis, growth, and bone maturation. *Genes Dev*, 13, 1329-41.
- GOUVEIA, C. H., SCHULTZ, J. J., BIANCO, A. C. & BRENT, G. A. (2001) Thyroid hormone stimulation of osteocalcin gene expression in ROS 17/2.8 cells is mediated by transcriptional and post-transcriptional mechanisms. *J Endocrinol*, 170, 667-75.
- GRASBERGER, H., DE DEKEN, X., MAYO, O. B., RAAD, H., WEISS, M., LIAO, X. H. & REFETTOFF, S. (2012) Mice deficient in dual oxidase maturation factors are severely hypothyroid. *Mol Endocrinol*, 26, 481-92.
- HARADA, S. & RODAN, G. A. (2003) Control of osteoblast function and regulation of bone mass. *Nature*, 423, 349-55.
- HARTMANN, C. (2006) A Wnt canon orchestrating osteoblastogenesis. *Trends Cell Biol*, 16, 151-8.
- HARVEY, C. B. & WILLIAMS, G. R. (2002) Mechanism of thyroid hormone action. *Thyroid*, 12, 441-6.
- HARVEY, N., DENNISON, E. & COOPER, C. (2010) Osteoporosis: impact on health and economics. *Nat Rev Rheumatol*, 6, 99-105.

-
- HASHIMOTO, K., CURTY, F. H., BORGES, P. P., LEE, C. E., ABEL, E. D., ELMQUIST, J. K., COHEN, R. N. & WONDISFORD, F. E. (2001) An unliganded thyroid hormone receptor causes severe neurological dysfunction. *Proc Natl Acad Sci U S A*, 98, 3998-4003.
- HENS, J. R., WILSON, K. M., DANN, P., CHEN, X., HOROWITZ, M. C. & WYSOLMERSKI, J. J. (2005) TOPGAL mice show that the canonical Wnt signaling pathway is active during bone development and growth and is activated by mechanical loading in vitro. *J Bone Miner Res*, 20, 1103-13.
- HERNANDEZ, A., MARTINEZ, M. E., FIERING, S., GALTON, V. A. & ST GERMAIN, D. (2006) Type 3 deiodinase is critical for the maturation and function of the thyroid axis. *J Clin Invest*, 116, 476-84.
- HERO, M., NORJAVAARA, E. & DUNKEL, L. (2005) Inhibition of estrogen biosynthesis with a potent aromatase inhibitor increases predicted adult height in boys with idiopathic short stature: a randomized controlled trial. *J Clin Endocrinol Metab*, 90, 6396-402.
- HEUER, H. & VISSER, T. J. (2012) The pathophysiological consequences of thyroid hormone transporter deficiencies: Insights from mouse models. *Biochim Biophys Acta*.
- HIDESHIMA, T., CHAUHAN, D., PODAR, K., SCHLOSSMAN, R. L., RICHARDSON, P. & ANDERSON, K. C. (2001) Novel therapies targeting the myeloma cell and its bone marrow microenvironment. *Semin Oncol*, 28, 607-12.
- HOFBAUER, L. C., KHOSLA, S., DUNSTAN, C. R., LACEY, D. L., SPELSBERG, T. C. & RIGGS, B. L. (1999) Estrogen stimulates gene expression and protein production of osteoprotegerin in human osteoblastic cells. *Endocrinology*, 140, 4367-70.
- HOLMEN, S. L., ZYLSTRA, C. R., MUKHERJEE, A., SIGLER, R. E., FAUGERE, M. C., BOUXSEIN, M. L., DENG, L., CLEMENS, T. L. & WILLIAMS, B. O. (2005) Essential role of beta-catenin in postnatal bone acquisition. *J Biol Chem*, 280, 21162-8.
- HSU, H., LACEY, D. L., DUNSTAN, C. R., SOLOVYEV, I., COLOMBERO, A., TIMMS, E., TAN, H. L., ELLIOTT, G., KELLEY, M. J., SAROSI, I., WANG, L., XIA, X. Z., ELLIOTT, R., CHIU, L., BLACK, T., SCULLY, S., CAPPARELLI, C., MORONY, S., SHIMAMOTO, G., BASS, M. B. & BOYLE, W. J. (1999) Tumor necrosis factor receptor family member RANK mediates osteoclast differentiation and activation induced by osteoprotegerin ligand. *Proc Natl Acad Sci U S A*, 96, 3540-5.
- HUBER, D. M., BENDIXEN, A. C., PATHROSE, P., SRIVASTAVA, S., DIENGER, K. M., SHEVDE, N. K. & PIKE, J. W. (2001) Androgens suppress osteoclast formation induced by RANKL and macrophage-colony stimulating factor. *Endocrinology*, 142, 3800-8.
- IMAI, Y., KONDOH, S., KOUZMENKO, A. & KATO, S. (2009) Regulation of bone metabolism by nuclear receptors. *Mol Cell Endocrinol*, 310, 3-10.
- IWANIEC, U. T., YUAN, D., POWER, R. A. & WRONSKI, T. J. (2006) Strain-dependent variations in the response of cancellous bone to ovariectomy in mice. *J Bone Miner Res*, 21, 1068-74.
- JEE, W. S. & YAO, W. (2001) Overview: animal models of osteopenia and osteoporosis. *J Musculoskelet Neuronal Interact*, 1, 193-207.
- JOHNSON, M. L. & KAMEL, M. A. (2007) The Wnt signaling pathway and bone metabolism. *Curr Opin Rheumatol*, 19, 376-82.
- JUUL, A. (2001) The effects of oestrogens on linear bone growth. *Hum Reprod Update*, 7, 303-13.
- KANATANI, M., SUGIMOTO, T., SOWA, H., KOBAYASHI, T., KANZAWA, M. & CHIHARA, K. (2004) Thyroid hormone stimulates osteoclast differentiation by a mechanism independent of RANKL-RANK interaction. *J Cell Physiol*, 201, 17-25.
- KANESHIGE, M., KANESHIGE, K., ZHU, X., DACE, A., GARRETT, L., CARTER, T. A., KAZLAUSKAITE, R., PANKRATZ, D. G., WYNSHAW-BORIS, A., REFETOFF, S., WEINTRAUB, B., WILLINGHAM, M. C., BARLOW, C. & CHENG, S. (2000) Mice with a targeted mutation in the thyroid hormone beta receptor gene exhibit impaired growth and resistance to thyroid hormone. *Proc Natl Acad Sci U S A*, 97, 13209-14.
- KANESHIGE, M., SUZUKI, H., KANESHIGE, K., CHENG, J., WIMBROW, H., BARLOW, C., WILLINGHAM, M. C. & CHENG, S. (2001) A targeted dominant negative mutation of the thyroid hormone

-
- alpha 1 receptor causes increased mortality, infertility, and dwarfism in mice. *Proc Natl Acad Sci U S A*, 98, 15095-100.
- KANIS, J. A., BORGSTROM, F., DE LAET, C., JOHANSSON, H., JOHNELL, O., JONSSON, B., ODEN, A., ZETHRAEUS, N., PFLEGER, B. & KHALTAEV, N. (2005a) Assessment of fracture risk. *Osteoporos Int*, 16, 581-9.
- KANIS, J. A., JOHNELL, O., ODEN, A., JOHANSSON, H., DE LAET, C., EISMAN, J. A., FUJIWARA, S., KROGER, H., MCCLOSKEY, E. V., MELLSTROM, D., MELTON, L. J., POLS, H., REEVE, J., SILMAN, A. & TENENHOUSE, A. (2005b) Smoking and fracture risk: a meta-analysis. *Osteoporos Int*, 16, 155-62.
- KARAGUZEL, G. & HOLICK, M. F. (2010) Diagnosis and treatment of osteopenia. *Rev Endocr Metab Disord*, 11, 237-51.
- KARAS, R. H., BAUR, W. E., VAN EICKLES, M. & MENDELSON, M. E. (1995) Human vascular smooth muscle cells express an estrogen receptor isoform. *FEBS Lett*, 377, 103-8.
- KARSENTY, G. (2006) Convergence between bone and energy homeostases: leptin regulation of bone mass. *Cell Metab*, 4, 341-8.
- KHOSLA, S., MELTON, L. J., 3RD, ATKINSON, E. J., O'FALLON, W. M., KLEE, G. G. & RIGGS, B. L. (1998) Relationship of serum sex steroid levels and bone turnover markers with bone mineral density in men and women: a key role for bioavailable estrogen. *J Clin Endocrinol Metab*, 83, 2266-74.
- KHOSLA, S., MELTON, L. J., 3RD & RIGGS, B. L. (2011) The unitary model for estrogen deficiency and the pathogenesis of osteoporosis: is a revision needed? *J Bone Miner Res*, 26, 441-51.
- KHOSLA, S., OURSLER, M. J. & MONROE, D. G. (2012) Estrogen and the skeleton. *Trends Endocrinol Metab*.
- KHOSLA, S., RIGGS, B. L., ATKINSON, E. J., OBERG, A. L., MCDANIEL, L. J., HOLETS, M., PETERSON, J. M. & MELTON, L. J., 3RD (2006) Effects of sex and age on bone microstructure at the ultradistal radius: a population-based noninvasive in vivo assessment. *J Bone Miner Res*, 21, 124-31.
- KIMBLE, R. B., SRIVASTAVA, S., ROSS, F. P., MATAYOSHI, A. & PACIFICI, R. (1996) Estrogen deficiency increases the ability of stromal cells to support murine osteoclastogenesis via an interleukin-1 and tumor necrosis factor-mediated stimulation of macrophage colony-stimulating factor production. *J Biol Chem*, 271, 28890-7.
- KLINGE, C. M. (2001) Estrogen receptor interaction with estrogen response elements. *Nucleic Acids Res*, 29, 2905-19.
- KLINGE, C. M., JERNIGAN, S. C., MATTINGLY, K. A., RISINGER, K. E. & ZHANG, J. (2004) Estrogen response element-dependent regulation of transcriptional activation of estrogen receptors alpha and beta by coactivators and corepressors. *J Mol Endocrinol*, 33, 387-410.
- KRAUSE, C. (2008) Signal Transduction Cascades Controlling Osteoblast Differentiation. IN ROSEN, C. (Ed.) *Primer on the Metabolic Bone Diseases and Disorders of Mineral Metabolism*. Seventh ed., ASBMR.
- KREGE, J. H., HODGIN, J. B., COUSE, J. F., ENMARK, E., WARNER, M., MAHLER, J. F., SAR, M., KORACH, K. S., GUSTAFSSON, J. A. & SMITHIES, O. (1998) Generation and reproductive phenotypes of mice lacking estrogen receptor beta. *Proc Natl Acad Sci U S A*, 95, 15677-82.
- KRONENBERG, H. M. (2003) Developmental regulation of the growth plate. *Nature*, 423, 332-6.
- KRUM, S. A., MIRANDA-CARBONI, G. A., HAUSCHKA, P. V., CARROLL, J. S., LANE, T. F., FREEDMAN, L. P. & BROWN, M. (2008) Estrogen protects bone by inducing Fas ligand in osteoblasts to regulate osteoclast survival. *Embo J*, 27, 535-45.
- KUIPER, G. G., CARLSSON, B., GRANDIEN, K., ENMARK, E., HAGGBLAD, J., NILSSON, S. & GUSTAFSSON, J. A. (1997) Comparison of the ligand binding specificity and transcript tissue distribution of estrogen receptors alpha and beta. *Endocrinology*, 138, 863-70.
- KULAR, J., TICKNER, J., CHIM, S. M. & XU, J. (2012) An overview of the regulation of bone remodelling at the cellular level. *Clin Biochem*, 45, 863-73.

-
- LANFRANCO, F., ZIRILLI, L., BALDI, M., PIGNATTI, E., CORNELI, G., GHIGO, E., AIMARETTI, G., CARANI, C. & ROCHIRA, V. (2008) A novel mutation in the human aromatase gene: insights on the relationship among serum estradiol, longitudinal growth and bone mineral density in an adult man under estrogen replacement treatment. *Bone*, 43, 628-35.
- LANGER, G., BADER, B., MEOLI, L., ISENSEE, J., DELBECK, M., NOPPINGER, P. R. & OTTO, C. (2010) A critical review of fundamental controversies in the field of GPR30 research. *Steroids*, 75, 603-10.
- LANHAM, S. A., FOWDEN, A. L., ROBERTS, C., COOPER, C., OREFFO, R. O. & FORHEAD, A. J. (2011) Effects of hypothyroidism on the structure and mechanical properties of bone in the ovine fetus. *J Endocrinol*, 210, 189-98.
- LAW, M. R. & HACKSHAW, A. K. (1997) A meta-analysis of cigarette smoking, bone mineral density and risk of hip fracture: recognition of a major effect. *Bmj*, 315, 841-6.
- LAZAR, M. A. (1993) Thyroid hormone receptors: multiple forms, multiple possibilities. *Endocr Rev*, 14, 184-93.
- LEVIN, E. R. (2009) Plasma membrane estrogen receptors. *Trends Endocrinol Metab*, 20, 477-82.
- LINDBERG, M. K., WEIHUA, Z., ANDERSSON, N., MOVERARE, S., GAO, H., VIDAL, O., ERLANDSSON, M., WINDAHL, S., ANDERSSON, G., LUBAHN, D. B., CARLSTEN, H., DAHLMAN-WRIGHT, K., GUSTAFSSON, J. A. & OHLSSON, C. (2002) Estrogen receptor specificity for the effects of estrogen in ovariectomized mice. *J Endocrinol*, 174, 167-78.
- LIU, Y. Y., SCHULTZ, J. J. & BRENT, G. A. (2003) A thyroid hormone receptor alpha gene mutation (P398H) is associated with visceral adiposity and impaired catecholamine-stimulated lipolysis in mice. *J Biol Chem*, 278, 38913-20.
- LO IACONO, N., BLAIR, H. C., POLIANI, P. L., MARRELLA, V., FICARA, F., CASSANI, B., FACCHETTI, F., FONTANA, E., GUERRINI, M. M., TRAGGIALI, E., SCHENA, F., PAULIS, M., MANTERO, S., INFORZATO, A., VALAPERTA, S., PANGRAZIO, A., CRISAFULLI, L., MAINA, V., KOSTENUIK, P., VEZZONI, P., VILLA, A. & SOBACCHI, C. (2012) Osteopetrosis rescue upon RANKL administration to Rankl(-/-) mice: a new therapy for human RANKL-dependent ARO. *J Bone Miner Res*, 27, 2501-10.
- LORENZO, J. A., NAPRTA, A., RAO, Y., ALANDER, C., GLACCUM, M., WIDMER, M., GRONOWICZ, G., KALINOWSKI, J. & PILBEAM, C. C. (1998) Mice lacking the type I interleukin-1 receptor do not lose bone mass after ovariectomy. *Endocrinology*, 139, 3022-5.
- MACCHIA, P. E., TAKEUCHI, Y., KAWAI, T., CUA, K., GAUTHIER, K., CHASSANDE, O., SEO, H., HAYASHI, Y., SAMARUT, J., MURATA, Y., WEISS, R. E. & REFETOFF, S. (2001) Increased sensitivity to thyroid hormone in mice with complete deficiency of thyroid hormone receptor alpha. *Proc Natl Acad Sci U S A*, 98, 349-54.
- MACKIE, E. J., TATARCZUCH, L. & MIRAMS, M. (2011) The skeleton: a multi-functional complex organ: the growth plate chondrocyte and endochondral ossification. *J Endocrinol*, 211, 109-21.
- MANOLAGAS, S. C. (2010) From estrogen-centric to aging and oxidative stress: a revised perspective of the pathogenesis of osteoporosis. *Endocr Rev*, 31, 266-300.
- MANOLAGAS, S. C. & PARFITT, A. M. (2010) What old means to bone. *Trends Endocrinol Metab*, 21, 369-74.
- MANSOURI, A., CHOWDHURY, K. & GRUSS, P. (1998) Follicular cells of the thyroid gland require Pax8 gene function. *Nat Genet*, 19, 87-90.
- MARTIN-MILLAN, M., ALMEIDA, M., AMBROGINI, E., HAN, L., ZHAO, H., WEINSTEIN, R. S., JILKA, R. L., O'BRIEN, C. A. & MANOLAGAS, S. C. (2010) The estrogen receptor-alpha in osteoclasts mediates the protective effects of estrogens on cancellous but not cortical bone. *Mol Endocrinol*, 24, 323-34.
- MARTIN, R. B. & BURR, D. B. (1982) A hypothetical mechanism for the stimulation of osteonal remodelling by fatigue damage. *J Biomech*, 15, 137-9.

-
- MARUYAMA, Z., YOSHIDA, C. A., FURUICHI, T., AMIZUKA, N., ITO, M., FUKUYAMA, R., MIYAZAKI, T., KITAURA, H., NAKAMURA, K., FUJITA, T., KANATANI, N., MORIISHI, T., YAMANA, K., LIU, W., KAWAGUCHI, H., NAKAMURA, K. & KOMORI, T. (2007) Runx2 determines bone maturity and turnover rate in postnatal bone development and is involved in bone loss in estrogen deficiency. *Dev Dyn*, 236, 1876-90.
- MAYERL, S., VISSER, T. J., DARRAS, V. M., HORN, S. & HEUER, H. (2012) Impact of Oatp1c1 deficiency on thyroid hormone metabolism and action in the mouse brain. *Endocrinology*, 153, 1528-37.
- MCCAULEY, L. K., TOZUM, T. F., KOZLOFF, K. M., KOH-PAIGE, A. J., CHEN, C., DEMASHKIEH, M., CRONOVICH, H., RICHARD, V., KELLER, E. T., ROSOL, T. J. & GOLDSTEIN, S. A. (2003) Transgenic models of metabolic bone disease: impact of estrogen receptor deficiency on skeletal metabolism. *Connect Tissue Res*, 44 Suppl 1, 250-63.
- MEDICI, M., RIVADENEIRA, F., VAN DER DEURE, W. M., HOFMAN, A., VAN MEURS, J. B., STYRKARSDOTTIR, U., VAN DUJIN, C. M., SPECTOR, T., KIEL, D. P., UITTERLINDEN, A. G., VISSER, T. J. & PEETERS, R. P. (2012) A large-scale population-based analysis of common genetic variation in the thyroid hormone receptor alpha locus and bone. *Thyroid*, 22, 223-4.
- MEIKLE, M. C., BORD, S., HEMBRY, R. M., COMPSTON, J., CROUCHER, P. I. & REYNOLDS, J. J. (1992) Human osteoblasts in culture synthesize collagenase and other matrix metalloproteinases in response to osteotropic hormones and cytokines. *J Cell Sci*, 103 (Pt 4), 1093-9.
- MILLER, B. G. (1979) Delayed interactions between progesterone and low doses of 17 beta-estradiol in the mouse uterus. *Endocrinology*, 104, 26-33.
- MIRAOUI, H. & MARIE, P. J. (2010) Fibroblast growth factor receptor signaling crosstalk in skeletogenesis. *Sci Signal*, 3, re9.
- MITTAG, J., FRIEDRICHSEN, S., HEUER, H., POLSFUSS, S., VISSER, T. J. & BAUER, K. (2005) Athyroid Pax8^{-/-} mice cannot be rescued by the inactivation of thyroid hormone receptor alpha1. *Endocrinology*, 146, 3179-84.
- MIURA, M., TANAKA, K., KOMATSU, Y., SUDA, M., YASODA, A., SAKUMA, Y., OZASA, A. & NAKAO, K. (2002) A novel interaction between thyroid hormones and 1,25(OH)(2)D(3) in osteoclast formation. *Biochem Biophys Res Commun*, 291, 987-94.
- MIYAURA, C., TODA, K., INADA, M., OHSHIBA, T., MATSUMOTO, C., OKADA, T., ITO, M., SHIZUTA, Y. & ITO, A. (2001) Sex- and age-related response to aromatase deficiency in bone. *Biochem Biophys Res Commun*, 280, 1062-8.
- MONFOULET, L. E., RABIER, B., DACQUIN, R., ANGINOT, A., PHOTSAVANG, J., JURDIC, P., VICO, L., MALAVAL, L. & CHASSANDE, O. (2011) Thyroid hormone receptor beta mediates thyroid hormone effects on bone remodeling and bone mass. *J Bone Miner Res*, 26, 2036-44.
- MORIISHI, T., FUKUYAMA, R., ITO, M., MIYAZAKI, T., MAENO, T., KAWAI, Y., KOMORI, H. & KOMORI, T. (2012) Osteocyte network; a negative regulatory system for bone mass augmented by the induction of rankl in osteoblasts and sost in osteocytes at unloading. *PLoS One*, 7, e40143.
- MOSEKILDE, L. & MELSEN, F. (1978) A tetracycline-based histomorphometric evaluation of bone resorption and bone turnover in hyperthyroidism and hyperparathyroidism. *Acta Med Scand*, 204, 97-102.
- MULLER, R. E. & WOTIZ, H. H. (1979) Kinetics of estradiol entry into uterine cells. *Endocrinology*, 105, 1107-14.
- MUNNS, C. F., RAUCH, F., TRAVERS, R. & GLORIEUX, F. H. (2005) Effects of intravenous pamidronate treatment in infants with osteogenesis imperfecta: clinical and histomorphometric outcome. *J Bone Miner Res*, 20, 1235-43.
- MURPHY, E. & WILLIAMS, G. R. (2004) The thyroid and the skeleton. *Clin Endocrinol (Oxf)*, 61, 285-98.
- NAKAMURA, T., IMAI, Y., MATSUMOTO, T., SATO, S., TAKEUCHI, K., IGARASHI, K., HARADA, Y., AZUMA, Y., KRUST, A., YAMAMOTO, Y., NISHINA, H., TAKEDA, S., TAKAYANAGI, H., METZGER, D., KANNO, J., TAKAOKA, K., MARTIN, T. J., CHAMBON, P. & KATO, S. (2007) Estrogen

-
- prevents bone loss via estrogen receptor alpha and induction of Fas ligand in osteoclasts. *Cell*, 130, 811-23.
- NAKASHIMA, T., HAYASHI, M., FUKUNAGA, T., KURATA, K., OH-HORA, M., FENG, J. Q., BONEWALD, L. F., KODAMA, T., WUTZ, A., WAGNER, E. F., PENNINGER, J. M. & TAKAYANAGI, H. (2011) Evidence for osteocyte regulation of bone homeostasis through RANKL expression. *Nat Med*, 17, 1231-4.
- NG, L., HURLEY, J. B., DIERKS, B., SRINIVAS, M., SALTO, C., VENNSTROM, B., REH, T. A. & FORREST, D. (2001) A thyroid hormone receptor that is required for the development of green cone photoreceptors. *Nat Genet*, 27, 94-8.
- NGUYEN, T. V., CENTER, J. R. & EISMAN, J. A. (2000) Osteoporosis in elderly men and women: effects of dietary calcium, physical activity, and body mass index. *J Bone Miner Res*, 15, 322-31.
- NICHOLLS, J. J., BRASSILL, M. J., WILLIAMS, G. R. & BASSETT, J. H. (2012) The skeletal consequences of thyrotoxicosis. *J Endocrinol*, 213, 209-21.
- O'SHEA, P. J., BASSETT, J. H., CHENG, S. Y. & WILLIAMS, G. R. (2006) Characterization of skeletal phenotypes of TRalpha1 and TRbeta mutant mice: implications for tissue thyroid status and T3 target gene expression. *Nucl Recept Signal*, 4, e011.
- O'SHEA, P. J., BASSETT, J. H., SRISKANTHARAJAH, S., YING, H., CHENG, S. Y. & WILLIAMS, G. R. (2005) Contrasting skeletal phenotypes in mice with an identical mutation targeted to thyroid hormone receptor alpha1 or beta. *Mol Endocrinol*, 19, 3045-59.
- O'SHEA, P. J., HARVEY, C. B., SUZUKI, H., KANESHIGE, M., KANESHIGE, K., CHENG, S. Y. & WILLIAMS, G. R. (2003) A thyrotoxic skeletal phenotype of advanced bone formation in mice with resistance to thyroid hormone. *Mol Endocrinol*, 17, 1410-24.
- OHLSSON, C., NILSSON, A., ISAKSSON, O., BENTHAM, J. & LINDAHL, A. (1992) Effects of tri-iodothyronine and insulin-like growth factor-I (IGF-I) on alkaline phosphatase activity, [3H]thymidine incorporation and IGF-I receptor mRNA in cultured rat epiphyseal chondrocytes. *J Endocrinol*, 135, 115-23.
- ONAL, M., XIONG, J., CHEN, X., THOSTENSON, J. D., ALMEIDA, M., MANOLAGAS, S. C. & O'BRIEN, C. A. (2012) RANKL expression by B lymphocytes contributes to ovariectomy-induced bone loss. *J Biol Chem*.
- ONGHIPHADHANAKUL, B., ALEX, S., BRAVERMAN, L. E. & BARAN, D. T. (1992) Excessive L-thyroxine therapy decreases femoral bone mineral densities in the male rat: effect of hypogonadism and calcitonin. *J Bone Miner Res*, 7, 1227-31.
- OZ, O. K., ZERWEKH, J. E., FISHER, C., GRAVES, K., NANU, L., MILLSAPS, R. & SIMPSON, E. R. (2000) Bone has a sexually dimorphic response to aromatase deficiency. *J Bone Miner Res*, 15, 507-14.
- PACE, P., TAYLOR, J., SUNTHARALINGAM, S., COOMBES, R. C. & ALI, S. (1997) Human estrogen receptor beta binds DNA in a manner similar to and dimerizes with estrogen receptor alpha. *J Biol Chem*, 272, 25832-8.
- PACIFICI, R. (2007) T cells and post menopausal osteoporosis in murine models. *Arthritis Res Ther*, 9, 102.
- PARLE, J. V., FRANKLYN, J. A., CROSS, K. W., JONES, S. R. & SHEPPARD, M. C. (1993) Thyroxine prescription in the community: serum thyroid stimulating hormone level assays as an indicator of undertreatment or overtreatment. *Br J Gen Pract*, 43, 107-9.
- PATERNOSTER, L., LORENTZON, M., LEHTIMAKI, T., ERIKSSON, J., KAHONEN, M., RAITAKARI, O., LAAKSONEN, M., SIEVANEN, H., VIIKARI, J., LYYTIKAINEN, L. P., MELLSTROM, D., KARLSSON, M., LJUNGGREN, O., GRUNDBERG, E., KEMP, J. P., SAYERS, A., NETHANDER, M., EVANS, D. M., VANDENPUT, L., TOBIAS, J. H. & OHLSSON, C. (2013) Genetic determinants of trabecular and cortical volumetric bone mineral densities and bone microstructure. *PLoS Genet*, 9, e1003247.

-
- PELLETIER, P., GAUTHIER, K., SIDELEVA, O., SAMARUT, J. & SILVA, J. E. (2008) Mice lacking the thyroid hormone receptor-alpha gene spend more energy in thermogenesis, burn more fat, and are less sensitive to high-fat diet-induced obesity. *Endocrinology*, 149, 6471-86.
- PENG, Y., SHI, K., WANG, L., LU, J., LI, H., PAN, S. & MA, C. (2013) Characterization of Osterix protein stability and physiological role in osteoblast differentiation. *PLoS One*, 8, e56451.
- PEREIRA, R. C., JORGETTI, V. & CANALIS, E. (1999) Triiodothyronine induces collagenase-3 and gelatinase B expression in murine osteoblasts. *Am J Physiol*, 277, E496-504.
- PETTERSSON, K., GRANDIEN, K., KUIPER, G. G. & GUSTAFSSON, J. A. (1997) Mouse estrogen receptor beta forms estrogen response element-binding heterodimers with estrogen receptor alpha. *Mol Endocrinol*, 11, 1486-96.
- PETTIT, A. R., CHANG, M. K., HUME, D. A. & RAGGATT, L. J. (2008) Osteal macrophages: a new twist on coupling during bone dynamics. *Bone*, 43, 976-82.
- PFEFFER, U., FECAROTTA, E., ARENA, G., FORLANI, A. & VIDALI, G. (1996) Alternative splicing of the estrogen receptor primary transcript normally occurs in estrogen receptor positive tissues and cell lines. *J Steroid Biochem Mol Biol*, 56, 99-105.
- PIGNOLO, R. J., SHORE, E. M. & KAPLAN, F. S. (2011) Fibrodysplasia ossificans progressiva: clinical and genetic aspects. *Orphanet J Rare Dis*, 6, 80.
- POCOCK, N. A., EISMAN, J. A., HOPPER, J. L., YEATES, M. G., SAMBROOK, P. N. & EBERL, S. (1987) Genetic determinants of bone mass in adults. A twin study. *J Clin Invest*, 80, 706-10.
- POLI, V., BALENA, R., FATTORI, E., MARKATOS, A., YAMAMOTO, M., TANAKA, H., CILIBERTO, G., RODAN, G. A. & COSTANTINI, F. (1994) Interleukin-6 deficient mice are protected from bone loss caused by estrogen depletion. *Embo J*, 13, 1189-96.
- QUARTO, R., CAMPANILE, G., CANCEDDA, R. & DOZIN, B. (1992) Thyroid hormone, insulin, and glucocorticoids are sufficient to support chondrocyte differentiation to hypertrophy: a serum-free analysis. *J Cell Biol*, 119, 989-95.
- QUAYNOR, S. D., STRADTMAN, E. W., JR., KIM, H. G., SHEN, Y., CHORICH, L. P., SCHREIHOFFER, D. A. & LAYMAN, L. C. (2013) Delayed puberty and estrogen resistance in a woman with estrogen receptor alpha variant. *N Engl J Med*, 369, 164-71.
- QUIGNODON, L., VINCENT, S., WINTER, H., SAMARUT, J. & FLAMANT, F. (2007) A point mutation in the activation function 2 domain of thyroid hormone receptor alpha1 expressed after CRE-mediated recombination partially recapitulates hypothyroidism. *Mol Endocrinol*, 21, 2350-60.
- RAGGATT, L. J. & PARTRIDGE, N. C. (2010) Cellular and molecular mechanisms of bone remodeling. *J Biol Chem*, 285, 25103-8.
- RAUNER, M., SIPOS, W., THIELE, S. & PIETSCHMANN, P. (2013) Advances in osteoimmunology: pathophysiologic concepts and treatment opportunities. *Int Arch Allergy Immunol*, 160, 114-25.
- RAVN, P., CIZZA, G., BJARNASON, N. H., THOMPSON, D., DALEY, M., WASNICH, R. D., MCCLUNG, M., HOSKING, D., YATES, A. J. & CHRISTIANSEN, C. (1999) Low body mass index is an important risk factor for low bone mass and increased bone loss in early postmenopausal women. Early Postmenopausal Intervention Cohort (EPIC) study group. *J Bone Miner Res*, 14, 1622-7.
- REFETTOFF, S. (1993) Resistance to thyroid hormone. *Clin Lab Med*, 13, 563-81.
- RICHES, P. L., MCRORIE, E., FRASER, W. D., DETERMANN, C., VAN'T HOF, R. & RALSTON, S. H. (2009) Osteoporosis associated with neutralizing autoantibodies against osteoprotegerin. *N Engl J Med*, 361, 1459-65.
- RIGGS, B. L. (2002) Endocrine causes of age-related bone loss and osteoporosis. *Novartis Found Symp*, 242, 247-59; discussion 260-4.
- RIVKEES, S. A., BODE, H. H. & CRAWFORD, J. D. (1988) Long-term growth in juvenile acquired hypothyroidism: the failure to achieve normal adult stature. *N Engl J Med*, 318, 599-602.

-
- RIZZOLI, R., ADACHI, J. D., COOPER, C., DERE, W., DEVOGELAER, J. P., DIEZ-PEREZ, A., KANIS, J. A., LASLOP, A., MITLAK, B., PAPAPOULOS, S., RALSTON, S., REITER, S., WERHYA, G. & REGINSTER, J. Y. (2012) Management of Glucocorticoid-Induced Osteoporosis. *Calcif Tissue Int*.
- ROBINSON, L. J., YAROSLAVSKIY, B. B., GRISWOLD, R. D., ZADOROZNY, E. V., GUO, L., TOURKOVA, I. L. & BLAIR, H. C. (2009) Estrogen inhibits RANKL-stimulated osteoclastic differentiation of human monocytes through estrogen and RANKL-regulated interaction of estrogen receptor-alpha with BCAR1 and Traf6. *Exp Cell Res*, 315, 1287-301.
- ROBLING, A. G., NIZIOLEK, P. J., BALDRIDGE, L. A., CONDON, K. W., ALLEN, M. R., ALAM, I., MANTILA, S. M., GLUHAK-HEINRICH, J., BELLIDO, T. M., HARRIS, S. E. & TURNER, C. H. (2008) Mechanical stimulation of bone in vivo reduces osteocyte expression of Sost/sclerostin. *J Biol Chem*, 283, 5866-75.
- ROBSON, H., SIEBLER, T., STEVENS, D. A., SHALET, S. M. & WILLIAMS, G. R. (2000) Thyroid hormone acts directly on growth plate chondrocytes to promote hypertrophic differentiation and inhibit clonal expansion and cell proliferation. *Endocrinology*, 141, 3887-97.
- ROCHIRA, V., ZIRILLI, L., MADEO, B., ARANDA, C., CAFFAGNI, G., FABRE, B., MONTANGERO, V. E., ROLDAN, E. J., MAFFEI, L. & CARANI, C. (2007) Skeletal effects of long-term estrogen and testosterone replacement treatment in a man with congenital aromatase deficiency: evidences of a priming effect of estrogen for sex steroids action on bone. *Bone*, 40, 1662-8.
- ROSCHGER, P., FRATZL, P., ESCHBERGER, J. & KLAUSHOFER, K. (1998) Validation of quantitative backscattered electron imaging for the measurement of mineral density distribution in human bone biopsies. *Bone*, 23, 319-26.
- ROSS, F. P. (2006) M-CSF, c-Fms, and signaling in osteoclasts and their precursors. *Ann N Y Acad Sci*, 1068, 110-6.
- RUBIN, L. A., HAWKER, G. A., PELTEKOVA, V. D., FIELDING, L. J., RIDOUT, R. & COLE, D. E. (1999) Determinants of peak bone mass: clinical and genetic analyses in a young female Canadian cohort. *J Bone Miner Res*, 14, 633-43.
- RUSSELL, R. G. (2011) Bisphosphonates: the first 40 years. *Bone*, 49, 2-19.
- SAMBROOK, P. & COOPER, C. (2006) Osteoporosis. *Lancet*, 367, 2010-8.
- SAMPATH, T. K., SIMIC, P., SENDAK, R., DRACA, N., BOWE, A. E., O'BRIEN, S., SCHIAVI, S. C., MCPHERSON, J. M. & VUKICEVIC, S. (2007) Thyroid-stimulating hormone restores bone volume, microarchitecture, and strength in aged ovariectomized rats. *J Bone Miner Res*, 22, 849-59.
- SARAIVA, P. P., TEIXEIRA, S. S., PADOVANI, C. R. & NOGUEIRA, C. R. (2008) Triiodothyronine (T3) does not induce Rankl expression in rat Ros 17/2.8 cells. *Arq Bras Endocrinol Metabol*, 52, 109-13.
- SEELEY, D. G., BROWNER, W. S., NEVITT, M. C., GENANT, H. K., SCOTT, J. C. & CUMMINGS, S. R. (1991) Which fractures are associated with low appendicular bone mass in elderly women? The Study of Osteoporotic Fractures Research Group. *Ann Intern Med*, 115, 837-42.
- SEEMAN, E. & DELMAS, P. D. (2006) Bone quality--the material and structural basis of bone strength and fragility. *N Engl J Med*, 354, 2250-61.
- SEGNI, M., LEONARDI, E., MAZZONCINI, B., PUCARELLI, I. & PASQUINO, A. M. (1999) Special features of Graves' disease in early childhood. *Thyroid*, 9, 871-7.
- SHEVDE, N. K., BENDIXEN, A. C., DIENGER, K. M. & PIKE, J. W. (2000) Estrogens suppress RANK ligand-induced osteoclast differentiation via a stromal cell independent mechanism involving c-Jun repression. *Proc Natl Acad Sci U S A*, 97, 7829-34.
- SILVA-FERNANDEZ, L., ROSARIO, M. P., MARTINEZ-LOPEZ, J. A., CARMONA, L. & LOZA, E. (2013) Denosumab for the treatment of osteoporosis: a systematic literature review. *Reumatol Clin*, 9, 42-52.
- SIMS, N. A., CLEMENT-LACROIX, P., MINET, D., FRASLON-VANHULLE, C., GAILLARD-KELLY, M., RESCHE-RIGON, M. & BARON, R. (2003) A functional androgen receptor is not sufficient to allow estradiol to protect bone after gonadectomy in estradiol receptor-deficient mice. *J Clin Invest*, 111, 1319-27.

-
- SIMS, N. A., DUPONT, S., KRUST, A., CLEMENT-LACROIX, P., MINET, D., RESCHE-RIGON, M., GAILLARD-KELLY, M. & BARON, R. (2002) Deletion of estrogen receptors reveals a regulatory role for estrogen receptors-beta in bone remodeling in females but not in males. *Bone*, 30, 18-25.
- SMIT, T. H., BURGER, E. H. & HUYGHE, J. M. (2002) A case for strain-induced fluid flow as a regulator of BMU-coupling and osteonal alignment. *J Bone Miner Res*, 17, 2021-9.
- SMITH, E. P., BOYD, J., FRANK, G. R., TAKAHASHI, H., COHEN, R. M., SPECKER, B., WILLIAMS, T. C., LUBAHN, D. B. & KORACH, K. S. (1994) Estrogen resistance caused by a mutation in the estrogen-receptor gene in a man. *N Engl J Med*, 331, 1056-61.
- SNELLING, A. M., CRESPO, C. J., SCHAEFFER, M., SMITH, S. & WALBOURN, L. (2001) Modifiable and nonmodifiable factors associated with osteoporosis in postmenopausal women: results from the Third National Health and Nutrition Examination Survey, 1988-1994. *J Womens Health Gen Based Med*, 10, 57-65.
- SOROKO, S. B., BARRETT-CONNOR, E., EDELSTEIN, S. L. & KRITZ-SILVERSTEIN, D. (1994) Family history of osteoporosis and bone mineral density at the axial skeleton: the Rancho Bernardo Study. *J Bone Miner Res*, 9, 761-9.
- SOWERS, M. R., JANNAUSCH, M., MCCONNELL, D., LITTLE, R., GREENDALE, G. A., FINKELSTEIN, J. S., NEER, R. M., JOHNSTON, J. & ETTINGER, B. (2006) Hormone predictors of bone mineral density changes during the menopausal transition. *J Clin Endocrinol Metab*, 91, 1261-7.
- SRIVASTAVA, S., TORALDO, G., WEITZMANN, M. N., CENCI, S., ROSS, F. P. & PACIFICI, R. (2001) Estrogen decreases osteoclast formation by down-regulating receptor activator of NF-kappa B ligand (RANKL)-induced JNK activation. *J Biol Chem*, 276, 8836-40.
- ST GERMAIN, D. L., GALTON, V. A. & HERNANDEZ, A. (2009) Minireview: Defining the roles of the iodothyronine deiodinases: current concepts and challenges. *Endocrinology*, 150, 1097-107.
- STEVENS, D. A., HARVEY, C. B., SCOTT, A. J., O'SHEA, P. J., BARNARD, J. C., WILLIAMS, A. J., BRADY, G., SAMARUT, J., CHASSANDE, O. & WILLIAMS, G. R. (2003) Thyroid hormone activates fibroblast growth factor receptor-1 in bone. *Mol Endocrinol*, 17, 1751-66.
- STEVENS, D. A., HASSERJIAN, R. P., ROBSON, H., SIEBLER, T., SHALET, S. M. & WILLIAMS, G. R. (2000) Thyroid hormones regulate hypertrophic chondrocyte differentiation and expression of parathyroid hormone-related peptide and its receptor during endochondral bone formation. *J Bone Miner Res*, 15, 2431-42.
- SUN, L., PENG, Y., SHARROW, A. C., IQBAL, J., ZHANG, Z., PAPACHRISTOU, D. J., ZAIDI, S., ZHU, L. L., YAROSLAVSKIY, B. B., ZHOU, H., ZALLONE, A., SAIRAM, M. R., KUMAR, T. R., BO, W., BRAUN, J., CARDOSO-LANDA, L., SCHAFFLER, M. B., MOONGA, B. S., BLAIR, H. C. & ZAIDI, M. (2006) FSH directly regulates bone mass. *Cell*, 125, 247-60.
- SUN, L., VUKICEVIC, S., BALIRAM, R., YANG, G., SENDAK, R., MCPHERSON, J., ZHU, L. L., IQBAL, J., LATIF, R., NATRAJAN, A., ARABI, A., YAMOA, K., MOONGA, B. S., GABET, Y., DAVIES, T. F., BAB, I., ABE, E., SAMPATH, K. & ZAIDI, M. (2008) Intermittent recombinant TSH injections prevent ovariectomy-induced bone loss. *Proc Natl Acad Sci U S A*, 105, 4289-94.
- TAKAHASHI, N., AKATSU, T., UDAGAWA, N., SASAKI, T., YAMAGUCHI, A., MOSELEY, J. M., MARTIN, T. J. & SUDA, T. (1988) Osteoblastic cells are involved in osteoclast formation. *Endocrinology*, 123, 2600-2.
- TINNIKOV, A., NORDSTROM, K., THOREN, P., KINDBLUM, J. M., MALIN, S., ROZELL, B., ADAMS, M., RAJANAYAGAM, O., PETTERSSON, S., OHLSSON, C., CHATTERJEE, K. & VENNSTROM, B. (2002) Retardation of post-natal development caused by a negatively acting thyroid hormone receptor alpha1. *Embo J*, 21, 5079-87.
- TOMKINSON, A., REEVE, J., SHAW, R. W. & NOBLE, B. S. (1997) The death of osteocytes via apoptosis accompanies estrogen withdrawal in human bone. *J Clin Endocrinol Metab*, 82, 3128-35.
- TOTH, M. J., TCHERNOF, A., SITES, C. K. & POEHLMAN, E. T. (2000) Menopause-related changes in body fat distribution. *Ann N Y Acad Sci*, 904, 502-6.

-
- TRAJKOVIC, M., VISSER, T. J., MITTAG, J., HORN, S., LUKAS, J., DARRAS, V. M., RAIVICH, G., BAUER, K. & HEUER, H. (2007) Abnormal thyroid hormone metabolism in mice lacking the monocarboxylate transporter 8. *J Clin Invest*, 117, 627-35.
- TURNER, C. H. & PAVALKO, F. M. (1998) Mechanotransduction and functional response of the skeleton to physical stress: the mechanisms and mechanics of bone adaptation. *J Orthop Sci*, 3, 346-55.
- VAN DER EERDEN, B. C., KARPERIEN, M. & WIT, J. M. (2003) Systemic and local regulation of the growth plate. *Endocr Rev*, 24, 782-801.
- VAN MULLEM, A., VAN HEEREBEEK, R., CHRYSIS, D., VISSER, E., MEDICI, M., ANDRIKOULA, M., TSATSOULIS, A., PEETERS, R. & VISSER, T. J. (2012) Clinical phenotype and mutant TRalpha1. *N Engl J Med*, 366, 1451-3.
- VARGA, F., RUMPLER, M., ZOEHRER, R., TURECEK, C., SPITZER, S., THALER, R., PASCHALIS, E. P. & KLAUSHOFER, K. (2010) T3 affects expression of collagen I and collagen cross-linking in bone cell cultures. *Biochem Biophys Res Commun*, 402, 180-5.
- VARLAKHANOVA, N., SNYDER, C., JOSE, S., HAHM, J. B. & PRIVALSKY, M. L. (2010) Estrogen receptors recruit SMRT and N-CoR corepressors through newly recognized contacts between the corepressor N terminus and the receptor DNA binding domain. *Mol Cell Biol*, 30, 1434-45.
- VESTERGAARD, P. & MOSEKILDE, L. (2003) Hyperthyroidism, bone mineral, and fracture risk--a meta-analysis. *Thyroid*, 13, 585-93.
- VESTERGAARD, P., REJNMARK, L. & MOSEKILDE, L. (2005) Influence of hyper- and hypothyroidism, and the effects of treatment with antithyroid drugs and levothyroxine on fracture risk. *Calcif Tissue Int*, 77, 139-44.
- VLADUSIC, E. A., HORNBY, A. E., GUERRA-VLADUSIC, F. K. & LUPU, R. (1998) Expression of estrogen receptor beta messenger RNA variant in breast cancer. *Cancer Res*, 58, 210-4.
- WANG, L., SHAO, Y. Y. & BALLOCK, R. T. (2007) Thyroid hormone interacts with the Wnt/beta-catenin signaling pathway in the terminal differentiation of growth plate chondrocytes. *J Bone Miner Res*, 22, 1988-95.
- WAUNG, J. A., BASSETT, J. H. & WILLIAMS, G. R. (2012) Thyroid hormone metabolism in skeletal development and adult bone maintenance. *Trends Endocrinol Metab*, 23, 155-62.
- WEINER, S. & WAGNER, H. (1998) THE MATERIAL BONE: Structure-Mechanical Function Relations. *Annual Review of Materials Science*, 28, 271-298.
- WEINSTEIN, R. S., NICHOLAS, R. W. & MANOLAGAS, S. C. (2000) Apoptosis of osteocytes in glucocorticoid-induced osteonecrosis of the hip. *J Clin Endocrinol Metab*, 85, 2907-12.
- WEISS, R. E. & REFETTOFF, S. (1996) Effect of thyroid hormone on growth. Lessons from the syndrome of resistance to thyroid hormone. *Endocrinol Metab Clin North Am*, 25, 719-30.
- WEISS, R. E. & REFETTOFF, S. (2000) Resistance to thyroid hormone. *Rev Endocr Metab Disord*, 1, 97-108.
- WESTENDORF, J. J. (2006) Transcriptional co-repressors of Runx2. *J Cell Biochem*, 98, 54-64.
- WILLIAMS, G. R. (2000) Cloning and characterization of two novel thyroid hormone receptor beta isoforms. *Mol Cell Biol*, 20, 8329-42.
- WILLIAMS, G. R. & BASSETT, J. H. (2011) Deiodinases: the balance of thyroid hormone: local control of thyroid hormone action: role of type 2 deiodinase. *J Endocrinol*, 209, 261-72.
- WILLIAMS, G. R. & FRANKLYN, J. A. (1994) Physiology of the steroid-thyroid hormone nuclear receptor superfamily. *Baillieres Clin Endocrinol Metab*, 8, 241-66.
- WINDAHL, S. H., ANDERSSON, G. & GUSTAFSSON, J. A. (2002) Elucidation of estrogen receptor function in bone with the use of mouse models. *Trends Endocrinol Metab*, 13, 195-200.
- XIONG, J., ONAL, M., JILKA, R. L., WEINSTEIN, R. S., MANOLAGAS, S. C. & O'BRIEN, C. A. (2011) Matrix-embedded cells control osteoclast formation. *Nat Med*, 17, 1235-41.
- YAMAMOTO, M., MARKATOS, A., SEEDOR, J. G., MASARACHIA, P., GENTILE, M., RODAN, G. A. & BALENA, R. (1993) The effects of the aminobisphosphonate alendronate on thyroid hormone-induced osteopenia in rats. *Calcif Tissue Int*, 53, 278-82.

-
- ZAMAN, G., CHENG, M. Z., JESSOP, H. L., WHITE, R. & LANYON, L. E. (2000) Mechanical strain activates estrogen response elements in bone cells. *Bone*, 27, 233-9.
- ZHANG, X. K. & KAHL, M. (1993) Regulation of retinoid and thyroid hormone action through homodimeric and heterodimeric receptors. *Trends Endocrinol Metab*, 4, 156-62.
- ZHU, L. L., BLAIR, H., CAO, J., YUEN, T., LATIF, R., GUO, L., TOURKOVA, I. L., LI, J., DAVIES, T. F., SUN, L., BIAN, Z., ROSEN, C., ZALLONE, A., NEW, M. I. & ZAIDI, M. (2012) Blocking antibody to the beta-subunit of FSH prevents bone loss by inhibiting bone resorption and stimulating bone synthesis. *Proc Natl Acad Sci U S A*.

PUBLICATIONS FROM THESIS

Papers

BASSETT, J. H., LOGAN, J. G., BOYDE, A., **CHEUNG, M. S.**, EVANS, H., CROUCHER, P., SUN, X. Y., XU, S., MURATA, Y. & WILLIAMS, G. R. (2012) Mice lacking the calcineurin inhibitor Rcan2 have an isolated defect of osteoblast function. *Endocrinology*, 153, 3537-48.

CHEUNG, M. S., GOGAKOS, A., BASSETT, J. H. D. & WILLIAMS, G. R. (2011) Thyroid disease and osteoporosis. IN WASS, J. A. H. & STEWART, P. M. (Eds.) *The Oxford Textbook of Endocrinology and Diabetes*. 2 ed., Oxford University Press.

GOGAKOS, A., **CHEUNG, M.**, BASSETT, J. & WILLIAMS, G. (2009) Bone signalling pathways and treatment of osteoporosis. *Expert Rev. Endocrinol. Metab.*

Abstracts, Oral Presentations and Awards

6th International Conference on Children's Bone Health, Rotterdam, Netherlands, 2013

Skeletal effects of hypothyroidism are mediated by thyroid hormone receptor α

Cheung M, Boyde A, Evans H, Bassett JHD, Williams GR 2013, Bone Abstracts Vol 2, OP2

(DOI:10.1530/boneabs.2.OP1)

Oral poster presentation

Awarded: New Investigator Award

40th Meeting of the British Society of Paediatric Endocrinology and Diabetes, Leeds, UK, 2012

Skeletal effects of hypothyroidism are mediated by thyroid hormone receptor alpha

Cheung M, Boyde A, Evans H, Bassett JHD, Williams GR

Oral presentation

Awarded: Travel Grant

Imperial Graduate Summer School Research Symposium, London, UK, 2012

Skeletal effects of hypothyroidism are mediated by thyroid hormone receptor α

Cheung M, Boyde A, Evans H, Bassett JHD, Williams GR

Poster presentation

Awarded: 2nd Prize

Department of Medicine Young Scientist Day, London, UK, 2012

Skeletal effects of hypothyroidism are mediated by thyroid hormone receptor α

Cheung M, Boyde A, Evans H, Bassett JHD, Williams GR

Poster presentation

Awarded: 2nd Prize

9th International Workshop on Resistance to Thyroid Hormone, Cambridge, UK, 2010

Thyroid hormone and oestrogen cross talk in the regulation of the skeleton

Cheung M, Boyde A, Evans H, Bassett JHD, Williams GR

Oral presentation

Annual Meeting of The American Society of Bone and Mineral Research, Toronto, Canada, 2010

Optimising quantitation of mineral apposition and bone formation rate in mice

MS Cheung, A Boyde, JHD Bassett, GR Williams, 2010, J Bone Miner Res 25 (Suppl 1) SU0203

available at <http://www.asbmr.org/Meetings/AnnualMeeting/AbstractDetail.aspx?aid=b7ccdb28-f7bc-4c31-a505-f8e9dd2c1d63>

Poster presentation

Mice Lacking the Calcineurin Inhibitor *Rcan2* Have an Isolated Defect of Osteoblast Function

J. H. Duncan Bassett, John G. Logan, Alan Boyde, Moira S. Cheung, Holly Evans, Peter Croucher, Xiao-yang Sun, Sai Xu, Yoshiharu Murata, and Graham R. Williams

Molecular Endocrinology Group (J.H.D.B., J.G.L., M.S.C., G.R.W.), Department of Medicine, Imperial College London, Hammersmith Campus, London W12 0NN, United Kingdom; Centre for Oral Growth and Development (A.B.), Queen Mary College, University of London, London E1 4NS, United Kingdom; The Mellanby Centre for Bone Research (H.E., P.C.), Department of Human Metabolism, University of Sheffield, Sheffield S10 2RX, United Kingdom; Garvan Institute for Medical Research (P.C.), Sydney, New South Wales 2010, Australia; and Department of Genetics (X.S., S.X., Y.M.), Research Institute of Environmental Medicine, Nagoya University, Nagoya 464-8601, Japan

Calcineurin-nuclear factor of activated T cells signaling controls the differentiation and function of osteoclasts and osteoblasts, and regulator of calcineurin-2 (*Rcan2*) is a physiological inhibitor of this pathway. *Rcan2* expression is regulated by T_3 , which also has a central role in skeletal development and bone turnover. To investigate the role of *Rcan2* in bone development and maintenance, we characterized *Rcan2*^{-/-} mice and determined its skeletal expression in T_3 receptor (TR) knockout and thyroid-manipulated mice. *Rcan2*^{-/-} mice had normal linear growth but displayed delayed intramembranous ossification, impaired cortical bone formation, and reduced bone mineral accrual during development as well as increased mineralization of adult bone. These abnormalities resulted from an isolated defect in osteoblast function and are similar to skeletal phenotypes of mice lacking the type 2 deiodinase thyroid hormone activating enzyme or with dominant-negative mutations of TR α , the predominant TR isoform in bone. *Rcan2* mRNA was expressed in primary osteoclasts and osteoblasts, and its expression in bone was differentially regulated in TR α and TR β knockout and thyroid-manipulated mice. However, in primary osteoblast cultures, T_3 treatment did not affect *Rcan2* mRNA expression or nuclear factor of activated T cells c1 expression and phosphorylation. Overall, these studies establish that *Rcan2* regulates osteoblast function and its expression in bone is regulated by thyroid status *in vivo*. (*Endocrinology* 153: 3537–3548, 2012)

Regulator of calcineurin (RCAN)-2 belongs to a family of conserved proteins (RCAN1, RCAN2, and RCAN3) that inhibit calcineurin (1, 2). Calcineurin is a Ca^{2+} - and calmodulin-activated serine-threonine protein phosphatase that consists of a calmodulin-binding catalytic subunit and Ca^{2+} -binding regulatory subunit (3). Activation of calcineurin results in dephosphorylation of nuclear factor of activated T cells (NFAT), enabling it to enter the nucleus and regulate gene expression in association with other transcription factors, including activator protein 1 (1, 2, 4, 5). Interaction of RCAN2 with the cat-

alytic subunit of calcineurin blocks NFAT-regulated gene expression (6, 7), indicating RCAN2 is a physiological inhibitor of calcineurin-NFAT signaling.

Calcineurin and NFAT are essential for osteoclast differentiation and bone resorption. NFAT is a master transcription factor for osteoclast differentiation, functioning as a point of convergence for the receptor activator of nuclear factor- κ B ligand, TNF receptor-associated factor 6 and c-Fos signaling pathways required for osteoclastogenesis (8). In addition to its important role in osteoclasts, NFAT also regulates bone mass by acting in osteoblasts, in

ISSN Print 0013-7227 ISSN Online 1945-7170

Printed in U.S.A.

Copyright © 2012 by The Endocrine Society

doi: 10.1210/en.2011-1814 Received September 28, 2011. Accepted April 26, 2012.

First Published Online May 16, 2012

Abbreviations: BFR, Bone formation rate; BS, bone surface; BSE, backscattered electron; CT, computed tomography; DIO2, type 2 deiodinase enzyme; MAR, mineral apposition rate; MS, mineralizing surface; NFAT, nuclear factor of activated T cells; nt, nucleotide; Oc.N, osteoclast numbers; Oc.S, osteoclast surface; P, postnatal day; qBSE-SEM, quantitative BSE-SEM; RCAN, regulator of calcineurin; SEM, scanning electron microscopy; TR, T_3 receptor; TRAP, tartrate-resistant acid phosphatase; WT, wild type.

which its functions are more controversial. Initial studies in mice with global disruption or activation of calcineurin-NFAT signaling suggested the pathway stimulates osteoblast differentiation and bone formation *in vivo* and *in vitro* (9–11), whereas recent studies specifically targeting osteoblasts suggest the calcineurin-NFAT pathway is a negative regulator of osteoblast differentiation and bone formation that also inhibits osteoclastogenesis indirectly via its effects on osteoprotegerin and receptor activator of nuclear factor- κ B ligand in osteoblasts (12). The negative effects on bone formation are supported by findings that low doses of the calcineurin antagonist cyclosporin A increase osteoblast differentiation and bone mass (13). Nevertheless, cyclosporin A has biphasic effects on osteoblasts (12), and treatment of organ transplant patients with calcineurin inhibitors is associated with high bone turnover osteoporosis (14). Taken together, these data indicate the regulatory effects of the calcineurin-NFAT pathway on bone turnover are complex and involve direct actions in osteoblasts and osteoclasts as well as indirect osteoblast-mediated effects on osteoclastogenesis.

The human homolog of RCAN2 (previously named ZAKI-4) was originally identified as a thyroid hormone (T_3)-responsive gene in skin fibroblasts by differential display (15), and ZAKI-4 α and - β mRNA isoforms were identified subsequently (16). RCAN2-3 expression (previously named ZAKI-4 α) is restricted to brain and encodes a 197-amino acid short protein isoform RCAN2-S. By contrast, RCAN2-1 (previously named ZAKI-4 β) is distributed widely, with the highest levels of expression in brain, heart, skeletal muscle, and kidney, and encodes a 243-amino acid long protein isoform RCAN2-L (2, 16) (Fig. 1). Although the two isoforms display tissue-specific differences in expression, it is unknown whether they are functionally distinct. Nevertheless, only RCAN2-3 (ZAKI-4 α) mRNA was found to be T_3 responsive in fibroblasts (16), and this response was mediated by a non-genomic signaling cascade involving T_3 receptor (TR)- β , phosphatidylinositol 3-kinase-Akt/protein kinase B, and mammalian target of rapamycin (17). T_3 treatment also

resulted in reduced endogenous calcineurin activity, and RCAN2 proteins were shown to interact directly with calcineurin and inhibit calcineurin-NFAT signaling, indicating RCAN2 is a T_3 -responsive endogenous inhibitor of the calcineurin-NFAT pathway (16).

In developing brain, *Rcan2* mRNA was expressed widely, increased with age, and colocalized with the expression of calcineurin in some regions. The temporal increase in *Rcan2* expression during brain maturation was blunted in hypothyroid animals (18, 19). In particular, *Rcan2*-3 mRNA expression was reduced in cerebral cortex in hypothyroid mice, but levels in other brain regions were not affected by thyroid status (19). Thus, Rcan2-modulated calcineurin activity was suggested to influence brain development leading to the hypothesis that reduced Rcan2 expression could account for some of the adverse consequences of hypothyroidism during brain development (18, 19). In additional studies, the expression of *Rcan2*-1 in the heart was increased after T_3 administration (19, 20), but no effects were observed in other tissues in response to hyperthyroidism (19). Taken together, these findings indicate that T_3 regulation of *Rcan2*-3 and *Rcan2*-1 expression *in vivo* is isoform and tissue specific and suggest that Rcan2 may mediate some of the effects of thyroid hormones in T_3 -target tissues (18–20).

Although Rcan2 functions as an endogenous inhibitor of the calcineurin-NFAT signaling, it is not known whether *Rcan2* is also expressed in bone. To investigate and determine the physiological importance of *Rcan2* in bone, we generated *Rcan2*^{-/-} knockout mice and characterized their skeletal phenotype. We further hypothesized that *Rcan2* may be a T_3 -responsive target gene in the skeleton because both T_3 and the calcineurin-NFAT pathway regulate bone mass via actions in osteoblasts and osteoclasts (8, 12, 21). Thus, we also investigated expression of *Rcan2* in skeletal cells and in T_3 receptor mutant and thyroid manipulated mice. The effect of T_3 on *Rcan2* expression and downstream signaling was investigated in primary osteoblast cultures.

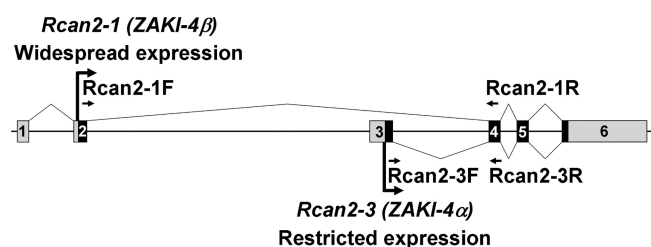


FIG. 1. Mouse *Rcan2* gene. Genomic organization of the mouse *Rcan2* gene showing the alternative splicing events that lead to expression of *Rcan2*-1 and *Rcan2*-3 isoforms. The locations of RT-PCR primers are also shown.

Materials and Methods

Rcan2^{+/-} and *Rcan2*^{-/-} mice

Rcan2 knockout mice (*Rcan2*^{-/-}) were generated by replacing exon 4, common to both *Rcan2*-1 (ZAKI-4 β) and *Rcan2*-3 (ZAKI-4 α), with a LacZ/Neo cassette, and Northern blot analysis confirmed the absence of both transcripts in *Rcan2*^{-/-} mice (22) (Fig. 1). Heterozygous *Rcan2*^{+/-} mice were backcrossed and established in a C57B/6J genetic background in the animal facility at the Research Institute of Environmental Medicine (Nagoya University, Nagoya, Japan) using protocols approved by the institutional review board. The adult mice were given two ip

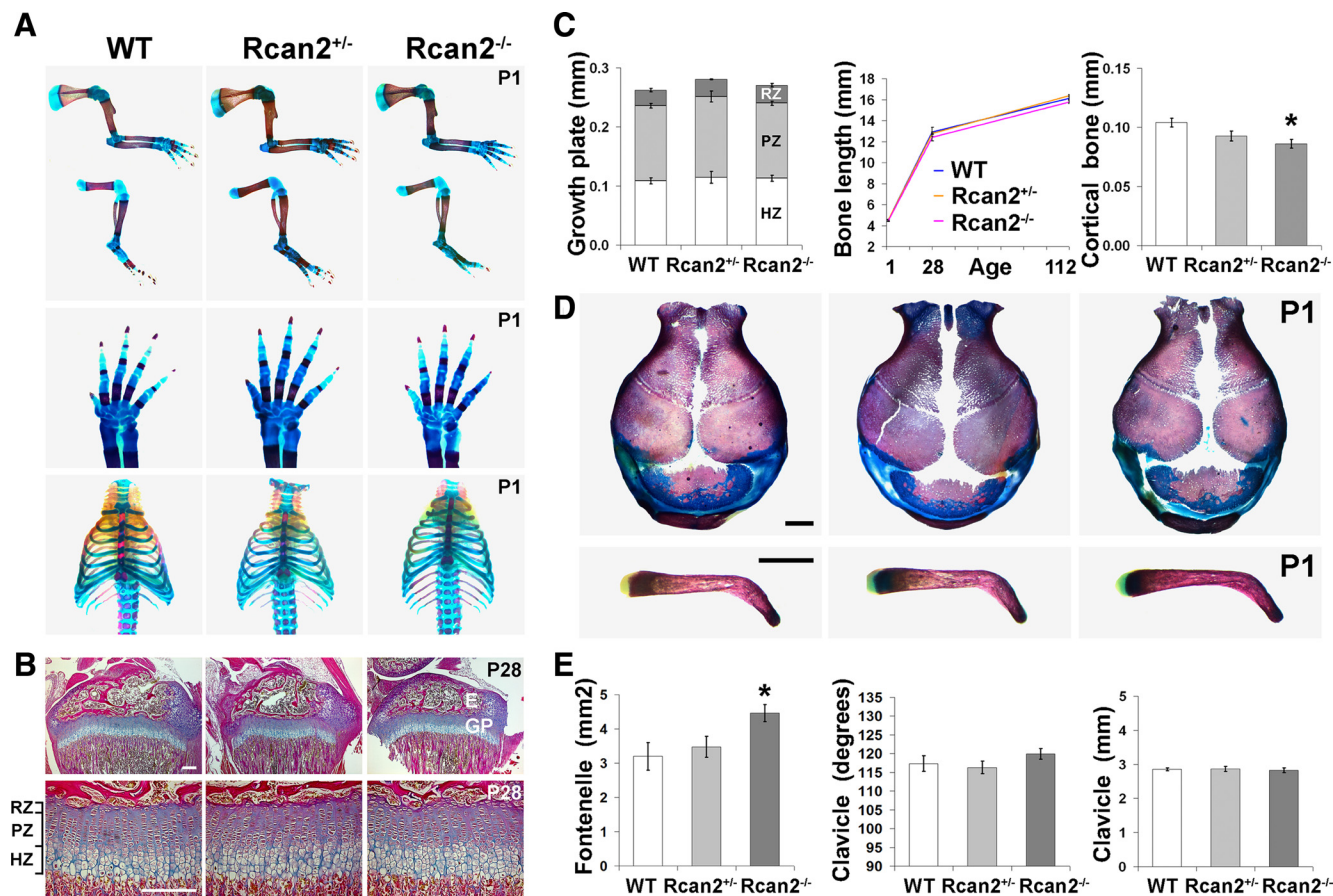


FIG. 2. Skeletal development and growth in *Rcan2*^{-/-} mice. **A**, Upper and lower limbs show detail of the upper limb paws and rib cages from P1 WT, *Rcan2*^{+/-}, and *Rcan2*^{-/-} mice stained with alcian blue (cartilage) and alizarin red (bone). **B**, Proximal tibia growth plates from P28 WT, *Rcan2*^{+/-}, and *Rcan2*^{-/-} mice stained with alcian blue and van Gieson (osteoid) ($\times 50$ and $\times 200$). E, Epiphysis; GP, growth plate; RZ, reserve zone; PZ, proliferative zone; HZ, hypertrophic zone. Bars, 200 μm . **C**, Growth plate and chondrocyte zone heights in P28 mice ($n = 3$ per genotype) and linear growth analysis from birth to P112 ($n = 3$ –4 per genotype). No statistical differences, ANOVA, *Rcan2*^{+/-}, and *Rcan2*^{-/-} vs. WT. Humerus middiaphysis cortical bone thickness at P28 ($n = 4$ per genotype), ANOVA, *Rcan2*^{+/-}, and *Rcan2*^{-/-} vs. WT. *, $P < 0.05$, Tukey's *post hoc* test. **D**, Skulls and clavicles from P1 WT, *Rcan2*^{+/-}, and *Rcan2*^{-/-} mice. Bars, 1000 μm . **E**, Area of skull fontanelles, clavicle angle, and length in P1 WT, *Rcan2*^{+/-}, and *Rcan2*^{-/-} mice ($n = 4$ per genotype), ANOVA, *Rcan2*^{+/-}, and *Rcan2*^{-/-} vs. WT. *, $P < 0.05$, Tukey's *post hoc* test.

injections of calcein (15 mg/kg in saline with 2% NaHCO₃) 7 and 4 d before the animals were killed at postnatal day (P) 112.

Manipulation of thyroid status in wild-type (WT) mice

Hypothyroid mice were fed a low iodine diet containing 0.15% (wt/vol) of the antithyroid drug propylthiouracil from P70 for 6 wk. Hyperthyroid mice were treated with TSH-suppressive doses of T₄ (1.2 $\mu\text{g}/\text{ml}$ in drinking water) from P70 for 6 wk. Manipulation of thyroid status was performed under license in compliance with the Animals (Scientific Procedures) Act 1986, and the studies were approved by the local Imperial College London Biological Services Unit ethical review process.

Skeletal preparations and histology

P1 mice and limbs from older animals were stained with alizarin red and alcian blue (23, 24) and photographed using a Leica MZ75 binocular microscope, KL1500 light source, DFC320 digital camera, and IM50 Digital Image Manager (all from Leica AG, Heerbrugg, Switzerland). The angle of the clavicle, skull dimensions, and open fontanelle and suture areas were calcu-

lated using ImageJ 1.43n (<http://rsb.info.nih.gov/ij/>). Limbs were fixed in 10% neutral buffered formalin and decalcified in 10% EDTA. Sections were stained with van Gieson and alcian blue. Proliferative and hypertrophic zones in growth plate sections were identified as described (25–27). Measurements from at least four separate positions across the width of tibial growth plates were obtained using a Leica DM LB2 microscope and Leica DFC320 digital camera to calculate mean values for the heights of the reserve, proliferative, and hypertrophic zones and total growth plate. Results from two levels of sectioning were compared with ensure consistency.

Faxitron digital x-ray microradiography

Digital x-ray images were recorded at 10 μm resolution using a Faxitron MX20 variable kilovolt point projection x-ray source and digital image system operating at 26 kV and $\times 5$ magnification (Qados; Cross Technologies PLC, Berkshire, UK). Images were calibrated with a digital micrometer and bone lengths and caudal vertebra heights determined using ImageJ [National Institutes of Health (NIH)]. Cortical bone thickness and diameter were determined at 10 locations in the middiaphysis. Relative

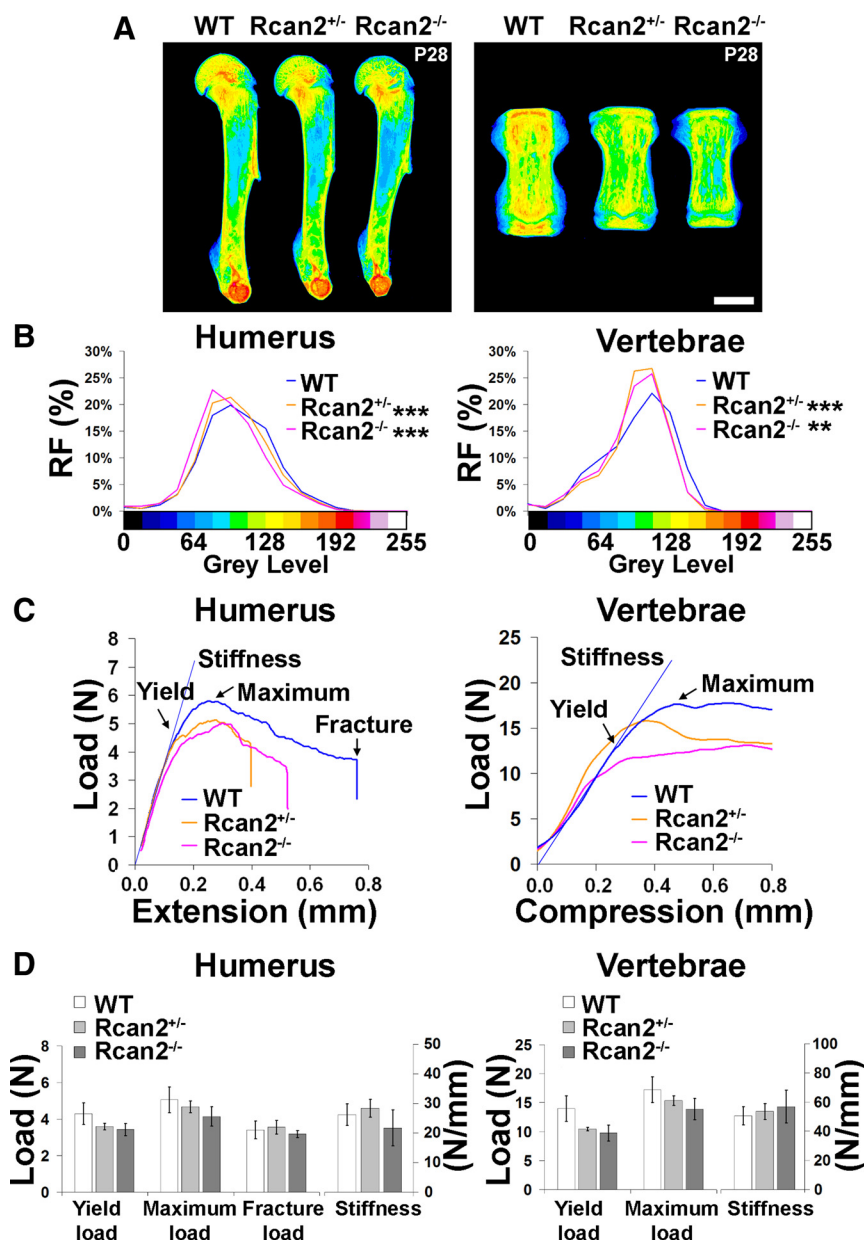


FIG. 3. Faxitron and biomechanical analysis in *Rcan2*^{-/-} mice during growth. **A**, Images of humerus and vertebrae from P28 WT, *Rcan2*^{+/-}, and *Rcan2*^{-/-} mice. Gray-scale images were pseudocolored according to a 16-color palette in which low mineral content is black and high mineral content is white. Bars, 1000 μ m. No statistical differences in humerus length or caudal vertebra height, ANOVA, *Rcan2*^{+/-}, and *Rcan2*^{-/-} vs. WT were seen. **B**, Relative and cumulative frequency histograms of bone mineralization densities ($n = 3$ per genotype). Kolmogorov-Smirnov test, *Rcan2*^{+/-}, or *Rcan2*^{-/-} vs. WT. **, $P < 0.01$; ***, $P < 0.001$. **C**, Representative load-displacement curves from destructive three-point bend testing of P28 WT, *Rcan2*^{+/-}, and *Rcan2*^{-/-} humeri showing yield load, maximum load, fracture load, and the gradient of the linear elastic phase (stiffness). Load-displacement curves from compression testing of P28 WT, *Rcan2*^{+/-}, and *Rcan2*^{-/-} caudal vertebrae show yield load, maximum load, and stiffness. **D**, Graphs showing yield, maximum, and fracture loads and stiffness of WT, *Rcan2*^{+/-}, and *Rcan2*^{-/-} humeri. No statistical differences, ANOVA ($n = 4$ per genotype), were seen. Graphs showing yield and maximum loads and stiffness of WT, *Rcan2*^{+/-}, and *Rcan2*^{-/-} vertebrae. No statistical differences, ANOVA ($n = 4$ per genotype), were seen.

mineral content was determined by comparison with steel, aluminum wire, and polyester fiber standards. The 2368×2340 16-bit DICOM images were converted to 8-bit Tiff images using

ImageJ (NIH), and the histogram stretched between polyester (gray level 0) and steel (gray level 255) standards. Gradations of mineralization density were represented in 16 equal intervals by a pseudocolor scheme (28).

Biomechanical testing

Bones were stored and tested in 70% ethanol. Destructive three-point bend tests were performed using an Instron 5543 load frame and 100 N load cell (Instron Ltd., High Wycombe, Buckinghamshire, UK). Bones were positioned horizontally and centered on custom supports, and the load was applied vertically to the midshaft with a constant rate of displacement of 0.03 mm/sec until fracture. A span of 5.6 mm was used. Biomechanical variables were derived from the load displacement curves as described previously (28–31).

Destructive compression tests were also performed on caudal vertebrae 6 and 7 (Ca6 and Ca7) using a 500 N load cell. Vertebral height and diameter was determined using ImageJ (NIH). Parallel surfaces were cut through adjacent intervertebral discs, and vertebrae were fixed to the center of the lower compression anvil with cyanoacrylate glue. The load was applied vertically with a constant rate of displacement of 0.03 mm/sec until failure with load displacement data acquired at 100 Hz. Load-displacement curves were plotted and yield load, displacement at maximum load, and stiffness were determined. Work energy was calculated from the area under the load displacement curve at maximum load. Elastic stored energy at maximum load was determined by calculating the area of a right-angled triangle with the vertex at the point of maximum load and a hypotenuse with a slope equal to that of the linear phase of the load-displacement curve. Energy dissipated at maximum load was calculated by subtracting the elastic stored energy from the work energy at maximum load.

Backscattered electron (BSE) scanning electron microscopy (SEM)

Long bones were fixed in 70% ethanol and opened longitudinally along anatomical curvatures as described (28). Samples were coated with carbon and imaged using backscattered electrons at 20 kV beam potential in a Zeiss DSM962 digital scanning electron microscope equipped with an annular solid state BSE detector (KE Electronics, Toft, Cambridgeshire, UK). The images provide detailed views of bone

mineral content was determined by comparison with steel, aluminum wire, and polyester fiber standards. The 2368×2340 16-bit DICOM images were converted to 8-bit Tiff images using

TABLE 1. 3 point bend and compression testing

			Yield load (N)	Maximum Load (N)	Fracture Load (N)	Stiffness (N/mm)	Energy dissipated at max load (%)	Energy dissipated at fracture load (%)
WT	P28	Humerus	4.3 ± 0.6	5.1 ± 0.7	3.4 ± 0.5	26 ± 4	43 ± 4	90 ± 2
<i>Rcan2</i> ^{+/-}	P28	Humerus	3.6 ± 0.2	4.7 ± 0.3	3.6 ± 0.4	28 ± 3	58 ± 5	89 ± 3
<i>Rcan2</i> ^{-/-}	P28	Humerus	3.4 ± 0.3	4.1 ± 0.5	3.2 ± 0.2	22 ± 6	51 ± 11	88 ± 2
WT	P28	Ca6+Ca7	13.9 ± 2.2	17.2 ± 2.2		51 ± 6.2	35 ± 2	
<i>Rcan2</i> ^{+/-}	P28	Ca6+Ca7	10.5 ± 0.3	15.4 ± 0.8		54 ± 5.4	52 ± 3	
<i>Rcan2</i> ^{-/-}	P28	Ca6+Ca7	9.8 ± 1.4	13.9 ± 1.8		56 ± 11.5	52 ± 10	
WT	P112	Humerus	8.2 ± 0.1	13.2 ± 1.9	11.6 ± 1.5	61 ± 2	33 ± 5	46 ± 11
<i>Rcan2</i> ^{-/-}	P112	Humerus	8.3 ± 0.5	10.9 ± 1.5	12.3 ± 0.6	54 ± 7	29 ± 10	35 ± 8
WT	P112	Ca6+Ca7	88 ± 9	97 ± 8		321 ± 20	17 ± 2	
<i>Rcan2</i> ^{-/-}	P112	Ca6+Ca7	77 ± 6	86 ± 6		329 ± 12	18 ± 1	

P28: WT, *Rcan2*^{+/-}, and *Rcan2*^{-/-} mice (n = 3 per genotype); >P112: WT and *Rcan2*^{-/-} mice (n = 3 per genotype).

surfaces and microarchitecture from which surface activity states (forming, resting, resorbing, resorbed) can be investigated (32, 33). The fraction of the trabecular and endosteal surfaces that displayed osteoclastic bone resorption was quantified using ImageJ (NIH).

Quantitative BSE-SEM (qBSE-SEM)

Bone micromineralization density was determined at cubic micron resolution by qBSE-SEM. Block faces were cut through polymethylmethacrylate-embedded specimens and analyzed in the SEM operated at 20 kV and 0.5 nA at a working distance of 17 mm (11 mm sample to detector). Gradations of micromineralization density were represented in eight equal intervals by a pseudocolor scheme as described (28, 34–36).

Microcomputed tomography(CT) analysis

Humeri were analyzed by micro-CT (Skyscan 1172a; Kon-tich, Belgium) at 50 kV and 200 μ A using a 0.5-mm aluminum filter and a detection pixel size of 4.3 μ m². Scanned images were reconstructed using Skyscan NRecon software (28). One cubic millimeter of area, 0.2 mm from the growth plate, was selected as the region of interest. Trabecular bone volume as proportion of tissue volume (percentage), trabecular thickness (millimeters), trabecular number (millimeters⁻¹), and structure model index were analyzed in the region of interest using the Skyscan CT analysis software. Cortical bone volume (cubic millimeters) was also determined in the region of interest.

Osteoclastic bone resorption

Osteoclast numbers were determined in samples fixed in 10% neutral buffered formalin and decalcified in 10% EDTA (pH 7.4). Sections were stained for tartrate-resistant acid phosphatase (TRAP) using a Sigma TRAP kit (386A-1KT; Sigma, Poole, Dorset, UK) and photographed at \times 200 magnification using a Leica DM LB2 microscope and DFC320 digital camera and a montage of nine overlapping fields constructed for each bone, representing an area of approximately 1 mm². Osteoclast numbers (Oc.N) and surface (Oc.S) were determined in trabecular bone and normalized to total bone surface (BS). Measurements commenced 0.2 mm below the growth plate (25, 26).

Osteoblastic bone formation

Midline longitudinal and midcoronal block faces were cut through methacrylate embedded specimens and examined using a Leica SP2 reflection confocal microscope with 488 nm excitation and \times 10/1.0 and \times 40/1.25 objectives to determine the fraction of bone surface undergoing active bone formation as described (28, 37). Mineral apposition rate (MAR) was calculated by determining calcein separation at between 10 and 20 locations per specimen using ImageJ (NIH). Montages of trabecular bone were generated and the BS and mineralizing surface (MS) measured using ImageJ. Bone formation rate (BFR) was calculated from the product of MS and MAR. Measurements commenced 0.2 mm below the growth plate.

Semiquantitative RT-PCR

cDNA was synthesized from total RNA (2.5 μ g), and 1 μ l cDNA was used for PCR amplification of *Rcan2-1*, *Rcan2-3*, and *Gapdh* (38). The nucleotide (nt) positions indicate the locations of PCR primers within the GenBank reference sequence: *Rcan2-1* forward primer, Rcan2-1 F (nt 294–313), reverse primer Rcan2-1R (nt 530–511) (GenBank NM_207649); *Rcan2-3* forward primer, Rcan2-3 F (nt 205–224), reverse primer, Rcan2-3R (nt 423–404) (NM_030598); *Gapdh* forward primer, GapdhF (nt 658–677), reverse primer, GapdhR (nt 881–863) (NM_008084) (Fig. 1). PCR were performed with an initial denaturation step at 94 C for 2 min, cycles of 30 sec at 94 C, 30 sec at an annealing temperature of 55 C, and 30 sec at 72 C, followed by a termination step at 72 C for 3 min. Semiquantitative RT-PCR was optimized as described (39) and cDNA amplified using the optimized number of PCR cycles for each gene (25 cycles for *Gapdh*; 28 cycles for *Rcan2-1* and *Rcan2-3*).

Osteoblast cultures

Calvaria were removed from 2-d-old mice and osteoblasts isolated by sequential collagenase digestion. Osteoblasts were cultured in 75-cm² flasks in modified Eagle's medium supplemented with 10% fetal calf serum, L-glutamine, penicillin, and streptomycin for 72 h. Cells were replated in six-well plates (250,000 cells/well) and maintained for 48 h before culture in serum-free medium overnight. Cells were treated with vehicle or T₃ (100 nM) for 6 h before RNA extraction with Trizol or isolation of nuclear and cytoplasmic protein fractions using an NE-PER kit (Thermo Scientific, Waltham, MA).

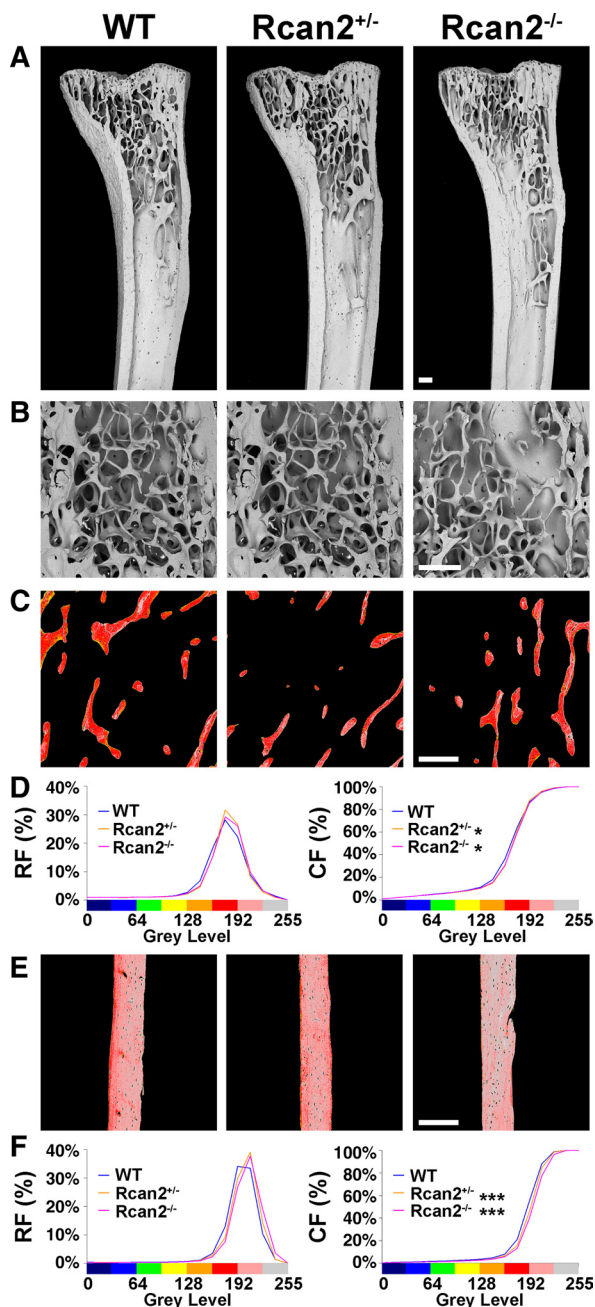


FIG. 4. Bone microarchitecture and micromineralization in adult *Rcan2*^{-/-} mice. A and B, Low-power BSE-SEM views of proximal tibia and high-power views of distal femur from P112 WT, *Rcan2*^{+/-}, and *Rcan2*^{-/-} mice (n = 3 per genotype). Bars, 200 μ m. C, qBSE-SEM images of trabecular bone from proximal humerus of P112 WT, *Rcan2*^{+/-}, and *Rcan2*^{-/-} mice (n = 2–4 per genotype). Gray-scale images were pseudocolored according to an eight-color palette in which the low mineralization density is blue and the high density is gray. Bar, 200 μ m. D, Relative and cumulative frequency histograms of trabecular bone micromineralization densities. *, $P < 0.05$, *Rcan2*^{+/-} or *Rcan2*^{-/-} vs. WT, Kolmogorov-Smirnov test, WT (n = 4), *Rcan2*^{+/-} (n = 2), and *Rcan2*^{-/-} (n = 4). E, qBSE-SEM images of cortical bone from the midshaft of the humerus in WT, *Rcan2*^{+/-}, or *Rcan2*^{-/-} mice. Bar, 200 μ m. F, Frequency histograms of cortical bone micromineralization densities. ***, $P < 0.001$, *Rcan2*^{+/-} or *Rcan2*^{-/-} vs. WT, Kolmogorov-Smirnov test, WT (n = 4), *Rcan2*^{+/-} (n = 2), and *Rcan2*^{-/-} (n = 4).

Real-time RT-PCR

Total RNA was extracted from calvarial osteoblasts and whole bones, and 1 μ g was reverse transcribed (QunatiTect reverse transcriptase kit; QIAGEN, Hilden, Germany). cDNA was amplified using *Rcan2*-1 and *Rcan2*-3 primers described above and β -actin and *18s rRNA* primers as follows: β -actin forward primer, β -ActinF (nt 1035–1058), reverse primer, β -ActinR (nt 1234–1209) (NM_007393); *18s rRNA* forward primer, 18sF (nt 1443–1461), reverse primer, 18sR (nt 1549–1530) (NM_003278). RT-PCR was performed using a 7900HT Fast real-time machine (Applied Biosystems, Foster City, CA) and analyzed with SDS2.3 software (Applied Biosystems). PCRs were performed with an initial denaturation step at 95 C for 10 min followed by 40 cycles of 95 C for 15sec, 30 sec at an annealing temperature of 60 C, and 30 sec at 72 C, followed by a dissociation stage to allow melt curve analysis.

Immunoprecipitation

Nuclear and cytoplasmic protein fractions were isolated from primary calvarial osteoblasts using a NE-PER kit (Thermo Scientific). 20 μ g of each fraction was pre-cleared using protein G-Sepharose beads (GE Healthcare, Hatfield, Hertfordshire, UK) for 1 h. Cleared lysates were incubated overnight with 5 μ g of anti-NFATc1 monoclonal antibody (Santa Cruz Biotechnology, Santa Cruz, CA) before the addition of protein-G-Sepharose beads for 1 h and collection of immunoprecipitates by centrifugation. Samples were washed four times in PBS and eluted in protein sample buffer. SDS-PAGE and Western blotting were then performed using anti-NFATc1 monoclonal antibody (Santa Cruz Biotechnology) or an antiphosphoserine antibody (Abcam, Cambridge UK).

Statistics

Normally distributed data were analyzed by ANOVA followed by Tukey's multiple comparison *post hoc* test. $P < 0.05$ was considered significant. Frequency distributions of bone micromineralization densities obtained by Faxitron and qBSE were compared using the Kolmogorov-Smirnov test, in which P values for the D statistic in 1024 pixel data sets were $D =$ greater than 6.01, $P < 0.05$; $D =$ greater than 7.20, $P < 0.01$, and $D =$ greater than 8.62 $P < 0.001$.

Results

Bone development in *Rcan2*^{-/-} mice

To determine whether deletion of *Rcan2* affects bone formation, endochondral and intramembranous ossification was analyzed in neonatal P1 mice, and linear growth was characterized between P1 and P112 (Fig. 2, A–E). There were no differences in endochondral bone formation or linear growth between WT and mutant mice (Fig. 2, A–C). Consistent with these findings, histological analysis of the growth plate revealed no differences between WT and *Rcan2* mutant mice at P28 (Fig. 2, B and C). By contrast, intramembranous ossification was delayed in P1 *Rcan2*^{-/-} mice, in which wider skull sutures and fonta-

nelles were present compared with WT mice and heterozygotes, although clavicle morphology was normal (Fig. 2, D and E). Cortical bone thickness was also reduced by 17% in *Rcan2*^{-/-} mice in the middiaphysis of the humerus at P28 (Fig. 2C), although this difference in cortical thickness was not maintained at P112 (data not shown). Thus, during skeletal development *Rcan2*-deficient mice display normal endochondral ossification in the growth plate but impaired intramembranous ossification and cortical bone formation.

Bone mineralization and strength in juvenile *Rcan2*^{-/-} mice

To determine whether deletion of *Rcan2* affects bone mineralization, bone mineral content in P28 mice was analyzed by Faxitron digital x-ray microradiography. Relative and cumulative frequency histograms revealed reduced bone mineral content in *Rcan2*^{-/-} mice and reduced vertebral bone mineral content in both *Rcan2*^{-/-} and *Rcan2*^{+/-} mice (Fig. 3, A and B). To determine whether reduced bone mineral content and cortical bone thickness in juvenile *Rcan2*^{-/-} mice was accompanied by impaired bone strength, destructive three-point bend testing was performed on humeri and compression testing on caudal vertebrae from P28 mice. Although biomechanical analysis demonstrated a trend to suggest that bone strength is impaired in *Rcan2*^{-/-} mice, the data did not reach statistical significance (Fig. 3, C and D, and Table 1).

Bone microarchitecture in adult *Rcan2*^{-/-} mice

To investigate the structure of adult bone in *Rcan2*^{-/-} mice, bone microarchitecture was analyzed. Low-power BSE-SEM views of proximal tibia revealed no differences in cortical or trabecular bone between mutant and WT mice at P112 (Fig. 4A). In higher-power views, the thickness and connectivity of individual trabeculae was similar among *Rcan2*^{+/-} and *Rcan2*^{-/-} and WT mice (Fig. 4B). Accordingly, trabecular and cortical bone parameters determined by micro-CT (Table 2), and cortical thickness determined by Faxitron (data not shown), did not differ between mutant and WT mice. Thus, adult *Rcan2* mutant mice have normal bone microarchitecture.

Bone mineralization and strength in adult *Rcan2*^{-/-} mice

Detailed studies of bone mineralization were performed using qBSE-SEM (Fig. 4, C–F). Frequency histograms of micromineralization densities from trabecular (Fig. 4D) and cortical bone (Fig. 4F) demonstrated increased mineralization in *Rcan2*^{+/-} and *Rcan2*^{-/-} mice. Thus, in contrast to the reduced bone mineral content identified in juveniles, adult *Rcan2* mutant mice display increased bone mineralization. To determine whether this increased bone mineralization was accompanied by altered bone strength three-point bend and compression testing was performed. Despite the observed changes in mineralization, biomechanical parameters did not differ between *Rcan2*^{-/-} and WT mice (Table 1).

Bone resorption and bone formation in *Rcan2*^{-/-} mice

To investigate whether changes in osteoclastic bone resorption also occur in *Rcan2* mutant mice, histomorphometry and BSE-SEM analyses were performed. Sections were stained for TRAP to determine the Oc.N and quantify Oc.S in relation to the total trabecular BS (Fig. 5, A and B), but no differences in these parameters were identified between mutant and WT mice. The areas of osteoclastic bone resorption on trabecular and endosteal bone surfaces were quantified in higher resolution BSE-SEM images (Fig. 5, C and D), and no differences were identified in the resorption surface relative to total BS between mutant and WT mice.

To investigate osteoblast function and bone formation parameters, mineralizing surfaces, MAR, and BFR were quantified in bones from the calcein-labeled mice (Fig. 5, E and F). Mineralizing surfaces were reduced by 54% and MAR by 29% in *Rcan2*-deficient mice, and consequently, bone formation rate was reduced by 67% in *Rcan2*^{-/-} mice. Thus, *Rcan2*-deficient mice exhibit an isolated defect in osteoblast function but have normal osteoclast function.

Rcan2 expression in bone

Expression of *Rcan2* in the skeleton and its regulation by thyroid hormones were investigated in primary bone

TABLE 2. Micro-CT analysis

			BV/TV (%)	Tb.Th (mm)	Tb.N (mm ⁻¹)	SMI	Cortical BV (mm ³)
WT	P112	Humerus	8.1% ± 0.7	0.038 ± 0.001	2.1 ± 0.18	1.91 ± 0.07	0.59 ± 0.02
<i>Rcan2</i> ^{-/-}	P112	Humerus	8.8% ± 2.7	0.038 ± 0.001	2.3 ± 0.71	1.94 ± 0.28	0.53 ± 0.05

WT and *Rcan2*^{-/-} mice (n = 3 per genotype). BV/TV, Trabecular bone volume as proportion of tissue volume; Tb.Th, trabecular thickness; Tb.N, trabecular number; SMI, structure model index; Cortical BV, Cortical bone volume.

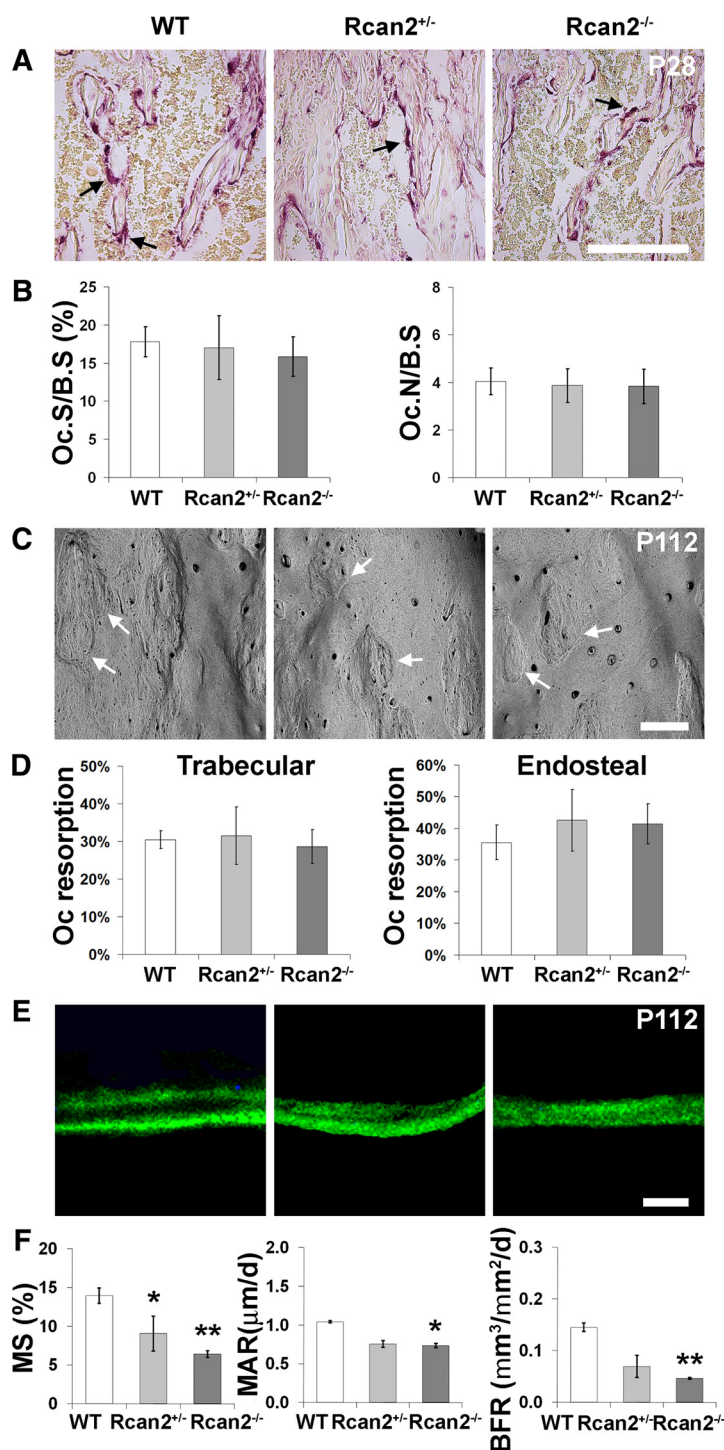


FIG. 5. Bone turnover in *Rcan2*^{-/-} mice. **A**, TRAP-stained sections of tibia trabecular bone from P112 WT, *Rcan2*^{+/-}, and *Rcan2*^{-/-} mice. *Black arrows* indicate TRAP-stained osteoclasts. *Bar*, 200 μm. **B**, Quantitative analysis of Oc.S and the Oc.N relative to BS. No statistical differences, ANOVA, WT (n = 4), *Rcan2*^{+/-} (n = 2), and *Rcan2*^{-/-} (n = 4), were seen. **C**, Endosteal bone surfaces from P112 WT, *Rcan2*^{+/-}, and *Rcan2*^{-/-} mice imaged by BSE-SEM. *White arrows* indicate roughened osteoclast resorption surfaces. *Bar*, 200 μm. **D**, Quantitative analysis of trabecular and endosteal osteoclast resorption surfaces (percentage of total bone surface). No statistical differences, ANOVA, WT (n = 4), *Rcan2*^{+/-} (n = 2) and *Rcan2*^{-/-} (n = 4), were seen. **E**, Calcein labeling of trabecular bone from WT, *Rcan2*^{+/-}, and *Rcan2*^{-/-} mice. *Bar*, 10 μm. **F**, Trabecular bone MS, MAR, and BFR determined by dual-calcein labeling. ANOVA, *Rcan2*^{+/-} (n = 2) and *Rcan2*^{-/-} (n = 4) vs. WT (n = 4), *, *P* < 0.05 and **, *P* < 0.01, Tukey's *post hoc* test.

cell cultures from WT mice and in bones obtained from TR knockout and thyroid-manipulated mice. In primary osteoclast cultures, bone marrow monocytes and osteoclast precursors expressed *Rcan2-1* but not *Rcan2-3*, whereas mature osteoclasts expressed only *Rcan2-3*. By contrast, primary osteoblasts expressed both isoforms (Fig. 6).

Mice lacking TRα (TRα^{0/0}) have impaired T₃ signaling in bone because they lack expression of TRα, the predominant functional TR isoform in the skeleton (26, 40). By contrast, mice lacking TRβ (TRβ^{-/-}) have increased thyroid hormone signaling in bone due to activation of the normal TRα isoform by elevated circulating thyroid hormones (25, 26). The level of *Rcan2-1* expression was similar in juvenile and adult TRα^{0/0}, TRβ^{-/-}, and WT mice, whereas expression of *Rcan2-3* was reduced by 50% in juvenile TRα^{0/0} mice (Fig. 7). Consistent with these findings, skeletal *Rcan2-3* mRNA expression was increased by more than 2-fold in thyrotoxic WT mice compared with hypothyroid animals (Fig. 8A).

In vitro studies in primary osteoblasts

In primary cultures of WT calvarial osteoblasts, T₃ treatment did not affect the levels of *Rcan2-1* or *Rcan2-3* mRNA expression (Fig. 8B). Furthermore, T₃ treatment did not alter levels of NFATc1 protein expression or phosphorylation and did not affect its relative distribution between nuclear and cytoplasmic compartments (Fig. 8C).

Discussion

These studies demonstrate that, despite normal endochondral ossification and linear growth, juvenile *Rcan2*^{-/-} mice display delayed intramembranous ossification, impaired cortical bone formation, and reduced bone mineral accrual.

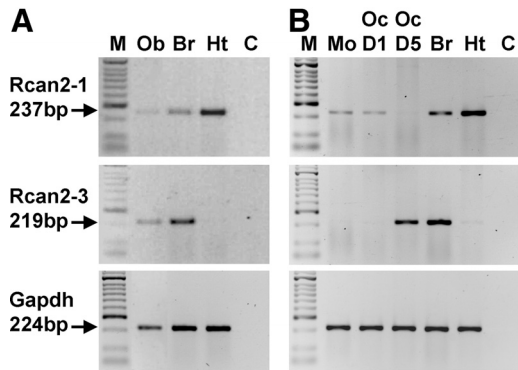


FIG. 6. *Rcan2* mRNA expression in primary osteoblasts and osteoclasts. A, *Rcan2-1*, *Rcan2-3*, and *Gapdh* mRNA expression in primary osteoblasts (M; size marker). Ob, Osteoblasts; Br, brain; Ht, heart; and C, no template control. B, *Rcan2-1* and *Rcan2-3* expression in primary osteoclasts (Mo; bone marrow monocytes). Oc D1, Osteoclast precursors (d 1 of culture); and Oc D5, mature osteoclasts (d 5 of culture).

Adult *Rcan2*^{-/-} mice exhibit normal bone microarchitecture but increased mineralization. Heterozygous *Rcan2*^{+/-} mice have an intermediate phenotype consistent with a gene dosage effect. The skeletal abnormalities in *Rcan2*^{-/-} mice were accompanied by normal bone resorption but reduced bone formation, indicating an isolated defect in osteoblast function. The resulting reduction in mineral apposition rate leads to an extended bone formation phase and prolongation of the bone remodeling cycle. This protracted phase of osteoblastic bone formation is accompanied by a longer period of secondary mineralization (41, 42), which results in the observed increase in bone mineralization in adult *Rcan2*^{-/-} mice.

Thyroid hormones have major effects on skeletal development and adult bone maintenance (43, 44). Hypothyroidism delays bone formation and linear growth, whereas thyrotoxicosis accelerates skeletal development and is an important risk factor for osteoporosis. In previous studies we characterized mice with mutation or deletion of TR α and TR β in several genetic backgrounds (21, 23–27). Juvenile TR α mutants exhibit delayed endochondral ossification and impaired growth, whereas juvenile TR β mutants have advanced ossification. By contrast, adult TR α mutants have increased bone mass resulting from disrupted T₃ action in bone, whereas adult TR β mutants are osteoporotic due to increased T₃ signaling in the skeleton as a consequence of elevated circulating thyroid hormone concentrations (23, 40). Taken together, these studies indicate TR α mediates T₃ action in bone (21).

In studies to investigate the role of TR α in skeletal development, we characterized a series of TR α mutant mice (23, 25, 26). Mice lacking TR α (TR α ^{0/0}) had delayed endochondral ossification but normal intramembranous ossification and normal adult bone mineralization. By con-

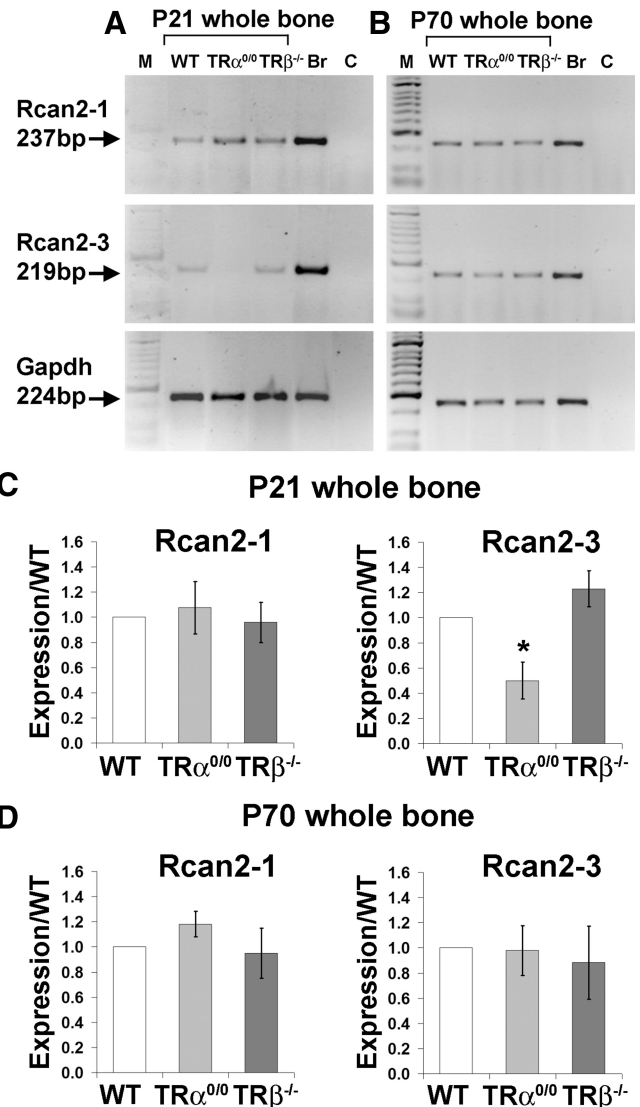


FIG. 7. *Rcan2* mRNA expression in bone from TR knockout mice. A, *Rcan2-1* and *Rcan2-3* mRNA expression in juvenile WT, TR α ^{0/0}, and TR β ^{-/-} bone at age P21. B, *Rcan2-1* and *Rcan2-3* mRNA expression in adult WT, TR α ^{0/0}, and TR β ^{-/-} bone at age P70. C, Graphs showing *Rcan2-1* and *Rcan2-3* mRNA expression, normalized to *Gapdh*, in bone from juvenile TR α ^{0/0} and TR β ^{-/-} mice compared with WT. ANOVA, *Rcan2*^{+/-} and *Rcan2*^{-/-} vs. WT. *, $P < 0.05$, Tukey's *post hoc* test, $n = 4$ per genotype. D, Graphs showing *Rcan2-1* and *Rcan2-3* mRNA expression, normalized to *Gapdh*, in bone from adult TR α ^{0/0} and TR β ^{-/-} mice compared with WT. No significant difference, ANOVA, $n = 4$ per genotype, was seen.

trast, mice harboring a dominant-negative mutation of TR α (TR α 1^{PV/+} and TR α 1^{R384C/+}) had delayed endochondral and intramembranous ossification accompanied by increased adult bone mineralization (23, 25, 26). In further studies we showed that expression of the type 2 deiodinase enzyme (DIO2), which generates T₃ in thyroid hormone-responsive target cells, is restricted to differentiated osteoblasts in the skeleton (45). Accordingly, *Dio2* knockout mice (*Dio2*^{-/-}) exhibited a discrete defect of osteoblast function, resulting in increased adult bone min-

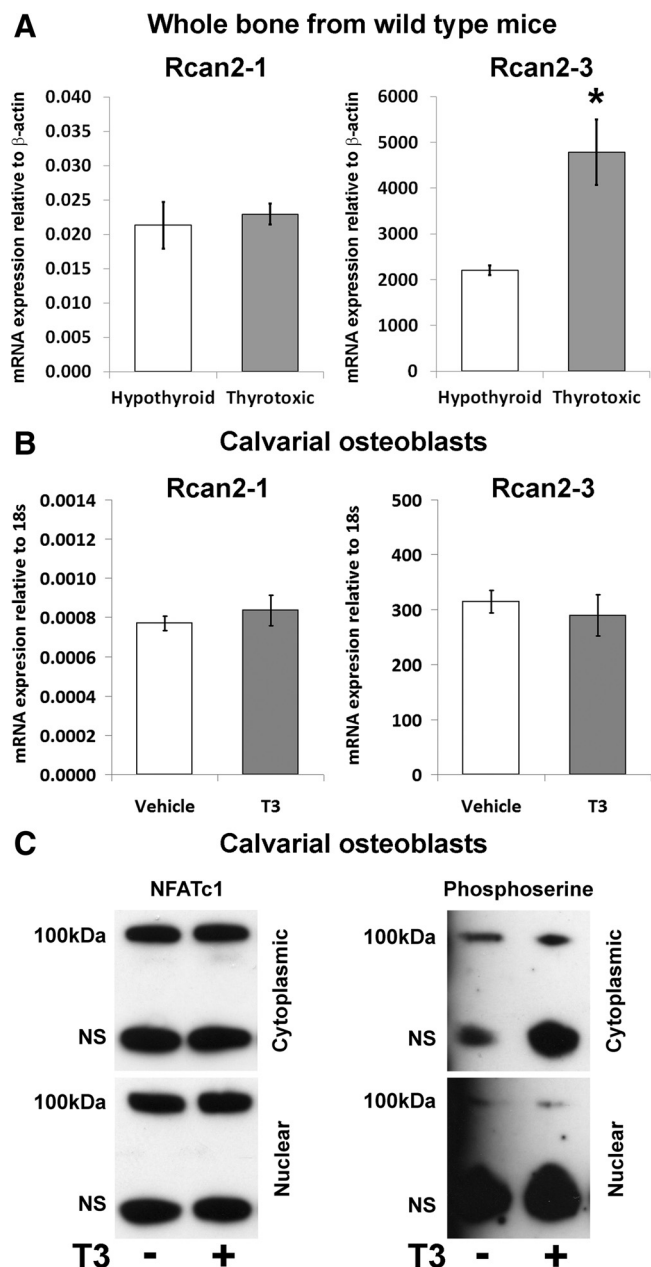


FIG. 8. *Rcan2* mRNA expression in whole bone and primary osteoblasts from WT mice and expression and phosphorylation of NFATc1 in WT osteoblasts treated with T_3 . **A**, *Rcan2-1* and *Rcan2-3* mRNA expression in whole bone from hypothyroid and thyrotoxic P112 WT mice. Unpaired Student's *t* test, hypothyroid vs. thyrotoxic. *, $P < 0.05$, $n = 3$ per group. **B**, *Rcan2-1* and *Rcan2-3* mRNA expression in primary calvarial osteoblasts obtained from WT mice. No significant difference, unpaired Student's *t* test, hypothyroid vs. thyrotoxic, $n = 3$ per group, was seen. **C**, Immunoprecipitation and Western blot analysis of total and phosphorylated NFATc1 in nuclear and cytoplasmic protein fractions from cultured primary calvarial osteoblasts treated with vehicle or T_3 (100 nM). No significant difference, unpaired Student's *t* test, vehicle vs. T_3 , $n = 3$ per group, was seen.

eralization (28). Thus, the findings of delayed intramembranous ossification and increased adult bone mineralization identified in *Rcan2*^{-/-} mice are similar to those in

mice with osteoblast defects due to dominant negative mutations of TR α or deletion of *Dio2*.

Cell-specific gene targeting has demonstrated that the calcineurin-NFAT pathway is a negative regulator of osteoblast differentiation (12). Thus, deletion of the endogenous calcineurin inhibitor RCAN2 would be expected to inhibit osteoblast activity further by removal of tonal inhibition of calcineurin activity in osteoblasts. The findings of delayed intramembranous ossification, impaired cortical bone formation, and reduced bone mineral accrual during development, together with increased bone mineralization in adult *Rcan2*^{-/-} mice are all consistent with this hypothesis. Together with the previous similar findings in TR α and *Dio2* mutant mice (23, 25, 26, 28), the skeletal phenotype of *Rcan2*^{-/-} mice suggests that Rcan2 may lie downstream of T_3 signaling in osteoblasts.

We therefore investigated thyroid hormone regulation of *Rcan2* expression in skeletal cells *in vivo* and *in vitro*. Both *Rcan2-1* and *Rcan2-3* mRNA were expressed in bone *in vivo* and, consistent with previous studies in fibroblasts (16), only the *Rcan2-3* isoform was regulated by thyroid status or deletion of TR α . *In vitro* studies demonstrated that expression of *Rcan2-1* and *Rcan2-3* was bone cell lineage specific and dependent on the stage of cell differentiation. Osteoblasts expressed both *Rcan2* mRNA isoforms and immature osteoclast precursor cells expressed only *Rcan2-1*, whereas mature differentiated osteoclasts expressed only *Rcan2-3*. The absence of an osteoclast phenotype in *Rcan2*^{-/-} mice suggests the actions of Rcan2 are dispensable in the osteoclast lineage, and this may reflect redundancy in regulation of calcineurin/NFAT signaling. Expression of both *Rcan2* transcripts in osteoblasts suggests that Rcan2 may mediate some of the actions of T_3 in osteoblasts.

To address this, primary osteoblasts were treated with T_3 . Even though skeletal *Rcan2-3* expression was increased in thyrotoxic animals, T_3 treatment did not affect *Rcan2-3* or *Rcan2-1* expression in primary osteoblasts. Furthermore, immunoprecipitation studies to investigate expression of the calcineurin target gene NFATc1 and its phosphorylation in cytoplasmic and nuclear compartments also revealed no response to T_3 . These *in vitro* studies suggest that, even though skeletal expression of *Rcan2* is regulated by thyroid status *in vivo*, the phenotype identified in *Rcan2*^{-/-} mice is unlikely to result directly from disruption of T_3 signaling in osteoblasts.

Nevertheless, the current studies establish that Rcan2 regulates osteoblast activity during growth and maintenance of bone mineralization in adults.

Acknowledgments

We thank Maureen Arora for SEM studies.

Address all correspondence and requests for reprints to: Graham R. Williams, Molecular Endocrinology Group, Room 7N2a, Commonwealth Building, Hammersmith Hospital, Du Cane Road, London W12 0NN, United Kingdom. E-mail: graham.williams@imperial.ac.uk.

This work was supported by Medical Research Council research grants (to J.H.D.B. and G.R.W.) and a grant from the Horserace Betting Levy Board (to A.B.). The SEM study was funded by the Medical Research Council. P.C. is supported by the Mrs. Janice Gibson and the Ernest Heine Family Foundation.

Disclosure Summary: The authors have nothing to disclose.

References

- Kingsbury TJ, Cunningham KW 2000 A conserved family of calcineurin regulators. *Genes Dev* 14:1595–1604
- Davies KJ, Ermak G, Rothermel BA, Pritchard M, Heitman J, Ahnn J, Henrique-Silva F, Crawford D, Canaider S, Strippoli P, Carinci P, Min KT, Fox DS, Cunningham KW, Bassel-Duby R, Olson EN, Zhang Z, Williams RS, Gerber HP, Pérez-Riba M, Seo H, Cao X, Klee CB, Redondo JM, Maltais LJ, Bruford EA, Povey S, Molkentin JD, McKeon FD, Duh EJ, Crabtree GR, Cyert MS, de la Luna S, Estivill X 2007 Renaming the DSCR1/Adapt78 gene family as RCAN: regulators of calcineurin. *FASEB J* 21:3023–3028
- Klee CB, Crouch TH, Krinks MH 1979 Calcineurin: a calcium- and calmodulin-binding protein of the nervous system. *Proc Natl Acad Sci USA* 76:6270–6273
- Crabtree GR 1999 Generic signals and specific outcomes: signaling through Ca²⁺, calcineurin, and NF-AT. *Cell* 96:611–614
- Stern PH 2006 The calcineurin-NFAT pathway and bone: intriguing new findings. *Mol Interv* 6:193–196
- Fuentes JJ, Genescà L, Kingsbury TJ, Cunningham KW, Pérez-Riba M, Estivill X, de la Luna S 2000 DSCR1, overexpressed in Down syndrome, is an inhibitor of calcineurin-mediated signaling pathways. *Hum Mol Genet* 9:1681–1690
- Rothermel B, Vega RB, Yang J, Wu H, Bassel-Duby R, Williams RS 2000 A protein encoded within the Down syndrome critical region is enriched in striated muscles and inhibits calcineurin signaling. *J Biol Chem* 275:8719–8725
- Takayanagi H 2007 The role of NFAT in osteoclast formation. *Ann NY Acad Sci* 1116:227–237
- Sun L, Blair HC, Peng Y, Zaidi N, Adebajo OA, Wu XB, Wu XY, Iqbal J, Epstein S, Abe E, Moonga BS, Zaidi M 2005 Calcineurin regulates bone formation by the osteoblast. *Proc Natl Acad Sci USA* 102:17130–17135
- Koga T, Matsui Y, Asagiri M, Kodama T, de Crombrugge B, Nakashima K, Takayanagi H 2005 NFAT and Osterix cooperatively regulate bone formation. *Nat Med* 11:880–885
- Winslow MM, Pan M, Starbuck M, Gallo EM, Deng L, Karsenty G, Crabtree GR 2006 Calcineurin/NFAT signaling in osteoblasts regulates bone mass. *Dev Cell* 10:771–782
- Yeo H, Beck LH, Thompson SR, Farach-Carson MC, McDonald JM, Clemens TL, Zayzafoon M 2007 Conditional disruption of calcineurin B1 in osteoblasts increases bone formation and reduces bone resorption. *J Biol Chem* 282:35318–35327
- Yeo H, Beck LH, McDonald JM, Zayzafoon M 2007 Cyclosporin A elicits dose-dependent biphasic effects on osteoblast differentiation and bone formation. *Bone* 40:1502–1516
- Epstein S, Shane E, Bilezikian JP 1995 Organ transplantation and osteoporosis. *Curr Opin Rheumatol* 7:255–261
- Miyazaki T, Kanou Y, Murata Y, Ohmori S, Niwa T, Maeda K, Yamamura H, Seo H 1996 Molecular cloning of a novel thyroid hormone-responsive gene, ZAKI-4, in human skin fibroblasts. *J Biol Chem* 271:14567–14571
- Cao X, Kambe F, Miyazaki T, Sarkar D, Ohmori S, Seo H 2002 Novel human ZAKI-4 isoforms: hormonal and tissue-specific regulation and function as calcineurin inhibitors. *Biochem J* 367:459–466
- Cao X, Kambe F, Moeller LC, Refetoff S, Seo H 2005 Thyroid hormone induces rapid activation of Akt/protein kinase B-mammalian target of rapamycin-p70S6K cascade through phosphatidylinositol 3-kinase in human fibroblasts. *Mol Endocrinol* 19:102–112
- Siddiq A, Miyazaki T, Takagishi Y, Kanou Y, Hayasaka S, Inouye M, Seo H, Murata Y 2001 Expression of ZAKI-4 messenger ribonucleic acid in the brain during rat development and the effect of hypothyroidism. *Endocrinology* 142:1752–1759
- Mizuno Y, Kanou Y, Rogatcheva M, Imai T, Refetoff S, Seo H, Murata Y 2004 Genomic organization of mouse ZAKI-4 gene that encodes ZAKI-4 α and β isoforms, endogenous calcineurin inhibitors, and changes in the expression of these isoforms by thyroid hormone in adult mouse brain and heart. *Eur J Endocrinol* 150:371–380
- Yang J, Rothermel B, Vega RB, Frey N, McKinsey TA, Olson EN, Bassel-Duby R, Williams RS 2000 Independent signals control expression of the calcineurin inhibitory proteins MCIP1 and MCIP2 in striated muscles. *Circ Res* 87:E61–E68
- Bassett JH, Williams GR 2009 The skeletal phenotypes of TR α and TR β mutant mice. *J Mol Endocrinol* 42:269–282
- Sun XY, Hayashi Y, Xu S, Kanou Y, Takagishi Y, Tang YP, Murata Y 2011 Inactivation of the Rcan2 gene in mice ameliorates the age- and diet-induced obesity by causing a reduction in food intake. *PLoS One* 6:e14605
- O'Shea PJ, Bassett JH, Srisankharajah S, Ying H, Cheng SY, Williams GR 2005 Contrasting skeletal phenotypes in mice with an identical mutation targeted to thyroid hormone receptor α 1 or β . *Mol Endocrinol* 19:3045–3059
- O'Shea PJ, Harvey CB, Suzuki H, Kaneshige M, Kaneshige K, Cheng SY, Williams GR 2003 A thyrotoxic skeletal phenotype of advanced bone formation in mice with resistance to thyroid hormone. *Mol Endocrinol* 17:1410–1424
- Bassett JH, Nordström K, Boyde A, Howell PG, Kelly S, Vennström B, Williams GR 2007 Thyroid status during skeletal development determines adult bone structure and mineralization. *Mol Endocrinol* 21:1893–1904
- Bassett JH, O'Shea PJ, Srisankharajah S, Rabier B, Boyde A, Howell PG, Weiss RE, Roux JP, Malaval L, Clement-Lacroix P, Samarut J, Chassande O, Williams GR 2007 Thyroid hormone excess rather than thyrotropin deficiency induces osteoporosis in hyperthyroidism. *Mol Endocrinol* 21:1095–1107
- Bassett JH, Williams AJ, Murphy E, Boyde A, Howell PG, Swinhoe R, Archanco M, Flamant F, Samarut J, Costagliola S, Vassart G, Weiss RE, Refetoff S, Williams GR 2008 A lack of thyroid hormones rather than excess thyrotropin causes abnormal skeletal development in hypothyroidism. *Mol Endocrinol* 22:501–512
- Bassett JH, Boyde A, Howell PG, Bassett RH, Galliford TM, Archanco M, Evans H, Lawson MA, Croucher P, St Germain DL, Galton VA, Williams GR 2010 Optimal bone strength and mineralization requires the type 2 iodothyronine deiodinase in osteoblasts. *Proc Natl Acad Sci USA* 107:7604–7609
- Dai XM, Zong XH, Akhter MP, Stanley ER 2004 Osteoclast deficiency results in disorganized matrix, reduced mineralization, and abnormal osteoblast behavior in developing bone. *J Bone Miner Res* 19:1441–1451
- Schriefer JL, Robling AG, Warden SJ, Fournier AJ, Mason JJ,

- Turner CH 2005 A comparison of mechanical properties derived from multiple skeletal sites in mice. *J Biomech* 38:467–475
31. Silva MJ, Brodt MD, Uthgenannt BA 2004 Morphological and mechanical properties of caudal vertebrae in the SAMP6 mouse model of senile osteoporosis. *Bone* 35:425–431
 32. Geoffroy V, Kneissel M, Fournier B, Boyde A, Matthias P 2002 High bone resorption in adult aging transgenic mice overexpressing *cbfa1/runx2* in cells of the osteoblastic lineage. *Mol Cell Biol* 22:6222–6233
 33. Saftig P, Hunziker E, Wehmeyer O, Jones S, Boyde A, Rommerskirch W, Moritz JD, Schu P, von Figura K 1998 Impaired osteoclastic bone resorption leads to osteoporosis in cathepsin-K-deficient mice. *Proc Natl Acad Sci USA* 95:13453–13458
 34. Boyde A, Firth EC 2005 Musculoskeletal responses of 2-year-old Thoroughbred horses to early training. 8. Quantitative back-scattered electron scanning electron microscopy and confocal fluorescence microscopy of the epiphysis of the third metacarpal bone. *N Z Vet J* 53:123–132
 35. Boyde A, Jones SJ, Aerssens J, Dequeker J 1995 Mineral density quantitation of the human cortical iliac crest by backscattered electron image analysis: variations with age, sex, and degree of osteoarthritis. *Bone* 16:619–627
 36. Boyde A, Travers R, Glorieux FH, Jones SJ 1999 The mineralization density of iliac crest bone from children with osteogenesis imperfecta. *Calcif Tissue Int* 64:185–190
 37. Doube M, Firth EC, Boyde A 2007 Variations in articular calcified cartilage by site and exercise in the 18-month-old equine distal metacarpal condyle. *Osteoarthritis Cartilage* 15:1283–1292
 38. Bassett JH, Swinhoe R, Chassande O, Samarut J, Williams GR 2006 Thyroid hormone regulates heparin sulfate proteoglycan expression in the growth plate. *Endocrinology* 147:295–305
 39. Williams GR 2000 Cloning and characterization of two novel thyroid hormone receptor β isoforms. *Mol Cell Biol* 20:8329–8342
 40. O'Shea PJ, Bassett JHD, Cheng SY, Williams GR 2006 Characterization of skeletal phenotypes of TR α 1PV and TR β PV mutant mice: implications for tissue thyroid status and T3 target gene expression. *Nuclear Receptor Signaling* 4:e011 (<http://www.nursa.org/article.cfm?doi=010.1621/nrs.04011>)
 41. Bala Y, Farlay D, Delmas PD, Meunier PJ, Boivin G 2010 Time sequence of secondary mineralization and microhardness in cortical and cancellous bone from ewes. *Bone* 46:1204–1212
 42. Boivin G, Farlay D, Bala Y, Doublier A, Meunier PJ, Delmas PD 2009 Influence of remodeling on the mineralization of bone tissue. *Osteoporos Int* 20:1023–1026
 43. Bassett JH, Williams GR 2008 Critical role of the hypothalamic-pituitary-thyroid axis in bone. *Bone* 43:418–426
 44. Murphy E, Williams GR 2004 The thyroid and the skeleton. *Clin Endocrinol (Oxf)* 61:285–298
 45. Williams AJ, Robson H, Kester MH, van Leeuwen JP, Shalet SM, Visser TJ, Williams GR 2008 Iodothyronine deiodinase enzyme activities in bone. *Bone* 43:126–134



THE
ENDOCRINE
SOCIETY®



Members have FREE online access
to the journal *Hormones & Cancer*.

www.endo-society.org/HC

4.8

Thyroid disorders and bone disease

Moira S. Cheung, Apostolos I. Gogakos,
J.H. Duncan Bassett, Graham R. Williams

Introduction

Osteoporosis is defined as a bone mineral density (BMD) of 2.5 or more standard deviations below that of a young adult (T score ≤ -2.5). It is characterized by reduced bone mass, low BMD, deterioration of bone microarchitecture, and an increased susceptibility to fragility fracture. The prevalence of postmenopausal osteoporosis increases with age from 6% at 50 years of age to over 50% at age 80 and the lifetime incidence of fracture for a 50 year old in the UK is 40% for women and 13% for men. Osteoporosis is a worldwide public health burden that costs an estimated £1.7 billion in the UK, \$15 billion in the USA, and £32 billion in Europe per annum (see Chapter 4.7).

Low BMD, a prior or parental history of fracture, low body mass index, use of glucocorticoids, smoking, excessive alcohol consumption, untreated thyrotoxicosis, and other risk factors increase susceptibility to osteoporosis and fracture. Even subclinical hyperthyroidism, defined by a suppressed thyroid stimulating hormone (TSH) level in the presence of normal thyroid hormone concentrations, is associated with fracture while treatment with thyroxine (T_4) at doses that suppress TSH is associated with increased bone turnover and low BMD in postmenopausal women (1).

Thyroid disease occurs 10-fold more frequently in women and its prevalence increases with age. Hypothyroidism is a common disorder with a prevalence of 0.5% in women between the ages of 40 and 60 and greater than 2% over the age of 70. Thyrotoxicosis has a prevalence of 0.45% in women between the ages of 40 and 60 and 1.4% over the age of 60. As a result, 3% of women over 50 receive T_4 replacement for either primary hypothyroidism or the consequences of surgical or radio-iodine treatment for thyrotoxicosis, and at least 20% of them are overtreated (2). Moreover, subclinical hyperthyroidism affects an additional 1.5% of women over 60 and its prevalence also increases with age. Nevertheless, the role of thyroid hormone in the pathogenesis of osteoporosis has been under-recognized and the extent of its contribution remains uncertain.

Bone strength and fracture susceptibility are determined by the acquisition of peak bone mass and the rate of bone loss in adulthood (3). In children, congenital hypothyroidism is the most

common congenital endocrine disorder with an incidence of 1 in 1800. Hypothyroidism in children results in delayed bone age and growth arrest and treatment with T_4 reverses these changes by inducing rapid 'catch-up' growth. Although juvenile Graves' disease is rare, it remains the commonest cause of thyrotoxicosis in children, being characterized by advanced bone age and accelerated growth that results in short stature due to premature fusion of the growth plates (4). In adults, histomorphometry studies reveal that hypothyroidism results in reduced bone turnover but a net gain in bone mass per remodelling cycle, whereas thyrotoxicosis increases bone resorption and bone formation but induces a net 10% loss of bone per remodelling cycle (5, 6). Taken together, these studies indicate the juvenile and adult skeleton is exquisitely sensitive to thyroid hormones. Thus, euthyroid status is essential for skeletal development, bone mineralization, and acquisition of peak bone mass, and the regulation of bone maintenance in adults. Importantly, recent large population studies have shown that both hypothyroidism and thyrotoxicosis are associated with an increased risk of fracture, demonstrating the physiological importance of euthyroid status for optimization of skeletal integrity and bone strength (7–11).

In this chapter we provide an up to date analysis of the role of thyroid hormone in skeletal development and adult bone maintenance by discussing evidence from animal models and basic science in relation to a detailed review of the current clinical literature.

Thyroid hormone action

Circulating thyroid hormone levels are maintained in the euthyroid range by a classical endocrine negative feedback loop. Thyrotropin-releasing hormone is synthesized in the paraventricular nucleus of the hypothalamus and stimulates synthesis and secretion of TSH from thyrotrophs in the anterior pituitary gland. TSH, acting via the G-protein coupled TSH receptor (TSHR), stimulates growth of thyroid follicular cells and the synthesis and release of thyroid hormones. Thyroid hormones act via thyroid hormone receptors in the hypothalamus and pituitary to inhibit thyrotropin-releasing hormone and TSH synthesis and secretion. This negative feedback loop maintains circulating thyroid hormones

and TSH in a physiological inverse relationship, which defines the hypothalamic–pituitary–thyroid (HPT) axis set point (4).

The thyroid gland secretes the prohormone T_4 and a small amount of the physiologically active hormone 3,5,3'-L-triiodothyronine (T_3). The majority of circulating T_3 , however, is thought to be generated via 5'-deiodination of T_4 by the type 1 iodothyronine deiodinase enzyme (D1) in liver and kidney. Circulating free T_4 levels are maintained at approximately three to fourfold higher concentrations than free T_3 . Intracellular availability of T_3 is determined by active uptake of the free hormones by specific cell membrane transporters, including monocarboxylate transporter-8 and -10, and organic acid transporter protein-1c1, and by the activities of the type 2 and 3 deiodinase enzymes (D2 and D3). D2 converts T_4 to the active hormone T_3 by catalysing removal of a 5'-iodine atom. By contrast, D3 prevents activation of T_4 and inactivates T_3 by removal of a 5-iodine atom to generate the metabolites 3,3',5'-L-triiodothyronine (reverse T_3) and 3,3'-diiodothyronine (T_2), respectively. Thus, the relative levels of D2 and D3 ultimately determine the concentration of intracellular T_3 available to the nuclear T_3 receptors (TRs) (12).

TRs act as hormone-inducible transcription factors that regulate expression of T_3 -responsive target genes. The *THRA* and *THRB* genes encode three functional TRs: TR α 1, TR β 1, and TR β 2. TR α 1 and TR β 1 are expressed widely but their relative levels differ during development and in adulthood due to tissue-specific and temporospatial regulation. Expression of TR β 2, however, is restricted. In the hypothalamus and pituitary it mediates inhibition of thyrotropin-releasing hormone and TSH expression whilst in the cochlea and retina it has a key role to control the timing of sensory organ development (13).

Skeletal development and bone maintenance

The skeleton develops via two distinct processes. Endochondral ossification is the process by which long bones form and linear growth occurs. A cartilage anlage forms from mesenchyme condensations to form a scaffold for subsequent bone formation. Mesenchyme progenitor cells differentiate into chondrocyte precursors, which undergo a tightly regulated sequence of clonal expansion, proliferation, hypertrophic differentiation, and apoptosis. Chondrocytes secrete a cartilage matrix that mineralizes and is subsequently remodelled by the activities of bone resorbing osteoclasts and bone forming osteoblasts, resulting in formation of the diaphysis. Linear growth continues throughout development by a similar process within the epiphyseal growth plates, which are located at the proximal and distal ends of long bones. By contrast, the skull vertex forms by intramembranous ossification, in which mesenchymal cells differentiate directly into osteoblasts, resulting in bone formation in the absence of a cartilage scaffold. Linear growth continues until fusion of the growth plates during puberty but bone mineralization and consolidation of bone mass accrual continues into early adulthood so that peak bone mass is achieved during the third to fourth decade (14, 15).

Functional integrity and strength of the skeleton is maintained by the process of bone remodelling, which is achieved by the integrated and coupled activities of osteocytes, osteoclasts, and osteoblasts. Osteocytes comprise 90–95% of all adult bone cells. They derive

from osteoblasts that have become embedded in bone matrix. The osteocyte network is thought to sense changes in mechanical load and regulate local initiation of bone remodelling by the release of cytokines and chemotactic signals or by osteocyte apoptosis. Bone remodelling begins with the recruitment of mature osteoclasts and their precursors to sites of altered mechanical load or micro-damage. Osteoclasts excavate a resorption cavity over a period of 3–5 weeks until this process is terminated by apoptosis and followed by recruitment of osteoblast precursors. Subsequently, osteoblasts undergo a programme of maturation during which they secrete and mineralize osteoid to replace the resorbed bone over a period of approximately 3 months. Coupling of osteoclast and osteoblast activities via signalling between the two cell lineages regulates the bone remodelling cycle and results in skeletal homeostasis with preservation of bone strength. In summary, the bone remodelling cycle is initiated and orchestrated by osteocytes, and regulated by coupled crosstalk between osteoblasts and osteoclasts.

Thyroid hormone action in bone

TR α 1 and TR β 1 are expressed in growth plate chondrocytes, bone marrow stromal cells, and osteoblasts but it is uncertain whether they are present in osteoclasts (4, 16).

In vivo and *in vitro* studies have shown that T_3 acts via the Indian hedgehog/ parathyroid hormone-related peptide feedback loop, growth hormone/ insulin-like growth factor-1, and fibroblast growth factor receptor-3 (FGFR3) signalling pathways to inhibit growth plate chondrocyte proliferation and stimulate hypertrophic chondrocyte differentiation. In childhood hypothyroidism, growth arrest and delayed bone formation are consequences of gross disruption of growth plate architecture (epiphyseal dysgenesis), which results from disorganization of the growth plates and a failure of hypertrophic chondrocyte differentiation. By contrast, thyroid hormone excess accelerates hypertrophic chondrocyte differentiation resulting in advanced bone formation (4, 16).

Studies of bone marrow stromal cells suggest that many of the actions of T_3 involve complex cytokine and growth factor signalling pathways that regulate communication between osteoblast and osteoclast cell lineages within the bone marrow microenvironment. *In vivo* and *in vitro* studies have further shown that T_3 regulates osteoblast differentiation and activity at least in part via the FGFR1 signalling pathway. Activating mutations of *FGFR1* cause Pfeiffer's craniosynostosis syndrome and, consistent with this, craniosynostosis is a recognized manifestation of severe juvenile thyrotoxicosis in which FGFR1 activity is increased in osteoblasts.

The regulation of adult bone turnover by thyroid hormones has been investigated by bone histomorphometry (5, 6). The skeletal manifestations of hypothyroidism include reduced osteoblast activity, impaired osteoid apposition, and a prolonged period of secondary bone mineralization. Consistent with a state of low bone turnover, osteoclast activity and bone resorption are also reduced. The effect of the low bone turnover state in hypothyroidism is a net increase in mineralization without a change in bone volume. By contrast, thyrotoxicosis results in a state of high bone turnover. The frequency of initiation of bone remodelling is markedly increased and the duration of the bone remodelling cycle is reduced. The net result is that the duration of bone formation and mineralization is reduced to a greater extent than the reduction in duration of

bone resorption. This leads to a net 10% loss of bone per remodeling cycle, resulting in high bone turnover osteoporosis.

Studies in genetically modified mice

In vivo studies in mutant mice have demonstrated that TR α 1 mediates T₃ action in bone (17). Mutation or deletion of TR α results in transient growth retardation, impaired ossification, and reduced bone mineralization during growth (Table 4.8.1). In adults, there is a defect in bone remodelling, a marked increase in bone mass, and increased bone mineralization. By contrast, mutation or deletion of TR β results in an opposite phenotype of accelerated growth, advanced ossification with increased mineralization during growth but short stature, which results from premature quiescence of the growth plates (Table 4.8.1). In adults, increased bone remodelling results in osteoporosis and reduced bone mineralization. Taken together, these features indicate that thyroid hormones exert anabolic actions during skeletal growth but catabolic responses in adult bone (17). Mutation of TR α disrupts T₃ action in bone cells resulting in skeletal hypothyroidism, whereas mutation of TR β disrupts the HPT axis, leading to elevated levels of circulating thyroid hormones which activate TR α in bone cells, resulting in skeletal hyperthyroidism. Consistent with these phenotypes, levels of TR α mRNA expression are 10- to 100-fold greater than TR β in adult bone.

Recently, a direct role for TSH as a negative regulator of bone turnover has also been proposed (4). Osteoblasts and osteoclasts were shown to express the TSHR, and congenitally hypothyroid TSHR knockout mice treated with thyroid hormone displayed a phenotype of high bone turnover osteoporosis. As a result of these findings, it was suggested that bone loss was a consequence of TSH deficiency. However, the susceptibility of patients with Graves' disease to osteoporosis and fracture is inconsistent with the hypothesis that TSH negatively regulates bone turnover because the presence of TSHR-stimulating antibodies would be predicted to protect patients from osteoporosis. Thus, the skeletal consequences of thyrotoxicosis are most likely to result primarily from thyroid hormone excess although TSH deficiency cannot be excluded as a contributing factor (4).

These two possibilities cannot be differentiated readily because the HPT axis maintains thyroid hormones and TSH in a physiological reciprocal relationship. Nevertheless, studies in mutant mice

have enabled the issue to be addressed *in vivo*. Thus, the skeletal phenotypes of two different mouse models of congenital hypothyroidism were compared. Pax8 knockout mice lack a transcription factor that is essential for thyroid follicular cell development and have undetectable thyroid hormone levels, a 2000-fold elevation of TSH, and a fully functional TSHR. By contrast, *hyt/hyt* mice have gross congenital hypothyroidism also accompanied by a 2000-fold increase in TSH but they harbour a point mutation in the *Tshr* gene, leading to complete loss of TSHR protein function. Both mutants exhibited a similar phenotype of growth retardation and delayed ossification typical of hypothyroidism despite the divergence in TSH signalling (4).

In summary, the skeleton is exquisitely sensitive to thyroid status during growth and in adulthood. T₃ exerts important anabolic responses during skeletal growth and has significant catabolic effects on adult bone. Both of these actions are mediated by TR α 1.

Skeletal consequences of altered thyroid status in humans

Studies in children

Childhood hypothyroidism

Congenital hypothyroidism results in growth arrest, epiphyseal dysgenesis, delayed bone age, and short stature. Thyroxine replacement therapy induces rapid catch-up growth and as a result children that are treated early ultimately reach their predicted adult height and achieve normal BMD after 8.5 years' follow-up. Nevertheless, a single study has suggested that adult BMD may be reduced despite treatment from the neonatal period. Children with juvenile acquired hypothyroidism also display growth arrest, delayed bone maturation, and short stature. T₄ replacement again induces rapid catch-up growth, but these individuals may fail to achieve final predicted height and the resulting permanent height deficit is related to the duration of thyroid hormone deficiency prior to replacement (18).

Childhood hyperthyroidism

Juvenile thyrotoxicosis results in accelerated growth, advanced bone age, and short stature, which is a consequence of the premature fusion of the epiphyseal growth plates due to accelerated skeletal maturation. In severe cases in young children, early closure of the cranial sutures may result in craniosynostosis (19). To date, there

Table 4.8.1 Skeletal phenotypes of thyroid hormone receptor mutant mice

	TR α mutant mice	TR β mutant mice
Systemic thyroid status	Euthyroid	Elevated T ₄ , T ₃ and TSH
Skeletal thyroid status	Hypothyroid	Thyrotoxic
Juvenile skeleton	Transient growth delay Delayed endochondral and intramembranous ossification Impaired chondrocyte differentiation Reduced calcified bone	Persistent short stature Advanced endochondral and intramembranous ossification Enhanced chondrocyte differentiation Increased calcified bone
Adult skeleton	Osteosclerosis Increased bone volume Increased mineralization Reduced osteoclastic bone resorption	Osteoporosis Reduced bone volume Reduced mineralization Increased osteoclastic bone resorption

See review (17).

TR, 3,5,3'-l-triiodothyronine receptor.

are no data relating to the effects of childhood thyrotoxicosis on BMD.

Resistance to thyroid hormone

Resistance to thyroid hormone is an autosomal dominant condition resulting from a dominant negative mutation of TR β (20). The mutant TR β protein disrupts negative feedback in the HPT axis, leading to increased circulating thyroid hormone concentrations in the presence of inappropriately normal or elevated TSH levels. The syndrome results in a complex mixed phenotype of hyperthyroidism and hypothyroidism depending on the target tissue studied and the specific mutation present in TR β . Thus, an individual patient can have symptoms of both thyroid hormone deficiency and excess. A broad range of skeletal abnormalities have been described in association with resistance to thyroid hormone. These include craniofacial abnormalities, craniosynostosis, delayed or advanced bone age, short stature, increased bone turnover, osteoporosis, and fracture, although only a few patients have been studied in detail.

Studies in adults

A large number of studies have attempted to characterize the skeletal consequences of altered thyroid function in adults. Unfortunately, many of these studies have been confounded by inclusion of patients with a variety of thyroid diseases and by comparison of mixed cohorts of patients, which have included pre- and postmenopausal women or men. Furthermore, many studies have lacked sufficient statistical power because of the inclusion of small numbers of patients and the absence of long-term follow-up. In addition, in many studies there has been inadequate control for other confounding factors that influence bone mass and fracture susceptibility, including: age, prior or family history of fracture, body mass index, physical activity, use of oestrogens, glucocorticoids, bisphosphonates, and vitamin D, prior history of thyroid disease or use of thyroxine, and smoking or alcohol intake. For these reasons, the literature in this field has been difficult to investigate by meta-analysis and conclusions can only be uncertain (1).

Studies of normal individuals

Bone turnover markers

Few studies have determined bone turnover markers in euthyroid populations. Zofkova *et al.* in a study of bone turnover markers in a population of 60 healthy postmenopausal women reported that high circulating TSH levels correlated with low urinary deoxypyridinoline concentrations but not with serum procollagen type I C

propeptide levels (21). This study illustrates difficulties with interpretation of thyroid hormone effects on bone turnover as only a small number of subjects were investigated and individuals with treated hypothyroidism, subclinical hyperthyroidism, and secondary hyperparathyroidism were not excluded.

Bone mineral density and fracture

Four large population studies have investigated the relationship between thyroid status and BMD (Table 4.8.2). van der Deure *et al.* studied a population of 1151 euthyroid men and women over 55 from Rotterdam (22). BMD at the femoral neck was positively correlated with TSH levels and inversely correlated with free T₄, and the association with free T₄ was much stronger than the association with TSH. No relationships between free T₄ or TSH and fracture were identified in this study. Kim *et al.* studied 959 Korean postmenopausal women and showed that individuals with low-normal TSH levels between 0.5 and 1.1 mU/l had lower lumbar spine and femoral neck BMD than women with high-normal TSH between 2.8 and 5.0 mU/l, although no fracture data were reported (23). Morris studied 581 postmenopausal American women and showed that subjects with a low-normal TSH were nearly five times more likely to have osteoporosis than women with a high-normal TSH (24). Grimnes *et al.* studied a population of 993 postmenopausal women and 968 men from Tromsø. This study revealed that individuals with TSH below the 2.5th percentile had a low forearm BMD whereas those with TSH above the 97.5th percentile had a high femoral neck BMD compared with the rest of the population (25). Neither of these studies investigated the incidence of fracture. Finally, the incidence of fracture in 367 UK women over 50 was prospectively studied for 10 years by Finigan *et al.* and no associations between free T₃, free T₄, or TSH and incident vertebral fracture were identified (26).

In summary, these studies suggest the hypothesis that thyroid status in the upper normal range is associated with reduced BMD whereas thyroid status in the lower normal range is associated with increased BMD. A definitive conclusion, however, is not possible as these studies unfortunately did not account for a number of confounding variables. Prospective population studies of sufficient size and duration will be required to determine the relationship between thyroid status and fracture risk.

Studies of patients with hypothyroidism

Bone turnover markers and BMD

Histomorphometric analyses have demonstrated that bone turnover is decreased in hypothyroidism (5, 6) but studies of the effect of

Table 4.8.2 Large studies of thyroid status and BMD

First author (reference)	Study design	Subjects (n)	Patient group	Fracture risk
Van der Deure (22)	Prospective cohort	479 men 672 women	Men and women >55 years of age	Free T ₄ negatively associated with spine and hip BMD
Grimnes (25)	Cross-sectional	968 men 993 women	Men and women >55 years of age	Decreased forearm BMD associated with low-normal TSH
Morris (24)	Cross-sectional	581 women	Postmenopausal women	Decreased spine BMD associated with low-normal TSH
Kim (23)	Cross-sectional	959 women	Postmenopausal women	Decreased spine and hip BMD associated with low-normal TSH
Jamal (9)	Cross-sectional	15 316 women	Postmenopausal women	Decreased hip BMD associated with abnormally low TSH

Abbreviations: BMD, bone mineral density; TSH, thyroid stimulating hormone.

hypothyroidism on bone turnover markers have included only very small numbers of patients and were inconclusive. Consistent with histomorphometric data showing normal bone volume in hypothyroid patients, Vestergaard and Mosekilde, and Stamato *et al.* have reported that BMD is normal in patients newly diagnosed with hypothyroidism (10, 27).

Fracture

Large population studies, however, have demonstrated an association between hypothyroidism and fracture. Patients with a prior history of hypothyroidism had a two to three-fold increased relative risk of fracture, which persisted for up to 10 years following initial diagnosis (7, 10, 11, 28) (Table 4.8.3).

In summary, hypothyroidism results in low bone turnover and an increased risk of fracture.

Studies of patients with thyrotoxicosis

The severe bone disease associated with overt uncontrolled thyrotoxicosis is now rare because of early diagnosis and treatment, although several studies have investigated the skeleton in thyrotoxic patients prior to treatment.

Bone turnover markers and BMD

The effect of thyrotoxicosis on bone turnover markers is consistent with histomorphometric data reported by Eriksen *et al.* (5). Thus, levels of bone resorption markers such as urinary pyridinoline and deoxypyridinoline are increased. Bone formation markers, including bone-specific alkaline phosphatase and osteocalcin, are also elevated. A meta-analysis of 20 eligible studies by Vestergaard and Mosekilde (37) calculated that BMD at the time of diagnosis of thyrotoxicosis was reduced compared to age-matched controls (Table 4.8.4).

Fracture

Two cross-sectional case–controlled (11, 43) and four population studies (7, 8, 29, 30) have identified an association between fracture and a prior history of thyrotoxicosis (Table 4.8.3). Similarly, a meta-analysis of patients with thyrotoxicosis revealed an increased relative risk of hip fracture (37). The majority of these studies did not determine whether the increased fracture risk could be accounted for by reduced BMD, although one prospective study (29) showed that a prior history of thyroid disease is associated with hip fracture even after adjustment for BMD. Furthermore, Bauer *et al.* (8, 44)

Table 4.8.3 Large studies of thyroid status and fracture risk

Reference	Study design	Subjects (n)	Patient group	Fracture risk
Positive studies				
Ahmed (7)	Cross-sectional	27 159 men and women	Nonvertebral fractures	Increased risk of fractures with both thyrotoxicosis and hypothyroidism
Vestergaard (11)	Cross-sectional case–control	124 655 men and women 373 962 controls	All fractures	Fracture risk increased for 5 years after thyrotoxicosis and 10 years after hypothyroidism
Jamal (9)	Cross-sectional	15 316 women	Postmenopausal women	Increased risk of vertebral fracture with low TSH
Vestergaard (10)	Cross-sectional	11 776 thyrotoxic 4473 hypothyroid 48 710 controls	National register	Increased risk of femur fracture with thyrotoxicosis and hypothyroidism
Sheppard (35)	Cross-sectional	23 183 men and women	T ₄ replacement	Increase risk of femur fracture in males
Bauer (8)	Prospective longitudinal	686 women	Women >65 years of age	Increased risk of hip and vertebral fracture with suppressed TSH
Lau (36)	Cross-sectional	1176 Asian men and women 1162 controls	>50 years with hip fracture	Increase risk of hip fracture with T ₄ treatment
Franklyn (31)	Retrospective cohort	1226 men 5983 women	Radio-iodine treated thyrotoxicosis	Increase risk of death from hip fracture
Seeley (30)	Longitudinal	9704 women	Women >65 years of age	Increased risk of foot fractures if prior thyrotoxicosis
Cummings (29)	Longitudinal	9516 women	Women >65 years of age	Increased fracture risk with prior thyrotoxicosis
Negative studies				
Van der Deure (22)	Prospective cohort	479 men 672 women	>55 years of age	Free T ₄ and TSH not associated with fracture
Van den Eeden (34)	Cross-sectional case–controlled	501 women 533 controls	Hip fracture	No association with T ₄ replacement
Melton (33)	Retrospective cohort	630 men and women	Thyroidectomy	No association with fracture
Leese (32)	Cross-sectional	1180 men and women	Thyroid register	No association between fracture risk and TSH

TSH, thyroid stimulating hormone.

Table 4.8.4 Meta-analyses and literature reviews

First author (reference)	Population	Studies (n)	Type	Conclusions
Heemstra (39)	Suppressive T ₄	21 BMD	Literature review	Postmenopausal women at risk of reduced BMD; no effect in premenopausal women or men
Murphy (1)	Suppressive T ₄ T ₄ replacement Thyroid disease	19 BMD 9 BMD 15 Fracture	Literature review	Prior history of thyrotoxicosis is associated with increased fracture risk Subclinical hyperthyroidism is associated with reduced BMD in postmenopausal women A suppressed TSH from any cause is associated with an increased fracture risk in postmenopausal women Appropriate T ₄ replacement does not affect BMD or fracture risk Suppressive T ₄ treatment does not affect BMD in premenopausal women or men; the situation is less clear in postmenopausal women
Vestergaard (37)	Thyrotoxicosis	20 BMD 5 Fracture	Meta-analysis	Spine and hip BMD reduced in untreated thyrotoxicosis Fractures risk increases with age at diagnosis
Schneider (42)	T ₄ replacement	63 BMD	Literature review	Insufficient evidence to draw formal conclusion
Quan (40)	Suppressive T ₄	11 BMD	Literature review	Effect in postmenopausal women unclear No effect in premenopausal women or men
Uzzan (41)	T ₄ replacement Suppressive T ₄	13 BMD 27 BMD	Meta-analysis	Suppressive doses of T ₄ associated with reduced BMD at radius, spine, and hip in postmenopausal women but not in premenopausal women or men
Faber (38)	Suppressive T ₄	13 BMD	Meta-analysis	Suppressive T ₄ associated with reduced BMD in postmenopausal women and an excess annual bone loss of 1% per year No effect in premenopausal women

BMD, bone mineral density; T₄, thyroid hormone; TSH, thyroid stimulating hormone.

demonstrated that low TSH was associated with a three to fourfold increased risk of fracture even though a relationship between TSH and BMD was not identified. In agreement with these observations, Franklyn *et al.* showed an increased standardized mortality ratio due to fractured femur in a follow-up register of thyrotoxic patients treated with radio-iodine (31). Nevertheless, several studies have failed to demonstrate an association between thyrotoxicosis and fracture (32–34).

In summary, a prior history of thyrotoxicosis may be associated with reduced bone density and a long-term increased risk of fracture, although data are conflicting and limited by confounding factors.

Studies of individuals with subclinical hyperthyroidism

Bone turnover markers and BMD

Either elevated or normal levels of the bone resorption markers urinary deoxypyridinoline and hydroxyproline have been reported in patients with subclinical hyperthyroidism. Similarly, levels of the bone formation markers osteocalcin, alkaline phosphatase, and procollagen I C-terminal extension propeptide have been reported to be elevated or normal. Subclinical hyperthyroidism has also been associated with reduced BMD at the femoral neck and other sites, although other studies have not found such a relationship. Accordingly, a meta-analysis was inconclusive (38) (Table 4.8.4).

Fracture

Although no prospective studies of fracture risk in subclinical hyperthyroidism have been published, data from Bauer *et al.* suggest that suppressed TSH levels may be associated with an increased risk of fracture (8). Additionally, Jamal *et al.* reported a subanalysis of the Fracture Intervention Trial and demonstrated that a TSH level suppressed below 0.5 mIU/l was associated with an increased risk of vertebral fracture (9). Unfortunately, there was insufficient

information provided to determine whether patients in this study had subclinical hyperthyroidism or untreated thyrotoxicosis.

In summary, subclinical hyperthyroidism may be associated with increased bone turnover, reduced BMD, and increased fracture risk although again insufficient data are currently available to draw definitive conclusions.

Studies in patients treated with suppressive doses of thyroxine

The long-term management of patients with differentiated thyroid cancer frequently involves treatment with doses of thyroxine that suppress circulating TSH concentrations and which may have detrimental effects on the skeleton.

Bone turnover markers

A number of small studies have investigated the effect of suppressive doses of T₄ on bone turnover markers. Three studies reported increased levels of bone resorption markers in patients receiving T₄ and two of these also demonstrated an increase in bone formation markers (45). Nevertheless, other studies reported no effect on markers of bone resorption or formation (46).

Bone mineral density

A large number of studies have investigated the effects of suppressive doses of T₄ on BMD in pre- and postmenopausal women and in men at various anatomical locations.

Most studies showed no effect of TSH suppression therapy on BMD at the lumbar spine, femur, or radius in premenopausal women. By contrast, three studies have reported reduced BMD at the femur in premenopausal women receiving suppressive doses of T₄. Heemstra *et al.* analysed 12 cross-sectional and four prospective studies of premenopausal women receiving suppressive doses of T₄, but a meta-analysis could not be performed due to heterogeneity of the cohorts (39). The authors concluded that treatment

with suppressive doses of T_4 did not affect BMD in premenopausal women (Table 4.8.4). This finding supported results of an earlier review of eight studies by Quan *et al.* (40).

The effects of suppressive doses of T_4 on BMD in postmenopausal women are less clear as the two most rigorous cross-sectional studies reported conflicting results (47, 48). Franklyn *et al.* investigated 26 UK postmenopausal women treated for 8 years and demonstrated no effect of TSH suppression on BMD (47), whereas Kung and Yeung studied 34 postmenopausal Asian women and found a decrease in total body, lumbar spine, and femoral BMD in patients treated with suppressive doses of T_4 (48). However, direct comparison between the two studies is difficult because in the study by Franklyn *et al.* TSH was fully suppressed in only 80% of patients, whilst mean calcium intake was low in the study by Kung *et al.* Similar conflicting results have been reported at various anatomical sites in less well-controlled cross-sectional and longitudinal studies. Eight cross-sectional studies also included investigation of male patients, but only Jodar *et al.* reported a reduction in lumbar spine and femur BMD in men receiving suppressive doses of T_4 (49).

A meta-analysis of 27 studies investigating the effect of suppressive doses of T_4 on BMD (41) concluded there were no effects on BMD in premenopausal women or men, although such treatment in postmenopausal women for up to 10 years led to reductions in BMD at the distal radius, lumbar spine, and femoral neck of between 5 and 7% (Table 4.8.4). Although the long-term effects of suppressive doses of T_4 on BMD in postmenopausal women remain uncertain, further reviews of this topic support the findings of Uzzan *et al.* and recommend monitoring of BMD in such patients (1, 39, 40).

Fracture

No studies with sufficient statistical power to determine the effect of treatment with suppressive dose of T_4 on fracture risk have been reported.

In summary, treatment with suppressive dose of T_4 does not affect BMD in premenopausal women or men but may lead to reduced BMD in postmenopausal women. Effects on bone turnover are inconclusive and there are no data regarding fracture risk.

Studies of patients treated for hypothyroidism

Bone turnover markers, BMD, and fracture

Histomorphometric studies have suggested an increase in bone turnover in response to T_4 replacement in hypothyroidism (5) but the effect on bone markers has not been reported. The majority of cross-sectional studies of pre- and postmenopausal women receiving long-term T_4 replacement for hypothyroidism have not identified any significant effect on BMD. However, in premenopausal women Paul *et al.* (50) reported a 10% reduction BMD in the femur but no change at the lumbar spine following T_4 replacement, whilst Kung and Pun (51) reported reduced BMD at both lumbar spine and hip. There are no prospective studies investigating the effects of T_4 replacement in hypothyroid patients on fracture risk, although population studies have not identified an association between T_4 replacement therapy and fracture (29, 33, 34).

Studies of patients treated for thyrotoxicosis

Bone turnover markers, BMD, and fracture

Two prospective studies of patients with thyrotoxicosis have shown that elevated levels of bone resorption and bone formation markers return to normal levels within 1 month of initiation of treatment. A meta-analysis of 20 studies investigating the effect of

treatment for thyrotoxicosis on BMD (37) demonstrated that the low BMD at diagnosis returned to normal after 5 years (Table 4.8.4). In a subsequent study, treatment for thyrotoxicosis was shown to result in a 4% increase in BMD within 1 year (52). Nevertheless, in a large population study Vestergaard *et al.* (11) reported that an increased relative risk of fracture risk persisted for 5 years following a diagnosis of thyrotoxicosis (Table 4.8.3).

In summary, treatment of patients with thyrotoxicosis results in normalization of bone turnover and BMD by 5 years, although the increased risk of fracture may persist for longer.

Human genetics

In healthy individuals free T_3 , free T_4 , and TSH levels fluctuate over a range that is less than 50% of the normal reference range. Thus, variation in thyroid status within an individual is narrower than the broad interindividual variation seen in the population. Each person has a unique HPT axis set point that lies within the population reference range, indicating there is variation in tissue sensitivity to thyroid hormones between normal individuals (53). Data from the UK Adult Twin Registry estimate heritability for free T_3 concentration at 23%, free T_4 at 39%, and TSH at 65%, whilst estimates from a Danish twin study were 64%, 65%, and 64%, respectively (54, 55). A genome-wide screen identified eight quantitative trait loci linked to circulating free T_3 , free T_4 , and TSH levels, indicating that thyroid status is inherited as a complex genetic trait (56). Similarly, unbiased genome-wide association studies and candidate gene approaches have shown that osteoporosis is a polygenic disorder in which many genes and signalling pathways exert small contributions that influence bone size, BMD, and fracture susceptibility (57).

These observations raise the possibility that variations in bone turnover, BMD, and fracture susceptibility in normal individuals may be associated with differences in their HPT axis set points. Furthermore, genes that establish the HPT axis set point and thus regulate thyroid status may also influence the acquisition of peak bone mass, skeletal growth, and bone turnover and thereby contribute to the genetic determination of fracture risk. This hypothesis is consistent with observations in other physiological complex traits including body mass index, blood pressure, heart rate, atherosclerosis, serum cholesterol, and psychological well-being, in which variations have been associated with small alterations in thyroid function and with polymorphisms in thyroid pathway genes that are themselves associated with altered serum thyroid hormone and TSH concentrations (58). These new developments in our understanding the physiological regulation of the HPT axis and thyroid hormone action in target tissues have been extended recently to investigation of the skeleton and these studies suggest common genetic factors may be involved in the determination of thyroid status, bone turnover, and BMD (22, 59).

Future prospective studies investigating the relationships between variations in the HPT axis set point and genes regulating thyroid hormone transport, metabolism, and action with bone mass and fracture risk will need to be well designed and adequately powered. Stringent exclusion criteria will be required to define large populations of individuals which can be followed up prospectively for prolonged periods. Nevertheless, such studies have the potential to individualize fracture risk prediction and inform the choice of preventative therapy (58).

Conclusions

- ◆ Bone strength and fracture susceptibility are determined by peak bone mass acquisition during growth and the rate of bone loss in adulthood.
- ◆ Large population studies indicate that both hypothyroidism and thyrotoxicosis are associated with increased fracture susceptibility, demonstrating the importance of euthyroid status for optimal bone strength.
- ◆ A negative feedback loop maintains circulating thyroid hormones and TSH in an inverse relationship which defines the HPT axis set point.
- ◆ The skeleton is exquisitely sensitive to thyroid status during growth and in adulthood. T₃ exerts anabolic responses during skeletal growth and has catabolic effects on adult bone.
- ◆ Many studies have investigated the consequences of altered thyroid function on bone. Unfortunately, many of these have been confounded by poor study design, lack of statistical power, and an absence of long-term follow-up analysis. Thus, definitive conclusions cannot be obtained from the current literature.
- ◆ Population studies suggest that reduced BMD is associated with thyroid status in the upper normal range whereas increased BMD is associated with thyroid status in the lower normal range.
- ◆ Hypothyroidism results in low bone turnover and may be associated with an increased risk of fracture.
- ◆ Untreated hyperthyroidism results in increased bone turnover, reduced BMD, and an increased risk of fracture. A prior history of thyrotoxicosis may be associated with reduced BMD and a long-term increased risk of fracture. Subclinical hyperthyroidism may be associated with increased bone turnover, reduced BMD, and increased risk of fracture. Treatment with suppressive dose of T₄ may lead to reduced BMD in postmenopausal women.
- ◆ Treatment of patients with thyrotoxicosis results in normalization of bone turnover and BMD within 5 years, although the increased risk of fracture may persist for much longer.

References

1. Murphy E, Williams GR. The thyroid, the skeleton. *Clin Endocrinol*, 2004; **61**: 285–98.
2. Parle JV, Franklyn JA, Cross KW, Jones SR, Sheppard MC. Thyroxine prescription in the community: serum thyroid stimulating hormone level assays as an indicator of undertreatment or overtreatment. *Br J Gen Pract Mar*, 1993; **43**: 107–9.
3. Ralston SH, de Crombrughe B. Genetic regulation of bone mass and susceptibility to osteoporosis. *Genes Dev*, 2006; **20**: 2492–506.
4. Bassett JH, Williams GR. Critical role of the hypothalamic-pituitary-thyroid axis in bone. *Bone*, 2008; **43**: 418–26.
5. Eriksen EF, Mosekilde L, Melsen F. Kinetics of trabecular bone resorption and formation in hypothyroidism: evidence for a positive balance per remodeling cycle. *Bone*, 1986; **7**: 101–8.
6. Mosekilde L, Eriksen EF, Charles P. Effects of thyroid hormones on bone and mineral metabolism. *Endocrinol Metab Clin North Am*, 1990; **19**: 35–63.
7. Ahmed LA, Schirmer H, Berntsen GK, Fonnebo V, Joakimsen RM. Self-reported diseases and the risk of non-vertebral fractures: the Tromso study. *Osteoporos Int*, 2006; **17**: 46–53.
8. Bauer DC, Ettinger B, Nevitt MC, Stone KL. Risk for fracture in women with low serum levels of thyroid-stimulating hormone. *Ann Intern Med*, 2001; **134**: 561–8.
9. Jamal SA, Leiter RE, Bayoumi AM, Bauer DC, Cummings SR. Clinical utility of laboratory testing in women with osteoporosis. *Osteoporos Int*, 2005; **16**: 534–40.
10. Vestergaard P, Mosekilde L. Fractures in patients with hyperthyroidism and hypothyroidism: a nationwide follow-up study in 16,249 patients. *Thyroid*, 2002; **12**: 411–9.
11. Vestergaard P, Rejnmark L, Mosekilde L. Influence of hyper- and hypothyroidism, and the effects of treatment with antithyroid drugs and levothyroxine on fracture risk. *Calcif Tissue Int*, 2005; **77**: 139–44.
12. St Germain DL, Galton VA, Hernandez A. Minireview: Defining the roles of the iodothyronine deiodinases: current concepts and challenges. *Endocrinology*, 2009; **150**: 1097–107.
13. Yen PM. Physiological and molecular basis of thyroid hormone action. *Physiol Rev*, 2001; **81**: 1097–142.
14. Karsenty G, Wagner EF. Reaching a genetic and molecular understanding of skeletal development. *Dev Cell*, 2002; **2**: 389–406.
15. Kronenberg HM. Developmental regulation of the growth plate. *Nature*, 2003; **423**: 332–6.
16. Bassett JH, Williams GR. The molecular actions of thyroid hormone in bone. *Trends Endocrinol Metab*, 2003; **14**: 356–64.
17. Bassett JH, Williams GR. The skeletal phenotypes of TRalpha and TRbeta mutant mice. *J Mol Endocrinol*, 2009; **42**: 269–82.
18. Rivkees SA, Bode HH, Crawford JD. Long-term growth in juvenile acquired hypothyroidism: the failure to achieve normal adult stature. *N Engl J Med*, 1988; **318**: 599–602.
19. Segni M, Leonardi E, Mazzoncini B, Pucarelli I, Pasquino AM. Special features of Graves' disease in early childhood. *Thyroid*, 1999; **9**: 871–7.
20. Weiss RE, Refetoff S. Resistance to thyroid hormone. *Rev Endocr Metab Disord*, 2000; **1**: 97–108.
21. Zofkova I, Hill M. Biochemical markers of bone remodeling correlate negatively with circulating TSH in postmenopausal women. *Endocr Regul*, 2008; **42**: 121–7.
22. van der Deure WM, Uitterlinden AG, Hofman A, Rivadeneira F, Pols HA, Peeters RP, et al. Effects of serum TSH and FT4 levels and the TSHR-Asp727Glu polymorphism on bone: the Rotterdam Study. *Clin Endocrinol*, 2008; **68**: 175–81.
23. Kim DJ, Khang YH, Koh JM, Shong YK, Kim GS. Low normal TSH levels are associated with low bone mineral density in healthy postmenopausal women. *Clin Endocrinol*, 2006; **64**: 86–90.
24. Morris MS. The association between serum thyroid-stimulating hormone in its reference range and bone status in postmenopausal American women. *Bone*, 2007; **40**: 1128–34.
25. Grimnes G, Emaus N, Joakimsen RM, Figenschau Y, Jorde R. The relationship between serum TSH and bone mineral density in men and postmenopausal women: the Tromso study. *Thyroid*, 2008; **18**: 1147–55.
26. Finigan J, Greenfield DM, Blumsohn A, Hannon RA, Peel NF, Jiang G, et al. Risk factors for vertebral and nonvertebral fracture over 10 years: a population-based study in women. *J Bone Miner Res*, 2008; **23**: 75–85.
27. Stamato FJ, Amarante EC, Furlanetto RP. Effect of combined treatment with calcitonin on bone densitometry of patients with treated hypothyroidism. *Rev Assoc Med Bras*, 2000; **46**: 177–81.
28. Vestergaard P, Rejnmark L, Weeke J, Mosekilde L. Fracture risk in patients treated for hyperthyroidism. *Thyroid*, 2000; **10**: 341–8.
29. Cummings SR, Nevitt MC, Browner WS, Stone K, Fox KM, Ensrud KE, et al. Risk factors for hip fracture in white women, Study of Osteoporotic Fractures Research Group. *N Engl J Med*, 1995; **332**: 767–73.
30. Seeley DG, Kelsey J, Jergas M, Nevitt MC. Predictors of ankle and foot fractures in older women. The Study of Osteoporotic Fractures Research Group. *J Bone Miner Res*, 1996; **11**: 1347–55.
31. Franklyn JA, Maisonneuve P, Sheppard MC, Betteridge J, Boyle P. Mortality after the treatment of hyperthyroidism with radioactive iodine. *N Engl J Med*, 1998; **338**: 712–8.

32. Leese GP, Jung RT, Guthrie C, Waugh N, Browning MC. Morbidity in patients on L-thyroxine: a comparison of those with a normal TSH to those with a suppressed TSH. *Clin Endocrinol*, 1992; **37**: 500–3.
33. Melton LJ, 3rd, Ardila E, Crowson CS, O'Fallon WM, Khosla S. Fractures following thyroidectomy in women: a population-based cohort study. *Bone*, 2000; **27**: 695–700.
34. Van Den Eeden SK, Barzilay JI, Ettinger B, Minkoff J. Thyroid hormone use and the risk of hip fracture in women > or = 65 years: a case-control study. *J Womens Health*, 2003; **12**: 27–31.
35. Sheppard MC, Holder R, Franklyn JA. Levothyroxine treatment and occurrence of fracture of the hip. *Arch Intern Med*, 2002; **162**: 338–43.
36. Lau EM, Suriwongpaisal P, Lee JK, Das De S, Festin MR, Saw SM, et al. Risk factors for hip fracture in Asian men and women: the Asian osteoporosis study. *J Bone Miner Res*, 2001; **16**: 572–80.
37. Vestergaard P, Mosekilde L. Hyperthyroidism, bone mineral, and fracture risk—a meta-analysis. *Thyroid*, 2003; **13**: 585–93.
38. Faber J, Gallo AM. Changes in bone mass during prolonged subclinical hyperthyroidism due to L-thyroxine treatment: a meta-analysis. *Eur J Endocrinol*, 1994; **130**: 350–6.
39. Heemstra KA, Hamdy NA, Romijn JA, Smit JW. The effects of thyrotropin-suppressive therapy on bone metabolism in patients with well-differentiated thyroid carcinoma. *Thyroid*, 2006; **16**: 583–91.
40. Quan ML, Pasieka JL, Rorstad O. Bone mineral density in well-differentiated thyroid cancer patients treated with suppressive thyroxine: a systematic overview of the literature. *J Surg Oncol*, 2002; **79**: 62–9.
41. Uzzan B, Campos J, Cucherat M, Nony P, Boissel JP, Perret GY. Effects on bone mass of long term treatment with thyroid hormones: a meta-analysis. *J Clin Endocrinol Metab*, 1996; **81**: 4278–89.
42. Schneider R, Reiners C. The effect of levothyroxine therapy on bone mineral density: a systematic review of the literature. *Exp Clin Endocrinol Diabetes*, 2003; **111**: 455–70.
43. Wejda B, Hintze G, Katschinski B, Olbricht T, Benker G. Hip fractures and the thyroid: a case-control study. *J Intern Med*, 1995; **237**: 241–7.
44. Bauer DC, Nevitt MC, Ettinger B, Stone K. Low thyrotropin levels are not associated with bone loss in older women: a prospective study. *J Clin Endocrinol Metab*, 1997; **82**: 2931–6.
45. Karner I, Hrgovic Z, Sijanovic S, Bukovic D, Klobucar A, Usadel KH, et al. Bone mineral density changes and bone turnover in thyroid carcinoma patients treated with supraphysiologic doses of thyroxine. *Eur J Med Res*, 2005; **10**: 480–8.
46. Reverter JL, Holgado S, Alonso N, Salinas I, Granada ML, Sanmarti A. Lack of deleterious effect on bone mineral density of long-term thyroxine suppressive therapy for differentiated thyroid carcinoma. *Endocr Relat Cancer*, 2005; **12**: 973–81.
47. Franklyn JA, Betteridge J, Daykin J, Holder R, Oates GD, Parle JV, et al. Long-term thyroxine treatment and bone mineral density. *Lancet*, 1992; **340**: 9–13.
48. Kung AW, Yeung SS. Prevention of bone loss induced by thyroxine suppressive therapy in postmenopausal women: the effect of calcium and calcitonin. *J Clin Endocrinol Metab*, 1996; **81**: 1232–6.
49. Jodar E, Begona Lopez M, Garcia L, Rigopoulou D, Martinez G, Hawkins F. Bone changes in pre- and postmenopausal women with thyroid cancer on levothyroxine therapy: evolution of axial and appendicular bone mass. *Osteoporos Int*, 1998; **8**: 311–6.
50. Paul TL, Kerrigan J, Kelly AM, Braverman LE, Baran DT. Long-term L-thyroxine therapy is associated with decreased hip bone density in premenopausal women. *JAMA*, 1988; **259**: 3137–41.
51. Kung AW, Pun KK. Bone mineral density in premenopausal women receiving long-term physiological doses of levothyroxine. *JAMA*, 1991; **265**: 2688–91.
52. Udayakumar N, Chandrasekaran M, Rasheed MH, Suresh RV, Sivaprakash S. Evaluation of bone mineral density in thyrotoxicosis. *Singapore Med J*, 2006; **47**: 947–50.
53. Andersen S, Bruun NH, Pedersen KM, Laurberg P. Biologic variation is important for interpretation of thyroid function tests. *Thyroid*, 2003; **13**: 1069–78.
54. Hansen PS, Brix TH, Sorensen TI, Kyvik KO, Hegedus L. Major genetic influence on the regulation of the pituitary-thyroid axis: a study of healthy Danish twins. *J Clin Endocrinol Metab*, 2004; **89**: 1181–7.
55. Panicker V, Wilson SG, Spector TD, Brown SJ, Falchi M, Richards JB, et al. Heritability of serum TSH, free T4 and free T3 concentrations: a study of a large UK twin cohort. *Clin Endocrinol*, 2008; **68**: 652–9.
56. Panicker V, Wilson SG, Spector TD, Brown SJ, Kato BS, Reed PW, et al. Genetic loci linked to pituitary-thyroid axis set points: a genome-wide scan of a large twin cohort. *J Clin Endocrinol Metab*, 2008; **93**: 3519–23.
57. Zmuda JM, Kammerer CM. Snipping away at osteoporosis susceptibility. *Lancet*, 2008; **371**: 1479–80.
58. Peeters RP, van der Deure WM, Visser TJ. Genetic variation in thyroid hormone pathway genes; polymorphisms in the TSH receptor and the iodothyronine deiodinases. *Eur J Endocrinol*, 2006; **155**: 655–62.
59. Heemstra KA, van der Deure WM, Peeters RP, Hamdy NA, Stokkel MP, Corssmit EP, et al. Thyroid hormone independent associations between serum TSH levels and indicators of bone turnover in cured patients with differentiated thyroid carcinoma. *Eur J Endocrinol*, 2008; **159**: 69–76.

Bone signaling pathways and treatment of osteoporosis

Expert Rev. Endocrinol. Metab. 4(6), 639–650 (2009)

Apostolos I Gogakos,
Moira S Cheung,
JH Duncan Bassett and
Graham R Williams[†]

[†]Author for correspondence
Molecular Endocrinology Group,
Imperial College London, MRC
Clinical Sciences Centre,
Room 7N2a, 7th Floor
Commonwealth
Building, Hammersmith Hospital,
Du Cane Road, London,
W12 0NN, UK
Tel.: +44 208 383 1383
Fax: +44 208 383 8306
graham.williams@imperial.ac.uk

Osteoporotic fractures are a major healthcare burden costing over US\$50 billion/per year. Bone turnover is a continuous process regulated by the coupled activities of osteocytes, osteoclasts and osteoblasts that maintain bone mass and strength. Osteoclastic bone resorption is regulated by the RANKL/osteoprotegerin/RANK pathway, while osteoblastic bone formation is controlled by canonical Wnt signaling. Antiresorptive bisphosphonates remain the mainstay of treatment but recombinant parathyroid hormone is increasingly being used as an anabolic agent. Nevertheless, these drugs are limited by patient compliance, efficacy and cost. Cathepsin K inhibitors and RANKL antibodies have been developed as new antiresorptive drugs, while short-acting calcilytics and antibodies to Dickkopf-1 and sclerostin are promising anabolics. The recent identification of adipocytes and duodenal enterochromaffin cells as novel regulators of bone mass represent exciting opportunities for future drug development.

KEYWORDS: anabolic • antiresorptive • bone remodeling • osteoblast • osteoclast • osteocytes • osteoporosis
• RANKL/OPG/RANK • Wnt signaling

Osteoporosis is characterized by reduced bone mineral density (BMD) and deterioration of the bone micro-architecture with increased susceptibility to fragility fracture. Osteoporosis affects 50% of women and 20% of men over the age of 50 years, accounting for over 9 million fractures worldwide with an annual estimated cost of US\$50 billion in Northern Europe and the USA [1,2]. Furthermore, osteoporotic fractures impair quality of life owing to chronic pain, skeletal deformities or disability and result in increased mortality [3]. Thus, the economic burden of osteoporosis is already substantial and will continue to rise as the average age of the population increases.

Bone is a dynamic tissue that continually senses load and mechanical stresses, and responds by maintaining optimal bone structure, mineralization and strength in addition to repairing areas of microdamage. This homeostatic process is mediated by the bone remodeling cycle, which is characterized by focal bone resorption followed by new bone formation [4]. Current therapies for osteoporosis manipulate this process to preserve bone mass and strength by either inhibiting bone resorption or stimulating bone formation. Nevertheless, current therapies are limited by patient compliance and efficacy, with 70% of individuals discontinuing treatment in the first

year [5]. Recent advances in our understanding of the signaling pathways that regulate bone turnover have identified new and promising therapeutic targets for the prevention and treatment of osteoporosis.

Bone cell biology

Skeletal remodeling is mediated by the integrated and tightly coupled actions of mechanosensing osteocytes, bone-resorbing osteoclasts and bone-forming osteoblasts (FIGURE 1).

Osteocytes

Osteocytes comprise 90–95% of all adult bone cells. They derive from osteoblasts that have become embedded in bone matrix. Osteocyte cell bodies lie within bone lacunae and their numerous dendritic processes ramify through networks of canaliculi that connect the periosteal and endosteal bone surfaces. Osteocytes sense fluid shear stresses within the canaliculi and communicate with each other via gap junctions at the tips of their dendritic processes [6,7]. Mechanical stresses and localized microdamage control osteocyte signaling pathways that result in release of cytokines and chemotactic signals, or they may induce osteocyte apoptosis. In general, increased mechanical stress stimulates local osteoblastic bone formation, whereas reduced loading or microdamage results in osteoclastic bone resorption [4,8].

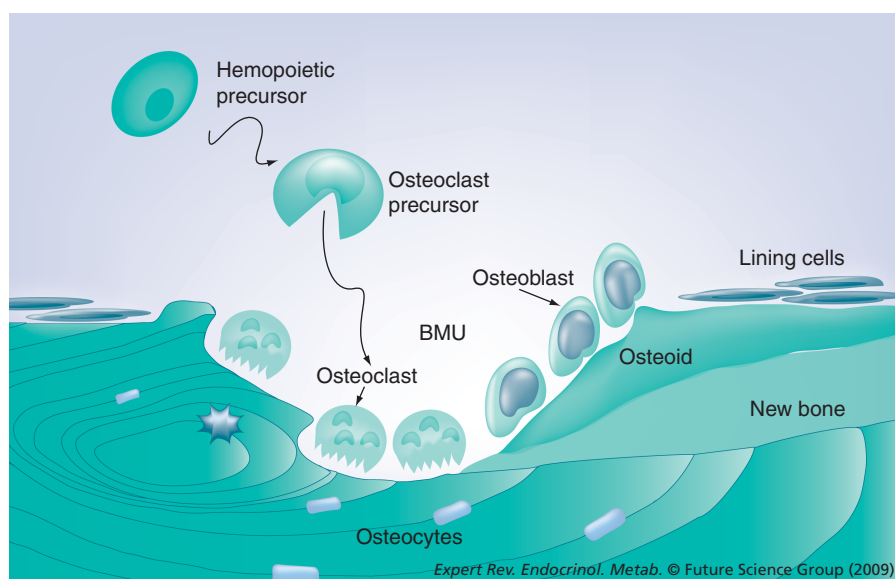


Figure 1. Bone remodeling. Bone remodeling occurs in the BMU. Osteocytes act as mechanosensors and respond to mechanical load and microdamage by recruiting osteoclasts to initiate bone resorption. Removal of bone by osteoclast resorption is followed by deposition of osteoid by osteoblasts, which subsequently mineralize the matrix to form new bone. During bone remodeling, osteoblasts may become embedded within newly formed bone as osteocytes and, following completion of the cycle, form lining cells or undergo apoptosis. BMU: Basic multicellular unit.

Osteoclasts

Osteoclasts comprise 1–2% of bone cells. They are polarized multinucleated cells derived from the monocyte–macrophage lineage that resorb bone matrix and minerals. Attachment of osteoclasts to bone is mediated by $\alpha\beta3$ integrins expressed on the surface of filamentous actin-containing podosomes. $\alpha\beta3$ integrins interact with bone matrix proteins that include osteopontin and vitronectin. These interactions lead to development of an actin ring and sealing zone with polarization of the osteoclast into functionally distinct ruffled border and basolateral membrane regions [9]. Carbonic anhydrase II generates protons (H^+) and bicarbonate (HCO_3^-) within the osteoclast cytoplasm [10] and the HCO_3^- is exchanged for extracellular chloride at the basolateral membrane by a specific Cl^-/HCO_3^- channel. An osteoclast-specific proton pump (H^+ -ATPase) transports the protons across the ruffled border, while the CLCN7 chloride channel balances the ionic charge by transporting chloride simultaneously. Within the resorption lacuna, the resultant acidic environment facilitates dissolution of hydroxyapatite [$Ca_{10}(PO_4)_6(OH)_2$] to release Ca^{2+} and HPO_4^{2-} , while a secreted cysteine protease, cathepsin K, digests the organic bone matrix [10]. The degradation products are endocytosed at the ruffled border, transported across the cytoplasm in tartrate-resistant acid phosphatase-rich vesicles and released at the basolateral membrane by exocytosis (FIGURE 2) [10].

Osteoblasts

Bone-forming osteoblasts comprise approximately 5% of bone cells and are derived from common multipotent mesenchymal stem cells that are capable of differentiation into chondrocytes, osteoblasts or adipocytes. Osteoblast maturation is a stepwise

process comprising precursor cell commitment to the osteoblast lineage, cell proliferation, bone matrix deposition, matrix maturation and bone mineralization. Following the program of bone formation, osteoblasts may ultimately form bone lining cells, become embedded within matrix as osteocytes or undergo apoptosis [11].

Bone remodeling cycle

The continual process of adult bone remodeling is essential for the maintenance of bone mass and skeletal microarchitecture [4]. The basic multicellular unit of bone remodeling comprises osteocytes, osteoclasts and osteoblasts [12]. Over 95% of the surface of the normal adult skeleton is quiescent because osteocytes exert a resting inhibition of both osteoclastic bone resorption and osteoblastic bone formation [11]. By contrast, when local skeletal microdamage occurs or when there is a reduction in mechanical loading, osteocytes respond either by releasing cytokines and chemoattractants or by undergoing apoptosis. These responses result in local

recruitment of osteoclast precursor cells and mature osteoclasts to initiate bone resorption [4]. Osteoclasts excavate a resorption cavity over a period of 3–5 weeks until this process is terminated by apoptosis and followed by recruitment of osteoblast precursors. Subsequently, osteoblasts undergo a program of maturation, during which they secrete and mineralize osteoid to replace the resorbed bone over a period of approximately 3 months [11]. Coupling of osteoclast and osteoblast activities via signaling between the two cell lineages regulates the bone remodeling cycle and results in skeletal homeostasis with preservation of bone strength [13]. In summary, the bone remodeling cycle is initiated and orchestrated by osteocytes, and regulated by coupled crosstalk between osteoblasts and osteoclasts.

Signaling pathways regulating osteoclast differentiation & bone resorption

Bone marrow stromal cells synthesize and secrete macrophage colony-stimulating factor (M-CSF), which promotes proliferation, survival and differentiation of osteoclast precursor cells that express RANK. The ligand that activates RANK (RANKL) is a key osteoclastogenic cytokine sufficient for mature osteoclast formation. RANKL acts via several downstream signaling molecules, including c-fos, NF- κ B, MAPK and TNF receptor-associated factor-6 [14–17]. RANKL also induces expression of the $\alpha\beta3$ integrin in osteoclast precursor cells, which signals via c-src to induce the activation of small GTPases that are critical for formation of the actin ring sealing zone and osteoclast migration and survival. In addition to RANKL, osteoblasts and bone marrow stromal cells also express osteoprotegerin

(OPG). OPG is a secreted decoy receptor for RANKL and functions as the physiological inhibitor of RANK–RANKL signaling (FIGURE 3) [10,18]. Thus, the ratio of RANKL to OPG expressed by osteoblasts determines osteoclast differentiation and activity. This ratio is determined by systemic hormones and local cytokines that regulate bone remodeling, which include estrogen, parathyroid hormone (PTH), glucocorticoids, thyroid hormone, TNF- α , IL-1 and prostaglandin E₂ [19].

Signaling pathways regulating osteoblast differentiation & bone formation

Osteoblast differentiation is predominantly regulated by Wnts, which are mammalian homologs of the *Drosophila* secreted morphogen wingless, and bone morphogenetic proteins, which are members of the TGF- β superfamily. Although commitment of mesenchyme precursors to the osteochondrogenic lineages requires both Wnt and bone morphogenetic protein signaling, the canonical Wnt pathway subsequently acts as the master regulator of osteogenesis [13,20]. In the absence of Wnt, glycogen synthase kinase (GSK)-3 β forms a stable complex with axin and adenomatous polyposis coli proteins and phosphorylates the transcription factor β -catenin in the cytoplasm. Phosphorylated β -catenin is targeted for ubiquitination and degradation by the proteasome, thereby preventing its entry into the nucleus. Binding of Wnt to its receptor Frizzled (Fz) and coreceptor low-density lipoprotein receptor-related protein (LRP) 5 or 6, results in inhibition and degradation of GSK-3 β by the cytoplasmic phosphoprotein dishevelled (Dsh). Anchoring of axin to LRP5/6 is also induced by Dsh and further disrupts the complex containing GSK-3 β and APC. This results in accumulation of β -catenin and its subsequent nuclear translocation. In the nucleus, β -catenin interacts with T-cell factor-4 or lymphoid enhancer binding factor-1 to regulate transcription of Wnt target genes [13,20]. Physiological negative regulation of this critical pathway is mediated by soluble and membrane proteins that interfere with the interaction between Wnt and its receptor and coreceptor. Soluble Fz-related proteins and Wnt inhibitory factor-1 are decoy receptors that bind Wnt and prevent its interaction with Fz. Alternatively, sclerostin and Dickkopf (Dkk) bind to LRP5 and 6 in association with Kremen, a transmembrane receptor for Dkk, resulting in internalization and degradation of LRP5/6 and, thus, inhibition of Wnt signaling (FIGURE 4) [11,20].

Human genetic disorders of bone remodeling

Studies of patients with osteopetrosis, a condition characterized by increased bone mass and mineralization resulting

from osteoclast dysfunction, have resulted in identification of many critical genes and signaling pathways and confirmed their requirement for osteoclast differentiation and activity in humans. Similarly, essential genes in the canonical Wnt signaling pathway that are required for osteoblast differentiation have been revealed by investigation of patients with skeletal dysplasias. Population studies have used polymorphisms in some of these important genes to identify associations with altered BMD and increased fracture risk.

Disruption of osteoclastic bone resorption

Homozygous loss-of-function mutations in RANKL (*TNFSF11*) have been identified in families with autosomal recessive osteopetrosis, in which osteoclast numbers are depleted [21]. In addition, polymorphisms adjacent to *TNFSF11* are associated with reduced BMD and increased fracture susceptibility [22]. Similarly, homozygous or compound heterozygous loss-of-function mutations in RANK (*TNFRSF11A*) have been identified in patients with severe autosomal recessive osteoclast-poor osteopetrosis. Furthermore, homozygous loss-of-function mutations in OPG (*TNFRSF11B*) have been found in patients with juvenile Paget's disease, a condition characterized by osteopenia, fractures and progressive skeletal deformity resulting from abnormal and rapid bone remodeling [23,24]. Polymorphisms adjacent to *TNFRSF11B* are also associated

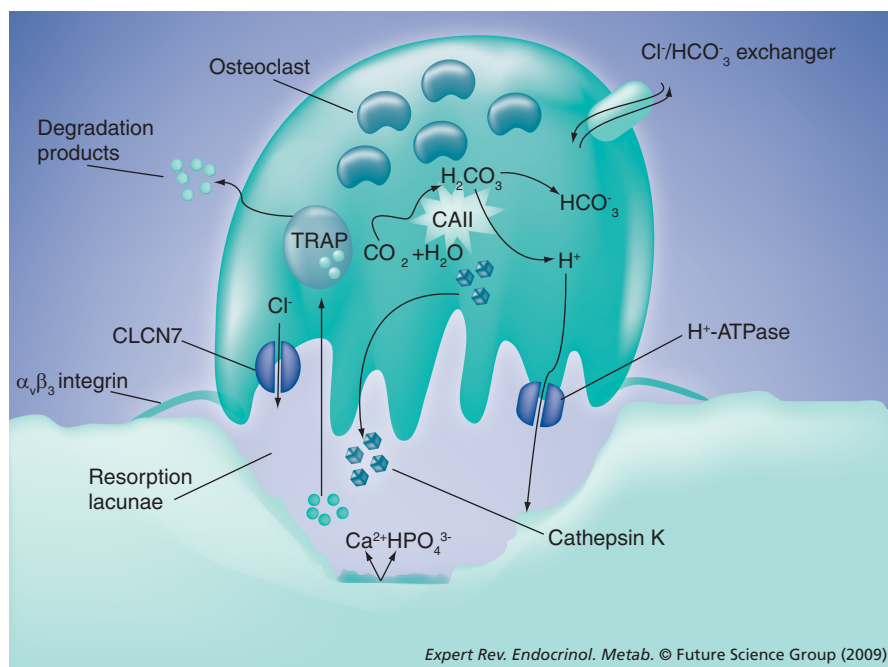


Figure 2. The osteoclast. Osteoclasts attach to bone via podosomes containing filamentous actin and $\alpha v \beta 3$ integrin. CAII generates H⁺ and HCO₃⁻ from CO₂ and H₂O. Protons and chloride ions are transported across the ruffled border into resorption lacunae by an osteoclast-specific H⁺-ATPase pump and the CLCN7 chloride channel. The chloride–bicarbonate exchanger facilitates the balance of ionic charge across the basolateral cell membrane. The acidic environment facilitates dissolution of bone mineral to release Ca²⁺, HPO₄³⁻ and H₂O. Organic matrix is degraded by cathepsin K and degradation products are transported across the cytoplasm in TRAP-containing vesicles and exocytosed at the basolateral membrane. CAII: Carbonic anhydrase II; TRAP: Tartrate-resistant acid phosphatase.

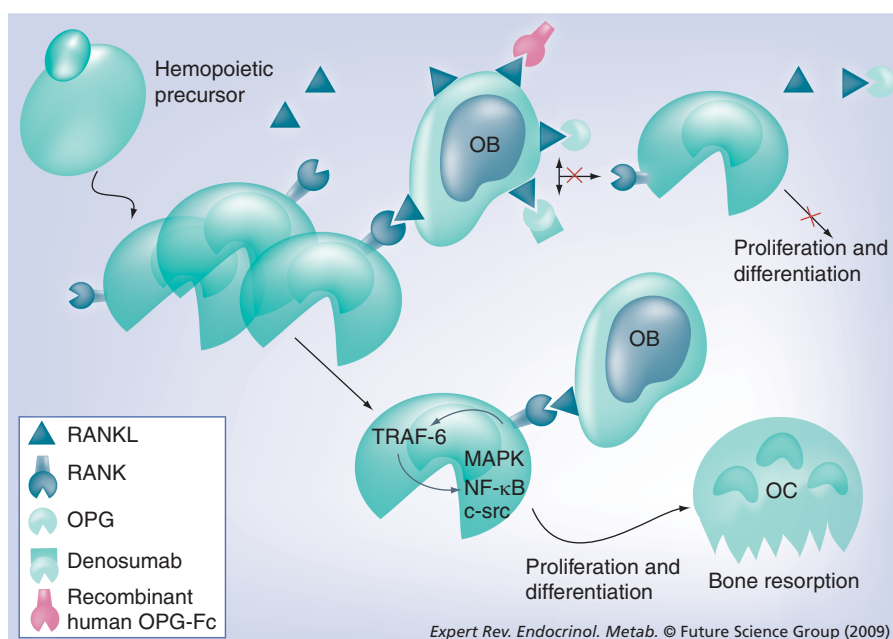


Figure 3. Therapeutic targeting of RANKL/OPG/RANK signaling. Osteoclasts express RANK, while osteoblasts express the RANKL and also secrete a decoy receptor and physiological inhibitor of the RANKL/RANK interaction, OPG. RANKL/RANK signaling stimulates osteoclastogenesis and the ratio of RANKL to OPG expressed by osteoblasts determines the level of osteoclast differentiation and activity. Denosumab, an anti-RANKL fully humanized monoclonal antibody acts like OPG to inhibit RANKL/RANK signaling and decrease bone resorption. A recombinant human OPG–Fc fusion protein was also used to inhibit RANKL/RANK signaling, but its clinical use was limited by the development of antibodies resulting in loss of efficacy. c-src: c-src tyrosine kinase; NF-κB: Nuclear factor-κB; OB: Osteoblast; OC: Osteoclast; OPG: Osteoprotegerin; OPG-Fc: Osteoprotegerin fused to the Fc portion of human IgG1; TRAF: TNF receptor-associated factor.

with altered BMD and fracture risk [22,25]. Together, these studies have confirmed the critical role of the RANKL/OPG/RANK pathway in osteoclastogenesis and control of bone turnover.

Similar investigations of patients with osteopetrosis but normal osteoclast numbers have resulted in identification of critical genes required for osteoclast function. Homozygous or compound heterozygous loss-of-function mutations of *CAII* (*CA2*) have been identified in patients with autosomal recessive osteopetrosis and renal tubular acidosis [26]. In addition to the impaired generation of protons resulting from *CA2* inactivation, mutations resulting in disruption of H^+ and Cl^- ion transport have also been described in patients with osteopetrosis. Thus, homozygous and compound heterozygous loss-of-function mutations of *CLCN7* encoding the osteoclast chloride channel cause the rare autosomal recessive infantile malignant osteopetrosis [27], while heterozygous dominant negative mutations result in the more common Albers–Schönberg autosomal dominant osteopetrosis [28]. Furthermore, homozygous mutations of osteopetrosis-associated transmembrane protein 1 (*OSTM1*) also cause a syndrome of autosomal recessive infantile malignant osteopetrosis. *OSTM1* localizes to late endosomes, lysosomes and the osteoclast ruffled border, and interacts with *CLCN7* facilitating acidification of the osteoclast resorption lacuna [29]. Homozygous or compound heterozygous loss-of-function mutations in the osteoclast-specific

H^+ -ATPase (*TCIRG1*) also cause autosomal recessive infantile malignant osteopetrosis in which osteoclast numbers are normal or elevated [30,31] but resorption lacuna acidification is impaired. Finally, a homozygous loss-of-function mutation in pleckstrin homology domain-containing protein, family M, member 1 (*PLEKHM1*) resulted in a less severe recessive adult osteopetrosis syndrome, in which osteoclast numbers were again normal. *PLEKHM1* is a prenylated protein thought to be important in vesicle acidification and exocytosis of tartrate-resistant acid phosphatase in osteoclasts [32]. An additional heterozygous missense mutation in *PLEKHM1* has been described in a patient with low BMD but areas of focal osteosclerosis [33], further confirming the critical importance of acidification and endosomal transport pathways in the function of mature osteoclasts and regulation of bone mass.

Disruption of osteoblastic bone formation

The central role of the canonical Wnt pathway in osteoblast function in humans was first shown following identification of homozygous loss-of-function mutations of *LRP5* in osteoporosis–pseudoglioma syndrome, in which patients have reduced BMD, skeletal fragility and congenital

blindness [34]. By contrast, a heterozygous G171V point mutation in *LRP5* causes an autosomal dominant high bone mass trait [35,36]. The mutant *LRP5* protein has impaired binding to Dkk1, sclerostin and other soluble inhibitors of Wnt signaling, and this mechanism is thought to result in increased osteoblastic bone formation [37,38]. Other missense mutations in the N-terminal of *LRP5* are associated with increased BMD, mainly affecting long bones and the skull [39]. Polymorphisms in *LRP5* have also been associated with BMD and fracture risk in population studies [40]. Consistent with these findings, homozygous loss-of-function mutations in the *SOST* gene encoding sclerostin result in the sclerosteosis syndrome, which is characterized by cortical hyperostosis and syndactyly [41]. Furthermore, homozygous genomic deletions adjacent to *SOST* reduce its expression and cause van Buchem disease, which is similarly characterized by cortical hyperostosis [42]. Polymorphisms within *SOST* are also associated with altered BMD, although no effects on fracture risk were observed in prospective studies [43].

Prevention & treatment of osteoporosis

The recent advances in understanding of the molecular mechanisms underlying homeostatic control of bone mass, together with characterization of the genetic basis of human skeletal

disorders, has identified novel therapeutic targets for the prevention and treatment of osteoporosis. In addition, these advances have clarified the underlying mechanisms by which currently available drugs act to inhibit bone resorption or promote bone formation.

Drugs that inhibit bone resorption: currently available drugs

Bisphosphonates

Nitrogen-containing bisphosphonates, including alendronate, risedronate, ibandronate and zoledronic acid, are the most widely used drugs for the primary and secondary prevention of osteoporosis. The skeletal selectivity of nitrogen-containing bisphosphonates is a consequence of their avid binding to calcium hydroxyapatite, and this property also accounts for their extended biological half-life in bone. The nitrogen-containing bisphosphonates inhibit farnesyl diphosphate synthase within the mevalonate pathway. Inhibition of farnesyl diphosphate synthase results in disruption of prenylation of small GTPases, including Ras, Rho, Rac and Rab. These GTPases are essential for osteoclast cytoskeletal organization, formation of the sealing zone and ruffled border, vesicle transport and osteoclast survival. Thus, the bisphosphonates inhibit osteoclast function and promote cellular apoptosis [44,45]. Inhibition of osteoclastic bone resorption by bisphosphonates results in reduced bone

turnover and a concomitant reduction in osteoblastic bone formation. Although long-term studies of up to 10 years have shown a persistent reduction in fracture risk with alendronate treatment [46], there remain concerns that prolonged suppression of bone remodeling may result in increased bone fragility. Indeed, a number of studies have reported atraumatic atypical subtrochanteric fractures of the femoral cortex in patients treated with alendronate for up to 8 years [47,48]. An additional problem that has been highlighted recently is osteonecrosis of the jaw, which is characterized by persistent exposure of necrotic mandibular or maxillary bone. Its association with high-dose intravenous bisphosphonate therapy was initially identified in patients treated for malignant disease. However, osteonecrosis of the jaw is rare in osteoporotic patients treated with bisphosphonates, its incidence being estimated at less than 1:100,000 patient years [49]. In summary, nitrogen-containing bisphosphonates are widely and safely used in the vast majority of patients and they are effective, with a 35–65% reduction in vertebral fracture risk and 25–50% reduction in hip fractures [50,51]. Despite this, the clinical effectiveness of oral bisphosphonates is limited by compliance and

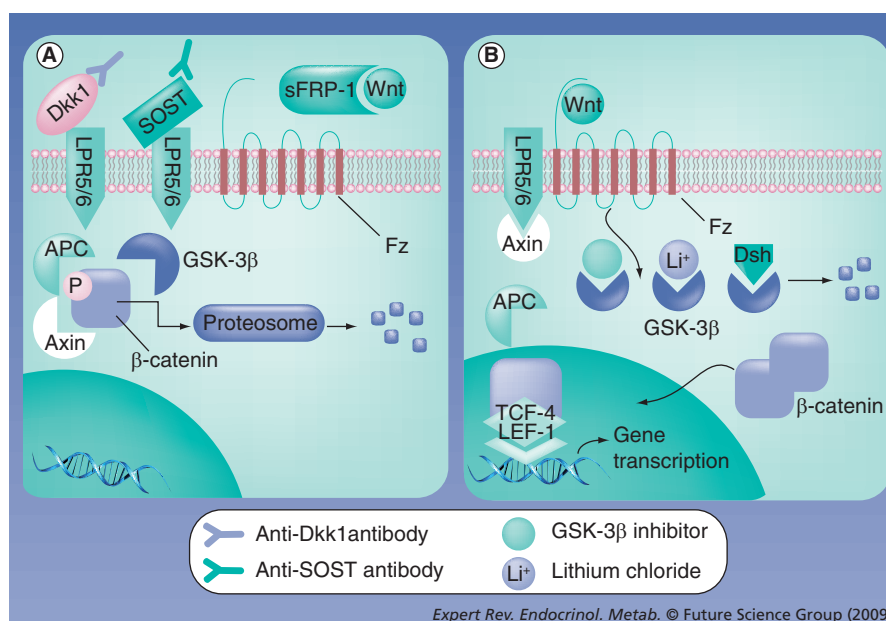


Figure 4. Therapeutic targeting of canonical Wnt signaling. (A) The canonical Wnt pathway acts as the master regulator of osteogenesis. Wnt signaling is physiologically inhibited by sFRP1, Dkk1 and SOST, which bind soluble Wnt or bind to the Wnt coreceptor LRP5/6 and target its degradation. In the absence of Wnt, β-catenin is phosphorylated by GSK-3β in a complex containing axin and APC, thus targeting its ubiquitination and degradation by the proteasome. Neutralizing humanized antibodies that target either Dkk1 or SOST relieve the physiological inhibition of Wnt signaling resulting in increased osteoblastic bone formation. (B) Binding of Wnt to its receptor Fz and coreceptor LRP5/6 causes Dsh-mediated degradation of GSK-3β and anchoring of axin to LRP5/6, thus resulting in inhibition of β-catenin phosphorylation. Unphosphorylated β-catenin accumulates and translocates to the nucleus where it activates Wnt target genes following interaction with the transcription factors TCF-4 or LEF-1. Li⁺ and other small-molecule inhibitors of GSK-3β enhance Wnt signaling by interfering with phosphorylation of β-catenin and facilitating its accumulation and translocation to the nucleus. APC: Adenomatous polyposis coli; Dkk: Dickkopf; Dsh: Dishevelled; Fz: Frizzled; GSK: Glycogen synthase kinase; LEF: Lymphoid enhancer factor; sFRP: Secreted frizzled related protein; SOST: Sclerostin; TCF: T-cell factor.

patient intolerance of gastrointestinal side-effects; up to 70% of patients have been reported to discontinue treatment during the first year of therapy [5].

Selective estrogen-receptor modulators

Estrogen acts via ligand-inducible nuclear receptors (estrogen receptors [ERs]) to regulate expression of target genes in skeletal cells. Estrogens act directly in monocytes, bone marrow stromal cells and osteoblasts, which respond by reducing the expression and secretion of cytokines, including IL-1, IL-6, TNF-α, granulocyte–monocyte colony-stimulating factor, M-CSF and RANKL, while increasing expression and secretion of OPG and TGF-β. The overall effect is that estrogen reduces osteoclast number and activity, and thus inhibits bone resorption and turnover [52–54]. Conversely, estrogen deficiency results in high bone turnover with accelerated bone loss leading to an increased risk of fragility fracture. While estrogen-replacement therapy reverses these skeletal effects, its detrimental actions in other tissues result in unacceptable side effects that now preclude its use in osteoporosis prevention and treatment; these include an increased risk of coronary

heart disease, breast cancer and thromboembolic disease [55–58]. Selective ER modulators (SERMs) are ligands that exhibit varying degrees of ER agonist activity leading to tissue selectivity. The ideal SERM would have ER agonist activity in bone, brain and the urogenital tract, while having no detrimental effects in the breast, endometrium or cardiovascular system. The second-generation SERM raloxifene is used as a second-line treatment for osteoporosis and reduces vertebral fracture risk, but is not effective at nonvertebral sites. Although raloxifene may have a protective effect against breast cancer, it has a similar risk of thromboembolic disease to estrogen. Furthermore, the frequent occurrence of menopausal vasomotor symptoms with raloxifene treatment limits patient tolerability and results in poor compliance [59].

Novel antiresorptive agents

Cathepsin K inhibitors

Cathepsin K is a key osteoclast-specific enzyme required for bone resorption and thus represents a potential drug target to inhibit bone loss [60]. A 12-month oral treatment with balicatib, a nonselective cathepsin inhibitor, resulted in a 2–4% increase in lumbar spine and hip BMD accompanied by a reduction in bone turnover [61]. Unfortunately, use of this agent was limited by adverse skin reactions and the drug was withdrawn. Subsequently, a 2-year randomized Phase IIB trial of odanacatib, a well-tolerated selective inhibitor of cathepsin K, revealed a 50% reduction in bone resorption and 10% reduction in bone formation accompanied by 3 and 6% gains in BMD at the femoral neck and lumbar spine, respectively [62]. The effect of odanacatib on vertebral, hip and nonvertebral fractures is currently being investigated in a worldwide Phase III study [31].

Inhibitors of RANKL/RANK signaling

RANKL is the key regulator of osteoclast function and survival, mediating crosstalk between osteoblasts and osteoclasts [14]. OPG is the physiologically negative regulator of RANKL and three different approaches have been adopted to pharmacologically inhibit RANKL signaling. Initially, subcutaneous injection of a recombinant human OPG–Fc fusion protein, a chimera comprising mature soluble OPG and the Fc fragment of IgG₁, was demonstrated to be an effective and potent inhibitor of bone resorption [63,64]. However, its clinical use was limited by the development of antibodies that resulted in a reduced effective half-life and the necessity for increasing doses and frequency of administration [65]. As a result, denosumab, a human monoclonal IgG₂ RANKL antibody, was developed as a direct inhibitor of RANKL/RANK signaling [66]. In six reported Phase II and III clinical trials, 3–6 monthly subcutaneous injections of denosumab administered for between 1 and 3 years have been demonstrated to reduce differentiation, activation and survival of osteoclasts, inhibit bone resorption and increase BMD [67–72]. Fracture risk was also reduced by 68% at the lumbar spine, 40% at the hip and 20% at other nonvertebral sites [72]. Despite these promising results, since RANKL/RANK signaling is also involved in regulation of the immune system there are concerns that general inhibition of

this pathway may result in significant side effects that will need to be addressed in long-term clinical trials [68,73]. Nevertheless, the recent identification of an intracellular motif of RANK that might be specifically involved in osteoclast differentiation may provide an opportunity for inhibition of RANK signaling specifically in osteoclasts. A cell permeable RANK receptor inhibitor peptide has been developed to target this motif and it was shown to protect against ovariectomy-induced bone loss in mice by inhibiting osteoclast maturation and activity [74].

C-src kinase inhibitors

C-src, a nonreceptor tyrosine kinase, is a key regulator of osteoclast cytoskeletal organization required for sealing zone formation. It is an important secondary messenger signaling molecule involved in mediating the actions of M-CSF and RANKL. Initial studies showed that inhibition of c-src reduces bone resorption *in vitro* and decreases bone loss in ovariectomized rodents [75], although preliminary results in humans have been less promising and this target has not been pursued further.

$\alpha\beta 3$ integrin inhibitors

The $\alpha\beta 3$ integrin is essential for formation of the osteoclast sealing zone and is, therefore, a potential therapeutic target for inhibition of osteoclast function. The orally active $\alpha\beta 3$ integrin antagonist, SB265123, prevented ovariectomy-induced bone loss in rodents [76], while in a multicenter, randomized, double-blind, placebo-controlled, 12-month study the $\alpha\beta 3$ integrin antagonist L-000845704 resulted in reduced bone turnover and a small increase in BMD at the hip and femoral neck [77]. However, $\alpha\beta 3$ integrin antagonists have not been pursued further as potential drugs for the treatment of osteoporosis because of limited efficacy and nonselective actions.

Drugs that promote bone formation: currently available drugs

Recombinant PTH

In bone, PTH activates the G-protein-coupled PTH receptor PTH receptor in cells of the osteoblast lineage. Continuous activation of the PTHR results in bone loss, whereas intermittent stimulation results in increased bone formation although the underlying molecular mechanisms are poorly understood. Continuous exposure of osteoblasts to PTH receptor increases expression of M-CSF and RANKL but reduces expression of OPG resulting in increased osteoclastogenesis and bone resorption. By contrast, intermittent PTH induces Runx-2 expression in osteoblasts, increases osteoblast cell number and delays cellular apoptosis. PTH augments differentiation of committed osteoblast precursors by stimulating exit of proliferating cells from the cell cycle. It is thought these effects sensitize osteoblasts to the actions of IGF-1, FGF2 and Wnts, thereby promoting an anabolic skeletal response to intermittent PTH administration [78].

Recombinant human PTH(1–34) fragment (teriparatide) is licensed for treatment of osteoporosis in Europe and the USA, whereas full-length intact PTH(1–84) is only licensed in Europe.

In an 18-month randomized double-blind study, treatment with teriparatide resulted in a twofold increase in bone formation and 60% increase in resorption [79]. In a separate study, treatment of postmenopausal women with teriparatide resulted in 10 and 2.5% increases in BMD at the spine and hip, respectively, with reductions in vertebral fractures and nonvertebral fragility fractures of 60 and 50% [80]. Similarly, treatment of postmenopausal women with PTH(1–84) in a double-blind, placebo-controlled study resulted in a 7% increase in BMD at the spine and 2% increase at the hip. These changes were accompanied by a relative risk reduction of 58% for vertebral fractures but no reduction in nonvertebral fractures [81]. Even though transient and mild increases in serum calcium are common in the first 6 months of treatment, teriparatide is generally well tolerated. Although initial safety studies suggested that administration of high and prolonged doses of teriparatide was associated with osteosarcoma in rats, only one case has been reported in more than 600,000 patients treated with the drug [82]. Nevertheless, widespread use of teriparatide is limited by its subcutaneous route of administration and high cost.

Novel anabolic agents

Modulators of calcium-sensing receptors to stimulate transient endogenous PTH release

Calcium-sensing receptors are G-protein coupled receptors expressed in the parathyroid glands that mediate inhibition of PTH synthesis and release in response to changes in serum calcium concentration to maintain negative feedback control of calcium homeostasis [83]. The success of subcutaneously and intermittently administered PTH as an anabolic agent has resulted in investigation of short-acting orally active calcilytic drugs to inhibit the calcium-sensing receptors and induce transient release of PTH. The first agent to be investigated in Phase II clinical trials, ronacaleret, did not have sufficient efficacy to be pursued. New calcilytic compounds have been developed subsequently and additional studies are continuing because of the current lack of an orally active anabolic agent [84].

Agonists of the canonical Wnt signaling pathway

GSK-3 β inhibitors

GSK-3 β is a multifunctional serine/threonine kinase that is central to Wnt signaling but also involved in the regulation of numerous other signaling pathways [20]. Nevertheless, GSK-3 β is amenable to pharmacological manipulation. Thus, treatment of ovariectomized rats with a nonspecific GSK-3 α and -3 β inhibitor (LY603281-31-8) increased bone mineral content and BMD and also improved bone strength [85]. Furthermore, treatment of mice with the selective GSK-3 β inhibitors lithium chloride or 6-bromoindirubin-3'-oxime resulted in enhanced bone formation and increased bone mass [86]. In addition, case-control studies have shown that long-term treatment of patients with bipolar disorder results in a reduced risk of fracture [87]. However, since GSK-3 β has also been implicated in the pathogenesis of Alzheimer's disease and noninsulin-dependent diabetes [20], clinical use of selective GSK-3 β inhibitors in osteoporosis may be limited by their extraskelatal actions [88].

Inhibitors of physiological antagonists of canonical Wnt signaling

Inhibitors of the negative regulators of Wnt signaling are potential candidates for the prevention and treatment of bone loss. In mice, *Dkk1* haploinsufficiency results in high bone mass, whereas its transgenic overexpression causes osteopenia [89,90]. Treatment of rats with antisense *Dkk1* oligonucleotides prevents the detrimental effects of ovariectomy by improving bone mineral content, BMD and bone strength [91]. In multiple myeloma, *Dkk1* levels are associated with the extent of osteolysis [92] and treatment is accompanied by a reduction in serum *Dkk1* levels [93]. Fully human monoclonal *Dkk1*-neutralizing antibodies enhanced bone formation, increased BMD and reduced osteolytic bone resorption, as well as reducing tumor burden in SCID-rab mice with multiple myeloma [94,95]. These promising preclinical data have resulted in further investigation of a human *Dkk1* monoclonal antibody BHQ880 in current Phase Ib and Phase II clinical trials in patients with multiple myeloma [3].

Reduced expression of sclerostin or impairment of its interaction with LRP5/6 results in sclerosteosis, van Buchem's disease or high bone mass trait, suggesting that pharmacological inhibition of sclerostin may prevent bone loss [96,97]. This represents a particularly attractive strategy as sclerostin expression is restricted to osteocytes [98]. Following 1 year of estrogen deficiency, treatment of ovariectomized rats with a sclerostin-neutralizing monoclonal antibody enhanced bone formation, resulting in increased bone mass and bone strength to levels greater than those in nonovariectomized controls [99]. As a result of these encouraging findings, the clinical efficacy of sclerostin neutralizing antibodies (AMG 785) is being tested in a Phase II clinical trial of postmenopausal women with low BMD [3].

Agents with dual actions on bone resorption & formation

Strontium ranelate

Strontium is a divalent cation with a molecular weight more than twice that of calcium. Strontium ranelate is currently used in Europe as a second-line agent for the treatment of osteoporosis, although it is not licensed in the USA [67]. Strontium ranelate is thought to inhibit osteoclast differentiation and activity directly, while also stimulating osteoblast proliferation and differentiation, perhaps acting via the calcium-sensing receptor and prostaglandins [100]. Treatment results in an approximately 30–45% reduction in vertebral fracture risk and 15–30% reduction at nonvertebral sites [101,102]. Strontium ranelate has been associated with an increased risk of venous thromboembolism [103]. Importantly, interpretation of bone densitometry data is complicated by the incorporation of x-ray dense strontium into bone; thus, any relative change in BMD following treatment must be corrected accordingly [104]. Furthermore, the requirement for daily administration of the drug limits patient compliance.

Expert commentary

Understanding of the molecular and genetic basis for regulation of bone remodeling has advanced rapidly in the last decade. Nevertheless, the incidence and financial burden of osteoporosis

is relentlessly increasing as the population progressively ages. Prevention and treatment of osteoporosis continues to rely on antiresorptive treatment with bisphosphonates, although a single anabolic agent, teriparatide, has recently become available. Poor tolerability and compliance in the case of bisphosphonates, and problems relating to route of administration and cost in the case of teriparatide, clearly highlight the need for development of new drugs. Two key signaling pathways that control osteoclast and osteoblast function have now been identified. Targeting the RANKL/OPG/RANK pathway has led to development of novel antiresorptive compounds, while targeting Wnt signaling has resulted in the emergence of new anabolic agents. SERMs and other drug classes are continuously being refined to increase their efficacy. Ensuring skeletal specificity of these new agents is a significant challenge and their pharmacodynamics, long-term safety and compliance will also require optimization. A further area under intense current study is whether combination or sequential administration of antiresorptive and anabolic drugs should be used to maximize therapeutic benefit and minimize dose-related side effects.

Five-year view

Although great progress has been made in our understanding of skeletal homeostasis, fundamental new pathways that control bone mass have recently been discovered. Leptin is an adipokine and its serum concentrations are proportional to fat mass. Leptin suppresses appetite via actions in the hypothalamic arcuate nucleus resulting in homeostatic maintenance of bodyweight via a classical negative-feedback loop [105]. Recent studies have shown that leptin also regulates bone mass through a regulatory loop that involves the ventromedial hypothalamic nuclei [106,107]. Leptin regulates bone mass by its effects on both osteoblasts and osteoclasts. It regulates bone formation by controlling the rate of osteoblast proliferation via two opposing pathways coordinated by the SNS [107–110]. Furthermore, leptin also regulates bone resorption via two opposing pathways. It promotes bone resorption by increasing osteoclast differentiation via its actions to induce RANKL expression in

osteoblasts [111], but also inhibits resorption by unknown mechanisms that involve the neurotransmitter cocaine- and amphetamine-regulated transcript [112]. Thus, leptin is a homeostatic hormone that links regulation of bodyweight by adipocytes to the control of bone mass. More recently, osteocalcin has been identified as a homeostatic regulator secreted by osteocytes that controls insulin sensitivity, glucose homeostasis and fat mass [113]. These landmark findings demonstrate communication between adipocytes, the hypothalamus and bone. In the coming years, detailed characterization of the cellular pathways involved in this regulatory loop will identify new therapeutic targets for treatment of obesity, diabetes and osteoporosis.

Of equal significance, the central role of the Wnt pathway in osteoblasts to regulate bone formation has been challenged. Analysis of mice with gut-specific deletion of the Wnt coreceptor LRP5 recapitulated the skeletal phenotype of low bone mass observed in *Lrp5*^{-/-} mice, whereas mice with osteoblast-specific deletion of LRP5 did not [114,115]. Microarray studies in *Lrp5*^{-/-} mice demonstrated greatly increased expression of *Tph1* encoding tryptophan hydroxylase, the rate-limiting enzyme responsible for synthesis of serotonin [114]. Subsequently, duodenal LRP5 activity was shown to inhibit serotonin synthesis in enterochromaffin cells of the duodenum and circulating serotonin was demonstrated to reduce bone formation by inhibiting osteoblast proliferation directly [114,116]. These findings suggest that Wnts act in duodenal enterochromaffin cells to reduce circulating serotonin levels and thus increase bone formation. Identification of serotonin as a new factor that contributes to the regulation of bone mass may offer further anabolic opportunities for the future.

Financial & competing interests disclosure

The authors have no relevant affiliations or financial involvement with any organization or entity with a financial interest in or financial conflict with the subject matter or materials discussed in the manuscript. This includes employment, consultancies, honoraria, stock ownership or options, expert testimony, grants or patents received or pending, or royalties.

No writing assistance was utilized in the production of this manuscript.

Key issues

- Osteoporosis results in over nine million fractures per year at a cost of more than US\$50 billion.
- Bone mass and strength are maintained by the bone remodeling cycle involving the integrated actions of osteocytes, osteoclasts and osteoblasts.
- Current therapies for the prevention and treatment of osteoporosis are limited by efficacy and patient compliance.
- RANKL/osteoprotegerin/RANK signaling regulates bone resorption and is essential for osteoclastogenesis, osteoclast activity and survival.
- Canonical Wnt signaling regulates bone formation and is essential for osteoblast proliferation, differentiation, function and survival.
- Antiresorptive agents are the mainstay of current osteoporosis treatment and include bisphosphonates, Selective estrogen receptor modulators and strontium ranelate.
- Novel antiresorptive agents include cathepsin K inhibitors and fully humanized RANKL-neutralizing antibodies.
- Teriparatide and parathyroid hormone(1–84) are the only currently available purely anabolic agents but require daily subcutaneous administration.
- Novel anabolic therapies include short-acting calcilytic agents and neutralizing antibodies to Dkk1 and sclerostin.
- Novel regulatory pathways linking fat mass, the CNS and the GI tract to the control of bone mass will offer many new therapeutic opportunities for the prevention and treatment of osteoporosis in the future.

References

Papers of special note have been highlighted as:

• of interest

•• of considerable interest

- 1 Kanis JA; on behalf of the World Health Organization Scientific Group. Assessment of osteoporosis at the primary health-care level: technical report. *World Health Organization Collaborating Centre for Metabolic Bone Diseases*. University of Sheffield, Sheffield, UK (2007).
- **Detailed review of osteoporosis epidemiology and fracture risk assessment.**
- 2 Sambrook P, Cooper C. Osteoporosis. *Lancet* 367(9527), 2010–2018 (2006).
- 3 Lewiecki ME. Emerging drugs for postmenopausal osteoporosis. *Expert Opin. Emerg. Drugs* 14(1), 129–144 (2009).
- 4 Seeman E, Delmas PD. Bone Quality – the material and structural basis of bone strength and fragility. *N. Engl. J. Med.* 354, 2250–2261 (2006).
- **Physiology and pathophysiology of bonemetabolism.**
- 5 Cotté FE, Fardellone P, Mercier F, Gaudin AF, Roux C. Adherence to monthly and weekly oral bisphosphonates in women with osteoporosis. *Osteoporos Int.* DOI: 10.1007/s00198-009-0930-1 (2009) (Epub ahead of print).
- 6 Bonewald LF, Johnson ML. Osteocytes, mechanosensing and Wnt signaling. *Bone* 42, 606–615 (2008).
- 7 Bilezikian JP, Matsumoto T, Bellido T *et al.* Targeting bone remodeling for the treatment of osteoporosis: summary of the proceedings of an ASBMR workshop. *J. Bone Miner. Res.* 24(3), 373–385 (2009).
- 8 Han Y, Cowin SC, Schaffler MB, Weinbaum S. Mechanotransduction and strain amplification in osteocyte cell processes. *Proc. Natl Acad. Sci. USA* 101, 16689–16694 (2004).
- 9 Vaananen HK, Zhao H, Mulari M, Halleen JM. The cell biology of osteoclast function. *J. Cell. Sci.* 113, 377–381 (2000).
- 10 Tolar J, Teitelbaum SL, Orchard PJ. Osteopetrosis. *N. Engl. J. Med.* 351, 2839–2849 (2004).
- 11 Martin TJ, Sims NA, Ng KW. Regulatory pathways revealing new approaches to the development of anabolic drugs for osteoporosis. *Osteoporos. Int.* 19, 1125–1138 (2008).
- 12 Koshla S, Westendorf JJ, Ousler MJ. Building bone to reverse osteoporosis and repair fractures. *J. Clin. Invest.* 118, 421–428 (2008).
- 13 Canalis E, Giustina A, Bilezikian JP. Mechanisms of anabolic therapies for osteoporosis. *N. Engl. J. Med.* 357, 905–916 (2007).
- **Very good review of the biological basis of many emerging anabolic agents.**
- 14 Kearns AE *et al.* Receptor activator of nuclear factor κ B ligand and osteoprotegerin regulation of bone remodeling in health and disease. *Endocr. Rev.* 29, 155–192 (2008).
- **RANK/RANKL/osteoprotegerin involvement in regulation of bone remodeling.**
- 15 Yasuda H, Shima N, Nakagawa N *et al.* Osteoclast differentiation factor is a ligand for osteoprotegerin/osteoclastogenesis-inhibitory factor and is identical to TRANCE/RANKL. *Proc. Natl Acad. Sci. USA* 95, 3597–3602 (1998).
- 16 Burgess TL, Qian Y, Kaufman S *et al.* The ligand for osteoprotegerin (OPGL) directly activates mature osteoclasts. *J. Cell. Biol.* 145, 527–538 (1999).
- 17 Lee ZH, Kim HH. Signal transduction by receptor activator of nuclear factor κ B in osteoclasts. *Biochem. Biophys. Res. Commun.* 305, 211–214 (2003).
- 18 Lacey DL, Timms E, Tan HL *et al.* Osteoprotegerin ligand is a cytokine that regulates osteoclast differentiation and activation. *Cell* 93, 165–176 (1998).
- 19 Teitelbaum SL, Ross FP. Genetic regulation of osteoclast development and function. *Nat. Rev. Genet.* 4, 638–649 (2003).
- 20 Baron R, Rawadi G. Minireview: targeting the Wnt/ β -catenin pathway to regulate bone formation in the adult skeleton. *Endocrinology* 148(6), 2635–2643 (2007).
- **Elucidation of Wnt signalling pathway and its implication in regulation of bone formation.**
- 21 Sobacchi C, Frattini A, Guerrini MM *et al.* Osteoclast-poor human osteopetrosis due to mutations in the gene encoding RANKL. *Nat. Genet.* 39(8), 960–962 (2007).
- 22 Styrkarsdottir U, Halldorsson BV, Gretarsdottir S *et al.* Multiple genetic loci for bone mineral density and fractures. *N. Engl. J. Med.* 358(22), 2355–2365 (2008).
- 23 Whyte MP, Obrecht SE, Finnegan PM *et al.* Osteoprotegerin deficiency and juvenile Paget's disease. *N. Engl. J. Med.* 347(3), 175–184 (2002).
- 24 Cundy T, Hegde M, Naot D *et al.* A mutation in the gene *TNFRSF11B* encoding osteoprotegerin causes an idiopathic hyperphosphatasia phenotype. *Hum. Mol. Genet.* 11(18), 2119–2127 (2002).
- 25 Arko B, Prezelj J, Komel R, Kocijancic A, Hudler P, Marc J. Sequence variations in the osteoprotegerin gene promoter in patients with postmenopausal osteoporosis. *J. Clin. Endocrinol. Metab.* 87(9), 4080–4084 (2002).
- 26 Venta PJ, Welty RJ, Johnson TM, Sly WS, Tashian RE. Carbonic anhydrase II deficiency syndrome in a Belgian family is caused by a point mutation at an invariant histidine residue (107 His→Tyr): complete structure of the normal human CA II gene. *Am. J. Hum. Genet.* 49(5), 1082–1090 (1991).
- 27 Kornak U, Kasper D, Bösl MR *et al.* Loss of the ClC-7 chloride channel leads to osteopetrosis in mice and man. *Cell* 104(2), 205–215 (2001).
- 28 Cleiren E, Bénichou O, Van Hul E *et al.* Albers-Schönberg disease (autosomal dominant osteopetrosis, type II) results from mutations in the CLCN7 chloride channel gene. *Hum. Mol. Genet.* 10(25), 2861–2867 (2001).
- 29 Chalhouh N, Benachenhou N, Rajapurohitam V *et al.* Grey-lethal mutation induces severe malignant autosomal recessive osteopetrosis in mouse and human. *Nat. Med.* 9(4), 399–406 (2003).
- 30 Frattini A, Orchard PJ, Sobacchi C *et al.* Defects in TCIRG1 subunit of the vacuolar proton pump are responsible for a subset of human autosomal recessive osteopetrosis. *Nat. Genet.* 25(3), 343–346 (2000).
- 31 Kornak U, Schulz A, Friedrich W *et al.* Mutations in the α 3 subunit of the vacuolar H(+)-ATPase cause infantile malignant osteopetrosis. *Hum. Mol. Genet.* 9(13), 2059–2063 (2000).
- 32 Van Wesenbeeck L, Odgren PR, Coxon FP *et al.* Involvement of PLEKHM1 in osteoclastic vesicular transport and osteopetrosis in incisors absent rats and humans. *J. Clin. Invest.* 117(4), 919–930 (2007).
- 33 Del Fattore A, Fornari R, Van Wesenbeeck L *et al.* A new heterozygous mutation (R714C) of the osteopetrosis gene, pleckstrin homolog domain containing family M (with run domain) member 1 (*PLEKHM1*), impairs vesicular acidification and increases TRACP secretion in osteoclasts. *J. Bone Miner. Res.* 23(3), 380–391 (2008).

- 34 Gong Y, Slee RB, Fukai N *et al.* LDL receptor-related protein 5 (LRP5) affects bone accrual and eye development. *Cell* 107(4), 513–523 (2001).
- 35 Boyden LM, Mao J, Belsky J *et al.* High bone density due to a mutation in LDL-receptor-related protein 5. *N. Engl. J. Med.* 346, 1513–1521 (2002).
- 36 Little RD, Carulli JP, Del Mastro RG *et al.* A mutation in the LDL receptor-related protein 5 gene results in the autosomal dominant high-bone-mass trait. *Am. J. Hum. Genet.* 70, 11–19 (2002).
- 37 Zhang Y, Wang Y, Li X *et al.* The LRP5 high-bone-mass G171V mutation disrupts LRP5 interaction with Mesd. *Mol. Cell. Biol.* 24(11), 4677–4684 (2004).
- 38 Ellies DL, Viviano B, McCarthy J *et al.* Bone density ligand, sclerostin, directly interacts with LRP5 but not LRP5G171V to modulate Wnt activity. *J. Bone Miner. Res.* 21(11), 1738–1749 (2006).
- 39 Ferrari SL, Deutsch S, Choudhury U *et al.* Polymorphisms in the low-density lipoprotein receptor-related protein 5 (LRP5) gene are associated with variation in vertebral bone mass, vertebral bone size, and stature in whites. *Am. J. Hum. Genet.* 74(5), 866–875 (2004).
- 40 Richards JB, Rivadeneira F, Inouye M *et al.* Bone mineral density, osteoporosis, and osteoporotic fractures: a genome-wide association study. *Lancet* 371(9623), 1505–1512 (2008).
- 41 Brunkow ME, Gardner JC, Van Ness J *et al.* Bone dysplasia sclerosteosis results from loss of the *SOST* gene product, a novel cystine knot-containing protein. *Am. J. Hum. Genet.* 68(3), 577–589 (2001).
- 42 Balemans W, Patel N, Ebeling M *et al.* Identification of a 52 kb deletion downstream of the *SOST* gene in patients with van Buchem disease. *J. Med. Genet.* 39(2), 91–97 (2002).
- 43 Uitterlinden AG, Arp PP, Paepker BW *et al.* Polymorphisms in the sclerosteosis/van Buchem disease gene (*SOST*) region are associated with bone-mineral density in elderly whites. *Am. J. Hum. Genet.* 75(6), 1032–1045 (2004).
- 44 McClung MR. Bisphosphonates. *Endocrinol. Metab. Clin. North Am.* 32, 253–271 (2003).
- 45 Russell RG, Xia Z, Dunford JE *et al.* Bisphosphonates: an update on mechanisms of action and how these relate to clinical efficacy. *Ann. NY Acad. Sci.* 1117, 209–257 (2007).
- 46 Black DM, Schwartz AV, Ensrud KE *et al.* Effects of continuing or stopping alendronate after 5 years of treatment: the Fracture Intervention Trial Long-term Extension (FLEX): a randomized trial. *JAMA* 296(24), 2927–2938 (2006).
- 47 Goh SK, Yang KY, Koh JS *et al.* Subtrochanteric insufficiency fractures in patients on alendronate therapy: a caution. *J. Bone Joint Surg. Br.* 89(3), 394–353 (2007).
- 48 Kwek EB, Goh SK, Koh JS, Png MA, Howe TS. An emerging pattern of subtrochanteric stress fractures: a long-term complication of alendronate therapy? *Injury* 39(2), 224–231 (2008).
- 49 Khosla S, Burr D, Cauley J *et al.* Bisphosphonate-associated osteonecrosis of the jaw: report of a task force of the American society for bone and mineral research. *J. Bone Miner. Res.* 22(10), 1479–1491 (2007).
- 50 Wells GA, Cranney A, Peterson J *et al.* Alendronate for the primary and secondary prevention of osteoporotic fractures in postmenopausal women. *Cochrane Database Syst. Rev.* 23(1), CD001155 (2008).
- 51 Wells G, Cranney A, Peterson J *et al.* Risedronate for the primary and secondary prevention of osteoporotic fractures in postmenopausal women. *Cochrane Database Syst. Rev.* 23(1), CD004523 (2008).
- 52 Zallone A. Direct and indirect estrogen actions on osteoblasts and osteoclasts. *Ann NY Acad. Sci.* 1068, 173–179 (2006).
- 53 Nakamura T, Imai Y, Matsumoto T *et al.* Estrogen prevents bone loss via estrogen receptor alpha and induction of fas ligand in osteoclasts. *Cell* 130, 811–823 (2007).
- 54 Charatcharoenwitthaya N, Khosla S, Atkinson EJ *et al.* Effect of blockade of TNF- α and interleukin-1 action on bone resorption in early postmenopausal women. *J. Bone Miner. Res.* 22, 724–729 (2007).
- 55 Chlebowski RT, Hendrix SL, Langer RD *et al.* Influence of estrogen plus progestin on breast cancer and mammography in healthy postmenopausal women: the Women's Health Initiative randomized trial. *JAMA* 289(24), 3243–3253 (2003).
- 56 Cauley JA, Robbins J, Chen Z *et al.* Effects of estrogen plus progestin on risk of fracture and bone mineral density: the Women's Health Initiative randomized trial. *JAMA* 290(13), 1729–1738 (2003).
- 57 Rossouw JE, Anderson GL, Prentice RL *et al.* Risks and benefits of estrogen plus progestin in healthy postmenopausal women: principal results from the Women's Health Initiative randomized controlled trial. *JAMA* 288(3), 321–333 (2002).
- 58 Anderson GL, Limacher M, Assaf AR *et al.* Effects of conjugated equine estrogen in postmenopausal women with hysterectomy: the Women's Health Initiative randomized controlled trial. *JAMA* 291(14), 1701–1712 (2004).
- 59 Barrett-Conno E, Mosca L, Collins P *et al.* Effects of raloxifene on cardiovascular events and breast cancer in postmenopausal women. *N. Engl. J. Med.* 355(2), 125–137 (2006).
- 60 Vasiljeva O, Reinheckel T, Peters C, Turk D, Turk V, Turk B. Emerging roles of cysteine cathepsins in disease and their potential as drug targets. *Curr. Pharm. Des.* 13, 387–403 (2007).
- 61 Adami S, Supronik J, Hala T *et al.* Effect of one year treatment with the cathepsin-K inhibitor, balicatib, on bone mineral density (BMD) in postmenopausal women with osteopenia/osteoporosis. *J. Bone Miner. Res.* 21, S24 (2006).
- **EvidencethatcathepsinKinhibition reducesboneresorption.**
- 62 Deal C. Potential new drug targets for osteoporosis. *Nat. Clin. Pract. Rheumatol.* 5(1), 20–27 (2009).
- 63 Bekker PJ, Holloway D, Nakanishi A, Arrighi M, Leese PT, Dunstan CR. The effect of a single dose of osteoprotegerin in postmenopausal women. *J. Bone Miner. Res.* 16(2), 348–360 (2001).
- 64 Body JJ, Greipp P, Coleman RE *et al.* A Phase I study of AMG-0007, a recombinant osteoprotegerin construct, in patients with multiple myeloma or breast carcinoma related bone metastases. *Cancer* 97(3 Suppl.), 887–892 (2003).
- 65 Boyce BF, Xing L. Functions of RANKL/RANK/OPG in bone modeling and remodeling. *Arch. Biochem. Biophys.* 473(2), 139–146 (2008).
- 66 Hamdy NA. Denosumab: RANKL inhibition in the management of bone loss. *Drugs Today (Barc.)* 44, 7–21 (2008).
- 67 Lewiecki EM, Miller PD, McClung MR *et al.* Two-year treatment with denosumab (AMG 162) in a randomized Phase 2 study of postmenopausal women with low BMD. *J. Bone Miner. Res.* 22(12), 1832–1841 (2007).
- 68 McClung MR, Lewiecki EM, Cohen SB *et al.* Denosumab in postmenopausal women with low bone mineral density. *N. Engl. J. Med.* 354(8), 821–831 (2006).

- 69 Brown JP, Prince RL, Deal C *et al.* Comparison of the effect of denosumab and alendronate on BMD and biochemical markers of bone turnover in postmenopausal women with low bone mass: a randomized, blinded, Phase 3 trial. *J. Bone Miner. Res.* 24(1), 153–161 (2009).
- **Phase II study of the skeletal effects of RANKL inhibition with a monoclonal antibody (denosumab) – comparison with bisphosphonates.**
- 70 Miller PD, Bolognese MA, Lewiecki EM *et al.* Effect of denosumab on bone density and turnover in postmenopausal women with low bone mass after long-term continued, discontinued, and restarting of therapy: a randomized blinded Phase 2 clinical trial. *Bone* 43(2), 222–229 (2008).
- 71 Kendler DL, Benhamou CL, Brown JP *et al.* Effects of denosumab vs alendronate on bone mineral density (BMD), bone turnover markers (BTM), and safety in women previously treated with alendronate. *J. Bone Miner. Res.* 23(Suppl.), S473 (2008).
- 72 Cummings S, McClung MR, Christiansen C *et al.* A Phase III study of the effects of denosumab on vertebral, nonvertebral, and hip fracture in women with osteoporosis: results from the FREEDOM trial. *J. Bone Miner. Res.* 23, (2008) (Abstract 1286).
- 73 Whyte MP. The long and the short of bone therapy. *N. Engl. J. Med.* 354(8), 860–863 (2006).
- 74 Kim H, Choi HK, Shin JH *et al.* Selective inhibition of RANK blocks osteoclast maturation and function and prevents bone loss in mice. *J. Clin. Invest.* 119(4), 813–825 (2009).
- 75 Missbach M, Jeschke M, Feyen J *et al.* A novel inhibitor of the tyrosine kinase Src suppresses phosphorylation of its major cellular substrates and reduces bone resorption *in vitro* and in rodent models *in vivo*. *Bone* 24(5), 437–449 (1999).
- 76 Lark MW, Stroup GB, Hwang SM *et al.* Design and characterization of orally active Arg–Gly–Asp peptidomimetic vitronectin receptor antagonist SB 265123 for prevention of bone loss in osteoporosis. *J. Pharmacol. Exp. Ther.* 291(2), 612–617 (1999).
- 77 Murphy MG, Cerchio K, Stoch SA *et al.* Effect of L-000845704, an $\alpha\text{v}\beta 3$ integrin antagonist, on markers of bone turnover and bone mineral density in postmenopausal osteoporotic women. *J. Clin. Endocrinol. Metab.* 90(4), 2022–2028 (2005).
- 78 Jilka RL. Molecular and cellular mechanisms of the anabolic effect of intermittent PTH. *Bone* 40(6), 1434–1446 (2007).
- 79 McClung MR, San Martin J, Miller PD *et al.* Opposite bone remodeling effects of teriparatide and alendronate in increasing bone mass. *Arch. Intern. Med.* 165(15), 1762–1768 (2005).
- 80 Neer RM, Arnaud CD, Zanchetta JR *et al.* Effect of parathyroid hormone (1–34) on fractures and bone mineral density in postmenopausal women with osteoporosis. *N. Engl. J. Med.* 344(19), 1434–1441 (2001).
- 81 Greenspan SL, Bone HG, Erttinger MP *et al.* Effect of recombinant human parathyroid hormone (1–84) on vertebral fracture and bone mineral density in postmenopausal women with osteoporosis: a randomized trial. *Ann. Intern. Med.* 146(5), 326–339 (2007).
- 82 Harper KD, Kregge JH, Marcus R, Mirlak BH. Osteosarcoma and teriparatide? *J. Bone Miner. Res.* 22(2), 334 (2007).
- 83 Brown M. The calcium-sensing receptor: physiology, pathophysiology and CaR-based therapeutics. *Subcell. Biochem.* 45, 139–167 (2007).
- 84 Balan G, Bauman J, Bhattacharya S *et al.* The discovery of novel calcium sensing receptor negative allosteric modulators. *Bioorg. Med. Chem. Lett.* 19(12), 3328–3332 (2009).
- 85 Kulkarni NH, Onyia JE, Zeng Q *et al.* Orally bioavailable GSK-3 α / β dual inhibitor increases markers of cellular differentiation *in vitro* and bone mass *in vivo*. *J. Bone Miner. Res.* 21, 910–920 (2006).
- 86 Clement-Lacroix P, Ai M, Morvan F *et al.* Lrp5-independent activation of Wnt signaling by lithium chloride increases bone formation and bone mass in mice. *Proc. Natl Acad. Sci. USA* 102, 17406–17411 (2005).
- 87 Vestergaard P, Rejnmark L, Mosekilde L. Reduced relative risk of fractures among users of lithium. *Calcif. Tissue Int.* 77, 1–8 (2005).
- 88 Wilting I, de Vries F, Thio BM *et al.* Lithium use and the risk of fractures. *Bone* 40, 1252–1258 (2007).
- 89 Morvan F, Boulukos K, Clement-Lacroix P *et al.* Deletion of a single allele of the Dkk1 gene leads to an increase in bone formation and bone mass. *J. Bone Miner. Res.* 21, 934–945 (2006).
- 90 Li J, Sarosi I, Cattley RC *et al.* Dkk1-mediated inhibition of Wnt signaling in bone results in osteopenia. *Bone* 39, 754–766 (2006).
- 91 Wang FS, Ko JY, Lin CL, Wu HL, Ke HJ, Tai PJ. Knocking down dickkopf-1 alleviates estrogen deficiency induction of bone loss. A histomorphological study in ovariectomized rats. *Bone* 40(2), 485–492 (2007).
- 92 Tian E, Zhan F, Walker R *et al.* The role of the Wnt-signaling antagonist DKK1 in the development of osteolytic lesions in multiple myeloma. *N. Engl. J. Med.* 349, 2483–2494 (2003).
- 93 Heider U, Kaiser M, Mieth M *et al.* Serum concentrations of DKK-1 decrease in patients with multiple myeloma responding to anti-myeloma treatment. *Eur. J. Haematol.* 82(1) 31–38 (2009).
- 94 Yaccoby S, Ling W, Zhan F, Walker R, Barlogie B, Shaughnessy JD Jr. Antibody-based inhibition of DKK1 suppresses tumor-induced bone resorption and multiple myeloma growth *in vivo*. *Blood* 109(5), 2106–2111 (2007).
- 95 Fulciniti M, Tassone P, Hideshima T *et al.* Anti-DKK1 mAb (BHQ880) as a potential therapeutic agent for multiple myeloma. *Blood* 114(2), 371–379 (2009).
- 96 Robling AG, Bellido T, Turner CH. Mechanical stimulation *in vivo* reduces osteocyte expression of sclerostin. *J. Musculoskelet. Neuronal Interact.* 6, 354 (2006).
- 97 Ominsky M, Warmongton KS, Asuncion FJ *et al.* Sclerostin monoclonal antibody treatment increases bone strength in aged osteopenic ovariectomized rats. *J. Bone Miner. Res.* 21, S44 (2006).
- 98 Poole KE, van Bezooijen RL, Loveridge N *et al.* Sclerostin is a delayed secreted product of osteocytes that inhibits bone formation. *FASEB J.* 19, 1842–1844 (2005).
- 99 Li X, Ominsky MS, Warmington KS *et al.* Sclerostin antibody treatment increases bone formation, bone mass and bone strength in a rat model of postmenopausal osteoporosis. *J. Bone Miner. Res.* 24(4), 578–588 (2009).
- **Evidence suggestive that sclerostin antagonism has anabolic effects on bone.**
- 100 Reginster JY, Sarlet N, Lejeune E, Leonori L. Strontium ranelate: a new treatment for postmenopausal osteoporosis with a dual mode of action. *Curr. Osteoporos. Rep.* 3(1), 30–34 (2005).
- 101 Meunier PJ, Roux C, Seeman E *et al.* The effects of strontium ranelate on the risk of vertebral fracture in women with postmenopausal osteoporosis. *N. Engl. J. Med.* 350(5), 459–468 (2004).
- **Evidence that strontium ranelate decreases fracture risk in vertebral sites.**

- 102 Reginster JY, Seeman E, De Vernejoul MC *et al.* Strontium ranelate reduces the risk of nonvertebral fractures in postmenopausal women with osteoporosis: Treatment of Peripheral Osteoporosis (TROPOS) study. *J. Clin. Endocrinol. Metab.* 90(5), 2816–2822 (2005).
- 103 Stevenson M, Davis S, Lloyd-Jones M, Beverley C. The clinical effectiveness and cost-effectiveness of strontium ranelate for the prevention of osteoporotic fragility fractures in postmenopausal women. *Health Technol. Assess.* 11(4), 1–134 (2007).
- 104 Blake GM, Lewiecki EM, Kendler DL *et al.* A review of strontium ranelate and its effect on DXA scans. *J. Clin. Densitom.* 10(2), 113–119 (2007).
- 105 Spiegelman BM, Flier JS. Obesity and the regulation of energy balance. *Cell* 104(4), 531–543 (2001).
- 106 Ducy P, Amling M, Takeda S *et al.* Leptin inhibits bone formation through a hypothalamic relay: a central control of bone mass. *Cell* 100(2) 197–207 (2000).
- 107 Karsenty G. Convergence between bone and energy homeostases: leptin regulation of bone mass. *Cell Metab.* 4(5), 341–348 (2006).
- 108 Fu L, Patel MS, Bradley A, Wagner EF, Karsenty G. The molecular clock mediates leptin-regulated bone formation. *Cell* 122(5), 803–815 (2005).
- 109 Rosen CJ. Bone remodeling, energy metabolism, and the molecular clock. *Cell Metab.* 7(1), 7–10 (2008).
- Excellent review of the central control of bone remodeling. A detailed view into the interactions between bone physiology and energy metabolism, central neuronal pathways, osteocalcin and serotonin.
- 110 Sato S, Hanada R, Kimura A *et al.* Central control of bone remodeling by neuromedin U. *Nat. Med.* 13(10), 1234–1240 (2007).
- 111 Eleftheriou F, Ahn JD, Takeda S *et al.* Leptin regulation of bone resorption by the sympathetic nervous system and CART. *Nature* 434(7032), 514–520 (2005).
- 112 Ahn JD, Dubern B, Lubrano-Berthelie C, Clement K, Karsenty G. Cart overexpression is the only identifiable cause of high bone mass in melanocortin 4 receptor deficiency. *Endocrinology* 147(7), 3196–3202 (2006).
- 113 Lee NK, Sowa H, Hinoi E *et al.* Endocrine regulation of energy metabolism by the skeleton. *Cell* 130(3), 456–469 (2007).
- 114 Yadav VK, Ryu JH, Suda N *et al.* Lrp5 controls bone formation by inhibiting serotonin synthesis in the duodenum. *Cell* 135(5), 825–837 (2008).
- 115 Collet C, Schiltz C, Geoffroy V, Maroteaux L, Launay JM, de Vernejoul MC. The serotonin 5-HT_{2B} receptor controls bone mass via osteoblast recruitment and proliferation. *FASEB J.* 22, 418–427 (2008).
- 116 Rosen CJ. Serotonin rising – the bone, brain, bowel connection. *N. Engl. J. Med.* 360(10), 957–959 (2009).

Affiliations

- Apostolos I Gogakos
Molecular Endocrinology Group, Imperial College London, MRC Clinical Sciences Centre, Room 7N2, 7th Floor Commonwealth Building, Hammersmith Hospital, Du Cane Road, London, W12 0NN, UK
Tel.: +44 208 383 4326
a.gogakos@imperial.ac.uk
- Moira S Cheung
Molecular Endocrinology Group, Imperial College London, MRC Clinical Sciences Centre, Room 7N2, 7th Floor Commonwealth Building, Hammersmith Hospital, Du Cane Road, London, W12 0NN, UK
Tel.: +44 208 383 4326
m.cheung@imperial.ac.uk
- JH Duncan Bassett
Molecular Endocrinology Group, Imperial College London, MRC Clinical Sciences Centre, Room 7N2b, 7th Floor Commonwealth Building, Hammersmith Hospital, Du Cane Road, London, W12 0NN, UK
Tel.: +44 (0) 208 383 4613
d.bassett@imperial.ac.uk
- Graham R Williams
Molecular Endocrinology Group, Imperial College London, MRC Clinical Sciences Centre, Room 7N2a, 7th Floor Commonwealth Building, Hammersmith Hospital, Du Cane Road, London, W12 0NN, UK
Tel.: +44 208 383 1383
Fax: +44 208 383 8306
graham.williams@imperial.ac.uk